UNIVERSITY OF ASTON IN BIRMINGHAM

SOLVENT INDUCED NMR CHEMICAL SHIFTS THAT ARISE FROM MOLECULAR ENCOUNTERS

by

PRITAM S VARMA, BSc (Hons), MSc

A thesis presented to the University of Aston for the degree of Doctor of Philosophy

DECEMBER 1987

ABSTRACT

"Solvent Induced NMR Chemical Shifts that Arise from Molecular Encounters"

A thesis prepared for the Degree of Doctor of Philosophy
by
Pritam S Varma
1987

Recently Homer and Percival have postulated that intermolecular van der Waals dispersion forces can be characterized by three mechanisms. The first arises via the mean square reaction field $<R_1^2>$ due to the transient dipole of a particular solute molecule that is considered situated in a cavity surrounded by solvent molecules; this was characterized by an extended Onsager approach. The second stems from the extra cavity mean square reaction field $<R_2^2>$ of the near neighbour solvent molecules. The third originates from square field electric fields E^2_{BI} due to a newly characterized effect in which solute atoms are "buffeted" by the peripheral atoms of adjacent solvent molecules.

The present work concerns more detailed studies of the buffeting screening, which is governed by sterically controlled parameter $(2\beta_T - \xi_T)^2$, where ß and ξ are geometric structural parameters. The original approach is used to characterise the buffeting shifts induced by large solvent molecules and the approach is found to be inadequate. Consequently, improved methods of calculating ß and ξ are reported. Using the improved approach it is shown that buffeting is dependent on the nature of the solvent as well as the nature of the solute molecule.

Detailed investigation of the buffeting component of the van der Waals chemical shifts of selected solutes in a range of solvents containing either H or Cl as peripheral atoms have enabled the determination of a theoretical acceptable value for the classical screening coefficient B for protons.

^1H and ^{13}C resonance studies of tetraethylmethane and ^1H, ^{13}C and ^{29}Si resonance studies of TMS have been used to support the original contention that three ($<R_1^2>$, $<R_2^2>$ and E^2_{BI}) components of intermolecular van der Waals dispersion fields are required to characterise vdW chemical shifts.

Key words

NMR, van der Waals - Nuclear screening, Generalized reaction field theory, Homer and Percivals Buffeting theory, Solvent induced NMR chemical shifts.

With love
to my wife, Kanta
my sons, Stephen and Vinay
and
my parents

ACKNOWLEDGEMENTS

I consider myself extremely fortunate to have been supervised by Dr J Homer during the course of this research, and in the subsequent reporting of it, and I would like to express my sincere gratitude for his guidance and encouragement, as well as many discussions and suggestions, in the fulfilment of this work.

Beyond their support and encouragements as research colleagues and friends, I would like to thank the following.

Dr HK Al-Daffaee, for private communication of data from his work, as noted.

SU Patel, for his assistance in graphical presentation.

Dr MS Mohammadi and JK Roberts for their assistance in writing the necessary computer programs.

I must also express my sincere gratitude to: The University and in particular to Miss S Jackson, University Student Support Officer, for providing financial assistance during the final years of my research.

CONTENTS

LIST OF TABLES

LIST OF FIGURES

CHAPTER ONE

SOME THEORETICAL CONSIDERATIONS OF NUCLEAR MAGNETIC RESONANCE SPECTROSCOPY

1.1 Introduction

Many atomic nuclei possess spin angular momentum and as a result of this spin and their inherent charge, they have magnetic moments. These spin and magnetic nuclear properties were first revealed indirectly through the very fine splittings of certain atomic spectral lines. In 1924 Pauli(1) suggested that this hyperfine structure resulted from the interaction of magnetic moments with those of electrons in the atoms (more precisely the nuclear and electron angular momenta couple). Analysis of the hyperfine structure permitted the determination of the spin angular momentum and magnetic moments of many nuclei.

Evidence for nuclear spin was strengthened by the discovery (through heat capacity measurements) of ortho and para hydrogen molecules(2) that differ only in having the two constituent nuclei spinning in the same or opposite directions respectively.

In the early 1920's Stern and Gerlach(3,4) showed that the measurable values of a nuclear magnetic moment are discrete in nature. When a nucleus is placed in an inhomogeneous magnetic field, the allowed values of the magnetic moment correspond to its space quantization. The magnetic moment of the hydrogen nucleus was determined by directing a beam of hydrogen atoms through a static magnetic field which deflected the beam. This method was developed by using two, oppositely inclined, magnetic fields of similar gradients. The atomic beam was diffused by the first magnetic field, and focussed by the second one onto a detector. The introduction of a radio-frequency signal between the two original fields, such that the oscillating magnetic component of the rf signal was perpendicular to the main field, showed that the density of the atoms reaching the detector was reduced when the energy of the radio frequency signal was equal to the energy required to induce transitions between the nuclear energy levels (corresponding to quantization of the nuclear magnetic moments)[5]. It was not until 1946 that nuclear magnetic resonance was demonstrated in bulk materials (solids and liquids). In that year Purcell and his co-workers at Harvard reported nuclear resonance absorption in paraffin wax[6], while Bloch and his colleagues at Stanford reported nuclear resonance in liquid water[7].

In 1949 it was found that the energy of the nuclear levels are dependent on the compound in which the nucleus is found and on its position on that compound[8]. The determination of nuclear properties and molecular structure thus became possible from a knowledge of precise resonance frequencies[8,9,10].

The detection of Nuclear Magnetic Resonance is dependent on the properties of the bulk sample, however it is convenient, initially, to discuss the theory of NMR in terms of an isolated nucleus in a magnetic field. Subsequently, consideration can be made for other factors relevant to resonance in bulk samples.

1.2 Magnetic and Related Properties of Nuclei

Nuclei of certain isotopes may be considered to behave as spinning spherical, or ellipsoidal, bodies possessing uniform charge distribution around at least one axis. Such a positively charged spinning nucleus produces a magnetic field with axis coincident with the axis of spin. The angular momentum and the magnetic moment behave as parallel vectors related by

$$\vec{\mu} = \gamma \vec{I} \hbar \qquad \text{..... 1.1}$$

where γ is a characteristic constant of each nuclear species called the magnetogyric ratio or magnetogyric constant, μ is the magnetic moment of the nucleus; I is the nuclear spin quantum number and $\hbar$ is the reduced Plank's constant ($h/2\pi$). Nuclear angular momentum is quantised and in magnetic fields the maximum measurable component of angular momentum (actually $\sqrt{I\,(I + 1)}\,.\,\hbar$) in the field direction is always an integral or half integral multiple of h.

There are $2I + 1$ such values given by $[+I, (+I - 1), ..., 0, ... (-I + 1), - I]$ h. If $I = 0$, then $\mu = 0$ and no magnetic characteristics are observed, but if I is non-zero, μ has a finite value. It is obvious from equation 1.1 that the quantization of the nuclear angular momentum parallels the quantization of the magnetic moment μ, which, therefore, possesses only discrete components corresponding to different orientations with respect to the reference axis of an applied magnetic field.

Therefore, when placed in a magnetic field, a nucleus of spin I has available to it $2I + 1$ energy states. NMR spectroscopy is concerned with observing nuclear transitions between the permitted energy states.

1.3 Nuclei in a Magnetic Field

The different values of the components of the angular momentum are degenerate in the absence of a magnetic field. However, the application of an external magnetic field, B_o, causes the degeneracy to be lifted. The resulting energy levels correspond to different nuclear spin orientations relative to the reference (z) direction of the applied static field. The energy of the nucleus is given classically by:

$$E = E_o - E_z \qquad ..... 1.2$$

where E_o is the energy of the nucleus in the absence of a magnetic field, and $E_z = -\mu_z B_o$. Therefore the change in energy when the external field is applied is given by:

$$E_z = - \mu_{Bo} \text{Cos}\, \theta \qquad ..... 1.3$$

when the magnetic moment, μ, is inclined at an angle θ to the static field direction (Figure 1.1), it is evident that $\cos \theta$ can be defined in terms of m, the magnetic quantum numbers, by m/I where m adopts the values I, I - 1 .... -I.

Consequently,

$$E_z = -\mu \frac{m}{I} B_o \qquad .....1.4$$

Therefore the energies of the allowed levels, characterised by the associated value sof m, are:

$$-\mu B_o, \frac{-(I-1)}{I} \mu B_o, ..., (\frac{I-1}{I}) \mu B_o, \mu B_o$$

The transition selection rule is that transitions are permitted only between adjacent levels, ie. $\Delta m = \pm 1$[11]. It follows that energy difference between two adjacent levels is given by:

$$E = \frac{\mu B_o}{I} \qquad ..... 1.5$$

Using the Bohr frequency condition $\Delta E = h\nu$ equation 1.5 may be rewritten as:

$$\nu = \mu \frac{B_o}{Ih} = \frac{\gamma B_o}{2\pi} \qquad ..... 1.6$$

which characterises the frequency in the electromagnetic spectrum at which nuclear transitions may be detected.

To appreciate the physical basis of equation 1.5, it is convenient to consider the case of the simplest nucleus, that of hydrogen. This consists of one proton for which I = 1/2 and only two energy levels are permitted. These correspond to m = +1/2 and m = -1/2. The situation for the proton can be represented by:

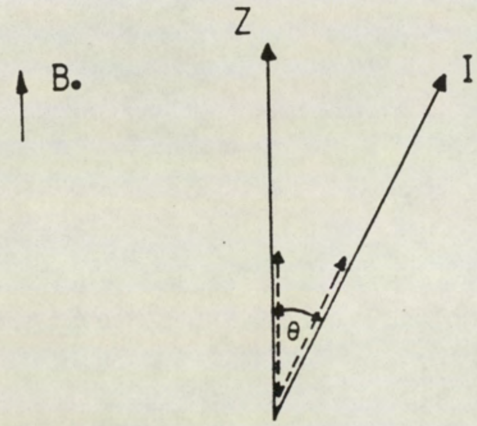

Figure 1.1: The relationship between the magnetic moment μ and the spin angular momentum I

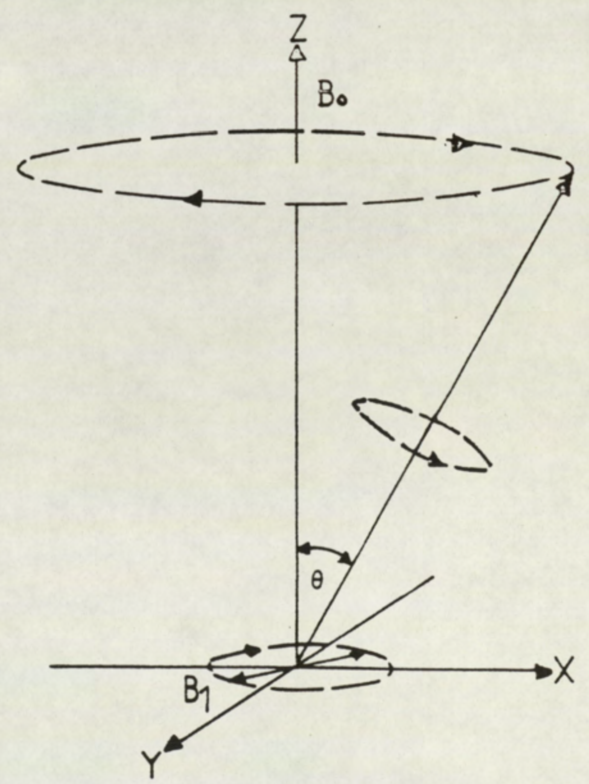

Figure 1.2: Vectorial representation of the classical Larmor precession

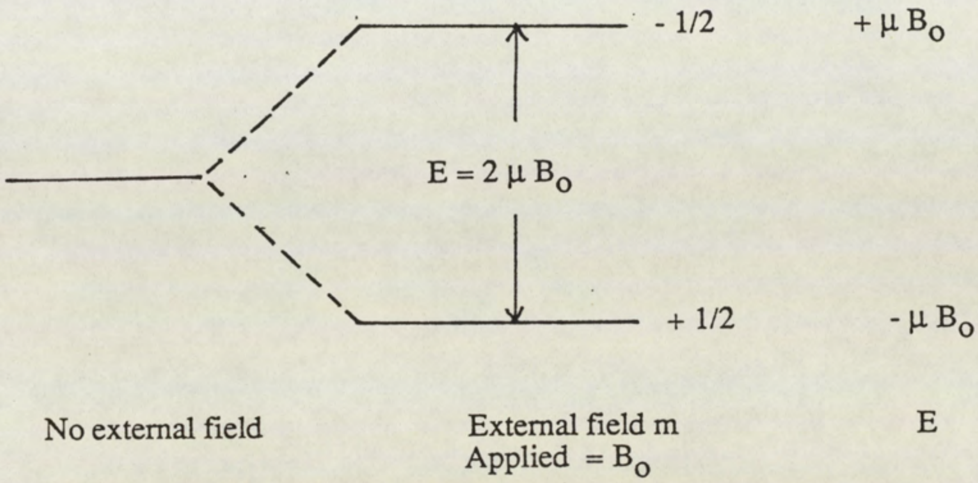

Because a particular nuclear species has constant values of μ and I, ν depends directly on B_o, so the magnetic resonance spectrum can occur under a variety of conditions. For example, for proton three typical conditions where resonance occurs are:

B_o = 1.4092 Tesla; ν = 60.004 MHz

B_o = 2.03329 Tesla; ν = 89.56 MHz

B_o = 2.3490 Tesla; ν = 100.00 MHz

1.4 The Conditions for and Classical Description of Nuclear Magnetic Resonance

An understanding of the mechanism of NMR can be approached by a classical treatment of the nuclear dipole. If a spinning charged particle, the nucleus, is placed in a magnetic field, B_o, with its magnetic moment making an angle θ to the direction of this field, it will experience a torque L to constrain it parallel to the field,

(Figure 1.2). Newton's law of motion states that the rate of change of angular momentum p with the time is equal to the torque or

$$\frac{dp}{dt} = \vec{L} \qquad \text{..... 1.7}$$

But according to magnetic theory:

$$\vec{L} = \vec{\mu} B_o \qquad \text{..... 1.8}$$

So

$$\frac{dp}{dt} = \vec{\mu} B_o = \gamma \vec{p} B_o \qquad \text{..... 1.9}$$

This equation describes the precession of the nuclear magnet around B_o with an angular velocity ω_o. The angular velocity may be defined by:

$$\frac{dp}{dt} = p\,\omega_o \qquad \text{..... 1.10}$$

Therefore

$$\omega_o = \gamma B_o \qquad \text{..... 1.11}$$

Equation 1.11 is called the Larmor equation. It can be written in terms of a precession frequency ν_o by:

$$\nu_o = \gamma \frac{B_o}{2\pi} \qquad \text{..... 1.12}$$

If a low intensity magnetic field B_1 is applied to the sample so that B_1 rotates in a plane at right angles to the main static field B_o, it is necessary, in order to exert the most torque on μ and change its orientation and thus the energy of the nucleus (Figure 1.2), for B_1 to rotate in synchronisation with the precession of μ about B_o, ie. the rotation of B_1 must be in resonance with the Larmor precession about B_o.

The rotating B_1 for nucleus resonance can be obtained by applying a rf signal to a coil surrounding the sample. This produces a linearly oscillating field, and such a field can be regarded as a superimposition of two fields rotating in opposite directions. One field component will be rotating in the opposite direction of the nucleus and will have little effect on it, while the other component is in phase with and can perturb the precessional motion and thus induce energy changes when its frequency is equivalent to the Larmor frequency.

1.5 The Distribution of Nuclei between Allowed Energy Levels

When a system of identical nuclei is at resonance, the probabilities P of transition occurring by absorption or simulated emission of energy are equal; the effect of spontaneous emission of energy is negligible(12).

Normally there is a Boltzmann distribution of nuclei between the various allowed energetically different nuclear levels. The probability of a given nucleus occupying a particular level characterised by a magnetic quantum number m, is given by

$$\frac{1}{2I+1} \exp \frac{m \mu B_o}{I k T} \qquad \text{..... 1.13}$$

which approximates to:

$$\frac{1}{2I+1}\left[1+\frac{m\,\mu\,B_o}{I\,k\,T}\right] \qquad \text{..... 1.14}$$

where k is the Boltzman constant and T is the temperature.

For a nucleus of spin I = $^1/2$, the populations of the upper or lower energy states respectively are governed at thermal equilibrium by:

$$^1/_2\left[1-\frac{\mu\,B_o}{kT}\right]$$

and

$$^1/_2\left[1+\frac{\mu\,B_o}{kT}\right] \qquad \text{..... 1.15}$$

There is, thus a distribution of nuclei favouring the lower energy state. The above equations also show that normal excess of nuclei in the lower energy states enables NMR to be observed by the net absorption of energy by the nuclear system.

If only two energy levels are considered, and N_1 and N_2 are the numbers of nuclei in the low and high energy levels respectively, the net change in the system at resonance is given by:

$P\,(N_1 - N_2) = P_n$ (excess) 1.16

where P is the probability of a transition occurring, and n is the excess of nuclei in the lower relative to the higher state.

The above equation also shows that, the absorption signal intensity increases with B_o. This latter parameter should therefore be as high as possible; because the higher the field, the greater the sensitivity due to the increase in the excess population of nuclei in the lower energy state.

Nuclear magnetic resonance spectroscopy differs from optical spectroscopy[13,14] in the rate of return of an energetically perturbed system to equilibrium. In the case of optical spectroscopy, after the absorption of energy, a very rapid recovery to equilibrium from an excited state to the ground state often occurs. However in nuclear magnetic resonance the recovery is relatively slow and signals can be weakened and eventually disappear with increasing intensity of radio-frequency field B_1 because the number of excess nuclei in the lower energy states tend to zero. This phenomena is known as saturation.

1.6 Saturation Effects

Absorption of energy from radio-frequency field B_1 reduces the excess population in the lower energy state with respect to the upper energy state. This results in a reduction in the net number of nuclei that can absorb energy from the radio-frequency field B_1. This effect will increase as the amplitude of the oscillating field is increased.

Saturation is reflected primarily as a reduction in signal intensity. Moreover it distorts the signal shape causing a broadening of the signal. If the spectrum includes several lines, the effect of saturation need not be the same because each absorption may have different relaxation times T_1 and T_2 (see 1.7 and 1.7.2).

1.7 Relaxation Processes

If the effects of saturation were not reversible, it would not be possible to reproduce the spectrum of a given sample.

However, a natural process known as relaxation removes the excess energy from a saturated system and allows it to reachieve the equilibrium Boltzman distribution of nuclei between the permitted levels.

There are two principal kinds of relaxation process, namely, the spin-lattice and spin-spin relaxation. Of these only the spin-lattice relaxation mechanism influences the net population of energy levels.

1.7.1 Spin-Lattice Relaxation

The term lattice refers to the molecular system as a whole which contains the nuclei being studied. All these molecules or their constituent particles in the lattice may have permanent or induced magnetic properties, and as they are undergoing transitional, rotational, and vibrational motions, a variety of time dependent magnetic fields are present in the lattice. When the resultant lattice field has a component at the resonance frequency which is sychronous with the precessional frequency of a given nucleus, this field will preferentially induce either stimulated emission or absorption transitions. However the probability of emission is greater than that of absorption, and the overall energy will be transferred from the spin-system to the surrounding lattice.

This is the mechanism of spin-lattice, or longitudinal relaxation and is responsible for the achievement of the Boltzmann population distribution of nuclear spin states when the sample is initially placed in a magnetic field. The rate at which a system returns to equilibrium after being perturbed is characterized by the spin-lattice relaxation time and this usually denoted by T_1.

The relation between the upward and the downward transition relaxation probabilities P_1 and P_2, follows from simple thermodynamics.

P_2 (upper to lower) > P_1 (lower to upper).

If a system is considered in which there are N_1 and N_2 nuclei in the lower and upper states respectively, then at equilibrium:

$$N_1 P_1 = N_2 P_2 \qquad \text{..... 1.17}$$

The excess number of nuclei in the lower level is

$$N(\text{excess}) = N_1 - N_2 \qquad \text{..... 1.18}$$

The normal Boltzman distribution for two energy states is given by[19]:

$$\frac{N_1}{N_2} = \exp\left(2\,\mu\,B_o/kT\right) \qquad \text{..... 1.19}$$

$$= 1 + 2\,\mu\,B_o/kT \qquad \text{..... 1.20}$$

and therefore

$$\frac{P_2}{P_1} = 1 + 2\,\mu\,B_o/kT \qquad \text{..... 1.21}$$

Hence the rate of change of the number of excess nuclei, is given by:

$$\frac{dN_{excess}}{dt} = 2\,N_2\,P_2 - 2\,N_1\,P_2 \qquad \text{..... 1.22}$$

where the factor of two comes from the fact that an upward transition decreases and a downward transition increases N(excess) by two, so:

$$\frac{dN_{excess}}{dt} = -2P\,(N\ excess - N\ equi) \qquad ..... 1.23$$

where $P = (P_1 + P_2)/2$

and

$$N_{equi} = \frac{\mu\, B_o}{kT}\,(N_1 + N_2) \qquad ..... 1.24$$

N_{equi} is the number of excess nuclei in the lower state at equilibrium.

Integration of equation 1.23 gives:

$$(N_{excess} - N_{equi}) = (N_o - N_{equi})\ \exp\,(2Pt) \qquad ..... 1.25$$

where N_o is the initial value of N excess per unit volume.

The spin relaxation time T_1 is given by(15):

$$T_1 = \frac{1}{2p} \qquad ..... 1.26$$

therefore from equation (1.25 and 1.26)

$$(N_{excess} - N_{equi}) = (N_o - N_{equi})\ \text{expt}\ \frac{-t}{T_1} \qquad ..... 1.27$$

This equation shows that the rate by which the excess population reaches its equilibrium value is governed exponentially by the spin-lattice time T_1.

1.7.2 Spin-Spin Relaxation

Besides the mechanism which has been described in the previous section, the nuclei also interact among themselves. The actual magnetic field felt by the nucleus is not only due to the steady magnetic field B_o, but it is this plus small magnetic fields produced locally by other surrounding nuclear magnets precessing about the direction of B_o. Those fields may be thought to have oscillating and static components.

A nucleus producing a magnetic field oscillating at its Larmor frequency, may induce a transition in a like neighbouring nucleus (and vice versa) in a similar way to an applied alternating magnetic field that is used to observe resonance. This will lead to an interchange of energy between the pair of spins, while the total energy of the pair is conserved. Thus there is no effect on the population distribution of nuclear spins.

The process is known as spin-spin relaxation. The characteristic spin-spin relaxation time is denoted by T_2.

1.8 NMR in Macroscopic Samples

So far the discussion of the resonance condition has considered the magnetic properties of isolated nuclei. In the treatment of the experimental observation of NMR for bulk systems, it is convenient to adopt the approach of Bloch[16,17,18] and consider the assembly of nuclei in macroscopic terms.

An assembly of nuclei in an applied field has its various spin states occupied to different extents, and this gives the sample a magnetic moment per unit volume, M_o, according to:

$$M_o = B_o \chi_o \qquad \text{..... 1.28}$$

where χ_o is the static magnetic susceptibility.

The bulk magnetisation is analogous to the nuclear moment μ, except for one important difference that in the absence of an applied radiofrequency field, M_o has only a z-component whereas μ has x, y and z components (ie. $Mx = \Sigma_i \mu_x = 0$, $My = \Sigma_i \mu_y = M_o$ and $M_z = \Sigma_i \mu_z = M_o$ the sums are over i nuclei). The individual nuclei precess about the z-axis with no phase coherence and so the x and y components average to zero in forming M_o.

When the assembly of nuclei is exposed to the rotating field B_1, then as this field approaches the values required for resonance, nuclei will start to precess in phase and give non-zero values to M_x and M_y (Figure 1.3).

The effect of B_1 will be to exert a torque on M tending to tip the moment toward the plane perpendicular to B_o; M will move away from the z-direction and precess about the effective field direction with the Larmor frequency at resonance. The precession of M can be described by the following equations:

$$\frac{dM_x}{dt} = \gamma \, [M_y \, B_o - M_z \, (B_1)_y] \qquad \text{..... 1.29}$$

$$\frac{dM_y}{dt} = \gamma \, [M_x \, B_o - M_z \, (B_1)_x] \qquad \text{..... 1.30}$$

$$\frac{dM_z}{dt} = \gamma \, [M_x \, (B_1) \, y - M_y \, (B_1)_x] \qquad \text{..... 1.31}$$

where $(B_1)_x$ and $(B_1)_y$ are the components of B_1 (rotating at angular frequency ω) along the x-y axis and are given by:

From Figure 1.4

$$(B_1)_x = B_1 \cos \omega t \qquad \text{..... 1.32}$$

$$(B_1)_y = -B_1 \sin \omega t \qquad \text{..... 1.33}$$

To proceed further the effect of relaxation processes must be taken into account. M_z does not remain constant, but after resonance approaches the equilibrium value M_o, at the rate governed by the spin relaxation time T_1, which in macroscopic systems is termed the longitudinal relaxation time. Additionally the effect of the transverse relaxation time T_2 must also be considered. The complete Bloch equations are therefore:

$$\frac{d\,M_x}{dt} = \gamma\ (M_y\, B_o + M_z B_1 \sin \omega t) - \frac{M_x}{T_2} \qquad \text{..... 1.34}$$

$$\frac{d\,M_y}{dt} = \gamma\ (M_z\, B_1 \cos \omega t - M_x\, B_o) - \frac{M_y}{T_2} \qquad \text{..... 1.35}$$

$$\frac{d\,M_z}{dt} = \gamma\ (M_x\, B_1 \sin \omega t + M_y\, B_1 \cos \omega t) - \frac{M_z - M_o}{T_1} \qquad \text{..... 1.36}$$

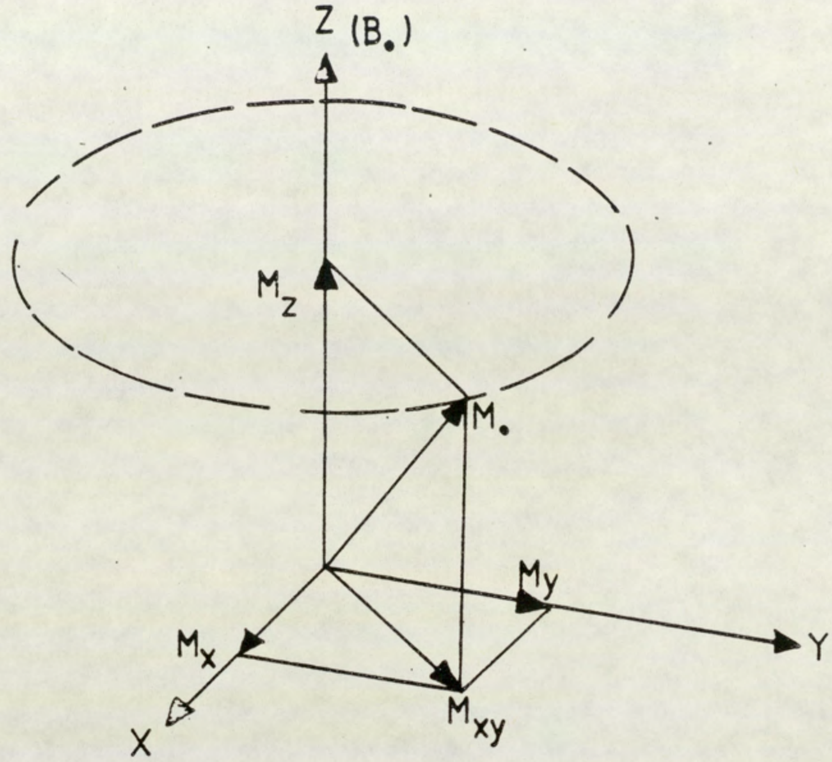

Figure 1.3: The resolving components of the magnetization vector

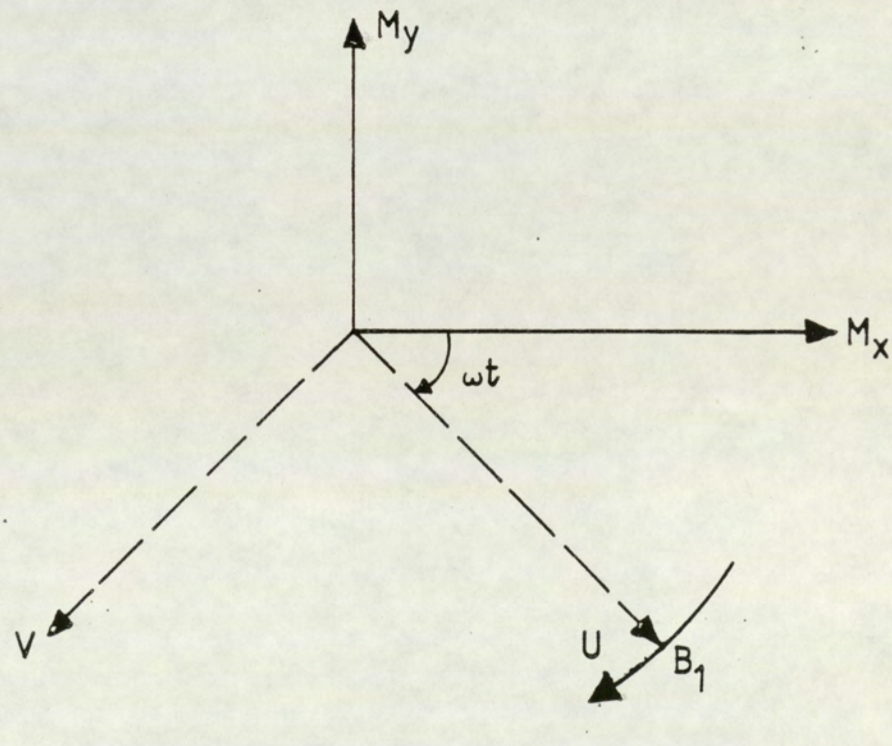

Figure 1.4: The transient components of the magnetization vector with respect to fixed and rotating axis

Assuming that resonance is passed through slowly (the slow passage approximation) the differentials with respect to time become zero and the solutions of equations (1.34, 1.35 and 1.36) are:

$$u = M_o \gamma B_1 T_2^2 (\omega_o - \omega)/D \qquad ..... 1.37$$

$$v = M_o \gamma B_1 T_2/D \qquad ..... 1.38$$

$$M_z = M_o [1 + T_2^2 (\omega_o - \omega)^2/D \qquad ..... 1.39$$

where

$$D = 1 + T_2^2 (\omega_o - \omega)^2 + \gamma^2 B_1 T_1 T_2 \qquad ..... 1.40$$

where u is the component of M that rotates in phase with B_1, and v is the component of M that rotates 90° out of phase with B_1.

Depending on whether u or v is observed a dispersion (u - mode signal) or absorption curve respectively will be obtained (Figure 1.5). It should be noted that the equation for v is almost an expression of the Lorenzian curve[16,19] which is the generally accepted absorption signal shape.

The area under an absorption curve can be obtained by integration of the v term over all values of $(\omega_o - \omega)$. The area under each resonance is therefore a direct indication of the number of nuclei of a particular type undergoing resonance.

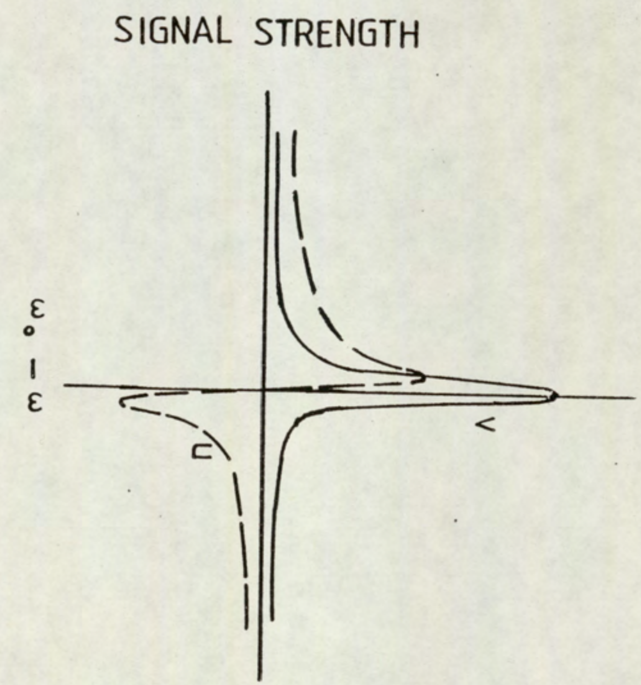

Figure 1.5: The absorption line shape (v mode) and dispersion line shape (u mode) of NMR signals

1.9 Factors Affecting the Line-Width

Superficially, it might be accepted that the NMR signal should appear as a sharp absorption line, but in practice absorption occurs over a finite frequency range due to several line broadening factors. Usually the signal width is defined as its width at half height expressed in terms of the applied field or more usually frequency.

The various factors affecting the line shape will now be discussed.

1.9.1 Spin-Lattice Relaxation

A nucleus may remain in a given energy state no longer than a factor of the spin-lattice relaxation time T_1. There is, therefore, some uncertainty in the life time of that particular spin-state that is characterized by the Heisenberg uncertainty principle which requires that:

$$\Delta E \, . \, \Delta T \simeq \frac{h}{2\pi} \qquad \text{..... 1.41}$$

Because energy and frequency are related by

$$\Delta E = h \, . \, \Delta \nu \qquad \text{..... 1.42}$$

where $\Delta \nu$ is the uncertainty in frequency of a particular resonance line, it follows from equations (1.41 and 1.42) that:

$$\Delta \nu = \frac{1}{2 \pi \Delta T} \qquad \text{..... 1.43}$$

and because $\Delta T = 2T_1$ 1.44

$$\Delta \nu = \frac{1}{4 \pi T_1} \qquad \text{..... 1.45}$$

This shows that small values of T_1 leads to line broadening.

1.9.2 Spin-Spin Relaxation

Spin-spin relaxation produces an uncertainty in the life time of any particular nuclear state in a similar manner to that of spin lattice relaxation and also leads to a broadened absorption signal.

1.9.3 Magnetic Dipole Interaction

The magnetic environment of a nucleus may be modified by fields due to magnetic moments of neighbouring nuclei. In solids or viscous liquids a nucleus at diatance r from the nucleus being considered produces a magnetic field at the nucleus of magnitude in the range of $+2\ \mu/r^3$ to $-2\ \mu/r^3$ where μ is the dipole moment of the nucleus. This means that the nuclei in a sample will experience a field spread over that range (derived from $\mu = \mu\ (3 \cos^2 \theta - 1)/r^3$ where θ is the angle between r and B_o) and the absorption will be broadened[20].

In liquids and gases where the molecules are subject to rapid random motion, the magnetic field at any nucleus due to neighbouring nuclei effectively averages to zero because $\langle\cos^2 \theta\rangle = {}^1/_3$; this occurs because the molecular correlation time is less than the time required for the observation of a nuclear magnetic resonance signal. Accordingly magnetic dipole broadening will be negligible in liquid and gas samples which are used for normal high resolution investigations.

1.9.4 Magnetic Field Inhomogeneity

Inhomogeneity of the applied static magnetic field over the sample volume can cause line broadening due to the fact that absorption occurs over a range of resonance conditions corresponding to the range of field inhomogeneity. This effect can be reduced by applying correcting fields and by rapid spinning of the sample.

1.9.5 Saturation

A large amplitude of the applied radio frequency field may cause the excess number of nuclei in the lower energy state to be reduced before the complete resonance line has been observed, if the effect of spin-lattice relaxation is inadequate to maintain a near Boltzmann ground state excess. Therefore the net radio frequency energy absorbed will decrease. The decrease is greater at the centre of an absorption mode signal and the height of the signal will decrease while the effective line width increases. If sufficient radio frequency power is applied the signal may disappear entirely.

1.9.6 Miscellaneous Effects

As the presence of any paramagnetic species will significantly decrease T_1, the absorption line will be broadened, as mentioned in section 1.9.1.

Finally a non-spherical nuclear charge distribution for nuclei of spin > $^1/_2$ confers on the nucleus a quadrupole moment q. Interaction of the quadrupole with environmental electric field gradients promotes relaxation which gives uncertainty in the resonance frequency and hence a broadening.

1.10 The Origins of the Chemical Shift and Nuclear Screening

1.10.1 Definition and Measurement

At an early stage in the history of NMR it was found that the resonant frequencies for isotopically similar nuclei in the same molecule could be different when using the same applied magnetic field. The magnitude of this effect was shown(21,22,23) to be related to the chemical environments of the resonant nuclei, which cause them to be screened differently from the applied magnetic field. These differences arise because in real systems the nuclei are not independent of their environment and this, by a variety of mechanisms, produces at the nuclei secondary magnetic fields. If the applied magnetic field is B_o, the actual field experienced by the nuclei is given by:

$$B = B_o (1 - \sigma) \qquad \text{..... 1.46}$$

where σ is the nuclear screening constant for the resonant nucleus.

Because of rapid molecular motions in gases and liquids, the screening value of the constant is the average for all molecular orientations relative to the applied field direction. Equation 1.46 must therefore be rewritten as:

$$\nu_1 = \mu B_o (1 - \sigma_i)/Ih \qquad \text{..... 1.47}$$

for a nucleus i.

It is the magnitude and composition of σ_i which holds the key to many chemical and physical problems; but unfortunately it cannot be determined experimentally as this would require the determination of ν_o for the appropriate isotope stripped of all its electrons. The best that can be done is to determine the difference between the screening constants of two nuclei of the same species. If σ_i and σ_j are the respective screening constants of two nuclei i and j, which resonate at fields B_i^R and B_j^R in a fixed frequency experiment, the chemical shift δ_{ij} of i relative to j is defined as:

$$\delta_{ij} = \sigma_i - \sigma_j \sim \frac{B_i^R - B_j^R}{B_j^R} (\times 10^6) \qquad \text{..... 1.48}$$

where the factor 10^6 is introduced to enable δ_{ij} to be quoted as a number of ppm. It is worth noting that a positive shift evaluated using equation (1.48) would appear to be negative if the experiment was conducted at a fixed field and the last term of the equation was redefined in frequency terms. It is helpful to remember that the screening constant is a nuclear parameter that in principle, can be "measured" by any technique, but it just happens that NMR is the only practical technique available for this purpose. The NMR chemical shift should, therefore, be defined in accordance with the fundamental significance of the screening constant. In other words, if it is found, for example, that in a fixed field experiment $\nu_i^R < \nu_j^R$ or correspondingly in a fixed frequency experiment that $B_i^R > B_j^R$, the absolute fact is that $\sigma_i > \sigma_j$ and δ_{ij} should be quoted as a positive number.

Usually the chemical shift of a particular isotope is measured relative to the resonance of a suitable reference. The most commonly used reference for proton resonance is tetramethylsilane (TMS)[24]. This is often chosen because its resonance is a clear sharp line occurring to a high (shielding) field of most resonances of interest and it is soluble in most organic compounds while being chemically inert. Moreover, it has low boiling point (26.7°C), so it is easy to remove from the sample after the experiment has been concluded. The position of the resonance of TMS when it is at infinite dilution in carbon tetrachloride CCl_4 is taken to be as $\delta = 0$. Signals to higher magnetic field, or greater screening, than TMS signal should have positive δ values, although common practice is to assign them (-) ve δ values. Another scale commonly used is the τ-scale[34], for which the TMS proton signal is taken as 10τ. The two scales are related as follows:

$$\tau = \delta + 10$$

As indicated above the δ and τ scales have been much abused and, many of the quoted values of chemical shifts must be treated with caution[25,26].

1.10.2 Some Details of Nuclear Screening

The nuclear screening parameter may be considered akin to many other observable physical properties. Consequently, its composition in the gas phase can be examined by using a Virial expansion(37).

$$x = A + \frac{B}{V_m} + \frac{C}{V_m^2} + \ldots \qquad \ldots\ldots 1.49$$

where x is the observable molecular parameter, A is the perfect gas value of x, B represents the effects of pairwise molecular interactions, C and higher terms represent the effects of multimolecular interactions; and V_m is the molar volume of the material studied.

Similarly, σ the screening constant can be given in terms of a virial expansion, as(27):

$$\sigma = \sigma_o + \frac{\sigma_1}{V_m} + \frac{\sigma_2}{V_m^2} + \ldots \qquad \ldots\ldots 1.50$$

where σ_o is the screening in the isolated molecule, σ_1 represents the effect of pairwise molecular interaction on the screening, σ_2 and higher terms represent the effects of three and higher body interactions on the screening.

For practical reasons equation (1.50) is better rewritten to represent the chemical shift as:

$$\delta_{obs} = (\sigma - \sigma_{ref}) = (\sigma - \sigma_{ref}) + \frac{\sigma_1}{V_m} + \frac{\sigma_2}{V_m^2} + \ldots \qquad \ldots\ldots 1.51$$

where σ_{ref} is the screening constant of the reference nucleus.

A significant observation has been that the relationship between the chemical shift ($\sigma - \sigma_{ref}$) and the bulk density of a gas is linear[28,29]. This relationship seems to extend into the liquid phase. The implication of this would lead to the conclusion that the only term additional to σ_o in the virial equation (1.51) is σ_1/V_m, and that the terms higher than first order can be ignored. This means that screening constant arises from two factors viz the absolute screening constant (intramolecular) and the screening contribution from the bimolecular interaction (intermolecular) σ_{inter}. Therefore, equation (1.50) may be reduced to:

$$\sigma = \sigma_o + \frac{\sigma_1}{V_m} \qquad \text{..... 1.52}$$

or

$$\sigma = \sigma_{intra} + \sigma_{inter} \qquad \text{..... 1.53}$$

Studies of σ_{intra}[30,31] have been carried out using quantum mechanical treatments. From these it has been suggested that the screening constant of a nucleus A is an isolated molecule is adequately represented by:

$$\sigma^{intra} = \sigma_{para}^{AA} + \sigma_{dia}^{AA} + \Sigma_{A \neq B}\, \sigma^{AB} + \sigma_{del}^{A} \qquad \text{..... 1.54}$$

In equation (1.54) σ_{para}^{AA} is the screening contribution that comes from the mixing of ground and excited electronic states by the magnetic field and leads to induced "paramagnetic" current around A. σ_{dia}^{A} is due to the diamagnetic currents resulting from electronic motion about A. The induced currents in bonds or atoms other than A provide the anisotropic contribution to the screening σ^{AB}, and σ_{del}^{A}

comes from the induced electronic motion of delocalized electrons in the molecular structure surrounding A.

Considering the second part of the screening constant σ_{inter} arises from the interaction of the molecule, containing the nucleus being studied and all other molecules.

It was suggested by Buckingham in 1960[32,27] that σ_{inter} may be generally formulated by:

$$\sigma_{inter} = \sigma_b + \sigma_w + \sigma_a + \sigma_E + \sigma_s \qquad \text{..... 1.55}$$

The individual terms of this equation generally represent the total contribution for all components of a mixture to the screening of a nucleus in one molecule (solute) and are as follows: σ_b is due to the bulk magnetization of the sample. σ_w is due to the effect of van der Waals, but principally attractive dispersion forces. σ_a is due to the secondary fields produced by magnetically antisotropic solvent molecules. σ_E is a composite term basically due to the effect on an electrically polar solute of the reaction field of the solvent which is induced by the solute, but includes the effects of electric fields due to permanent dipoles or quadrupole in the solvent. σ_s is due to the contribution of any specific or binding interactions between the solute and the solvent molecules, eg. when hydrogen bonding or complex formation occurs.

It is obvious from what has been explained above that σ_{intra} depends on the structure of the molecule of interest and so is a parameter of particular interest to most chemists. In this thesis however, investigations of aspects of σ_{inter} rather than σ_{intra} are reported, although there is an underlying interest in the elucidation of molecular structure using σ_{inter}.

Although extensive work has been carried out, over the past decades to establish theoretical models for the characterisation of the components of σ_{inter}, the magnetic susceptibility screening parameter σ_b, is the only parameter which can be considered adequately characterised. Dickinson[33] showed that

$$\sigma_b = (\alpha - q - \frac{4\pi}{3})\,\chi_v \qquad \text{..... 1.56}$$

where α is the sample shape factor, q is the magnetic field interaction factor, and χ_v is the volume magnetic susceptibility of the matter under test. It was shown that q can be considered approximately zero. α the sample shape factor is taken to be 2π for a cylindrical sample with a length at least four times its diameter[34,35]. As all the sample tubes used throughout this work meet the above criteria, the parameter σ_b can be easily calculated.

Experimentally the chemical shift is measured with respect to a reference. The physical way in which this reference is used may effect the contribution of σ_b to the measured shift. A common method of referencing is by mixing the reference substance homogenously with the sample. This procedure is called the internal referencing procedure. In this method the molecule of interest and the reference are in the same medium and hence, both the sample and the reference experience the same magnetic susceptibility screening contribution. This eliminates the σ_b contribution to the chemical shift measurement[36].

Another referencing procedure is that of external referencing which employs the reference material in a separate vessel surrounded by the subject compound. A common method of external referencing is to use two co-axial cylinders, so that the reference material is in a capillary tube situated inside the co-axial with the main cylindrical sample tube. The theoretical implications of such an arrangement have been considered by Frost and Hall(37) who extended Dickinson's approach. They deduced that the true chemical shift devoid of susceptibility effects of the sample of interest (A) relative to a reference material (B) is given by:

$$\delta^t_{A-B} = \delta^o_{A-B} - \frac{2\pi}{3}(\chi_A - \chi_B) \qquad \text{..... 1.57}$$

where $\delta^t{}_{A-B}$ is the true chemical shift of A from the reference B, $\delta^o{}_{A-B}$ is the corresponding observed shift, and χ_A and χ_B are the volume magnetic susceptibilities of A and B respectively.

The above equation applies for long perfectly cylindrical tubes. However, if the reference can be contained in a spherical vessel, the shape factor which is $\alpha = 4\pi/3$, it emerges that $\Delta\ \sigma_b = 0$, which means that there is no need for any susceptibility correction. Unfortunately, the last technique is difficult to employ with precision.

The disadvantage of the external reference is that its correction depends on the volume magnetic susceptibility of the sample used and errors can arise from the uncertainty in these values, especially in the case of mixtures(38).

It is obvious that the contribution of the volume magnetic susceptibility to chemical shifts can be estimated. However, the relative importance of the remaining screening parameters, need to be assessed. It is probably fair to observe that σ_w, σ_a and σ_E, which in this order represent the relative ease of their experimental accessibility, have not been characterised precisely.

The major part of this thesis is concerned with σ_w as the correct formulation of this may provide the key to the elucidation of σ_a and σ_E. Intensive work on σ_w has already been carried out by Homer and Percival[39]. The present work may be considered an extension and further substantiation of Homer's basic theory.

In order to isolate σ_w, it is necessary to measure the chemical shift of a solute molecule with respect to a suitable reference in two physically different situations. The first one is when the solute is in the gas phase (at zero pressure) to give $(\sigma_o - \sigma_{ref})$, and the second one is when the solute molecule is at infinite dilution in a solvent to give $(\sigma - \sigma_{ref})$. When the solute and solvent molecules are perfectly isotropic, the difference between the susceptibility corrected chemical shift in the liquid phase relative to the gas phase will give only σ_w.

$$\delta_{liquid\ -\ gas} = \sigma_b + \sigma_w \qquad ..... \ 1.58$$

$$\delta_{gas\text{-}to\text{-}liquid} \text{ (after susceptibility correction)} = \sigma_w \qquad ..... \ 1.59$$

There have been many ways proposed to calculate σ_w theoretically, but these have been considered to be incomplete by Homer. The past work and the recently proposed theory will be discussed in Chapter 3.

1.11 Nuclear Spin-Spin Coupling

High resolution spectra may reveal that chemically shifted absorption bands are composed of several lines. This added multiplicity is attributed to the intra molecular interaction between magnetically non-equivalent nuclear magnetic moments[40,41]. The multiplicity comes from the coupling interaction between neighbouring nuclear spins. Important features are exhibited by spin-spin interactions which distinguish them from the chemical shift. For example they are independent of B and temperature in most cases.

In the simplest case the spacings between these multiplet lines are equal and the magnitude of this splitting is known as the coupling or the spin-spin coupling constant. This is symbolised by J for which the unit is Hz.

The effect can be explained naively in terms of the fact that a nuclear spin tends to orient the spins of the nearest electrons which then orientate the spins of the electrons and subsequently the spins of other nuclei.

In general the magnitude of the coupling constant decreases as the number of bonds separating the interacting nuclei increases, and increases with the atomic number of each coupled nucleus.

The complexity of the spin patterns is largely dependent on the relative magnitude of the chemicals shift differences and spin-spin coupling constant between the interacting nuclei. When the chemical shift of the two nuclei is of the same order of magnitude as the coupling constant (both in Hz), the nuclei are identified by letters (A,B,C) closely positioned in the alphabet. When the chemical shift is greater than the coupling constant between the nuclei ($\delta >> J$) the latter are identified by letters widely spaced in the alphabet, eg. A and X. Nuclei with the same chemical shifts are assigned the same letter and the number of such nuclei is indicated by the appropriate numerical subscript. Such nuclei are deemed either chemically equivalent or magnetically equivalent. Chemical equivalent nuclei only have the same chemical shift.

Nuclei are said to be magnetically equivalent when they have the same chemical shift and couple equally to any other resonant nuclei in the molecule. Magnetically equivalent nuclei do not show any experimental evidence of any coupling between them, although such coupling does occur.

Magnetically non-equivalent but chemically equivalent nuclei are identified by right hand superscript primed, eg. AA', BB'.

The signal arising from one set of nuclei is termed an absorption band, while constituent lines of such a band arising from coupling may be called peaks. The number of the latter can be predicted simply for first order situation for which $\delta >> J$.

For a set of n_A equivalent nuclei of type A and n_X equivalent nuclei of type X, a first order coupling treatment gives $(2n_X I_X + 1)$ peaks of band A and $(2n_A I_A + 1)$ peaks for band X[42].

The relative intensities of the peaks comprising the multiplet structure are given by the n^{th} polynomial coefficients. These rules are strictly valid only if $\delta >> J$, when $\delta = J$, the spectra should be treated as second order spectra and the above simple spacing and intensity rules are no longer valid.

The spin-spin coupling aspect of NMR spectroscopy has not been encountered in the present work and therefore will not be considered further.

CHAPTER TWO

NMR INSTRUMENTATION

2.1 Introduction

The essential components of a high resolution nuclear magnetic resonance spectrometer are:

(a) A magnet producing a very stable homogeneous magnetic field together with facilities for varying this field over a small range in a controlled manner.

(b) A stable source of radio-frequency power.

(c) A detection and display system

A block diagram showing the main features of continuous wave NMR spectrometer is given in Figure 2.1.

2.2 Features Common to CW and FT Spectroscopy

Continuous wave (CW) and Fourier transform (FT) spectroscopy differ principally in that with the former approach the rf field is applied continuously where as with the latter it is pulsed for periods of time typically in the microsecond (μs) range. Despite these fundamental differences both types of spectrometers have many features in common and these will be outlined initially.

2.2.1 The Magnet

A suitable magnetic field of the required stability and homogeneity may be provided by permanent, electro or superconducting magnets. The essential differences between these is that the first two direct Bo perpendicular to the sample axis while the last produces Bo along the sample axis. Each of these magnets have various advantages and disadvantages and a suitable compromise between these, results in each finding use for specific applications.

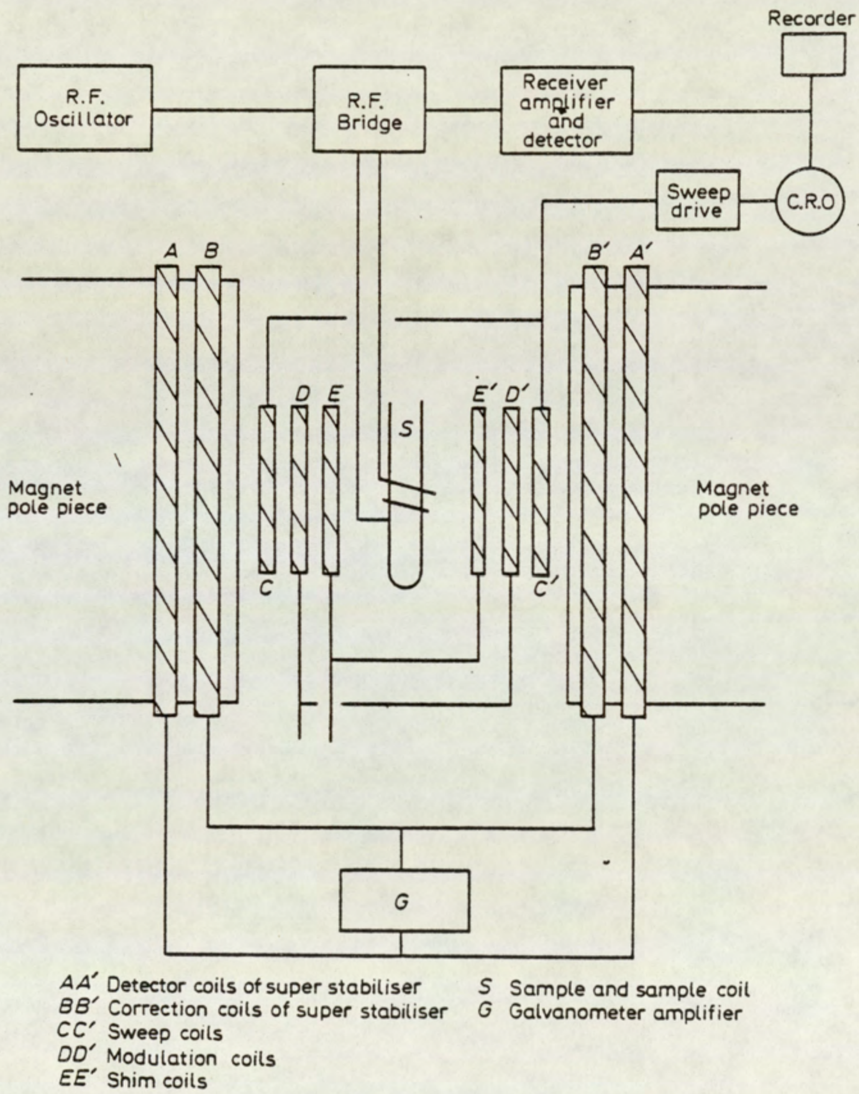

Figure 2.1: Block diagram of a continuous wave NMR spectrometer

Originally electromagnets were designed to operate at high voltage (2000-4000 volts) and low currents (1-2 amperes), but low impedence systems have been developed and these use solid state power supplies working at low voltage. Another development has been the introduction of super-conducting solenoids that can give fields of 5 tesla or more with adequate homogeneity and stability for high resolution work[43]. As these solenoids operate at liquid helium temperature much auxillary equipment is needed; such spectrometers are now quite common.

2.2.2 Magnetic Field Stability

In practice it is found that none of the above systems inherently provides a sufficiently stable magnetic field for high resolution nmr and a device known as a field corrector, flux stabiliser, or super stabiliser is incorporated in commercial instruments. This includes a pair of coils (AA', Figure 2.1) placed so that changes in the main magnetic field strength induce an emf in the coils. This emf is amplified (Figure 2.1) and used to control a current passing through a second set of coils (BB', Figure 2.1) in such a way as to compensate exactly for the original change in field strength. The response of this type of system is quite rapid and the residual magnetic field fluctuation can be reduced to less than 1 in 10^8 by these means. However, a very slow overall drift of the main field cannot be corrected in this way.

2.2.3 Magnetic Field Homogeneity

In addition to having high stability, the magnetic field needs to be uniform over the volume of the sample. If this is not so the absorption lines of the recorded spectrum will be excessively broad and narrow splittings will not be resolved.

By careful design each kind of magnet can achieve residual inhomogeneities of as little as 1 in 10^7 throughout a 0.5ml sample. This can be improved by spinning the sample tube about its axis at about 20 rev/sec. This helps to average out field gradients along the two other axes. Further improvement can be achieved by the use of shim (or Golay) coils[44] (EE', Figure 2.1). These coils are mounted on either the probe or the pole faces of the magnet, and are designed to produce weak magnetic fields having gradients that can be varied by altering the current passing through the coils. The shim coil currents are adjusted to produce a field gradient at the sample which cancels any gradient in the field of the laboratory magnet. This enables the residual inhomogeneity to be reduced to a few parts in 10^9. In practice it is found that the only shim coil to need frequent adjustment is the one which controls field gradients along the axis of spinning (the y-axis), and autoshim devices are now available to perform this operation automatically.

The autoshim is essentially a servomechanism which monitors a suitable control signal from the sample, and adjusts the current through the shim coil regulating the y-axis field gradient, so as to maintain maximum height and minimum width of the control signal.

The volume over which satisfactory homogeneity can be obtained limits the size of the sample that may be used. For high resolution work with ^{1}H, ^{19}F and ^{31}P, cylindrical sample tubes about 5mm in diameter can be conveniently used, but for other isotopes where low inherent receptivity causes problems it is common to use larger samples.

If necessary overall variation of the resultant magnetic field strength at the sample can be accomplished by passing a suitable current through a pair of Helmholtz coils (the sweep coils, CC', Figure 2.1) mounted in the gap of the magnet. Alternatively an artificial error signal can be fed into the super-stabiliser control system, this will then produce a correcting field change and so generate the required sweep. This generally offers a more precise means of achieving controlled variation of the magnetic field strength.

2.2.4 Radio-Frequency Circuits[45]

A source of radio-frequency energy, with a frequency stability of 1 in 10^9 is required. This is conveniently derived from either a fixed frequency oscillator or a frequency synthesizer, both of which may depend on a quartz crystal controlled oscillator. Usually the crystal itself is protected from rapid change in temperature to eliminate frequency drifts. Means of controlling the power output of the oscillator (or transmitter) are provided while facilities for modulating it with an audio-frequency are also often included.

2.2.5 The Detection System

This is one of the most important parts of an NMR spectrometer as the ultimate signal-to-noise ratio that can be attained depends on the detection system. The two types of detection in common use are:

(a) Single coil arrangement

Energy from the radio-frequency power supply is fed to a coil wound about the sample. The coil forms part of a radio-frequency bridge circuit; energy absorption by the sample produces changes in the balance of the bridge which are detected by the receiver. The use of this coil arrangement is usually confined to CW spectroscopy.

(b) Crossed coil arrangement

In this method use is made of two coils, these are arranged with their axes perpendicular to one another and also to the direction of the magnetic field. Energy from the rf oscillator is fed to the sample via the transmitter coil. When the sample absorbs energy an emf is induced in the second (sample or receiver) coil and this can be detected by the receiver. This is often known as the nuclear induction method and is used in both CW and FT spectroscopy. The coils are mounted in the probe unit. In practice, the receiver will detect a direct or leakage signal from the transmitter independently of any absorption by the sample and use is made of the leakage signal in the detection process. The relationship between this signal and that due to nmr absorption affects the shape of the recorded resonance. It may be altered by devices incorporated either in the detector circuitry or, for a crossed coil instrument, in the probe.

The signals to be detected are very weak, so the receiver must have a high sensitivity and care is needed to reduce spurious signals (noise) to a minimum. Noise may be normal electrical noise that occurs in all circuits or it may be generated mechanically by, for example, the spinning of the sample. To obtain the best signal-to-noise ratio the first stage of amplification of the signal takes place (as in CW spectroscopy) in a pre-amplifier unit, which is normally incorporated in the probe unit itself, as close as possible to the receiver coil. The transmitter and receiver proper are usually built into a single unit and in addition to control the power output of the transmitter a means of altering the gain of the receiver is also provided.

2.2.6 The Uses of Modulation

Originally audio frequency modulation was used in CW NMR spectroscopy as a means of calibrating spectra. Subsequently a number of improvements to spectrometers have been achieved by application of effects dependent on modulation. For present purposes it will be sufficient to consider modulation simply as a process which mixes signals of different frequencies. The convention will be adopted that the signal ν will be given to frequencies in the megahertz (or radio-frequency) region while audio frequencies will be given the signal f. When a radio-frequency ν is modulated by an audio-frequency f the resulting signal can be considered as being made up from the frequencies ν - f; ν; and ν + f. If the intensity of the audio-frequency field becomes sufficiently great it may be necessary to consider the resultant signal being made up from the frequencies ν - 2f; ν - f; ν; ν + f and ν + 2f.

Each of these frequencies can stimulate nmr transitions and it is possible by using suitable demodulation techniques to detect the signals due to the various frequencies in isolation.

2.2.7 Baseline Stabilizer

Small extraneous changes of conditions (such as temperature) in the probe will alter the strength of the signal detected by the receiver, and consequently the base-line will tend to fluctuate or drift. This can be overcome by using a device known as a phase-sensitive detector (psd) which depends on modulation for its operation. The radio-frequency signal or the magnetic field is modulated with a fixed audio-frequency signal f_B of a few kHz. The frequency f_B is also fed directly to the psd as a reference to ensure that only signals at the frequency of one of the side bands and with the correct phase relationship are detected by the receiver. Overall changes in rf power level will then have no effect and a stable baseline is achieved.

Baseline stabilisation by this method makes it extremely easy to record an integrated spectrum, that is a graph of the summation of the total spectral intensity. The output from the audio-frequency phase-sensitive detector is a voltage which can be transformed into a current. As a peak is traversed, the charges in detector output voltage are applied to the plates of a capacitor which acts as an integrator. The voltage produced across the terminals of the capacitor is proportional to the peak area, and it can be read to give the required integral trace.

2.2.8 Field-Frequency Locking System

The inherent long-term drifts of field strength, which occur particularly in spectrometers equipped with electromagnets, can be eliminated by use of the NMR phenomenon itself. A control sample of high proton or other resonant nucleus content is built into the probe as close as possible to the experimental sample. The control sample is provided with its own NMR circuitry and gives rise to a resonance signal in the usual way. Usually the dispersion mode signal is detected, so any variation from exact-resonance (zero-signal) generates either positive or negative signal that is used to actuate an electronic feed-back loop which restores the field strength to its original value. In this way the field strength can be held constant to 1 in 10^8 indefinitely. Strictly speaking it is not the strength of the field in absolute terms that must be held constant, but rather it is the ratio of field strength to frequency of irradiation signal that should not vary (see equation 1.8). The circuit mentioned above does not distinguish between changes in field and changes in frequency so it will, in fact, correct for both drifts in field and in frequency. This stabilisation arrangement is generally described as an external field-frequency lock, because the control sample is separate from the analytical sample. This type of locking system is particularly convenient for routine work because the field remains locked when the experimental sample is changed; it is rare for drifts to exceed 0.5 Hz. It is possible of course, to use a signal from the analytical sample for field/frequency locking.

External locking systems depend on the assumption that changes in the field strength at the experimental sample are paralleled by changes at the control sample. This will not be exactly true since the two samples are normally separated by a few centimetres and for this reason internal locking systems have been devised. In these, two separate frequencies are used to stimulate the analytical and lock signal discretely. The field strength is adjusted to X_1 corresponding to the f_1 sideband of a sharp line in the spectrum of the sample being examined and the rf detector output is passed through a phase-sensitive detector operating at a frequency f_1. The output from this psd is then used to actuate a control loop to the flux stabiliser, that maintains the ratio of field strength to frequency constant at a value governed by the relation

$$\frac{\nu - f_1}{B_o} = \frac{\gamma(1 - \sigma)}{2\pi} \qquad \text{..... 2.1}$$

In this relation ν is the frequency of the rf oscillator, and the lower sideband f_1 is used for locking; σ is the shielding constant of the nucleus giving the locking signal. Other resonances from the sample can now be detected by varying the frequency of the analytical circuits. The output of the analytical psd can then be fed to a recorder, oscilloscope or computer. It will be noticed that in this mode of operation the main magnetic field remains constant throughout, so this is a true frequency-sweep experiment. The stability achieved depends upon the sharpness of the line chosen to provide the locking signal, and upon the frequency stability of the oscillator used to generate f_1. Typically, the drift over several hours will be less than 0.1 Hz.

2.3 Other Accessories

2.3.1 Variable temperature attachment

Facilities for varying the temperature of the sample are commonly provided on commercial NMR spectrometers. Variation of temperature is usually achieved by passing a stream of air or nitrogen at the required temperature past the sample tube. The stream of hot or cold gas is transferred in and out of the probe through a dewar system so that the magnet is protected from the temperature changes. Temperatures above ambient may be attained by passing the air or nitrogen over an electrically heated nichrome spiral. A thermocouple placed in the gas stream close to the sample gives an indication of the actual temperature of the sample and can also be used to operate a proportional control system that regulates the current to the heater and/or the gas flow rate, so maintaining the sample temperature constant to about ± 1 degree. Temperatures below ambient are attained either by using a stream of cold nitrogen from a liquid nitrogen boiler (in which case the heater evaporating the nitrogen can be regulated by the proportional control system), or by passing dry gas through a spiral metal tube immersed in a dewar containing liquid nitrogen. In the latter case, the temperature of the sample could be adjusted by altering the gas flow rate.

2.3.2 Double resonance facilities

Manufacturers usually provide apparatus for homonuclear double resonance as a standard part of their NMR spectrometers, though it should be remembered that for some instruments this facility is an optional extra. The main additional instrumentation necessary for this type of experiment is a stable variable-frequency oscillator. The apparatus for heteronuclear double resonance almost invariably has to be obtained as an additional accessory for the spectrometer.

2.3.3 Spectral Accumulation

One early technique for enhancing the sensitivity of CW NMR spectrometers made use of a computer of average transients (cat). The spectrum is scanned many times and the output of the spectrometer is fed into the cat. Successive synchronised scans of the spectrum lead to reinforcement of the required positive signal, while random noise (either positive or negative) tends to be averaged out; this leads to improvement of the signal-to-noise ratio by a factor of $\sqrt{n}$, where n is the number of scans of the spectrum. This device has been largely superceeded by the use of FT spectrometers.

2.4 Special Features of CW Spectrometers

In CW spectroscopy a resonance spectrum is obtained either by fixing the radio frequency and linearly varying the applied field or fixing B_o and varying the radio-frequency. Methods of producing field sweep have been discussed in section 2.2.3. Often the variation in the applied field is synchronised to a chart recorder so that calibrated spectra can be output directly to the chart paper. Alternatively the repetitive signal derived from a saw tooth generator can be used to drive the field and time-base on oscilloscope on which spectra may be displayed repetitively.

Frequency swept spectra are often produced by linearly varying the audio-frequency modulation of the carrier rf signal.

Unlike FT spectrometers the use of a variable intensity, B_1, is possible to stimulate resonance. After resonance detection various receiver parameters may be varied to optimize the spectrum produced. For example, the time constant of the output circuit of the receiver may be varied so that the operator can vary the time constant and sweep-rate to obtain the most favourable signal-to-noise ratio for each sample. The output from the receiver is a voltage, which is fed to an appropriate presentation device (a chart recorder or a cathode ray oscilloscope).

2.4.1 The CW Spectrometer used in the Present Study

A Perkin-Elmer R12B NMR spectrometer was one of the instruments used in carrying out the work reported in this thesis for the study of some ^1H spectra.

While many of the principles applicable to this spectrometer, have been discussed, the salient features of Perkin-Elmer R12B NMR spectrometer will now be reviewed.

2.4.2 The Perkin-Elmer R12B Spectrometer

This spectrometer[46] has a permanent magnet giving a magnetic field strength of 1.492 Tesla, for ^1H resonances at 60 MHz. The magnet is of a rigid barrel construction that protects it from any distortion of the pole pieces. The field stability is maintained principally by keeping the magnet at constant temperature by passing heated air around the magnet, and by use of μ-metal screening. The field homogeneity is improved by means of Golay coils mounted near the pole tips. The sample is spun about its longitudinal axis using a plastic turbine fitted to the sample tube.

Sweep and shift coils are wound on a former on the magnet poles pieces. The magnetic field can be swept through a small range by passing a sawtooth current through the sweep coils. The sweep range may be varied by changing the amplitude of the sawtooth. In addition, the sweep current may be derived from a potentiometer driven by the pen recorder and this enables the spectrum to be observed on a recorder in addition to the oscilloscope.

Regions of the spectrum may be selected for expansion or study by field shift and widths controls; the adjustment of which changes the current passing through the appropriate coils.

The operational basis of the spectrometer is shown schematically in Figure 2.2.

The irradiation field (60 MHz) B_1 is derived from a highly stable crystal-controlled oscillator kept in a thermally regulated oven. The frequency stability of the oscillator is of the order 2 parts in 10^9 per hour. A 6 KHz signal, also derived from a crystal-controlled oscillator, is applied to coils orthogonally located relative to the probe radiofrequency coil and aligned with the magnet axis, so that the magnetic field in the sample region is audiofrequency modulated.

At resonance the sample acts as a mixing device, and NMR sidebands are produced at field strengths corresponding to 59.994 and 60.006 MHz. Each sideband, when stimulated, induces in the probe a 60 MHz radiofrequency response, amplitude-modulated at 6 KHz, the modulation containing information about the NMR signal. The probe output is applied to a radio frequency amplifier, located in the double resonance accessory, when fitted, the output of which is detected to obtain the 6KHz signal. This signal is amplified and compared with a reference signal of adjustable phase, so the v-mode or u-mode component of the 60.006 MHz sideband may be selected as required for observation or recording. The NMR signal may be

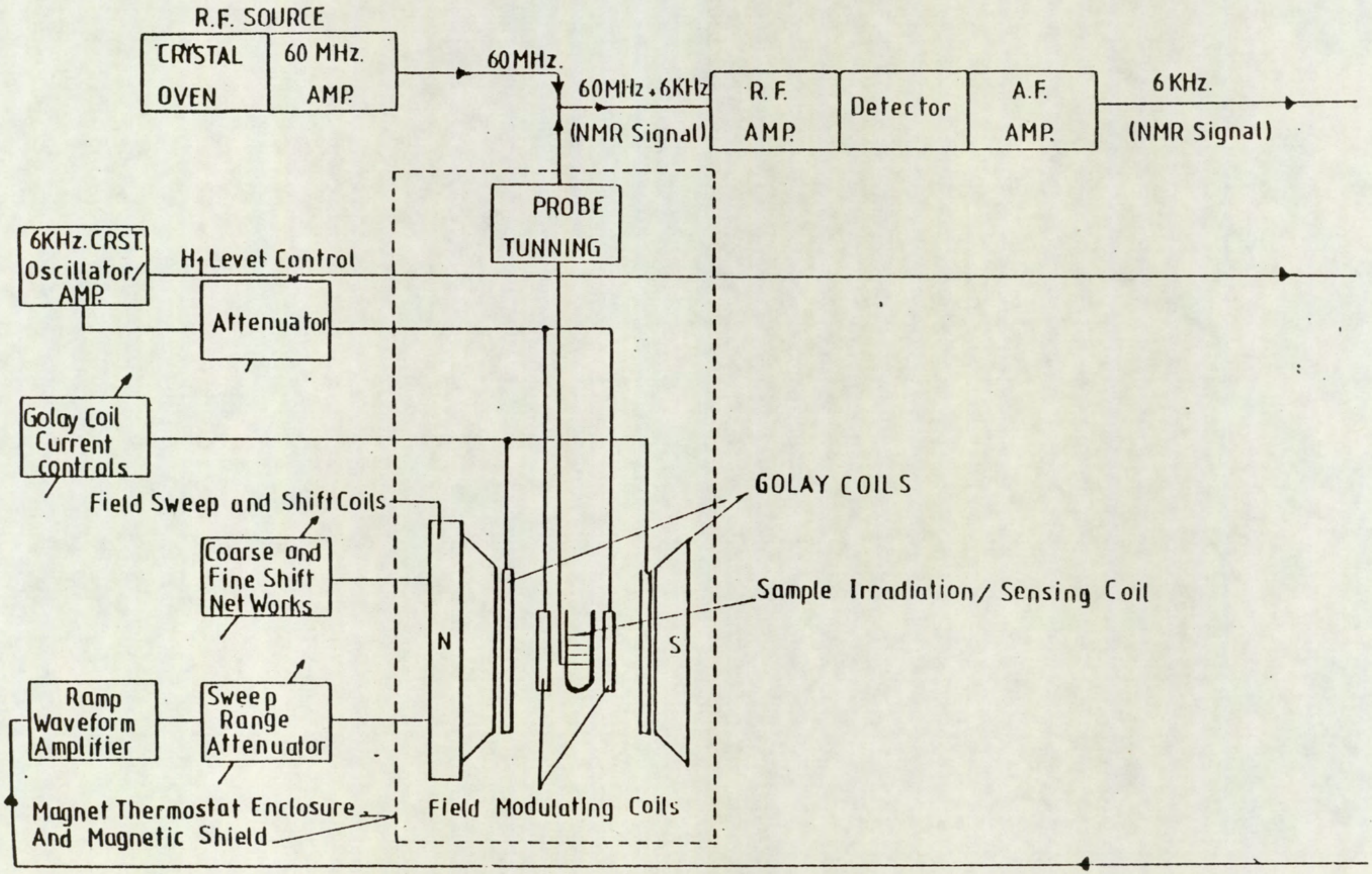

Figure 2.2: A Perkin Elmer R 12 B NMR Spectrometer block diagram

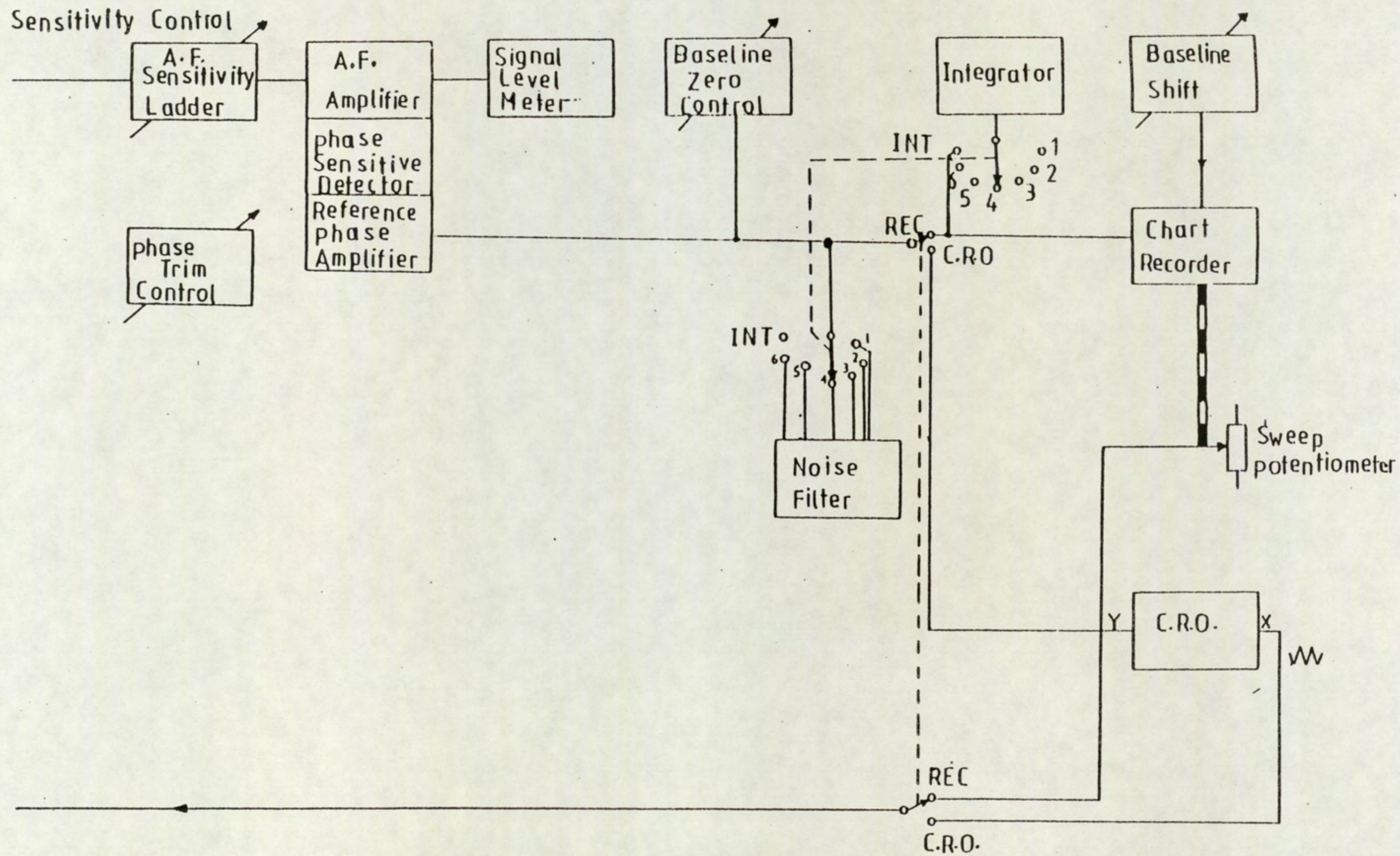

Figure 2.2 continued ...

filtered, integrated if necessary, and then presented.

2.5 FT NMR Spectroscopy

2.5.1 Introduction

Pulse FT spectrometers are characterized by their ability to provide information in a much shorter time than CW spectrometers.

Basically, if a radiofrequency signal produces a field B_1 by pulsing for a very short time, t_p. The equilibrium magnetization of the sample, M_o, is rotated from the direction of B_o by an angle θ radians according to:

$$\theta = \gamma B_1 t_p \qquad \text{..... 2.2}$$

The pulse time t_p is usually of the order of microseconds.

The radio frequency pulse envelope may be described as a square wave (Figure 2.3c) with many components covering a relatively wide range of frequency $\Delta\nu$. This allows all nuclei with their Larmor frequencies within $\Delta\nu$ to be stimulated and resonate. Essentially, therefore, the short rf pulse is equivalent to all of the frequencies that would have to be produced by many (CW) transmitters producing frequencies distributed over the spectral range required.

If a $\pi/2$ pulse is applied along the x-axis in the frame rotating at the rf (Figure 2.3a), M, lies entirely along the y-axis. Since the detector coil is usually arranged to detect signals in the (xy) plane, the magnitude of M_{xy} determines the strength of the observed signal. The nuclear signal is detected after the pulse is switched off as the free induction signal (FID), so called because the nuclei process freely and lose phase coherence in the absence of the applied rf (Figure 2.3b and d).

The decay component of the perturbed magnetization in the xy plane, is thus detected as the FID. The latter is sampled for a characteristic time and stored in the computer required for FT NMR. Successive FID's may be added to the computer to improve the signal to noise ratio and finally the resultant FID is subjected to Fourier transformation to produce a conventional frequency domain spectrum. Ideally pulse sequences should not be repeated within less than $5T_1$, after the last sequence, so that the nuclei can return to equilibrium before the next pulse.

If a $\pi/2$ pulse is applied and B_o is perfectly homogeneous, the magnetization should decay with a time constant T_2 (Figure 2.3d). In fact, however, M_{xy} decays in a time T^*_2 because of field inhomogeneity, that causes nuclei in different parts of the field to precess at slightly different frequencies, due to their different chemical shifts and/or spin-spin coupling. T^*_2 is given by:

$$\frac{1}{T^*_2} = \frac{1}{T_2} + \frac{\gamma}{2} \Delta B_o \qquad \text{..... 2.3}$$

where ΔB_o is the field inhomogeneity.

For a sample with chemically and magnetically equivalent nuclei a simple FID is obtained which after transformation yields a single absorption line. When the sample contains magnetically distinct nuclei, a more complex FID is obtained that may appear as a regular beat pattern. The Fourier transform of the latter gives an NMR spectrum composed of several lines.

2.5.2 The Basic Components of FT NMR Spectrometers

Although CW and FT spectrometers have similarities, they do have characteristic differences. Figure 2.4 is a schematic representation of the basic components of a FT spectrometer.

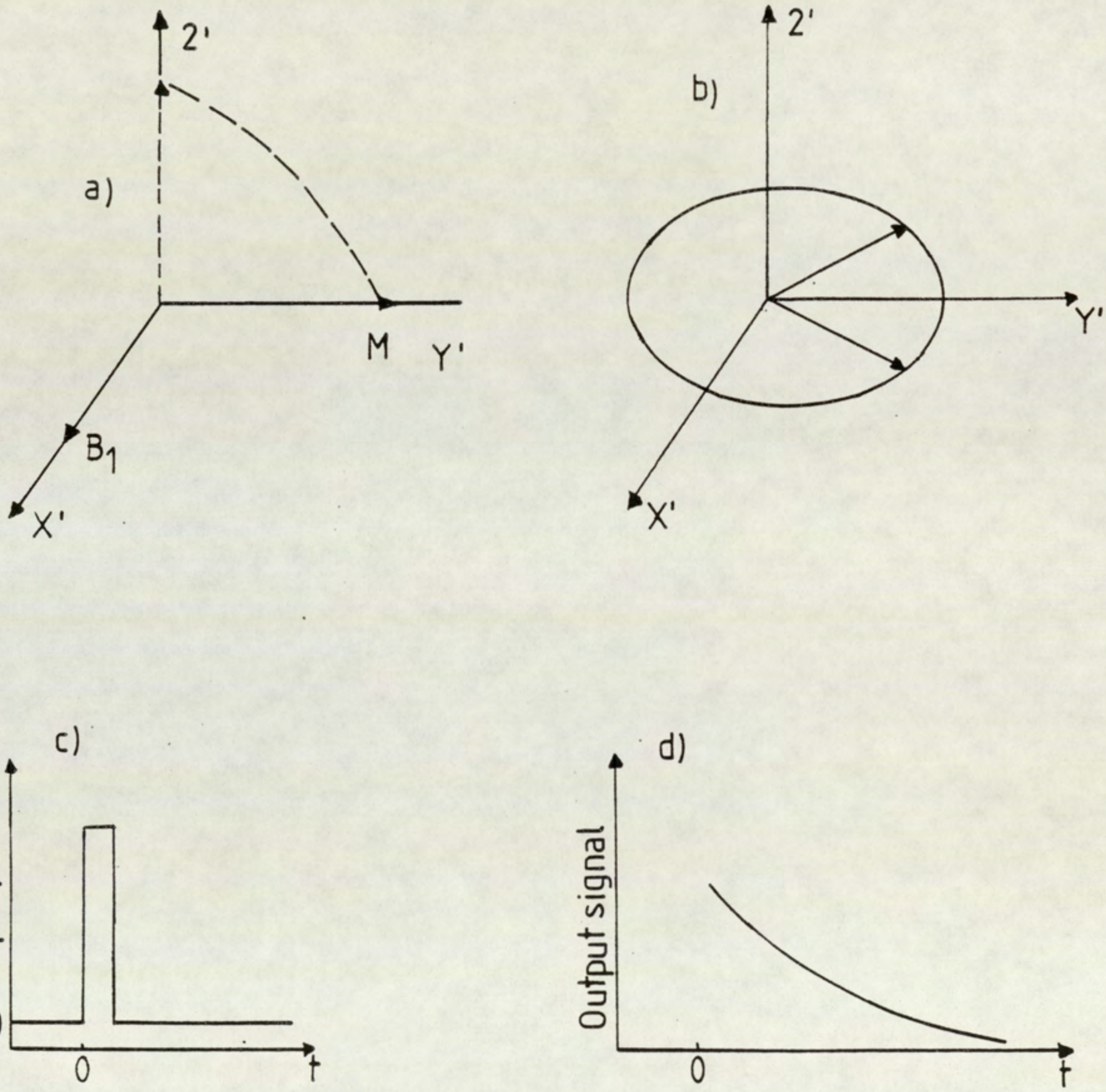

Figure 2.3: A representation of the FID

(a) 90° pulse along x' rotates M to the y' axis

(b) M_{xy} decays

(c) Input rf pulse

(d) Free induction decay signal FID corresponding to b

The short powerful rf pulse, needed for a FT spectrometer, necessitates a high power transmitter to produce B_1 in the range of 0.01-0.04 Tesla at the sample, and thus stimulate the whole resonance spectrum. Consequently, the pulse NMR receiver must be able to handle large voltages and recover very quickly, in order to detect the FID signal without interference.

Besides the requirements referred above, Fourier transform spectrometers have essentially similar basic units to those in CW spectrometers; the main differences being that the transmitter and receiver circuits are adapted for pulsed operation. In addition, there are several supplementary units such as a pulse programmer and a system for acquiring and processing the data.

2.5.2.1 The pulse programmer

The pulse programmer controls when, for how long and for which channel the rf gate will be opened. The output of the rf transmitter (usually derived from a frequency synthesizer to enable flexibility in the choice of operating frequency) is interrupted by a sequence of pulses. If it is a periodic single pulse of width t_p, it can be considered analogous to the sweep field in order to detect the absorption signal in CW NMR operations. More complex sequences of two or more pulses are used for more complex purposes, for example the measurement of relaxation times.

2.5.2.2 The RF Gate Unit

The rf output channel is provided with a gating device, which can be switched on and off, so that the rf is applied to the probe in pulses. The timing of the pulse generator is determined by digital programming. The rf gate is used to derive the transmitter which contains a very stable quartz crystal oscillator and usually the rf switch which is "on" in the presence of a dc pulse signal from the pulse programmer and in the "off" position otherwise[47].

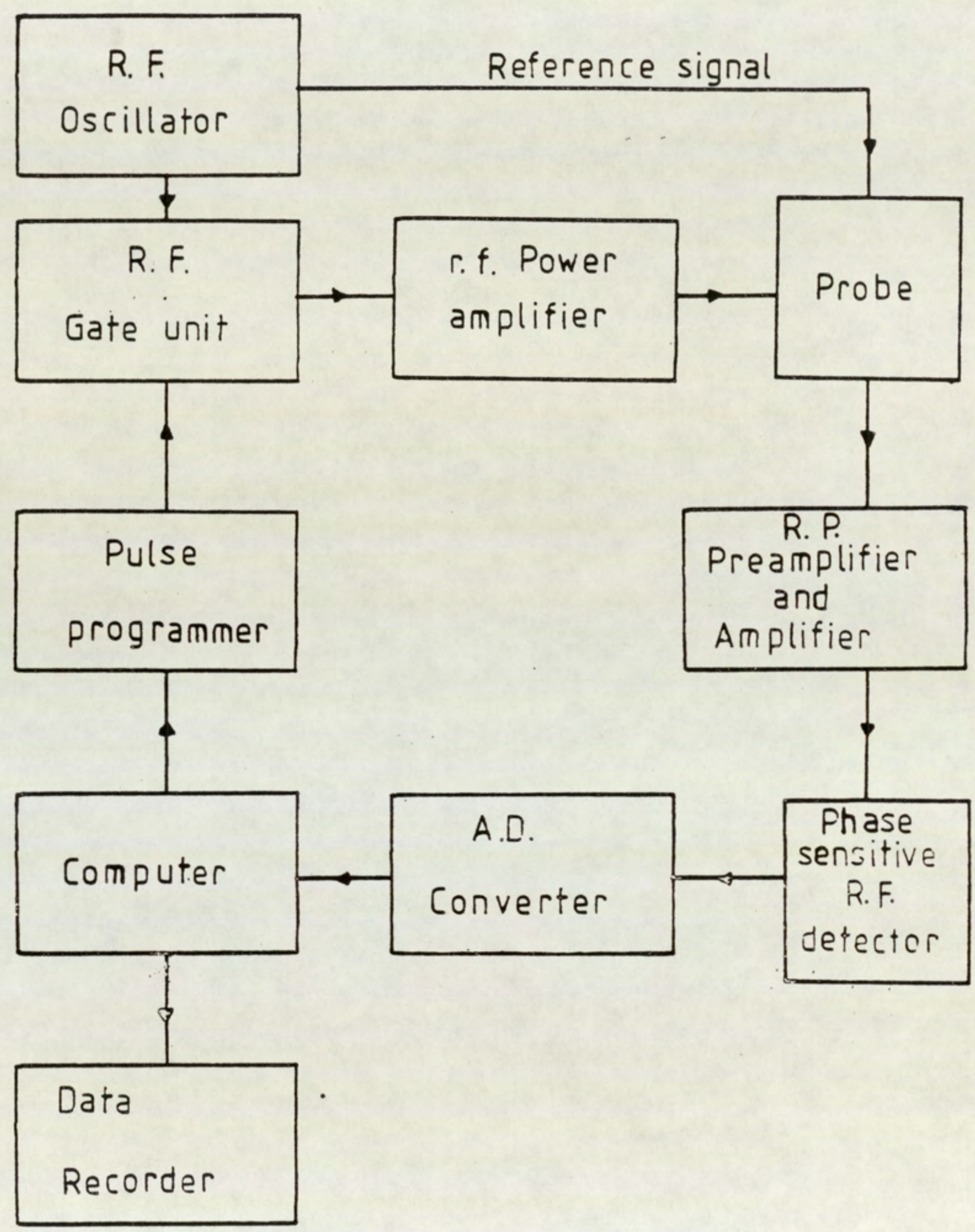

Figure 2.4: Basic components of FT NMR spectrometer

2.5.2.3 The RF Power Amplifier

The magnitude of the rf magnetic field B_1 used with FT spectrometers has to be high in order to ensure sufficiently uniform distribution of rf power across the spectrum.

The rf power required for pulse spectroscopy is higher than that needed for CW NMR spectroscopy; typically 100 watts is needed for FT NMR compared with 1 watt for a CW instrument. After the pulse less than 10^{-9} of the output power is radiated, so that the interferegram can be obtained by the receiver without perturbation.

2.5.2.4 The Probe

Beside the requirements for the probe used in the CW spectrometer, the FT technique necessitates that the probe has the following characteristics:

1 It must be able to handle the large rf voltage present while the pulse is on.

2 It must recover rapidly from the powerful pulse.

3 It should quickly receive and process the weak nuclear signals following the pulse.

4 In addition, in some cases, it must continuously deliver noise modulated or coherent decoupling power to the sample at the second rf frequency without interfering with the processing of the FID signal.

5 It must have facilities for essentially locking the magnetic field strength to the pulsed NMR frequency. This is usually achieved using a separate CW rf signal that enables locking to a heteronucleus.

6 The probe should have spinning facilities and a temperature detector necessary for conducting variable temperature studies.

2.5.2.5 The Receiver

The main two characteristics of the receiver within a FT spectrometer are; first, that it should recover very quickly from any overloads generated by the application of the rf pulse. Second, the receiver and the transmitter should be well isolated from one another in order to achieve minimum overload conditions and the fastest recovery time(48).

The receiver follows a preamplifier. The preamplifier should have a low noise figure, a fast recovery time from overloads and a modest gain. Both preamplifier and receiver should have linear response over a wide range(49).

The nuclear signal enters the receiver (rf detector) as a band of radiofrequencies near the basic transmitter frequency, during the free precession period after the pulse. Passing the signal through a phase detector results in a series of audiofrequencies which are filtered by being fed through a low pass filter with a band width usually just equal to the chosen spectral width. The rf carrier has to be positioned so that all the audio frequencies have the same sign, because the signal phase detection does not allow distinction between positive and negative frequencies. If the rf carrier is placed at the end of the spectrum and the set spectral width is larger than the chemical shift range, the frequencies can be digitized unambiguously. However, if the spectral width is set to a value smaller than the chemical shift range, some of the frequencies corresponding to lines at one end of the spectrum can be folded. This effect is avoided by using an experimental technique called quadrature detection. This employs two phase sensitive detectors to distinguish between high and low field frequencies; for this the rf carrier frequency is usually placed in the middle of the spectrum.

2.5.2.6 The Analogue to Digital Converter (ADC)

The detected FID is an analogue signal and because this has to be stored and processed by the spectrometer computer, it is necessary to digitalize the signal. An analogue to digital converter is used for this purpose. This analogue to digital converter samples the free induction decay at regular time intervals and converts each voltage measured to a binary number that can be stored in the corresponding memory location of the computer.

The rate at which a spectrum of width ΔF must be collected by the ADC is twice the spectral width, $2\Delta F$. In order to avoid line shape distortions, the FID should be sampled until its amplitude has fallen off to zero. As long as the signal is sampled over a period of time T seconds, this defines a total of $2\Delta FT$ sampling points. Since each point is stored, a memory of N words is needed ($N = 2\Delta FT$) where T is the acquisition time and is related to the digital resolution of the instrument.

The dynamic range of the signals that are to be digitized is a critical parameter when weak signals have to be detected in the presence of strong signals. When the interferogram is displayed on the screen of the oscilloscope, the minicomputer represents the maximum peak to peak amplitude by a number usually close to 2^{12}. Then if the largest signal detected has the intensity H_s, the smallest signal which can be recorded will have an intensity, H_w such that:

$$\frac{H_s}{H_w} = 2^{12}$$

This ratio is called the dynamic range of spectrum.

For an ADC of 12 bytes 'the signal' is normally measured in steps of $10/(2^{12}-1) = 2.44$ mV, if the voltage range is $\pm$ 10 volts. This means that all signals which correspond to a potential lower than 2.44 mV will not be read by the converter.

2.5.2.7 <u>The Computer</u>

The mathematical requirements of FT NMR necessitate the use of a computer. The computer is generally used for three types of mathematical manipulations of the data:

1 Data acquisition and coherent addition of repeated signals to improve the signal to noise ratio.

2 To carry out the Fourier transformation.

3 During the whole process between the above mentioned steps, or after them many other types of data processing have to be carried out by the computer, eg. setting of frequencies, display conditions etc.

A computer usually consists of input and output units, control, storage and arithmetic units. It controls the transmitter and receiver functions, stores and processes the FID and transfers the results to display units viz oscilloscope or the recorder. The minicomputer is characterized by two essential parameters that define its storage capacity. These are the number of memory location and the word length. Memory locations are counted in multiples of K; which stands for $2^{10} = 1024$.

According to the requirements of FT spectrometers, a computer with 12K memory is the minimum requirement for pulsed NMR. The word length determines the amount of data or their magnitude that can be stored in each memory location. The information is stored in binary form. In general, for n bytes the largest possible decimal number that can be represented is 2^{n-1}. Therefore, it is very important to have large values of n, eg. n=12 in order to detect small signals.

When collecting the FID, each pulse has the same characteristics. Any change in the field homogeneity will cause observed peak shapes to change on different passes, damaging the final spectrum. This problem can be overcome by the computer. In one approach, the height of an absorption peak of the reference compound (lock signal) is monitored. With field homogeneity optimized, the peaks show a maximum height. Any change from the optimal condition is detected. The error signal is then used to control the shim current and return the field to the optimum value.

2.5.3 The JEOL FX 90Q FT NMR Spectrometer

A JEOL FX 90Q FT NMR spectrometer was one of the instruments used in carrying out the work reported in this thesis. The spectrometer can be used to detect all NMR active nuclei in five different ranges of frequencies[50]. This pulsed FT NMR spectrometer permits the observation of proton resonance at a frequency of 89.6 MHz and ^{13}C at 22.5 MHz.

The instrument uses a tunable 10 mm probe that is optimized for the observation of ^{13}C resonances for which the instrument specifications are quoted. When studying ^{1}H, the performance is not guaranteed unless a dedicated ^{13}C-^{1}H probe is employed. This was not available for the present work.

This system has unique facilities in the form of, digital quadrature detection (DQD), light pen control system (LPCS) and autostacking software. Also the system has a computer having a memory of 24K words where 8K words are used for the program and 16K words for the data.

Figure 2.5 shows the basic units in the FX 90Q spectrometer. The specific components will be discussed now.

2.5.3.1 The Magnet System

The instrument is provided with an electromagnet, fed by a voltage and current regulated power supply system, that produces a magnetic field of 2.11 Telsa.

The magnet is accommodated in a compact console to help maintain it at constant temperature. The magnetic field homogeneity is controlled conventionally using Golay shim coils mounted on the probe between the pole pieces. The instrument is capable of producing a ^{13}C line width of less than 0.3 Hz. In the long term this may degrade and result in line broadening, although the magnetic field stability is 0.1 Hz per hour. This degradation may be corrected particularly by using an autoshim unit which corrects small field drifts in the y-direction.

It should be noted that during the early stages of this work, significant problems were encountered with maintaining resolution over a period of time exceeding 30 minutes. This was particularly evident when conducting ^{1}H studies. The fault was finally attributed to very low lock loop gain which resulted in superimposition of shifted spectra that appeared to result in poor resolution. Considerable time was spent by the manufacturers in improving the "resolution". In fact, the magnet was replaced by the manufacturers. However no significant improvement was achieved. Ultimately they improved the lock loop and the "resolution" was satisfactory. Consequently the experimental work presented herewith was subject to appreciable delay.

2.5.3.2 <u>The Probe</u>

The probe placed between the pole pieces of the magnet, has several modules:

1 The permabody which is fixed. It accommodates replacable modules, eg. the insert, which are housed in a double wall dewar for variable temperature experiments. On the permabody probe, irradiation coils and thermocouples are mounted. Spinning photosenser facilities are placed on the top to detect the spinning rate. Current shim boards are attached on both sides of the perma-body.

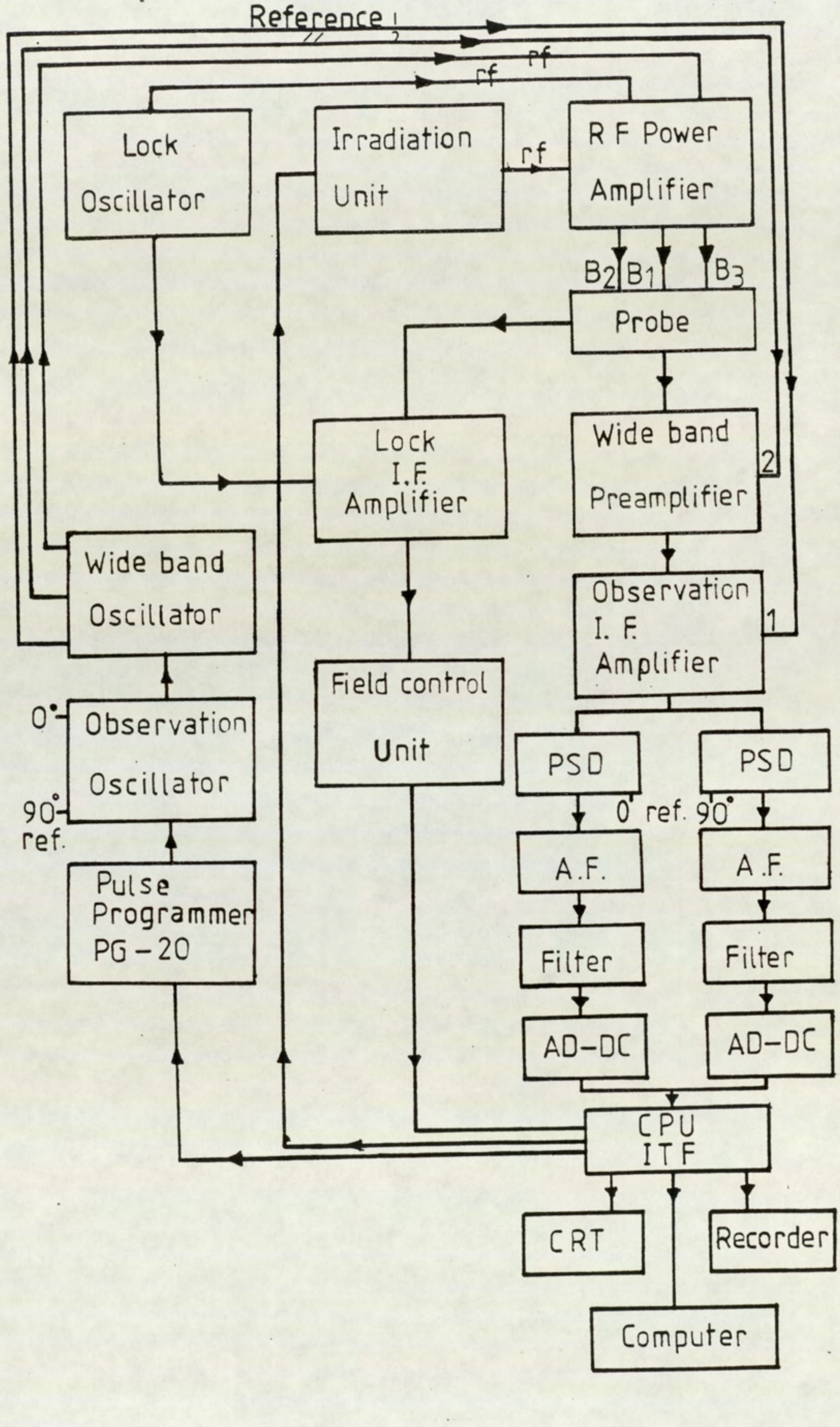

Figure 2.5: Schematic representation of the basic units in the JEOL FX 90 Q spectrometer

2 The rf tunable module which facilitates the selection of the nuclei. It has five ranges of frequencies, corresponding to five channels, and a fine tuner for optimizing the sensitivity for a given nucleus.

3 The irradiation module which enables the tuning of the irradiation circuit to use most of the energy in the irradiation coil and produce the maximum usable rf field.

4 The sample insert which is exchangable for different sample tube sizes and holds the sample coil and LOCK coil wound around the glass tube.

2.5.3.3 Transmitter, Receiver and Data System

The transmitter system has three channels which are based on the observation, irradiation and lock oscillator units which have a reference frequency of 44 MHz supplied by a master clock unit. The observation oscillator has a 4-phase generator which is used to generate the offset components of the radio frequency irradiation (OBS RF) output. A PG20 pulse programer operates the gates of the oscillator, generating the desired RF pulse sequence up to 2 pulses only. Two intermediate frequency (IF) reference signals that are out of phase are passed to the intermediate frequency observation (OBSIF) amplifier unit to be used in the Digital Quadrature detection (DQD) system. The signal frequency is then adjusted for the selected nucleus at the wide band local oscillator unit. Then the RF is amplified in the RF power amplifier unit. When the RF signal reaches the probe, the sample absorbs most of the energy generated at the transmitter coil.

The FID occurring after the RF pulse, is detected by the receiver coil and amplified in a wideband pre amplified unit, where a reference signal from the wideband local oscillator unit is used to reduce the signal level when they are mixed. Another amplification and frequency reduction occurs at the OBSIF amplifier where further 0 and $\pi/2$ reference signals from the OBS OSC unit are used to get the audiofrequencies 0 and $\pi/2$ out of phase. It is obvious now that the detection system has two phase sensitive detectors (PSD) rather than one; these are required in the digital quadrature detection DQD technique.

The DQD system allows the FT measurements to be carried out with the excitation pulse placed in the centre of the observation width. This reduces the observation band width to only half that required for single phase detection (SPD) resulting in $\sqrt{2}$ fold improvement in the signal to noise ratio. Consequently, as long as the rf pulse is delivered at the centre of the spectrum, the efficiency of the rf power is enhanced 4 times compared with the SPD, and this helps to obtain more accurate information.

The AD-DA Unit receives filtered analogue signals which are converted to digital form. They are then transferred to get the spectrum signal in digital form. The DA Unit changes the information to analogue signals which can be recorded or displayed on the oscilloscope screen.

The operator can deal with the FX 90Q instrument and the computer using a light pen unit. By pointing to a particular function or command on the screen, the order is transferred to establish a link between the computer and the spectrometer units controlling its operations.

2.5.3.4 Autostacking Program

The JEC-980B computer in the JEOL FX90Q spectrometer has a memory of 24K words. The program is stored in 8K words memory, the other 16K words of memory are used for the data. The different operations that can be done by the computer are stored in the autostacking program.

The autostacking program contains the following programs:

1 Normal program

2 Stacking program

3 Analysis program

Throughout the work reported in this thesis, the normal program was used to obtain results for liquid samples. The stacking program was used to obtain results for some of the gas samples.

2.5.3.5 The Locking System

The lock in the FX 90Q spectrometer can be obtained as in any CW spectrometer. The lock oscillator unit produces an rf signal at the appropriate resonance frequency which is amplified in the rf power amplifier. A field control unit produces a sawtooth signal which modulates the magnetic field and allows the observation of the lock resonance signal. This signal is phase sensitive detected at the LOCK IF amplifier unit, which receives a reference signal from the LOCK OSC unit. Besides being used for lock, the signal is also used for rapid resolution adjustments: ^{2}D and ^{7}Li can be used for locking purposes and are selected by simple switching.

For double irradiation purposes the rf irradiation oscillator units can be selected according to the experiment and allow noise and coherent rf irradiation. For both cases the irradiation rf is amplified, but at different levels that are controlled by the irradiation selector unit which is linked to the rf power amplifier.

The noise irradiation modulation width can be selected to be 0.5, 1, 2.5 and 5 KHz. For ^{13}C detection, an irradiation of 1 KHz is used normally for proton irradiation.

CHAPTER THREE

THE VAN DER WAALS SCREENING CONSTANT σ_W

3.1 Introduction

Characterisation of the van der Waals screening constant σ_w is the main aim of the present work reported in this thesis. Quite a few intermolecular phenomena may contribute to solvent shifts, but there is always the ubiquitous van der Waals effect σ_w. Contrary to such other effects as neighbour anisotropy, σ_a, the reaction field contribution σ_{RF}, or the complexation effect, σ_s, no major direct use has yet been found for the van der Waals screening or shift. So far the role of the van der Waals effect has been that of a disturbing phenomenon, something to be eliminated at all costs. But it is precisely in this latter respect where almost all solvent effect studies fall short. Not only is σ_w usually large (larger than σ_a and σ_E even in ^1H NMR and probably the dominating term with heavier nuclei), but it is strongly variable from one solute to another and even one nuclear site to another in the same molecule.

There appears to be only one possibility left and that is to develop models to calculate σ_w in any given circumstances. In the past twenty years models, each with many more refinements, have been proposed; yet the picture is far from complete. It has turned out that many physical and molecular parameters must be considered before a quantitative understanding may be expected.

Recently Homer and Percival(39) have developed a new reaction field treatment of gas-to-liquid shifts for isotropic molecules, ie. of σ_w. Their theory has three component parts. The first is based on an improved Onsager approach. The second part recognizes the deficiencies in the Onsager model that stem from ignoring the effect of near neighbour molecules. The third is a newly characterized "buffeting" contribution that arises only when solvent approaches to a solute resonant nucleus are sterically hindered. The major emphasis of the present work is to find direct experimental justification of the second and third contributions and use these to permit the elucidation of molecular structure through studies in the liquid phase.

Before detailing the results of the present investigations it is important to review the work which has been already done in characterizing the van der Waals screening constant.

3.2 Models characterizing σ_W

Essentially, three models have been proposed to characterize σ_W viz:

1 The gas phase model
2 The cage model
3 The continuum model

3.2.1 The Gas Phase Model

The gas theory[32,51] basically depends on the characterization of bimolecular interactions and the calculation of two centre potential energies. While it is tempting to extend this approach to liquids, it is unrealistic to consider that such a basis could be applicable to the liquid phase, because of the relatively small molecular separations involved and the fact that there must be simultaneous interactions between several molecules. Obviously multimolecular interactions would have to be considered. From an energetic point of view, this could be done by considering these as an average sum of several nonequivalent bimolecular interactions. Nevertheless, the potential difficulties with such an approach suggest that it would be unprofitable.

3.2.2 The Cage Model

This model(52) considers only the first solvent shell around a given solute molecule. The average effect of one solvent molecule on the nuclear screening of the solute has to be characterized and summed over a number of solvent molecules around the solute molecule in the first shell. Again it is possible to anticipate difficulties with this approach although some workers, eg. Homer and Redhead(53) have achieved some success with it when calculating σ_a.

Both the Gas Phase and Cage models were developed significantly by Rummens(51) but they undoubtedly underestimate the extensive properties of the solvent molecules in the bulk liquid.

3.2.3 The Continuum Model

The Continuum model(52,54) treats the solute molecule as being a single point species at the centre of a cavity surrounded by a continuum representing the solvent. This approach seems to afford a better representation of the liquid phase than the two models previously described, although it is demonstrably inadequate in accounting for σ_w.

Homer and Percival have used it as the basis for the most recent attempt to characterize physical properties of matter that depend entirely on inter-molecular van der Waals forces.

3.3 Application of the Continuum Model to σ_w

Its development and extension

Following Onsager[52], any treatment of σ_w on a continuum basis requires that one solute molecule is singled out and treated as being a point species at the centre of a cavity surrounded by a homogeneous continuum representing the solvent medium. In his work on electric dipole moments of molecules in liquids, Onsager specifically treated polar molecules but implied that there should be no real difference between this approach and that of non-polar molecules; the approach should therefore be suitable for the characterization of van der Waals forces. Following Onsager many workers have attempted to characterize σ_w on a continuum basis[32,55,56,57], eg. Howard and Linder, used the generally accepted equation for σ_w:

$$\sigma_w = - B < R_1{}^2 > \qquad ..... \; 3.1$$

where $< R_1{}^2 >$ is the mean square reaction field in the solute cavity and B is the screening coefficient. Other workers[58,59], eg. Lumbroso and Fontaine, have used the continuum theory to correct observed shifts in polar systems and obtain information about linear electric field effects on nuclear screening.

Equation 3.1 provides a test of the validity of different equations proposed for $< R_1{}^2 >$ that is necessary for calculating σ_w. A plot of gas-to-solution chemical shifts against $< R_1{}^2 >$ (which may generally be defined in terms of refractive indices as f $(n_1 \, n_2)$ should produce a straight line passing through the origin. Indeed the general trend of plots of this type produced by many workers do show a straight line regression with slopes generally similar to expected values of B but they do not pass through the origin[27]. This indicates that the formulae used for calculating $<R_1^2>$ are not correct, or there could be a term missing from equation (3.1) that would account for the y-intercepts.

The most consistent explanation of the variation of σ_w for a given solute with solvent properties was published by de Montgolfier[60,61,62,63]. He concluded that σ_w can be characterized by the following equation:

$$\sigma_w = -6 \left[\frac{(n_2^2 - 1)}{(2n_2^2 + 1)(n_2^2 + 1)}\right]_{\text{solution}} \left[\frac{K_1 \, B \, \Delta E_1}{\alpha_1}\right]_{\text{solute}} \qquad \text{..... 3.2}$$

where n_2 is the refractive index of the solvent, ΔE_1 is a complex transition energy of the solute molecule, α_1 is the mean polarizibility of the solute molecule, and K_1 is a site factor dependent on the geometry of the solute molecule.

De Montgolfier's theory was reconsidered by Rummens[64,65,66,67], who rejected the site factor K_1 as having no place in the continuum model. Nevertheless, Rummens later reintroduced another site factor and formulated the following quite widely accepted equation:

$$\sigma_w = \frac{-6 \, K_1 \, B \, \alpha_1 \, I_1}{a_1^6} \cdot \frac{n_2^2 - 1}{(2 \, n_2^2 + 1)^2} \cdot S \qquad \text{..... 3.3}$$

where S is the Rummens site factor that he introduced to account for the intercept found in the regression of σ_w against f (n_1, n_2), I_1 is the ionization energy of the solute molecules, a_1 is the solute cavity radius and K_1 is the reaction field solute factor constant.

Rummens took the correctly defined site factor for a pair of molecules in the gas phase, S pair[68,69] and transposed this to the liquid phase. The site factor for a pair of molecules is given by:

$$S_{pair} = \frac{1 + q^2}{(1 - q^2)\, 4} \qquad \text{..... 3.4}$$

where q = d/r, with d being the distance of the resonant nucleus from the centre of mass of the solute and solvent molecules.

Rummens derivation of his site factor has been criticized by Homer and Percival[39] who also demonstrated that it did not improve the regression of σ_w on $f(n_1, n_2)$, ie. an intercept remained. They have attempted to reformulate the site factor, which they nevertheless think as irrelevant:

$$S_{cont} = \frac{5}{6}\left[\frac{1 + q^2}{(1 - q^2)^3} + \frac{3 - 2\,q^2}{3\,q^4\,(1 - q^2)}\right] + \frac{5}{8\,q^5}\ \text{In}\left[\frac{1 - q}{1 + q}\right] \qquad \text{..... 3.5}$$

They demonstrated that the improved site factor was unable to complete the characterization of σ_w; However, Homer's site factor did improve the correlation of σ_w against $f\,(n_1\ n_2)$ as shown in table (3.1) for group IV B tetramethyl systems. This correlation still gives a straight line with finite intercept.

Before formulating this site factor, Homer[27] had concluded, from the literature and his own extensive work concerning chemical shifts due to intermolecular interactions, that there are major inadequacies in calculating σ_w. In a major review he noted:

"Superficially, it appears that little more than qualitative agreement between predicted and observed shifts is obtained. Indeed the general trend in the plots (of calculated parameters against the appropriate gas-to-solution shifts together with a theoretical line of slope B = 1 x 10^{-18} esu) away from the origin might be taken to indicate shortcoming in the general approach".

Homer has suggested that the reason for the inadequacies in existing theories might lie with facts alluded to by Buckingham:

"... dispersion screenings, because these may be considered to arise from two separate effects. The first effect is due to the interaction between the solute and solvent, in its equilibrium configuration, which causes the distortion of the electronic environment of the nucleus in the solute. The second is due to changes in the solvent equilibrium configuration, which leads to a "buffeting" of the solute and hence to a time dependent distortion of the electronic structure".

Essentially, this was the basis for Homer's recent theory for characterizing σ_w. This will be considered within the following sections.

Table 3.1 - Regression analysis of $-\sigma_w$ (expt) at 30°C and $(n_2^2 - 1)^2/(2n_2^2 - 1)^2$ for the group IV B Tetramethyl systems

Solute	Correlation coefficient	Intercept/PPM
CMe_4	0.885	0.100
Si Me_4	0.923	0.135
Ge Me_4	0.918	0.134
Sn Me_4	0.930	0.148
Pb Me_4	0.936	0.152

3.4 Homer's Theory for Characterizing σ_w

Homer's intention was to complete the characterization of the van der Waal's screening constant, which he saw to arise mainly from two sources. The first stems from interactions between solute and solvent molecules in their equilibrium situation. In order to deal with this, Onsager based reaction field theory was improved and extended which led to a term $\langle R_2^2 \rangle$ in addition to $\langle R_1^2 \rangle$. Even so, the results of this approach did not show complete characterization of σ_w and this led to the recognition of a second part. The second contribution comes from solvent-solute interactions in their non-equilibrium (continuum) situation. This was considered to arise from the unique effects of discrete pair-wise solvent-solute encounters. Homer characterized this by a buffeting interaction between the resonant nucleus in the solute molecule and the peripheral atoms of the solvent molecule.

Because van der Waals dispersion forces are additive, Homer has defined σ_w by:

$$\sigma_w = \sigma_{RF} + \sigma_{BI} \qquad \text{..... 3.6}$$

where σ_{RF} and σ_{BI} are the contributions to the screening, due to the reaction field and buffeting respectively.

3.4.1 Improvement and Extension of Reaction Field Theory

As Onsager's model and its previous improvements appeared to be inadequate, Homer and Percival's initial work was to extend the continuum approach. They considered the reaction field for transient dipoles in isotropic systems to be made up of two parts. The first is the classical reaction field or the primary reaction field that has been recognised before. The second arises from a further field stemming from the extra cavity reaction field of the nearest neighbour solvent molecules. Both parts were dealt with on a continuum basis. Therefore, the total mean square reaction field $\langle R_T^2 \rangle$ experienced by the solute molecule in a solvent will come from the sum of the primary reaction contribution and the contribution of the extra cavity fields arising from the solvent molecules surrouding the solute.

The following sections will describe the two parts of $\langle R_T^2 \rangle$.

3.4.1.1 The Primary Reaction Field R_1

The basic equation for calculating R_1 using Onsager's model (Figure 3.1) is represented by(52):

$$R_1 = \frac{2\,(\varepsilon_2 - \varepsilon_1)}{2\,(\varepsilon_2 + \varepsilon_1)} \quad \frac{\mu_1}{a_1\,3} \qquad \text{..... 3.7}$$

where ε_1 and ε_2 are the dielectric constants of the solute and the solvent molecules respectively, μ_1 is the dipole moment of the solute and a_1 is the radius of the Onsager cavity. The cavity in Onsager's model, was treated as being evacuated, so that $\varepsilon_1 = 1$ and equation 3.7 for R_1 becomes:

$$R_1 = \frac{2(\varepsilon_2 - 1)}{2(\varepsilon_2 + 1)} \quad \frac{\mu}{a_1^3} \qquad \text{..... 3.8}$$

where

$$g = \frac{2(\varepsilon_2 - 1)}{2(\varepsilon_2 + 1) \quad a_1^3} \qquad \text{..... 3.9}$$

g is the reaction field factor.

Therefore, $R_1 = g\mu$ 3.10

This reaction field, originating from the dipole moment μ, will induce further electric moments in the cavity that are proportional to the primary reaction field. Therefore, a true reaction field must be given by[70]:

$$R_1 = g\mu\,(1 - \alpha_1\, g)^{-1} \qquad \text{..... 3.11}$$

where α_1 is the solute molecule polarizability. It was assumed that, although the above equation is strictly for a permanent dipole moment, it applied also to transient dipole moments; This has been subsequently proved theoretically by Mohammadi[71].

Since σ_w is related to the mean square reaction field $< R_1{}^2 >$, the latter was given by:

$$<R_1{}^2> = g^2\,(1 - \alpha_1\, g)^{-2} <\mu^2> \qquad \text{..... 3.12}$$

By substituting for g in the above equation and following the approximation that $\varepsilon_2 = n^2{}_2$ for isotropic solvents, and employing the expression[52]:

$$\frac{n_1{}^2 - 1}{n_1{}^2 + 2} = \frac{\alpha}{a_1^3} \qquad \text{..... 3.13}$$

the mean square reaction field of a polarizable dipole was shown to given by:

$$\langle R_1^2 \rangle = \left[\frac{8 \pi L}{9 V_m} \right]^2 \frac{(n_1^2 + 2) \ (n_2^2 - 1)^2}{(2 n_1^2 + n_1^2)^2} \langle \mu_1^2 \rangle \qquad ..... \ 3.14$$

where L is Avogadro's Number and V_m is the molar volume of the solute.

The derivation of that equation is necessarily based on an oversimplified model because in reality a molecule is not a point as assumed, and there is no such thing as a microscopically indivisible continuum; also no account was taken of fields produced by higher electric moments of the solute molecule.

Homer demonstrated that equation 3.14 did not account completely for the reaction field and this led him to recognize the so called extra cavity reaction field.

3.4.1.2 <u>The Extra Cavity, Secondary Reaction Field of the Solvent R_2</u>

Homer and Percival[70] treated the nearest neighbour solvent molecules by accounting for the effect of their reaction fields, (recognized as R_2). With R_1, this makes up the total reaction field effecting the solute molecule in Onsager's cavity.

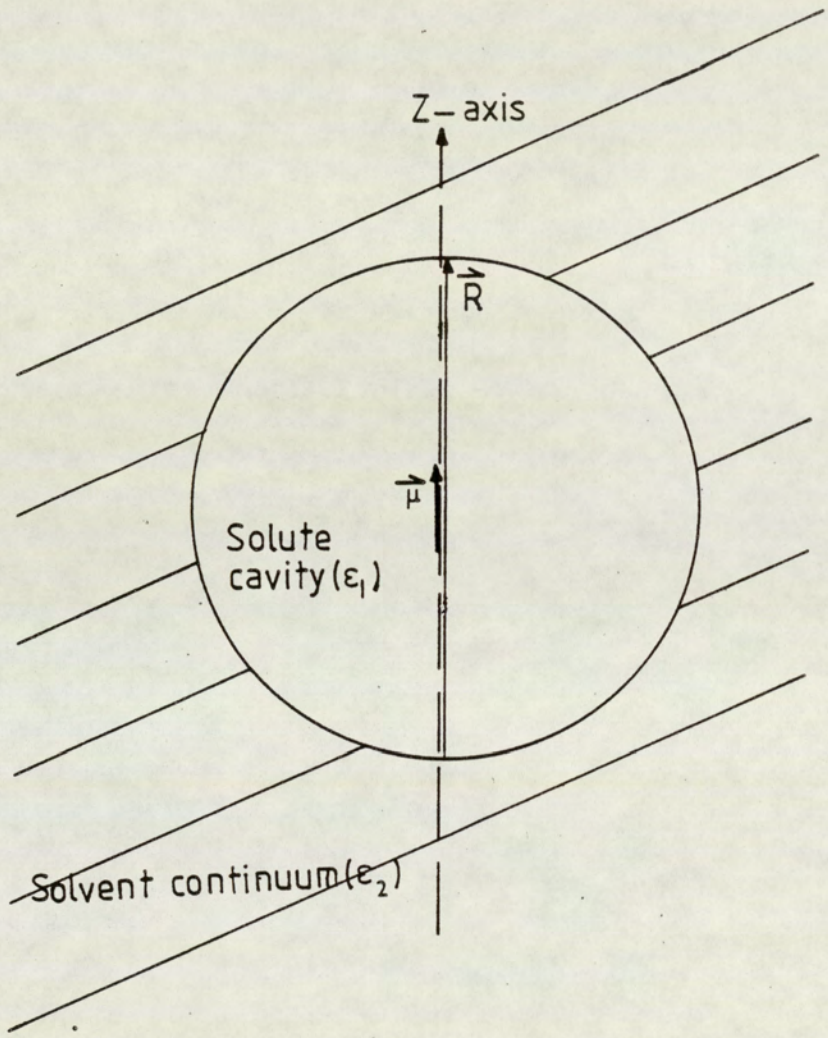

Figure 3.1: A representation of a solute cavity in the solvent continuum (Onsager type treatment)

The primary reaction field R_1 produces a uniform polarization of the cavity through the potential arising from the charge distribution on the cavity wall. The reaction field is continuous in the solvent medium, but its effect decreases rapidly with the separation from the cavity centre.

Homer and Percival's method for calculating $\langle R_2^2 \rangle$ depends on considering two cavities 1 and 2 (Figure 3.2) in the continuum. When the two cavities are well separated from each other, R_1 does not effect cavity 2 and R_2 does not effect cavity 1. However when the two cavities are close to each other, the reaction field of each molecule will effect the other one.

In the case of a (solute 1) at infinite dilution in solvent 2, the central solute molecule 1 will always be surrounded by solvent molecules 2. Consequently, the solute molecule will experience the reaction field arising from its own transient dipole, and additionally the sum of the extra cavity reaction fields due to the surrounding solvent molecules.

It was assumed that the number of the solvent molecules that can surround the solute molecules is Z_2, and the number of molecules that may surround the solvent molecules is Z_1.

Homer has shown that the additional secondary mean square field experienced by atoms at the periphery of the solute molecule is $2\,(Z_2/Z_1)\,\langle R_2^2 \rangle$.

The total mean square reaction field experienced by a solute molecule (really nuclei at the peripheries) is thus:

$$\langle R_T^2 \rangle = \langle R_1^2 \rangle + 2 \left(\frac{Z_2}{Z_1}\right) \langle R_2^2 \rangle \qquad \text{..... 3.15}$$

using the formula for the close packing of sphere, Z can be presented by:

$$Z_1 = \frac{(r_1 + r_2)^2}{r_1^2} \pi \qquad \text{..... 3.16}$$

where r_1 and r_2 are the radii of the solute and the solvent molecules, respectively. Consequently, equation 3.15 can be rewritten as:

$$\langle R_T^2 \rangle = \langle R_1^2 \rangle + 2 \left[\frac{r_1}{r_2} \right]^2 \langle R_2^2 \rangle \qquad \text{..... 3.17}$$

$\langle R^2{}_2 \rangle$ was formulated by an approach analogous to that for $\langle R_1^2 \rangle$. The final equation for the total mean square reaction field is:

$$\langle R_T^2 \rangle = \left[\frac{8\pi}{9} \right]^2 \frac{\mu_1}{V_1^2} \frac{(n_1^2 + 2)^2 (n_2^2 - 1)^2}{(2n_2^2 + n_1^2)^2} + 2 \left(\frac{r_1}{r_2}\right)^2 \times$$

$$\frac{\mu_2^2}{V_2^2} \frac{(n_2^2 + 2)^2 (n_2^2 - 1)^2}{9n_2^4} \qquad \text{..... 3.18}$$

Based on London's[72,73] treatment of a quantum mechanical oscillator, the required dipole moments can be expressed as:

$$\mu = 3 \alpha I/2 \qquad \text{..... 3.19}$$

where α is the polarizability of the appropriate molecule and I is the ionization potential.

The reaction field contribution to the nuclear screening constant σ_{RF} can now be expressed as:

$$\sigma_{RF} = -B \langle R_T^2 \rangle \qquad ..... \ 3.20$$

where B is the nuclear screening coefficient which depends on the nature of the nucleus and the chemical bonds to it.

Homer and Percival tested the validity of equation (3.18) by correlating the gas-to-solution chemical shifts for protons in the group IV B tetramethyls (as solute and solvent) against the calculated $\langle R^2{}_T \rangle$ for each system. The regressions were linear with correlation coefficients close to unity and slopes in good agreement with the theoretical value of B (Table 3.2). However, it can be seen from Table 3.2 that all the straight lines did not pass through the origin. This indicates that equation 3.18 presents an incomplete description of van der Waals forces effecting the molecules. This fact led Homer to recognize his buffeting theory which will be dealt with in the following section.

3.4.2 Buffeting Theory

Homer and Percival[(70)] characterized and recognized the buffeting interaction between the solute and the solvent molecules as analogous to the non-equilibrium situation first mentioned by Buckingham. The buffeting interaction was considered on the basis of a perturbation of the periphery of the solvent molecule. This was treated on the basis of pair-wise encounters. The reference for such encounters was a right hand triple taking the solute resonant nucleus at the origin with its bond to the other atom in the molecule colinear with a z-axis (Figure 3.3).

The electric field E produced at the solute atom containing the resonant nucleus of interest by a moment m in a solvent peripheral atom and separated from the solute nucleus by distance r, is given by[(74)]:

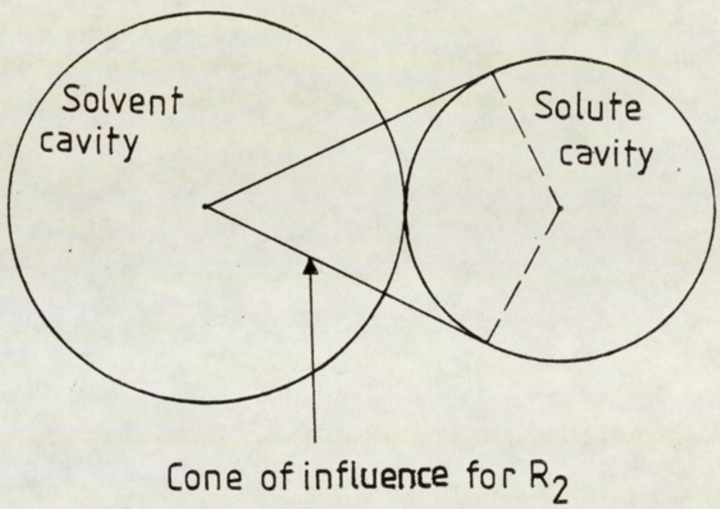

Figure 3.2: Cone of influence for R_2 with solute and solvent cavities in contact

$$\vec{E} = 3\,(\vec{m}\,.\,\vec{r})\,\frac{\vec{r}}{r^5} - \frac{\vec{m}}{r^3} \qquad ..... \; 3.21$$

Assuming that there is no restriction on the approach of the solvent molecule to the solute atom, the time average of the electric field over all space will be zero. However, the mean square value may still be finite. Therefore Homer evaluated the square of the instantaneous electric field at the resonant nucleus. This instantaneous value of the time average electric field was deduced by considering the situation in one octant about the solute's resonating nucleus. On time average the appropriate solvent atom can be considered to lie on an axis at an angle of 54° 44' ($\cos^{-1} 1/\sqrt{3}$) to each of the three co-ordinate axes based on the solute nucleus. The solvent moment $\vec{m}$ was characterized by considering the solvent electron moment in one octant about the solute atom.

Table 3.2 - Linear regression of $-\sigma_w$ (expt) at 30°C on $<R^2_T>$ for the Group IV B Tetramethyl systems

Solute	Correlation Coefficient	Gradient = 10^{18} B/esu	Intercept /ppm
C Me_4	0.933	0.81	0.128
Si Me_4	0.953	0.87	0.169
Ge Me_4	0.950	0.87	0.170
Sn Me_4	0.960	0.92	0.185
Pb Me_4	0.966	0.88	0.190

* Solute at infinite dilution in all five groups IV B Tetramethyls as solvents

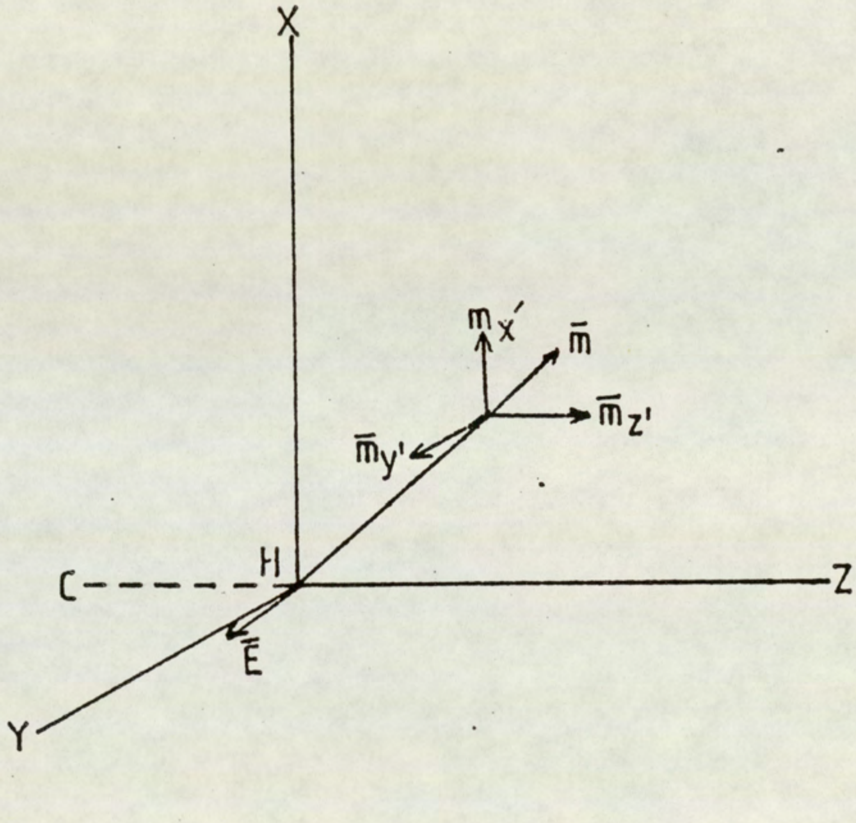

Figure 3.3: Space averaged situation of a solvent molecule average electric moment

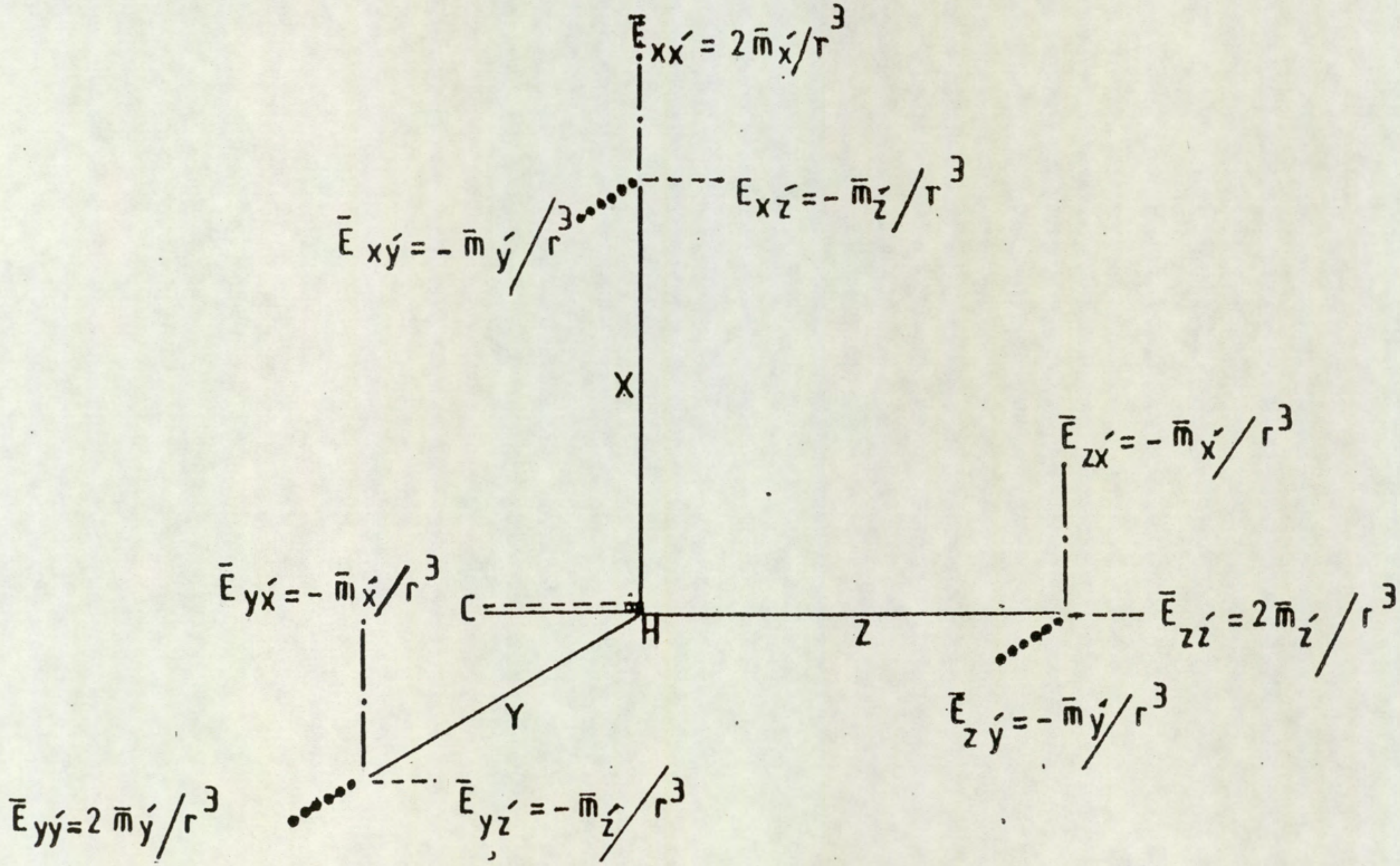

Figure 3.4: Time average electric fields with respect to directions parallel and perpendicular to the axis of the C-H bond

The electric fields at the solute resonant nucleus that are parallel and perpendicular to the bond containing the resonant nucleus are given by:

$$E_x = \frac{2\,m_x'}{r^3} - \frac{m_y'}{r^3} - \frac{m_z'}{r^3} \qquad \text{..... 3.22}$$

$$E_y = \frac{2\,m_y'}{r^3} - \frac{m_x'}{r^3} - \frac{m_z'}{r^3} \qquad \text{..... 3.23}$$

$$E_z = \frac{2\,m_z'}{r^3} - \frac{m_x'}{r^3} - \frac{m_y'}{r^3} \qquad \text{..... 3.24}$$

which is illustrated in Figure 3.4. It was accepted that because the accessibility of the solvent atom to the solute resonant nucleus is anisotropic, E_z, E_y and E_x are modulated by weighting factors which are considered to be a measure of the anisotropy of relative approach, accessibility or steric hinderance of the solvent molecule to the solute resonant nucleus. Solute-solvent encounters parallel to the bond are restricted by $0 \leq \beta \leq 1$, and those perpendicular to the bond are characterized by $0 \leq \alpha \leq 1$ and $0 \leq \alpha' \leq 1$. It is assumed also, for the axially symmetric bond around the z-axis (as in the case of C-H or C-F bonds) that $\alpha = \alpha'$ and $2\alpha = \varepsilon$. By taking the sum over four octants the final derivation of the mean square dispersion field was given by the simplified equation:

$$\langle E^2 \rangle = \frac{K}{r^6} (2\beta - \xi) \qquad \text{..... 3.25}$$

where K is a constant depending on the electron displacement around the peripheral solvent atom.

It follows that the contribution of the buffeting interaction to the nuclear screening constant is characterized by:

$$\sigma_{BI} = \frac{-BK}{r^6}(2\beta - \xi)^2 \qquad ..... 3.26$$

where γ is the interatomic distance between the resonant nucleus and the centre of the atom on the periphery of the solvent molecule (taken as the sum of van der Waals radii of the atoms considered), β and ξ describe the total effective accessibility of a solute atom to the solvent atom as a result of pair-wise encounters. They are based on a geometrical accessibility where the encountering species are rigid and passive (measurement of these parameters will be described in detail in Chapter 4).

The above discourse merely summarizes the salient factors of the evidently complex arguments leading to the derivation of σ_{BI}. The full details of the approach and of that leading to $\langle R_2{}^2 \rangle$ are contained in a lengthy paper in "J Chem Soc" Faraday II[39].

The application of buffeting theory is not limited just to the NMR field, but to other aspects of chemistry and physics. For example, Figure 3.5 shows the relationship between calculated van der Waals a-values, and those obtained from experimental data. The correlation is quite satisfactory and appears to be significant with the expected slope of unity and zero intercept.

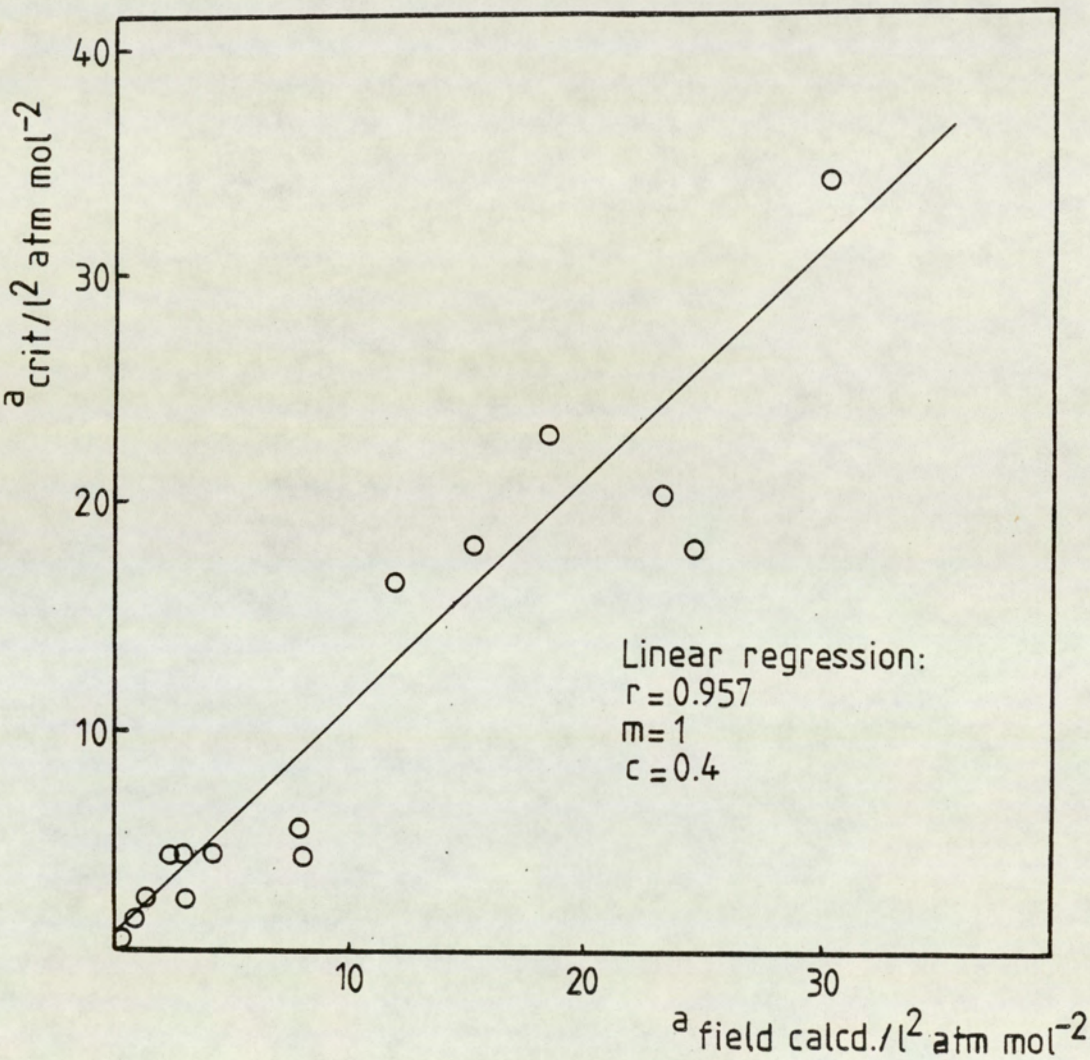

Figure 3.5: Relationship between critical constant and field calculated van der Waals a-values (reproduced from ref 39)

3.5 Conclusion

The overwhelming success obtained by the extensive tests of Homer and Percival's theory is beyond the realm of chance. Despite the acknowledged simplicity of Homer and Percival's approach it would appear that they have proved a working theory that can be used to accurately predict observable properties of matter that stem from van der Waals forces.

CHAPTER FOUR

EFFECT OF MOLECULAR VOLUME ON VAN DER WAALS NMR CHEMICAL SHIFTS

The original work on buffeting screening indicated that the magnitude of this should be significantly affected by both the electronic properties of the peripheral atoms of the solvent and also the molecular volume of the solvent. This chapter attempts to elucidate these possibilities by investigating the shifts induced in small solute molecules by lanthanide shift reagents (LSR). The purpose of using LSR is that they should provide enhancement of the buffeting effect. As discussed below LSR are normally used because of their ability to complex through interaction with the lone pairs on suitable substrates. The intention here is to avoid lone pairs containing substrates so that the normal LSR shift is not evident and examine the expectedly unpaired buffeting effect of these compounds.

An attempt has been made to simplify the 3-D Homer and Percival[39] "Buffeting Model" for determining the ß and ξ parameters into a two dimensional model, and assess the validity of this. This new method enables the minimization of human errors, which occur during the measurement of the buffeting parameters in the original three dimensional model.

4.1 Lanthanide Shift Reagents

Addition of paramagnetic material to a diamagnetic sample may result in:

(a) the loss of multiplicity due to spin-spin interaction; or

(b) changes in the chemical shifts.

Regarding the first affect, small amounts of nickel and cobalt compounds have been added to samples to remove the effects of spin-spin coupling from the spectrum. This has been successful for certain organo-phosphorus compounds, where it has been possible to remove the effect of ^{31}P splitting in the proton spectrum[75].

A more important development in recent years[76] has been the use of paramagnetic lanthanide complexes as 'shift reagents'. An early example of such a reagent is tris (dipvalomethanato) europium (usually abbreviated to $Eu(DPM)_3$). (I);

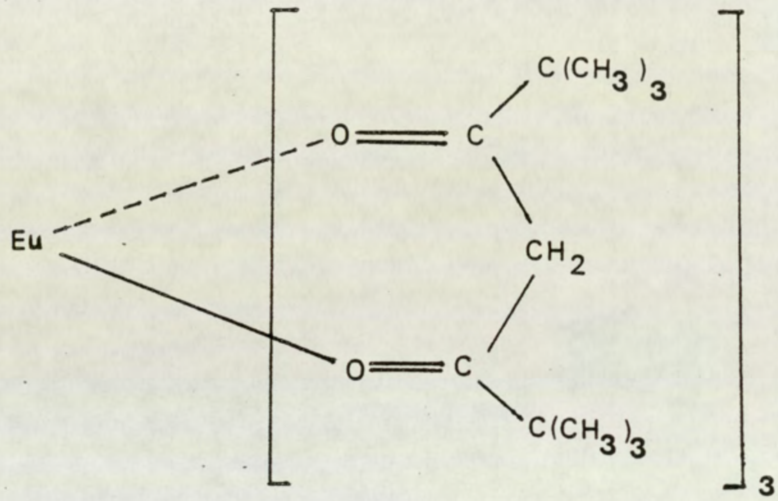

(I)

The lanthanide in such a complex can increase its co-ordination number by interaction with the lone pair electrons of other species. When the lanthanide complex is added to a suitable compound, association can occur and consequently the NMR chemical shifts in the substrate may be altered due to the effect of the LSR. The resulting change in shift differs from site to site in the molecule, so peaks that are close together in the spectrum obtained from the analytical compound alone may become separated in the spectrum when the shift reagent is added. Large shift differences may be produced so that the spectrum of the sample may also become more amenable to first-order spin-spin coupling analysis. Although most work involving shift reagents has been concerned with proton spectra, there have been reports[77,78] of the effects of shift reagents on the spectra of other nuclei such as ^{13}C and ^{14}N.

A number of different lanthanide complexes have been investigated. Usually $Eu(DPM)_3$ produces shifts to low field while $Pr(DPM)_3$ generally gives shifts to high field. The Pr complex gives the greater shifts and also produces greater broadening. The tris (1,1,1,2,2,3,3-heptafluoro-7,7-dimethyl-4,6-octanedione) complexes, Eu $(FOD)_3$ and Pr $(FOD)_3$ have the advantage of greater solubility in common organic solvents. It has been reported[78] that Dy $(DPM)_3$ is the best high-field, and Yb $(DPM)_3$ is the best low-field reagent for ^{14}N.

As the induced shift changes are dependent on the amount of shift reagent added, it is customary to report values of the induced shifts obtained by linear extrapolation to a molar ratio of 1:1. In addition the shifts are dependent on temperature because of the influence of this on the equilibrium process. It may be possible, therefore, to increase the shifts by lowering the sample temperature.

It has been of paramount importance to ensure that the LSR used in the present work should in no way react with the solutes selected, ie. the solutes do not contain lone pairs. This approach is of course contrary to the normal use of LSR when they are required to complex with lone pair containing substrates. An examination of the theory and computational techniques relevant to use of LSR is appropriate as now follows.

4.1.1 Paramagnetic Shifts

The lanthanide induced shift (LIS) value is defined as the difference between the resonance frequencies of a nucleus in the free substrate (S) and the shift in the adduct (Lanthanide reagent-substrate LS):

$$\Delta = \nu_{LS} - \nu_S \qquad \text{..... 4.1}$$

where Δ is the observed induced frequency shift. Because (S) normally exchanges rapidly between its free and complexed forms, Δ represents the average of the signal for the complexed and uncomplexed substrate. Moreover, because (S) is involved in an equilibrium process Δ is dependent on the concentration of reagent (L) in solution.

When a paramagnetic shift reagent is used, this Δ is called "The paramagnetic shift" implying that any diamagnetic component(79) on complex formation is negligible.

4.1.2 The McConnell-Robertson Equation for an Axially Symmetrical Dipolar Field

For a metal possessing unpaired electrons the paramagnetic shift (Δ para) has two components: the dipolar or pseudocontact term and the Fermi contact term.

$$\Delta_{para} = \Delta_{dipolar} + \Delta_{contact} \qquad \text{..... 4.2}$$

The first describes all magnetic dipolar types of effect, the latter accounts for possible spin-delocalisation within the complex. The first effect acts through space and can be formulated as a dipolar magnetic field. The latter acts through the bonds and represents a polarisation caused by a partially covalent bond between the substrate and lanthanide reagent.

4.1.3 Pseudocontact Shift

To calculate the dipolar or pseudocontact term, one assumes a dipolar magnetic field. The origin of the field is thought to be represented by the position of the lanthanide ion in the complex (point dipole) with co-ordinates (0,0,0) in Figure 4.1. The dipolar shift can be expressed(80) as a function of the internal co-ordinates of the nucleus under consideration: r is the length of a vector joining the paramagnetic centre and the resonant nucleus, θ is the angle between this vector and the Z-magnetic axis, and ω is the angle which the projection of r into the XY-plane makes with X magnetic field axis (Figure 4.1).

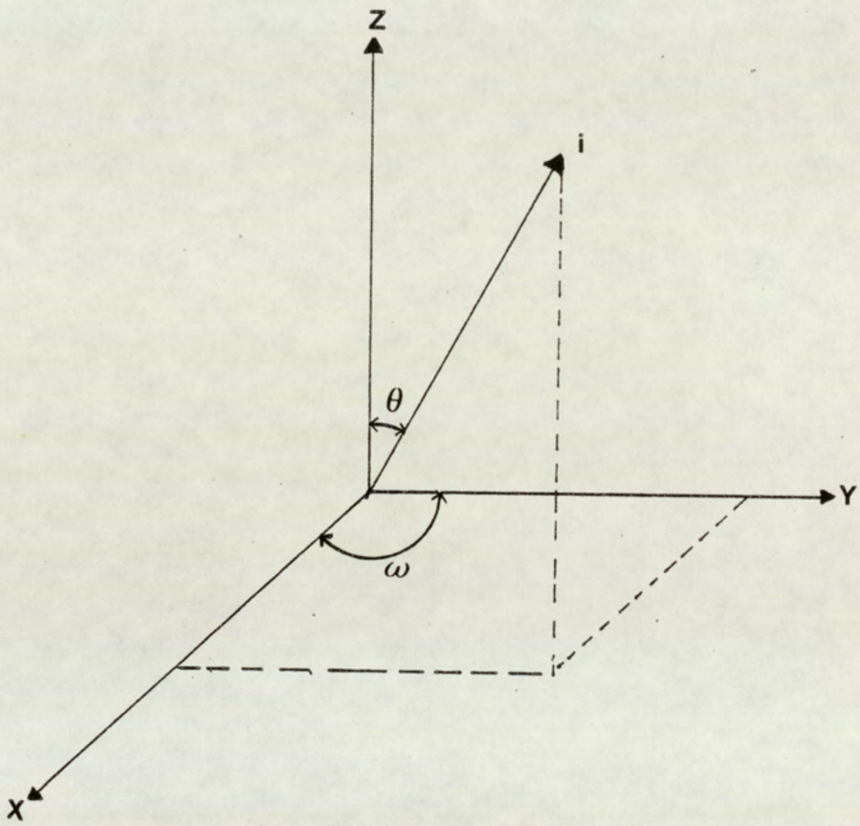

Figure 4.1 - Definition of co-ordinate parameters for the dipolar shifts. The lanthanide ion is at the origin of the co-ordinate system

The equation for this dipolar shift in its most general form is[84]

$$\Delta_{dip} = K_{ax} \left(\frac{3\cos^2\theta - 1}{r3}\right) + K_{non\ ax} \left(\frac{\sin^2\theta - \cos 2\omega}{r3}\right) \quad \text{..... 4.3}$$

The expressions in the brackets are called the "geometric factors". They are dependent on the geometry of the complex formed but independent of the lanthanide itself (except when the metallorganic molecule used as a shift reagent influences the substrate geometry significantly).

The magnitude and sign of the constants K_{ax} and $K_{non\ ax}$ are functions of the magnetic anistropy of the complex, and are determined by the electronic properties of the lanthanide. In the case of most common relaxation phenomena[80,81] (where the tumbling time of the complex is much longer than the electron spin relaxation time) these constants may be expressed as a function of the three principal molecular magnetic susceptibilities χ_x, χ_y and χ_z, corresponding to X, Y and Z in Figure 4.1.

$$K_{ax} = -\frac{1}{3L}\left(\chi_z - \frac{1}{2}\chi_x - \frac{1}{2}\chi_y\right) \qquad \text{..... 4.4}$$

$$K_{non\ ax} = -\frac{1}{2L}(\chi_x - \chi_y) \qquad \text{..... 4.5}$$

where L is the Avogadro number.

A special case is given for an axially symmetrical field where $\chi_z = \chi_{||}$ and $\chi_x = \chi_y = \chi_{\perp}$. $K_{non\ ax}$ then becomes zero, and the non axial term in equation (4.3) vanishes. Equation 4.3 is then reduced to equation 4.6 which is valid for all i observed resonances of a substrate.

$$\Delta i = K \,.\, \frac{3\cos^2\theta_i - 1}{r_i^{\,3}} \qquad \text{..... 4.6}$$

Equation 4.6 is the McConnell-Robertson equation[82] for an axially symmetrical dipolar magnetic field (point dipole). It is used in most calculations of LIS values.

4.1.4 Contact Shifts

Returning to equation 4.2, we see that in order to calculate the paramagnetic shift we need to know something about the contact contribution. Unfortunately the mathematical treatment of contact shifts is as yet rather uncertain, and the only choice we have in calculating Δ_{para} is to keep the contribution of $\Delta_{contact}$ as low as possible, so that the condition $\Delta_{contact} << \Delta_{dip}$ should hold.

There is much evidence that the contact shift for ^1H resonances is rather small. This was demonstrated by the calculation of the LIS on the basis of the complete pseudocontact equation (4.3) plus equations 4.4 and 4.5 using information on the geometry of the complex gained by X-ray chromatography(83).

The contact interaction is restricted to protons close to the co-ordination site, since the "through bond" interaction decreases rapidly and vanishes beyond three or four bonds, even in systems where substantial contact contributions are found (eg. for nuclei other than ^1H).

While ^1H contact shifts cannot be excluded a priori, they should represent a rather small contribution.

In the present study the intention is to avoid complexation between the LSR and the substrate by using solutes with no lone pairs. In this way the contact shift contribution can be eliminated and the "pseudo-contact" term transformed into an isotropic induced shift that should contain a buffeting contribution that is much larger than normally expected from diamagnetic solvents. The first problem to be addressed is how this buffeting contribution can be isolated from the measured LIS.

4.2 Isolation of σ_W from the experimental chemical shifts for molecules in the liquid phase

Neglecting bulk magnetic susceptibility effects the screening constant of an isotropic solute i in an isotropic solvent is:

$$\sigma^i_S = \sigma^i_O + \sigma^i_W \qquad \text{..... 4.7}$$

where σ^i_S is the screening constant of nucleus i in the solute contained in solution S,

σ^i_o is the absolute screening constant of nucleus i in the gas phase at zero pressure, and σ^i_w is the contribution of van der Waals dispersion forces to the screening of nucleus i. From equation 3.6:

$$\sigma^i_w = \sigma^i_{RF} + \sigma^i_{BI} \qquad \text{..... 4.8}$$

therefore,

$$\sigma^i_s = \sigma^i_o + \sigma^i_{RF} + \sigma^i_{BI} \, (+ \sigma_b{}^i) \qquad \text{..... 4.9}$$

where σ_{RF} and σ_{BI} are the reaction field and the buffeting interaction effects on the screening of constant of i.

Usually the chemical shift of each resonating nucleus is measured from a reference, which is one of the components in the solution when using the internal reference technique; this is the case adopted throughout the work reported in this chapter. Consequently, the reference will experience the same environment as the solute, and its chemical shift is, therefore, given by:

$$\sigma^r_s = \sigma^r_o + \sigma^r_w \qquad \text{..... 4.10}$$

where the superscript r in the above equation identifies the reference. Following equation (1.48) the chemical shift is defined by:

$$\delta^i_s = \sigma^i_s - \sigma^r_s \qquad \text{..... 4.11}$$

Therefore using equations 4.7 and 4.10 the above equation may be written as:

$$\delta^i_s = (\sigma^i_o - \sigma^r_o) + (\sigma^i_w - \sigma^r_w) \qquad \text{..... 4.12}$$

Since the term $(\sigma^i_o - \sigma^r_o)$ represents the difference between the single molecule or the absolute screening constants of nucleus i and that of the reference, r, this term is constant whereas the other term $(\sigma^i{}_w - \sigma^r{}_w)$ depends on the properties of the solvent. The difficulty of obtaining the absolute screening difference in the above equation may be avoided by finding the appropriate chemical shifts in two different solvents, so that the difference between these two chemical shifts for a given solute using the same reference will eliminate the term $(\sigma^i{}_o - \sigma^r{}_o)$ as explained below:

The chemical shift of the resonant nucleus i contained in an isotropic solute at infinite dilution in an isotropic solvent A is represented by:

$$\delta^{i/A} = (\sigma^i{}_o - \sigma^r{}_o) + (\sigma^{i/A}{}_w - \sigma^{r/A}{}_w) \quad ..... \; 4.13$$

and similarly the chemical shift of i using another isotropic solvent B is given by:

$$\delta^{i/B} = (\sigma^i{}_o - \sigma^r{}_o) + (\sigma^{i/B}{}_w - \sigma^{r/B}{}_w) \quad ..... \; 4.14$$

By subtracting equation 4.13 from equation 4.14, the difference of the chemical shifts of i on changing from solvent A to solvent B, is given by:

$$(\delta^{i/B} - \delta^{i/A}) = (\sigma^{i/B}{}_w - \sigma^{i/A}{}_w) - (\sigma_w{}^{r/B} - \sigma_w{}^{r/A}) \quad ..... \; 4.15$$

which may be rewritten as follows by using equation 4.8 with rearrangement:

$$(\delta^{i/B} - \delta^{i/A}) = (\sigma_{RF}{}^{i/B} - \sigma_{RF}{}^{i/A}) + (\sigma_{BI}{}^{i/B} - \sigma_{BI}{}^{i/A}) - (\sigma_w{}^{r/B} - \sigma_w{}^{r/A}) \quad ..... \; 4.16$$

For simplicity it will be assumed that both solute and reference are infinitely dilute so that there is no solute-reference interaction. Therefore, in equation 4.16 the term representing the difference of van der Waals dispersion force screening of the reference should be a constant value independent of the solute, provided the same solvents A and B are used.

It is convenient, therefore, to isolate the required difference in buffeting contribution to the nuclear screening constant, by rearranging equation 4.16 as:

$$(\delta^{i/B} - \delta^{i/A}) - (\sigma_{RF}{}^{i/B} - \sigma_{RF}{}^{i/A}) = (\sigma_{BI}{}^{i/B} - \sigma_{BI}{}^{i/A}) - (\sigma_w{}^{r/B} - \sigma_w{}^{r/A}) \text{ ..... } 4.17$$

The above equation enables the isolation of the difference in the buffeting interaction contribution to the screening, together with a constant factor on the right hand side. The left hand side of the equation contains the difference of the experimentally measured chemical shifts together with the difference of the reaction field contribution to the screening and this can be calculated using the established equation 3.18.

A test of the validity of equation 4.17 is provided in this chapter by studying the effect of the concentration of TMS (solute) in carbon tetrachloride (solvent).

In order to use equation 4.17 it is necessary to deduce σ_{BI} in addition to σ_{RF}. For this it is essential to have a reliable method for estimating ß and ξ parameters and this problem is addressed in the next section.

4.3 Measurement of the Buffeting Parameters ß and ξ

The geometrical buffeting parameters ß and ξ represent the effective accessibility of the solvent peripheral atom to the solute resonant nucleus, as a result of pair-wise encounters. In order to visualize this buffeting, the solvent molecule containing the peripheral atom is assumed to be spherical because of its rotational motion. Both solute and solvent molecules are taken to be rigid and passive. On this basis, Figure 4.2 shows the approach that is assumed to represent pair-wise encounters from a geometrical point of view. It shows that the solvent molecule is buffeting the solute atom under interest with a distance r between the centres of the resonant nucleus and the peripheral atom on the solvent. The figure shows a hypothetical two dimensional encounter situation.

If in Figure 4.2 the centre of the peripheral solvent atom can adopt all positions on the arc of radius r_c from the centre of the solute atom throughout the octant of interest, then $\beta = 1$ and $\alpha = 1$ ($\xi = 2$) and there will be no buffeting screening because $(2\beta - \xi)^2 = 0$. If the contact distance r_c is sterically precluded within the octant, β and α will be less than unity. If the two dimensional angle θ is the angle between the radius vector and the so-called α axis which defines the limit where r_c no longer applies (ie. $r > r_c$) the following equations are applicable:

$$\text{If } \theta \leq 45;\ \beta_c = 1,\ \alpha_c = \frac{45 - \theta}{45} \qquad \text{..... 4.18}$$

$$\text{If } \theta \geq 45;\ \alpha_c = 0,\ \beta_c = \frac{90 - \theta}{45} \qquad \text{.... 4.19}$$

The above equations enable the contact geometrical buffeting parameters β_c and ε_c to be deduced when the solvent peripheral atom is in contact with the solute atom. The remaining parts of β and α, $(1 - \beta_c)$ and $(1 - \alpha_c)$, may be deduced by distance modulation. The modulation is based on the inverse sixth power of distance, because of this distance dependence of van der Waals dispersion forces. If r^1 is the distance between the centres of the solute atom and the solvent atom at the α-axis, viz the extreme point of the octant of interest where direct atom-atom contact is prevented by steric hinderance, r_c is the distance between the centres of the solute-atom solvent atom

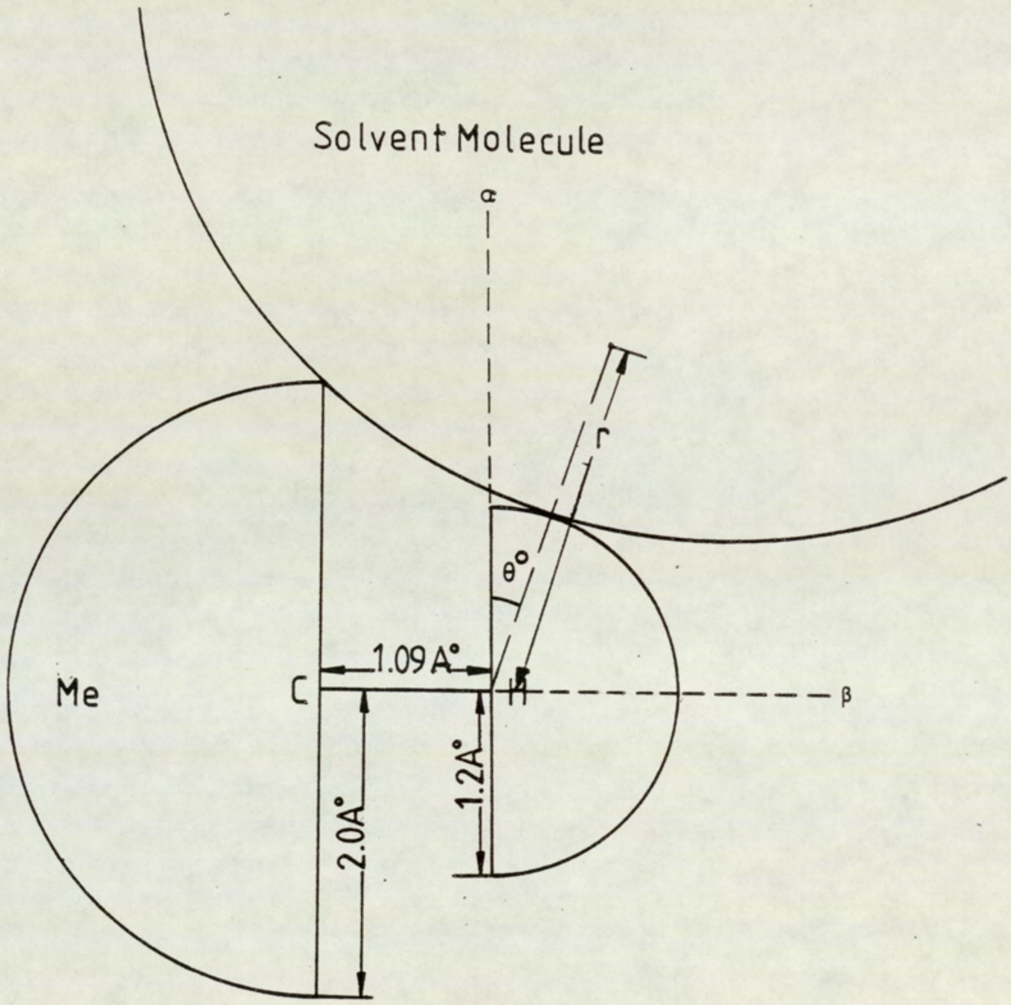

Figure 4.2: Two dimensional representation of a methane molecule (Hydrogen H and methyl group Me) encountered by an isotropic solvent molecule

at contact, and assuming a continuous change in distance from r_c to r^1, the average inverse power of the distance used for the modulation of $(1 - \beta_c)$ and $(1 - \alpha_c)$ is $< r^{-6} >$ where:

$$< r^{-6} > = \frac{\int_{r_c}^{r^1} r^{-6}\, dr}{\int_{r_c}^{r^1} dr} = \frac{r_c^{-5} - r^{1^{-5}}}{5\,(r^1 - r_c)} \qquad \text{..... 4.20}$$

The total values of ß and ξ are given by:

$$\beta_T = \beta_c + (1 - \beta_c)\, r^6{}_c < r^{-6} > \qquad \text{..... 4.21}$$

$$\alpha_T = \alpha_c + (1 - \alpha_c)\, r^6{}_c < r^{-6} > \qquad \text{..... 4.22}$$

$$\xi_T = \xi_c + (2 - \xi_c)\, r^6{}_c < r^{-6} > \qquad \text{..... 4.23}$$

for the appropriate situations.

4.4 Experimental Requirements

The contribution of the buffeting interaction to the solvent induced nuclear screening represents only a small part of the total chemical shifts; in some systems it is just few Hertz at 100 MHz. The isolation of such effects from the experimental shifts therefore requires high accuracy in the measurement of the latter. The factors that affect the chemical shift measurements, eg. the sample preparation and the concentration of the solute and LSRs under interest will be discussed now.

4.4.1 Measurement of Accurate Chemical Shifts

The chemical shifts measurements reported in this chapter, were performed using a Perkin-Elmer R12B60 MHz NMR spectrometer at 33°C, during the initial stages of the work, but the main results were obtained using a JEOL FX 90Q FT NMR spectrometer at 30°C. With the latter instrument it was possible to obtain absolute shifts without using TMS as reference. All the spectra were drawn out in expanded form, ie. minimum spectral width, and the measurements made several times to average any variations. Internal ^2H lock was used throughout to avoid any possible signal drifting.

For the few measurements made using the Perkin-Elmer R12 B instrument, TMS was used as the reference, the TMS signal being field/frequency locked at zero on δ scale. The chemical shifts were found by averaging several measurements for the same sample.

The temperature was kept constant throughout all the chemical shift measurements at 33°C to eliminate the effect of temperature variations.

4.4.2 Preparation of Samples

All the samples investigated were prepared at effectively infinite dilution (see Section 4.3.3) to eliminate any concentration effect. New 5mm and 10mm OD NMR tubes for each sample were used throughout.

To ensure that there was negligible dissolved oxygen that could affect the shifts, the samples were prepared under vacuum. The transference of solutions to NMR tube under vacuum was effected using special glassware designed[84] for this purpose. Figure 4.3 shows the vacuum manifold and syphoning apparatus used.

Initially, the three way tap and the rota flow taps were adjusted so that the flask was isolated from the rest of the apparatus. All parts of the manifold were then evacuated, except for the flask. Meanwhile the flask was cooled using liquid nitrogen. About 2.5 ml of prepared solution was quickly inserted in the flask. The solution inside the flask was frozen by liquid nitrogen. At this stage the flask was opened to the evacuated manifold while the solution was frozen. Vacuum was achieved using conventional rotary pump techniques and the pressure assessed using a mercury

'Vacustat' (manufactured by Edwards High Vacuum Ltd) connected to the manifold. The vacuum at this stage was checked using the 'Vacustat' for a pressure of 10^{-4} Torr or less. Subsequently the flask was isolated from the vacuum system by the three-way tap and allowed to warm up.

The NMR tubes were connected to the manifold using a special glass-to-metal joint with an O-ring seal. Each tube was evacuated and checked for any leakage. The NMR tube was warmed gently to remove any oxygen adhering to the wall. Then the vacuum manifold was isolated from the pump and the taps leading to the sample tube and the flask were opened. During this procedure the NMR tube was cooled and the flask containing the sample warmed while controlling the taps until enough sample in the NMR tube had been collected. At this stage the sample tube was frozen and the manifold re-evacuated. Finally the NMR tube was flame sealed under vacuum. In order to ensure effective sealing, the NMR tubes were prepared before use by flame heating around a point about 2cm from the open end prior to the installation on the vacuum system. This caused a restriction and thickening of the tube at the appropriate point. Subsequently, a very good seal was obtained by touching the narrow part of the tube with the flame. The sealed tube was kept under a glass beaker for at least two hours after the solution inside it had melted so that the effects of implosion could be monitored.

4.4.3 Effects of Concentration on NMR Chemical Shifts

For an accurate assessment of Homer and Percival theories, which ideally require the use of infinitely dilute solutions, it was important to establish the limit of concentration which could be considered to behave as an infinitely dilute solution.

This was done by investigating the dependence of an appropriate chemical shift on the solute concentration. The experiment was performed on the Jeol FX 90Q FT NMR spectrometer. Pure TMS sealed in a 5mm OD NMR tube was inserted

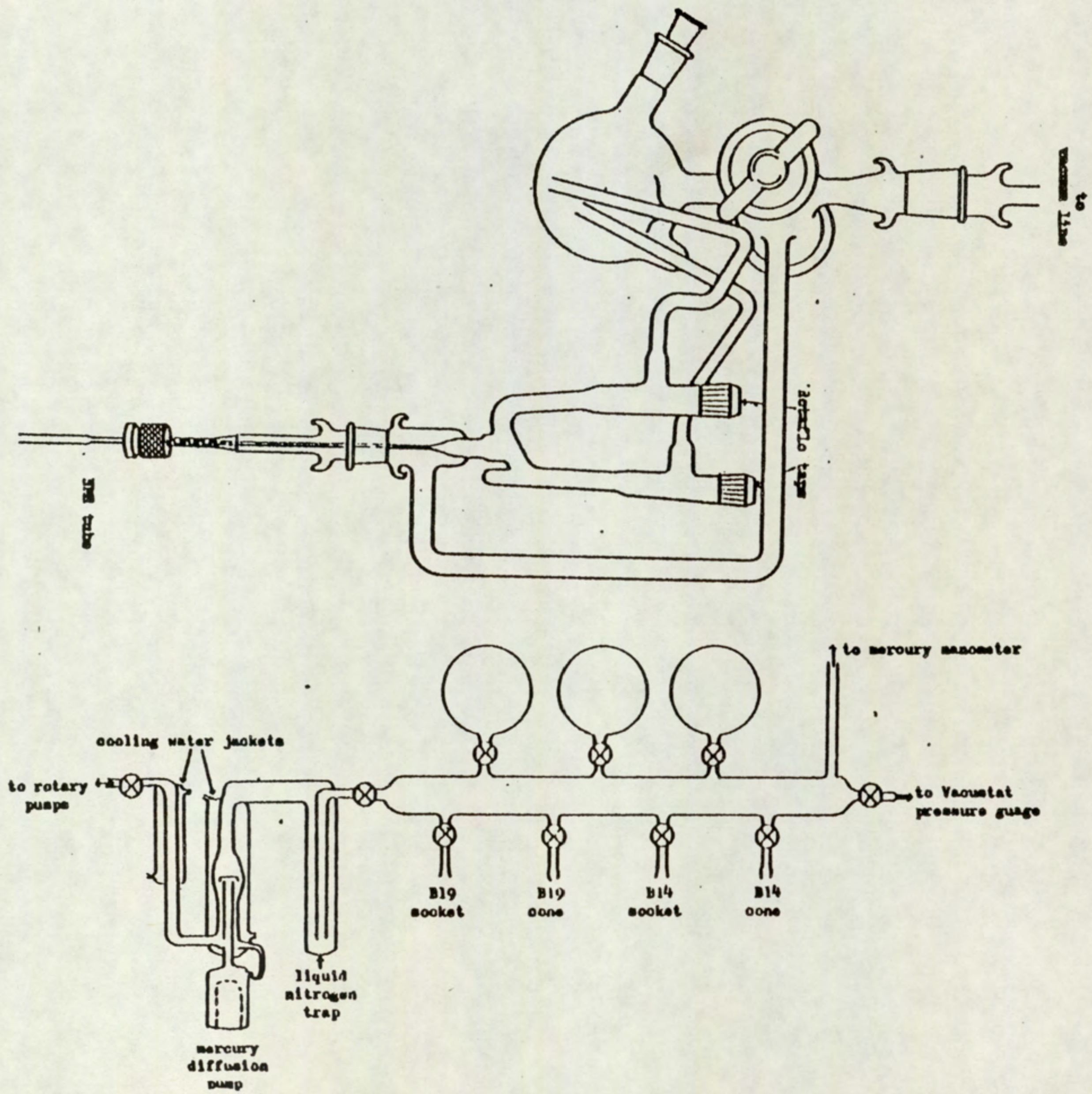

Figure 4.3: The manifold and the syphoning apparatus used together in sample preparation

coaxially into a 10mm OD NMR tube which contained D_2O (D_2O was used as the internal locking material). The proton chemical shift of TMS was measured. Different concentrations of TMS (solute) in CCl_4 (solvent) were prepared. Starting with a stock solution of 10 M solution of TMS in CCl_4, further dilute solution of 5, 2.5, 1.25, 0.613 and 0.31 M concentration were prepared.

The chemical shift was measured for each concentration, using the field/frequency locked spectrometer. Table 4.1 presents the resultant chemical shifts. A plot of these against concentration is shown in Figure 4.4; the Y-intercept represents the chemical shift of the sample at zero concentration viz: the infinite dilution chemical shift. While these shifts are not susceptibility corrected, it can be seen that below a concentration of 1.25 M the shifts are constant, therefore in practice a solution of 1 M can be assumed to be inifinitely diluted.

All the samples used throughout the remainder of this work were prepared at 0.5 M; this avoids any unwanted interaction that may occur between the solute and the solvent at higher concentrations.

	Concentration of TMS in CCl_4 (Molar)	TMS/in CCl_4 δ_o Hz	$\delta^{CCl_4}_{TMS} - \delta^{TMS}_{TMS}$ Hz
	TMS (Neat)	-199.95	-
X	10	-178.22	-21.73
1/2 X	5	-165.03	-34.92
1/4 X	2.5	-161.13	-38.82
1/8 X	1.25	-160.64	-39.31
1/16 X	0.625	-160.64	-39.31
1/32 X	0.313	-160.64	-39.31

Table 4.1 - Dependence of chemical shift of TMS in CCl_4 from internal TMS (neat) using FX 90Q FT NMR spectrometer at 303 K, at operating frequency of 89.60425 MHz.

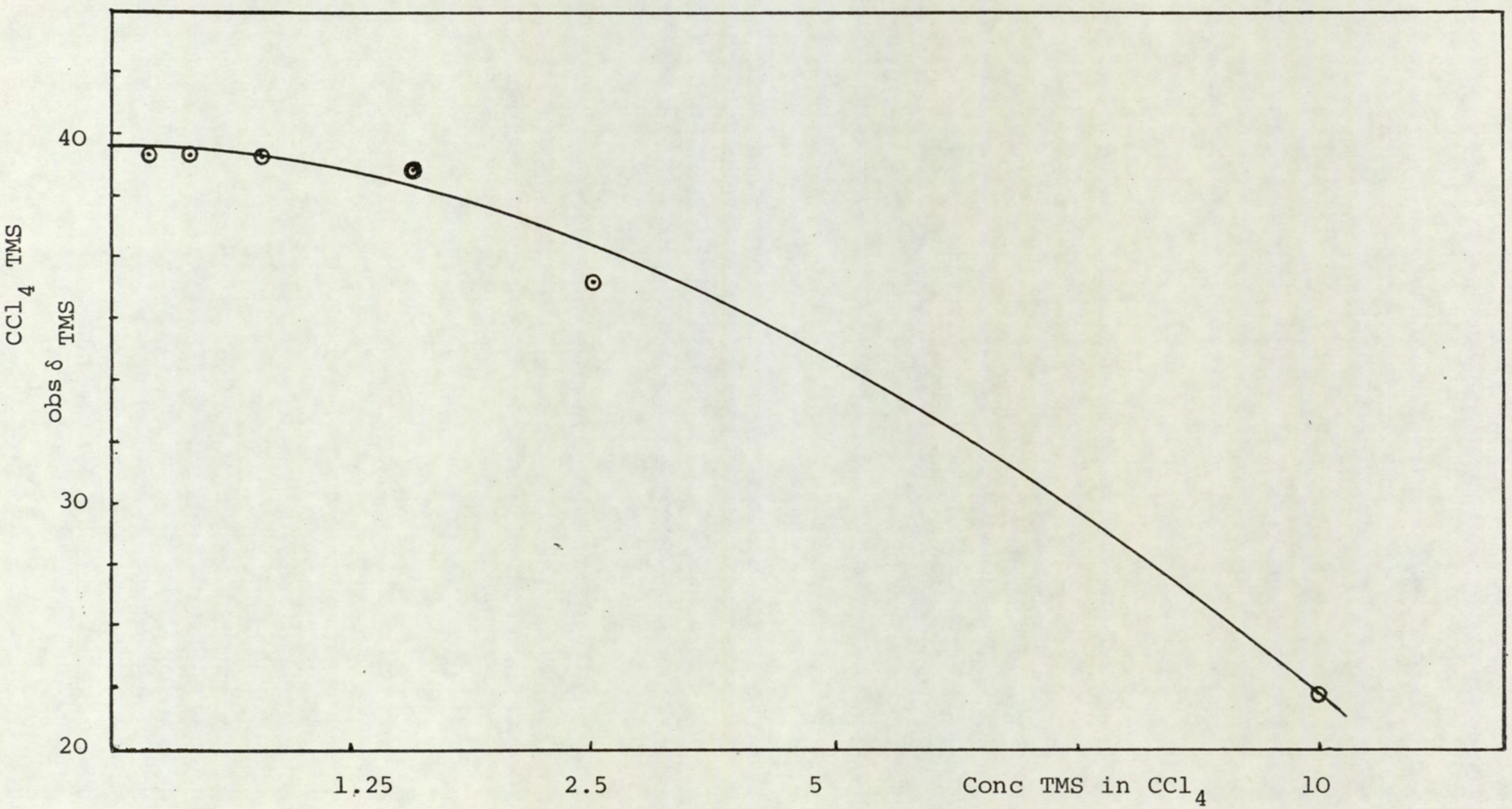

Figure 4.4: The dependence of ^1H shifts of TMS on concentration. Measurements were made employing JEOL FX 90 Q NMR Spectrometer at operating frequency of 89.60425 MHz at 303 K

4.5 σ_w for the reference TMS

If some correlation between the term on the left hand side of equation 4.17 and the first term of the right hand side can be demonstrated a further test of validity of this equation may be made by analysing the value obtained from the second term of the right hand side, ie. $(\sigma^{r/B}{}_w - \sigma^{r/A}{}_w)$. Consequently, the next stage of the work was to deduce, by an independent method, a value of this term for the reference. This term should be constant and can be estimated separately. The experiment that was described in Section 4.4.3 can be adopted for this purpose.

From equations (4.7 and 4.11) the chemical shift of TMS in the solvents CCl_4 and TMS can be represented respectively by:

$$\delta^{CCl_4}_{TMS} = \sigma_o + \sigma_b{}^1 + \sigma_w{}^1 \qquad \text{..... 4.24}$$

$$\delta^{TMS}_{TMS} = \sigma_o + \sigma_b + \sigma_w \qquad \text{..... 4.25}$$

Therefore

$$\delta^{CCl_4}_{TMS} - \delta^{TMS}_{TMS} = (\sigma_b{}^1 - \sigma_b) + (\sigma^1{}_w - \sigma_w) \qquad \text{..... 4.26}$$

In the above equation the term representing the screening effect of magnetic suspectibilities can be calculated using equation 1.57, where the volume magnetic susceptibilities are -0.536×10^{-6} for TMS[51] and -0.689×10^{-6} for CCl_4[85]. This would give $(\sigma_b{}^1 - \sigma_b) = -0.32$ ppm.

Using the value deduced in section 4.4.3 for the experimental differences in the chemical shifts of TMS on changing from CCl_4 to TMS as solvent (for infinitely dilute solutions) gives the term $(\delta^{CCl_4}_{TMS} - \delta^{TMS}_{TMS})$ as -39.44 Hz at 89.60425 MHz (from Table 4.1 and Figure 4.4). Therefore substituting this with $(\sigma_b{}^1 - \sigma_b)$ = -0.32ppm in equation (4.26) would give the difference in van der Waals screening for the reference $(\sigma^1{}_w - \sigma_w)$ equal to -10.75 Hz or 0.120ppm. This value is in good agreement with the value deduced by Homer(86) using a novel referencing system for the same purpose. He obtained -8.6 Hz at 60 MHz which is equivalent to -12.84 Hz at 89.60425 MHz. Figure 4.5 illustrates the above method schematically.

Having established the self-consistency of the earlier theoretical proposals it is now possible to use these to analyse the effects of LSR on non-bonding substrates.

4.6 Procedure for the use of Lanthanide Shift Reagent (LSR)

The most frequently used lanthanide shift reagents were found to be the lanthanide tris-ß-diketonates(76,87,88), eg. the dipivaloyl methanates, Ln $(dpm)_3$ (I) or the 1,1,1,2,2,3,3-heptafluoro-7,7-dimethyl-4,6,-octanedionates, Ln $(Fod)_3$ (II)(89,90).

Ln $(dpm)_3$ and Ln $(Fod)_3$ are readily soluble in $CDCl_3$ and CCl_4 and hence were an ideal choice for the present investigation.

The lanthanide chelates are very hygroscopic(91) and on adsorption of water, the chelates usually become white solids and their shifting power is drastically reduced(91). Precautions were taken to store all the LSR in a dessicator over phosphorous pentoxide.

4.6.1 Effect of concentration of LSR

As mentioned in Section 4.4.3, it was imperative to eliminate any dependence of the results obtained, on the LSR concentration, consequently it was necessary to establish the limit of concentration of the LSR which would give effectively concentration independent results.

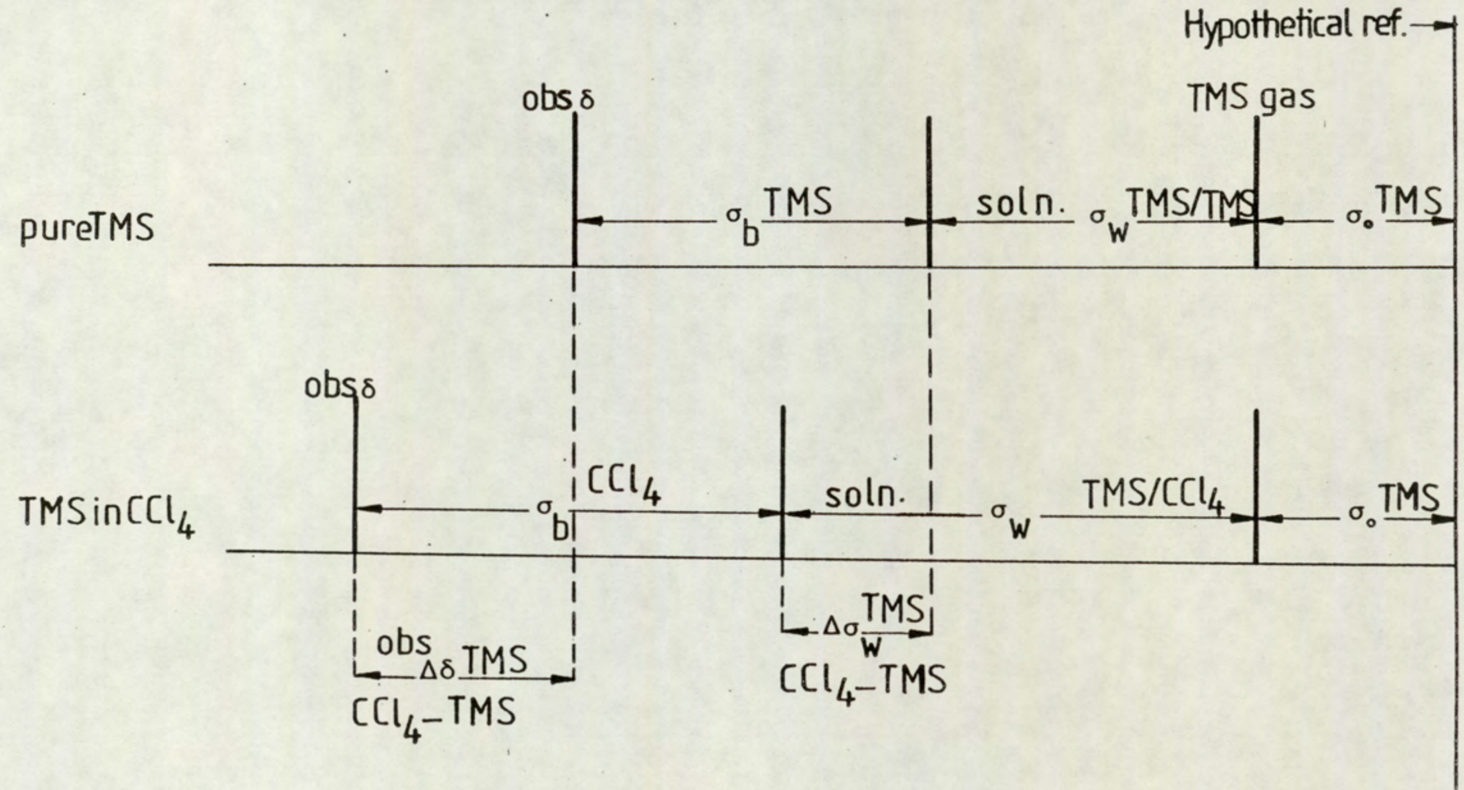

Figure 4.5: Schematic representation of evaluation of σ_w of TMS on changing from TMS in CCl_4 to pure TMS

This was established by preparing solutions of different concentration of Eu $(Fod)_3$ in 0.5 Molar TMS in CCl_4. The chemical shift was measured for each concentration using a field/frequency locked spectrometer by exactly the same procedure as mentioned in Section 4.4.3 The results are tabulated in Table 4.2.

Table 4.2 - Dependence of chemical shift of TMS in CCl_4 on the concentration of Eu $(Fod)_3$ using FX 90Q NMR at 303 K, at an operating frequency of 89.60425 MHz.

Concentration of Eu $(Fod)_3$ in (0.5M TMS in CCl_4)	TMS in CCl_4 Hz
0.254 (Molar)	41.5
0.127	24.41
0.064	14.16
0.037	13.3
0.018	7.81
0.009	7.81
0.005	7.81

It is evident from Table 4.2 that below the concentration of 0.018M the experimental differences in the chemical shifts of TMS (0.5M in CCl_4) are negligible. It has been assumed that the concentration of LSR other than Eu $(Fod)_3$ should have a similar effect on the chemical shifts, and normally follows the same trend. For accuracy and consistency the concentration of LSR was maintained at 0.01M throughout the present investigation.

4.6.2 Effect of LSR on the chemical shifts of some solute-solvent systems

The next stage was to measure chemical shifts from which some indication of the effect of LSR on chemical shifts could be obtained. Four sets of experiments were performed using different solute-solvent systems. The systems used were as follows:

(a) 0.5M Mesitylene in CCl_4

(b) 0.5M TMS in CCl_4

(c) 0.5M TMS in Mesitylene

(d) 0.5M 1,3,5-tri-iso propyl benzene in CCl_4.

The experiments for system (a) were performed on the Perkin Elmer 60 MHz R12 spectrometer, (the others being based on the JEOL FX 90 Q spectrometer).

A solution of 0.5M mesitylene was prepared using CCl_4 as solvent. The difference between the chemical shifts of the methyl and aryl protons in mesitylene was measured on a precalibrated chart. A set of LSR with concentration of 0.01M were prepared in the solution of 0.5M mesitylene in CCl_4 and similar measurements were made. The difference between the chemical shifts of the methyl and aryl protons in a solution of mesitylene in CCl_4 and that of a solution of mesitylene in CCl_4 containing LSR should reflect the effect of LSR on the mesitylene solute. The results are tabulated in Table 4.3.

Further experiments were conducted on JEOL FX 90Q FT NMR spectrometer at an operating frequency of 89.60425 MHz. The effects of LSR's on a solution of 0.5 Molar TMS in CCl_4, 0.5 Molar mesitylene in CCl_4 and 0.5 Molar 1,3,5-tri-iso-propyl benzene in CCl_4 were observed, the results are tabulated in Tables 4.4, 4.5 and 4.6 respectively.

Table 4.3 - Effect of LSR on the ^1H chemical shifts of mesitylene measured using a 60 MHz Perkin-Elmer R-12 spectrometer at 303 K

Concentration of mesitylene (solute) 0.5 Molar
Concentration of LSR: 0.01 Molar

Sample	δ ($-CH_3$) Hz	δ (-H) Hz	Difference Hz	Relative Shift Hz	Relative Shift ppm
Mesitylene in CCl_4 (reference)	23.31	289.71	266.4	-	-
Mesitylene in CCl_4 + Eu $(Fod)_3$	25.31	291.71	266.4	0	0
Mesitylene in CCl_4 + Ho $(Fod)_3$	14.65	278.65	264.0	-2.4	-0.04
Mesitylene in CCl_4 + Pr $(Fod)_3$	16.65	282.38	265.73	-0.67	-0.011
Mesitylene in CCl_4 + Dy $(Fod)_3$	27.97	295.7	267.73	+1.33	+0.022

Table 4.4 - Effect of LSR on the ^1H chemical shift of TMS, measured on JEOL FX 90Q FT NMR spectrometer at an operating frequency of 89.60425 MHz at 303 K.

Concentration of TMS (solute): 0.5 Molar
Concentration of LSR: 0.01 Molar

Sample	δ TMS Hz	Difference Hz	Difference ppm
TMS in CCl_4 (A)	-160.64	-	-
Eu $(Fod)_3$ in A	-169.30	8.66	0.097
Pr $(Fod)_3$ in A	-172.96	12.32	0.137
Yb $(Fod)_3$ in A	-170.76	10.12	0.113
Yb $(DPM)_3$ in A	-175.89	15.25	0.17
DY $(DPM)_3$in A	-188.35	27.71	0.309

Table 4.5 - Effect of LSR on the ^{1}H chemical shifts of mesitylene measured on JEOL FX 90Q FT NMR spectrometer at an operating frequency of 89.60425 MHz at 303 K

Concentration of mesitylene in CCl_4 (B) = 0.5 Molar
Concentration of LSR in (B) = 0.01 Molar

Sample	δ - CH_3 Hz	δ -H Hz	Difference Hz	Shift Hz	ppm
0.5M mesitylene in CCl_4 (B)	384.87	-17.08	401.35	-	-
Eu $(Fod)_3$ in B	375.48	-25.87	401.35	0	0
Pr $(Fod)_3$ in B	371.58	-28.8	400.38	0.97	0.011
Ho $(Fod)_3$ in B	282.22	-115.23	397.45	3.9	0.044
Yb $(Fod)_3$ in B	378.41	-22.46	400.87	0.48	0.005
Yb $(DPM)_3$ in B	364.26	-36.62	400.87	0	0
Ho $(DPM)_3$ in B	295.89	-104.98	400.87	0	0
DY $(DPM)_3$ in B	282.22	-118.65	400.87	0	0

Table 4.6 - Effect of LSR on the chemical shift between methyl and methine protons of 1,3,5-tri-isoproyl benzene measured on a JEOL FX 90Q FT NMR spectrometer at an operating frequency of 89.60425 MHz at 303 K

Concentration of 1,3,5-tri-isopropyl benzene in CCl_4 (C): 0.5 Molar
Concentration of LSR in C: 0.01 Molar

Sample	δ - CH Hz	δ - CH_3 Hz	δ (-CH)-(CH_3) Hz	Shift Hz	ppm
1,3,5-tri-isopropylbenzene in CCl_4 (C)	90.82	-50.78	141.6	-	-
Eu $(Fod)_3$ in C	80.56	-61.03	141.59	0.01	0
Pr $(Fod)_3$ in C	80.56	-61.03	141.59	0.01	0
Ho $(Fod)_3$ in C	68.84	-65.43	134.27	7.33	0.08
Yb $(Fod)_3$ in C	87.89	-53.71	141.6	0	0
Ho $(DPM)_3$ in C	49.80	-91.55	141.35	0.25	0.03
Dy $(DPM)_3$ in C	44.92	-97.17	142.09	0.49	0.005

Before interpreting the results presented in Tables 4.3, 4.4, 4.5 and 4.6 it is appropriate to consider equation 3.26:

$$\sigma_{BI} = \frac{BK}{r6} (2ß - \xi)^2$$

The constant K is essentially a factor which is dependent on the electron displacements about the peripheral solvent atoms. Due to the large electronic configuration in the case of LSR and the presence of lanthanide ions, which should have large values of K, one would obviously expect to obtain large values of σ_{BI}. Taking into consideration the capacity of LSR to produce large paramagnetic effects the shifts observed in Tables 4,3, 4.5 and 4.6 seem to be unexpectedly small.

The chemical shift differences indicated in Table 4.4 includes the buffeting σ_{BI},the bulk susceptibility σ_b and the reaction field σ_{RF} effects.

Unlike Table 4.4 the chemical shifts shown in Tables 4.3, 4.5 and 4.6 reflects only the effect of the buffeting parameter σ_{BI} and reaction field σ_{RF}.

This difference arises because in Table 4.4 the change between the shifts of TMS/CCl_4/LSR and TMS/CCl_4 solutions are reported. However in Tables 4.3 and 4.5, the chemical shift differences between the methyl and aryl proton of mesitylene for a series of LSR in mesitylene/CCl_4 solution are reported. Similarly Table 4.6 reflects the chemical shift differences between the methyl and methine proton of 1,3,5,-tri-isopropyl benzene, for a series of solutions of LSR in 1,3,5-tri-isopropyl benzene/CCl_4.

Hence two difference situations are encountered, one for Table 4.4 and the other for Tables 4.3, 4.5 and 4.6.

The two situations can be explained by the following set of equations.

(a) TMS system (Table 4.4)

$$\sigma^{i/CCl_4} = \sigma^{i}_{o} + \sigma_{RF}^{i/CCl_4} + \sigma_{BI}^{i/CCl_4} + \sigma_{b}^{i/CCl_4} \quad \text{.....} \ 4.27$$

$$\sigma^{i/CCl_4/LSR} = \sigma_{o}^{i} + \sigma_{RF}^{i/CCl_4/LSR} + \sigma_{BI}^{i/CCl_4/LSR} +$$

$$\sigma_{b}^{i/CCl_4/LSR} \quad \text{.....} \ 4.28$$

Subtracting equation 4.28 from equation 4.27:

$$\sigma^{i/CCl_4} - \sigma^{i/CCl_4/LSR} = (\sigma_{RF}^{i/CCl_4} - \sigma_{RF}^{i/CCl_4/LSR}) + (\sigma_{BI}^{i/CCl_4} -$$

$$\sigma_{BI}^{i/CCl_4/LSR}) + (\sigma_{b}^{i/CCl_4} - \sigma_{b}^{i/CCl_4/LSR}) \quad \text{.....} \ 4.29$$

Assuming that the reaction field difference term is negligible, the results in Table 4.4 should show the combined effect of buffeting σ_{BI} and bulk susceptibility σ_b.

(b) For the Mesitylene system (Tables 4.3 and 4.5) and the 1,3,5-iso-propyl benzene system (Table 4.6) the following equations apply:

$$\sigma^{CH/CCl_4} = \sigma_{o}^{CH} + \sigma_{RF}^{CH/CCl_4} + \sigma_{BI}^{CH/CCl_4} + \sigma_{b}^{CH/CCl_4}$$

$$\text{.....} 4.30$$

$$\sigma^{CH_3/CCl_4} = \sigma_{o}^{CH_3/CCl_4} + \sigma_{RF}^{CH_3/CCl_4} + \sigma_{BI}^{CH_3/CCl_4} +$$

$$\sigma_{b}^{CH_3/CCl_4} \quad \text{.....} \ 4.31$$

$$\sigma^{CH/CCl_4} - \sigma^{CH_3/CCl_4} = (\sigma_o^{CH} - \sigma_o^{CH_3}) + (\sigma_{RF}^{CH/CCl_4} -$$

$$\sigma_{RF}^{CH_3/CCl_4}) + (\sigma_{BI}^{CH/CCl_4} - \sigma_{BI}^{CH_3/CCl_4}) \qquad \text{..... 4.32}$$

Similarly it can be shown that:

$$\sigma^{CCl_4/LSR} = (\sigma_o^{CH} - \sigma_o^{CH_3}) + (\sigma_{RF}^{CH/CCl_4/LSR} - \sigma_{RF}^{CH_3/CCl_4/LSR})$$

$$+ (\sigma_{BI}^{CH/CCl_4/LSR} - \sigma_{BI}^{CH_3/CCl_4/LSR}) \qquad \text{..... 4.33}$$

$$\sigma^{CCl_4} - \sigma^{CCl_4/LSR} = (\sigma_{RF}^{CH/CCl_4} - \sigma_{RF}^{CH_3/CCl_4}) - (\sigma_{RF}^{CH/CCl_4/LSR} -$$

$$\sigma_{RF}^{CH_3/CCl_4/LSR}) + (\sigma_{BI}^{CH/CCl_4} - \sigma_{BI}^{CH_3/CCl_4}) - (\sigma_{BI}^{CH/CCl_4/LSR} -$$

$$\sigma_{BI}^{CH_3/CCl_4/LSR}) \qquad \text{..... 4.34}$$

Assuming that the reaction field term is negligible Tables 4.3, 4.5 and 4.6 should reflect the effect of the buffeting parameter σ_{BI}. It is evident from these tables that the largest chemical shift difference is 0.044 ppm for Ho $(Fod)_3$, with Dy $(Fod)_3$ showing a shift of 0.022ppm and the other LSR producing negligibly small shifts below 0.01ppm.

In Table 4.4 the chemical shift differences range between 0.1 and 0.31ppm, which on comparison with Table 4.3, 4.5 and 4.6 appear to reflect essentially the effect of bulk susceptibility with negligible buffeting. Chemical shifts measured for some of the above mentioned systems, using higher concentrations of LSR, show similar shift differences.

In a nutshell the results are contrary to the expectations of the author, clearly indicating that large solvent molecules do not necessarily produce large buffeting effect. This warrants further investigation into the relationship between the buffeting parameters and the molecular volume, which is addressed in the following section.

4.7 Effect of molecular volume of solvents on buffeting

The parameter $(2\beta - \xi)^2$ in equation 3.26 is relevant to the size of the solute and the solvent molecule and is one of the major factors affecting buffeting. Some sort of geometrical interpretation is necessary to visualize this effect.

LSR have large molecular volumes and therefore should result in significant values of β and ξ and normally produce large buffeting chemical shifts. The basic question one may ask is, why do LSR fail to produce appreciable shifts. The answer may emerge from an investigation of the buffeting parameter $(2\beta - \xi)^2$. To facilitate this the author proposes a two dimensional approach, which although essentially based on the method of calculating the parameters β and ξ suggested by Homer and Percival[39] is somewhat simpler.

4.7.1 Measurement of the buffeting parameters on the basis of the two-dimensional model

On the basis of the two dimensional model the solute and the solvent molecule are represented by circles corresponding to their relevant molecular volumes.

Let us consider one of the peripheral atoms of the solute molecule at the centre of a cartesian co-ordinate system with its centre lying at the origin (Figure 4.6). Let lines OX' and OY' represent the remaining part of the solute molecule, that restricts the mobility of the solvent molecules.

Let us consider various sizes of solvent molecules, represented by circles that can approach the solute atom quadrant of interest. The smaller the size of the solvent the smaller should be the degree of restriction, ie. small angle of contact θ. As the size of the solvent molecules is increased there comes a stage when, due to the large solvent molecules and a greater degree of restriction, (represented by the plane X' OY') it is no longer possible for the solvent molecule to maintain contact with the solute atom.

A set of readings was recorded for various sizes of solvent 'molecules' and from the angle of contact θ,β and ξ parameters were calculated using equations 4.18 and 4.19. The results are tabulated in Table 4.7. Regression of molar volumes of solvents on the parameter $(2\beta - \xi)^2$ is depicted in Figure 4.7.

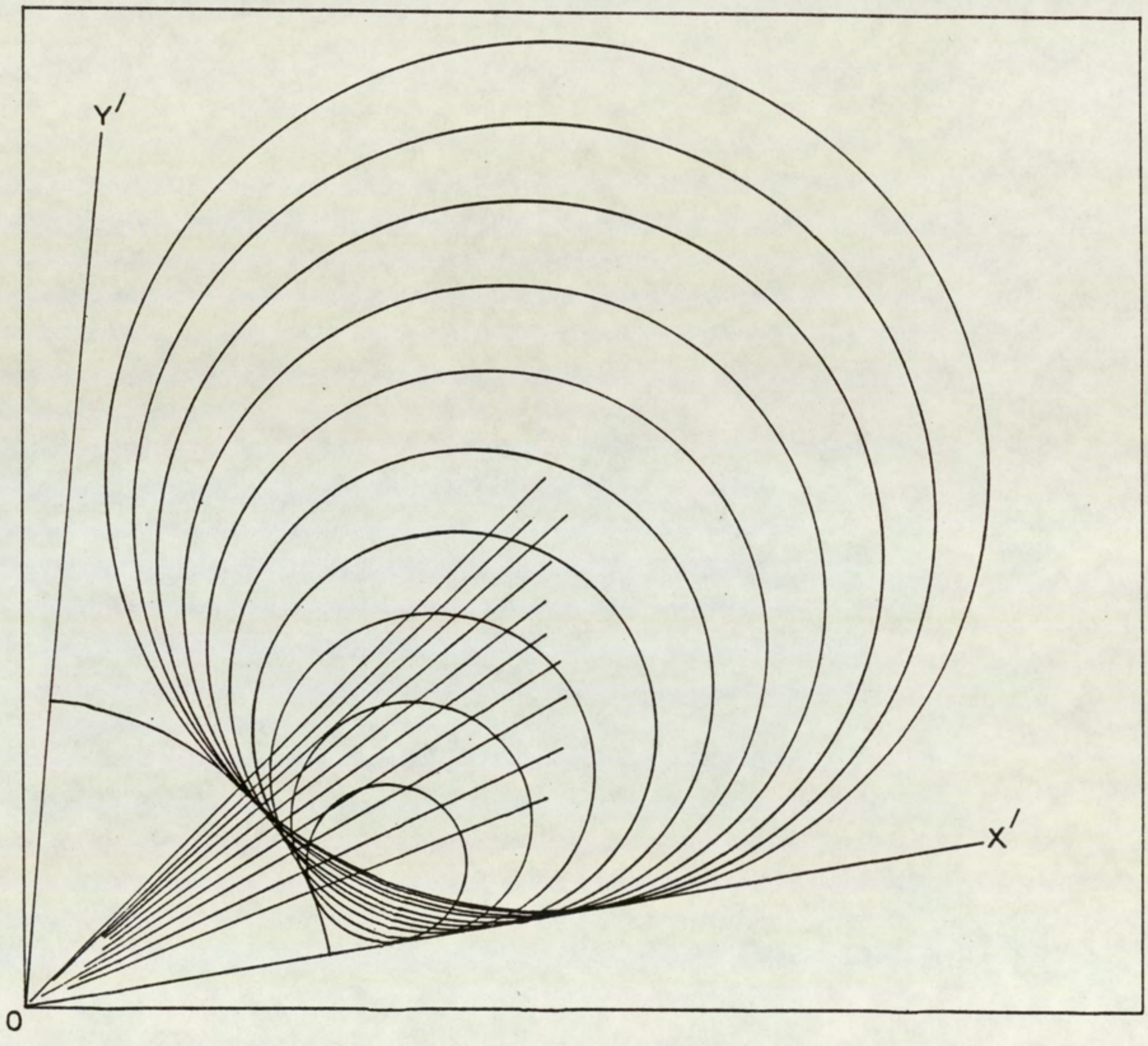

Figure 4.6: Representation of a two dimensional buffeting model

Table 4.7 - Values of $(2\beta - \xi)^2$ calculated from the angle of contact θ obtained on the basis of the condensed two dimensional model

Radius cm	Molar volume $cm^3 \times 10^{-2}$	Angle of contact θ°	α_c	β_c	$(2\beta_c - \xi_c)^2$
1.3	0.09	13.0	0.711	1	0.334
2	0.34	16.75	0.628	1	0.554
3	1.13	21.25	0.528	1	0.892
4	2.68	24.75	0.45	1	1.21
5	5.24	28.25	0.372	1	1.576
6	9.05	31.00	0.311	1	1.898
7	14.37	33.25	0.261	1	2.184
8	21.46	35.6	0.209	1	2.503
9	30.55	37.5	0.167	1	2.778
10	41.91	39.1	0.131	1	3.02
11	55.76	41.0	0.089	1	3.32
12	72.41	42.25	0.061	1	3.526

4.7.2 Interpretation of the results obtained by the two-dimensional model for buffeting

It is evident from Figure 4.7 that $(2\beta - \xi)^2$ increases significantly when the size of the solvent molecule is small compared to the solute molecules. As the size of the solvent molecules increases, the change in the parameter $(2\beta - \xi)^2$ tends to be relatively smaller. It appears that there comes a limiting stage when the change in $(2\beta - \xi)^2$ for very large molecules becomes negligible. This explains the failure of LSR to produce substantial chemical shifts despite the expectedly high value of K. It must be

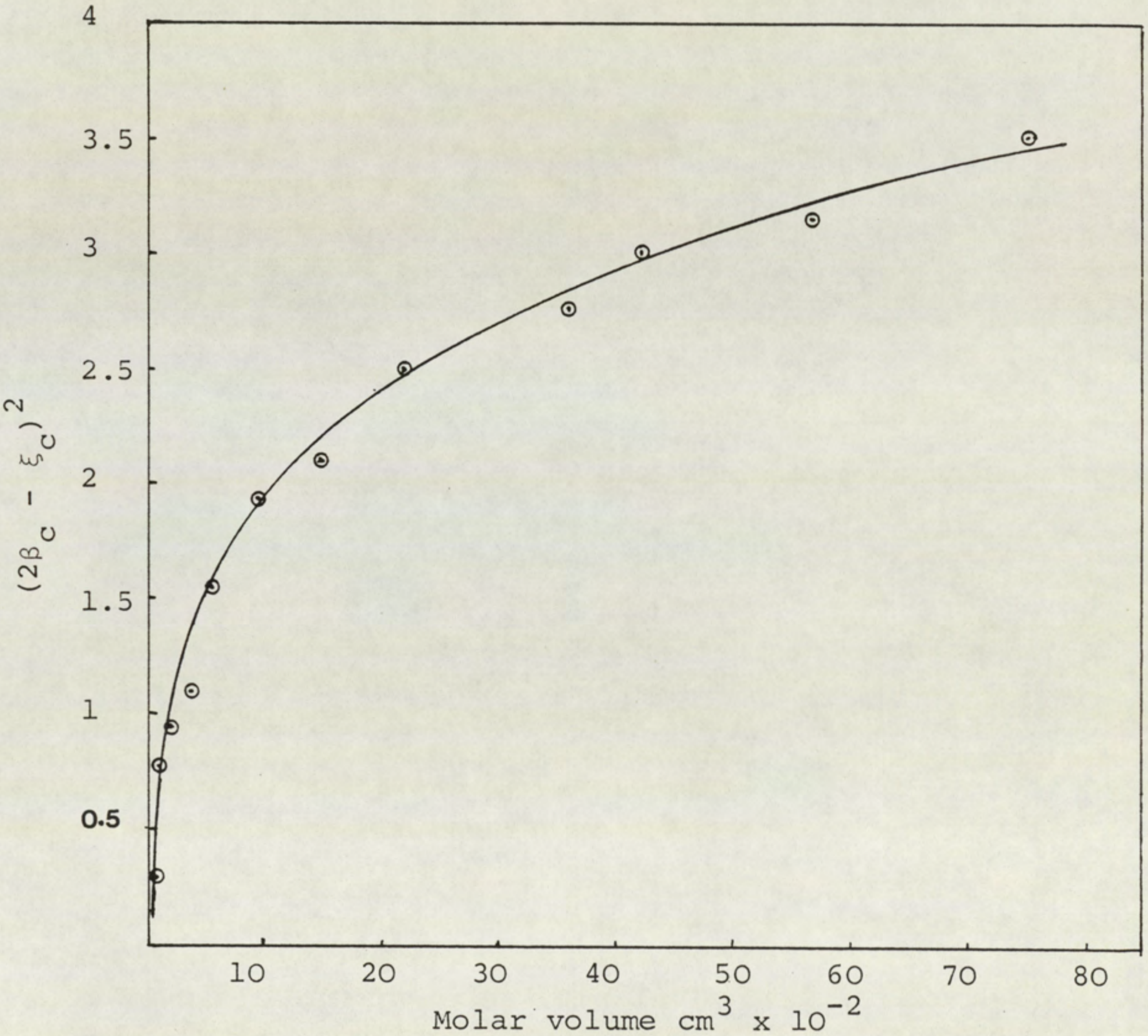

Figure 4.7: Regression of molar volume against $(2\beta_c - \xi_c)^2$ obtained from the condensed two dimensional buffeting model

emphasised that the two-dimensional model is purely an approximate model. In practice it is very difficult to draw all the possible combinations of the degree of restrictions that occur in real molecules. But this model does minimize the degree of human error which may occur during the measurement of β and ξ parameters according to the buffeting model suggested by Homer and Pervical[39].

The author feels that this model gives some insight into the effect of molecular volume on buffeting.

Although these results are based on the hypothetical sizes of the solute and solvent molecules, it is possible to encounter a similar situation in real molecules. Hence the results obtained should in no way alter the interpretation.

4.8 Conclusion

This chapter demonstrates that the buffeting screening, σ_{BI}, and thus the chemical shifts, do have marked dependence on the size of the solvent molecules, but there are factors which limit this effect.

Large values of K in equation 3.26 which should normally give large buffeting effect fail to do so.

Solvent molecules with large molecular volumes do not necessarily have large values for the parameter $(2\beta - \xi)^2$ and therefore may not contribute appreciable chemical shifts. There may be factors other than molecular volume, which may affect buffeting. For example, the detailed shape of the solute and the solvent molecules, internal rotations for the solute and the solvent molecules or the number and nature (atoms other than H such as Cl, Br, I etc) of the peripheral atoms of the solute and the solvent molecule. These possibilities will be investigated later.

CHAPTER FIVE

ASSESSMENT OF HOMER AND PERCIVAL'S BUFFETING THEORY AND REACTION FIELD THEORY

5.1 Introduction

The concept of buffeting has been successfully employed by Homer and Percival[39], to explain gas-to-solution NMR chemical shifts of van der Waals origin. So far no attempt has been made to study the effect of large solvent molecules on comparatively small solute molecules.

Although a fairly qualitative attempt was made to study the effect of large LSR molecules in Chapter 4 the intention now is to accurately determine the buffeting parameters of a wide cross section of solvents, using experimental shifts obtained in the author's laboratory. Before doing so, it is important to confirm the suitability of Homer's reaction field treatment of σ_w and illustrate that this approach does indeed reveal the necessity of introducing a term such as σ_{BI}that is embodied in σ_w.

The stepwise development of Homer's reaction field theory and the concept of the primary and secondary reaction fields have already been discussed in Section 3.4 (Chapter 3). Homer and Percival tested the validity of equation 3.18 by correlating the susceptibility corrected gas-to-solution chemical shifts for protons in the group IV B tetramethyls against the calculated reaction field $<R_T^2>$ for each system. The regression were linear with correlation coefficient close to unity and slopes in good agreement with the theoretical values of B (Table 3.2). This approach is extended in the following section.

5.2 Homer's Reaction Field

The physical constants requires to calculate the reaction fields according to equation 3.18 are tabulated in Table 5.1. The Homer and Percival total reaction field is analysed for the available σ_w data in Tables 5.2, 5.3 and 5.4.

Table 5.1: Physical Constants of the Species

Species	Molar volume cm^2/mole 30°C	Ref	I/ ev	Ref	α/ (A^3)	Ref	n^2 20°C	Ref
1,2,3,C_6H_3 $(CH_3)_3$	139	85	8.43	88	15.4	92	2.248	85
p-$C_6H_4(CH_3)_2$	125.2(35°C)	54	8.44	58	14.27	58	2.210	a
p-CH_3-C_6H_4F	111.0	85	8.80	b	12.28	c	2.1606	85
p-$C_6H_4F_2$	99.8(35°C)	93	9.15	c	10.29	c	2.054	a
$(CH_3)_2$ C = C $(CH_3)_2$	118.9	85	8.31	88	11.74	a	1.9943	85
CH_3 C = CCH_3	78.3	85	9.94	88	7.45	c	1.938	85
Si $(OCH_2CH_3)_4$	224.0(35°C)	94	9.25	d	20.40	c	1.8961	72
Si $(OCH_3)_4$	150.3(35°C)	94	9.25	d	12.90	c	1.8301	72
Si $(CH_2\,CH_3)_4$	191.3(35°C)	94	9.81	53	19.2	53	2.0357	85
Si $(CH_3)_4$	139.6	54	9.80	53	11.9	53	1.8266	67
Si Cl_4	117.2(35°C)	94	11.6	58	11.4	53	1.990	85
Si F_4	62.7	85	16.94	95	3.33	95	1.464	a
CH_4	33.6 (MP)	96	12.99	58	2.55	58	1.710	a
CF_4	66.8	85	17.81	95	2.89	95	1.2863	a
$CH_2\,Cl_2$	64.9	97	11.35	88	6.82	98	2.0294	85
C $(CH_3)_4$	131.4	51	10.36	53	10.2	53	1.7902	67
C $(CH_2\,CH_3)_4$	171.9	54	10.36	99	17.5	c	2.041	a
n-$C_5\,H_{12}$	115.2(20°C)	85	10.35	88	10.02	a	1.8428	85
Cyclo-C_5H_{10}	96.0(35°C)	85	10.53	88	9.1	53	1.978	85
C_6H_6	90.5(35°C)	85	9.24	58	10.39	58	2.242	85

Table 5.1 continued ...

C_6F_6	117.4(35°C)	93	9.97	85	10.1	99	1.8968	100
Cyclo-C_4F_8	116.0(0°C)	85	13.3	71	7.66	c	1.5136	101
n-C_6H_{14}	130.5(20°C)	85	10.18	85	12.9	c	1.8908	85
n-C_7H_{16}	146.5(20°C)	85	9.9	85	14.96	c	1.9256	85
Sn $(CH_2CH_3)_4$	199.2(35°C)	94	8.36	71	21.7	c	2.1362	a
SF_6	77.7	85	19.32	95	4.53	95	1.570	a
1,2-dichloro ethane	79.92	85	11.10	85	8.16	c	2.087	85
$CHCl_3$	81.17	97	11.62	85	8.12	102	2.091	85
1,1-dichloro ethane	85.3	85	11.10	85	8.16	c	2.006	85
CCl_4	97.0	94	11.42	58	10.5	58	2.114	85
1,1,2,2-tetrachloro-ethane	106.33	85	11.09	85	8.16	c	2.232	85
Cyclohexane	110.13	85	9.81	56	10.42	56	2.034	85
2,3-dimethyl butane	132.08	85	10.02	103	11.28	a	1.891	85
2-methyl pentane	133.49	85	10.09	103	11.28	c	1.88	85
2,2-dimethyl butane	134.08	85	10.06	103	11.28	c	1.874	85
Decalin	157.84	85	9.4	b	16.7	c	2.193	85
Bicyclohexyl	195.13	85	9.41	b	19.98	c	2.18	85
n-Decane	196.78	85	10.19	103	18.23	c	1.99	85
Hexadecane	295.37	85	10.19	b	28.65	c	2.055	85

a - estimated from Lorentz-Lorentz equation(104), using either α or n^2
b - estimated from data on similar compounds
c - estimated from bond polarizabilities given in ref 105

Table 5.2: Results of comparison between Expt $-\sigma_w$ (ppm) at 35°C (94) and $\langle R_T^2 \rangle \times 10^{-12}$ erg/cm^2 (ref: equation 3.18)

Solvent	$Si(OCH_2CH_3)_4$	$Si(OCH_3)_4$	$C(CH_3)_4$	$Si(OCH_2CH_3)_4$	$Si(CH_3)_4$	$Sn(CH_3)_4$	CH_4
Si (OEt_4)	0.160	0.182	0.173	0.193	0.217	0.270	0.295
$\langle R_T^2 \rangle$	0.059	0.067	0.070	0.059	0.067	0.072	0.186
Si $(oMe)_4$	0.155	0.198	0.190	0.190	0.252	0.272	0.310
$\langle R_T^2 \rangle$	0.067	0.074	0.077	0.067	0.074	0.079	0.181
Si $(Et)_4$	0.162	0.170	0.197	0.193	0.250	0.292	0.305
$\langle R_T^2 \rangle$	0.082	0.091	0.095	0.082	0.090	0.097	0.234
Sn (Et_4)	0.172	0.192	0.205	0.208	0.260	0.310	0.316
$\langle R_T^2 \rangle$	0.108	0.118	0.123	0.108	0.118	0.125	0.279
Sn (Me_4)	0.185	0.187	0.205	0.205	0.267	0.310	0.322
$\langle R_T^2 \rangle$	0.102	0.116	0.107	0.116	0.116	0.123	0.263
$SiCl_4$	0.188	0.200	0.223	0.228	0.298	0.325	0.346
$\langle R_T^2 \rangle$	0.142	0.150	0.154	0.142	0.150	0.156	0.286
CCl_4	0.302	0.332	0.345	0.349	0.375	0.433	0.472
$\langle R_T^2 \rangle$	0.206	0.216	0.220	0.206	0.215	0.223	0.373
Cor coeff	0.931	0.862	0.941	0.932	0.973	0.874	0.949
Slope (B)	0.940	1.026	1.042	1.041	0.960	1.037	0.800
Intercept	0.085	0.098	0.091	0.109	0.160	0.186	0.110

Table 5.3: Results of comparison between experimental σ_w at 35°C (66,94,106) and $\langle R_T^2 \rangle \times 10^{-12}$ erg/cm^3 (ref: equation 3.18)

	Solvents							
Solute	$SnEt_4$	$SiEt_4$	$SnMe_4$	$SiCl_4$	CCl_4	CC	Slope (B)	Intercept
C_5H_{10}	0.178	0.165	0.185	0.203	0.295			
$\langle R_T^2 \rangle$	0.156	0.124	0.150	0.181	0.252	0.982	0.1047	0.024
C_6H_6	0.273	0.240	0.277	0.293	0.443			
	0.169	0.135	0.162	0.192	0.265	0.980	1.578	0.014
$CH_3{\equiv}CCH_3$	0.300	0.277	0.288	0.318	0.477			
$\langle R_T^2 \rangle$	0.165	0.132	0.160	0.189	0.261	0.968	0.1633	0.035
$(CH_3)\,C = C\,(CH_3)_2$	0.232	0.218	0.230	0.237	0.340			
$\langle R_T^2 \rangle$	0.130	0.101	0.127	0.160	0.227	0.950	0.983	0.105
$C\underline{H}_3\,C_6H_4\,C\underline{H}_3$	0.267	0.242	0.268	0.283	0.423			
$\langle R_T^2 \rangle$	0.139	0.109	0.135	0.167	0.235	0.970	1.453	0.068
$CH_3\,\underline{C}_6\underline{H}_4\,CH_3$	0.230	0.200	0.227	0.245	0.340			
$\langle R_T^2 \rangle$	0.139	0.109	0.135	0.167	0.235	0.988	1.101	0.075
1,3,5 $C_6H_3\,(C\underline{H}_3)_2$	0.272	0.250	0.278	0.295	0.417			
$\langle R_T^2 \rangle$	0.131	0.102	0.128	0.161	0.228	0.977	1.333	0.102
1,3,5 $\underline{C}_6\underline{H}_3(CH_3)_3$	0.202	0.183	0.205	0.220	0.292			
$\langle R_T^2 \rangle$	0.131	0.102	0.128	0.161	0.228	0.989	0.862	0.092
$F\text{-}\underline{C}_6\underline{H}_4\text{-}F$	0.287	0.253	0.290	0.315	0.492			
$\langle R_T^2 \rangle$	0.150	0.119	0.145	0.176	0.246	0.979	0.910	0.007
$Sn\,(CH_2C\underline{H}_3)_4$	0.207	-	0.187	0.205	0.282			
$\langle R_T^2 \rangle$	0.121	0.093	0.119	0.152	0.218	0.956	0.872	0.087
$Si\,(CH_2C\underline{H}_3)_4$	-	0.153	0.153	0.162	0.257			
$\langle R_T^2 \rangle$	0.113	0.086	0.112	0.146	0.211	0.922	0.864	0.061

Table 5.4: Results of comparison between experimental ^{19}F-σ_w (ppm) at 35°C (66, 93, 71) and $<R_T^2> \times 10^{-12}$ erg/cm^2 (ref: equation 3.18)

Solvent	Solute CF_4	SF_6	SiF_4	P-Me-C_6H_4F	P-$C_6H_4F_2$	C_6F_6
Si $(OEt)_4$	5.97	6.36	8.95	5.74	6.12	6.31
$<R_T^2>$	0.082	0.110	0.108	0.087	0.090	0.077
Si $(OEt)_4$	5.54	5.96	8.31	5.21	5.77	5.16
$<R_T^2>$	0.088	0.113	0.111	0.092	0.095	0.084
Si $(Et)_4$	6.00	6.35	9.82	6.98	7.21	7.16
$<R_T^2>$	0.109	0.143	0.140	0.115	0.119	0.104
Sn $(Et)_4$	6.26	6.70	9.12	7.25	7.43	7.21
$<R_T^2>$	0.138	0.177	0.173	0.146	0.150	0.133
Sn $(Me)_4$	6.82	7.05	10.05	7.61	7.74	7.89
$<R_T^2>$	0.135	0.170	0.167	0.142	0.145	0.130
$SiCl_4$	6.85	7.03	10.10	7.83	7.96	8.45
$<R_T^2>$	0.167	0.199	0.197	0.173	0.176	0.162
CCl_4	7.60	7.98	11.15	8.14	8.27	8.81
$<R_T^2>$	0.235	0.273	0.270	0.243	0.246	0.230
Cor coeff	0.939	0.957	0.882	0.850	0.869	0.859
Slope (B)	12.40	11.21	14.60	17.29	15.15	20.59
Intercept	4.74	4.88	7.20	4.50	5.00	4.58

5.2.1 Interpretation of the Results

From the results of the regression given in Tables 5.2, 5.3 and 5.4 the following inferences can be made:

1 Homer and Percival RF Model appears to be the only pure RF formulation for σ_w that apparently works for nearly all the systems (with the exception of some ^{19}F systems) and gives regressions with reasonable correlation coefficients.

2 The slopes or B values with the overall average of 1.06 ± 0.3 for ^1H are in agreement with literature values, such as the empirical value of 1.06 found by Raynes et al[28] for hydrocarbons.

The B values are not constant and vary by a factor of 2.46 (0.774 to 1.91). Some of this variation is due to the site of the hydrogen atom in the molecule, for example, compare the ring and methyl hydrogens of 1,2,3-$C_6H_3(CH_3)_3$. The B value of $(16.9 \pm 4.4) \times 10^{-12}$ cm^3/erg for ^{19}F agrees well with the Kromhout and Linder[107] value of B = 18 for the CF_4 ... CF_4 interaction.

3 The distinctive feature of the RFT is the existance of positive intercepts for the regressions for all the systems as is shown in Tables 5.2, 5.3 and 5.4. These intercepts led Homer and Percival to the rediscovery of a well known effect in liquid and solid state theories, namely the interaction between the peripheral atoms of solvent and solute molecules, accordingly the characterization of σ_w must be changed to

$$\sigma_w = - B \langle R_T{}^2 \rangle + \text{Intercept} \qquad \ldots.. \; 5.2$$

which is essentially the source for the development of equation 3.6, ie.

$$\sigma_w = \sigma_{RF} + \sigma_{BI}$$

It appears reasonable, therefore, to accept Homer and Percival's contention that σ_w embraces both a reaction field and a buffeting screening term. The intention now is to examine more closely the buffeting screening term for a selected solute in a range of solvents. This procedure involves three stages, viz:

1 The determination of the buffeting parameter $(2\beta_T - \xi_T)^2$.

2 The evaluation of σ_{RF}.

3 Measurement of gas-to-liquid shifts and corrections of these for bulk susceptibility.

These various stages will now be addressed in the order stated, because various factors implicit in 1 dictate the choice of suitable solute solvent systems.

5.3 Measurement of the Geometrical Parameters ß and ξ

The geometrical parameters ß and ξ were measured according to Homer and Percival's "buffeting model" as described in Section 4.3 (Chapter 4).

The solvent, considered as a sphere of the appropriate size with the solvent hydrogen atoms around the periphery, is envisaged to encounter the solute hydrogen atom of interest from two different aspects with equal probability. The two encounter aspects are depicted in Figures 5.1 and 5.2 with the total ß and ξ values calculated in terms of one octant, consistent with the theory described in Chapter 3.

The most reliable way of predicting ß and ξ has been found to be by the use of a 'Courtauld Atomic model' of the solute molecule and spheres of appropriate size[108] for the encountering solvent molecule. The ß and ξ's estimated in this way are probably not very accurate but thought to be a reasonably good estimate for the purpose of this study.

The example in Figures 5.1 and 5.2 represents a TMS solute molecule encountered by an isotropic solvent molecule(s). Let us consider a three dimensional Courtauld model representing TMS as a solute molecule. One of the methyl groups is assumed to be fixed in space, while the rest of the TMS molecule is free to rotate. Let us consider one of the hydrogen atoms of the fixed methyl group and divide it into four octants. A sphere representing a solvent molecule, can approach this hydrogen atom from within all four octants (see Figure 5.1). However the solvent molecule will experience varying degrees of restriction due to the structure of the solute molecule. A 'snap shot' of the situation will enable us to measure four different angles of contact between the solvent sphere and the peripheral hydrogen atom, thus enabling us to calculate four values of ß and ξ's. If the position of the rest of the TMS molecule is altered, with respect to the fixed methyl group, the degree of restriction will change at least in one of the four quardrant of interest and hence a different set of four angles of

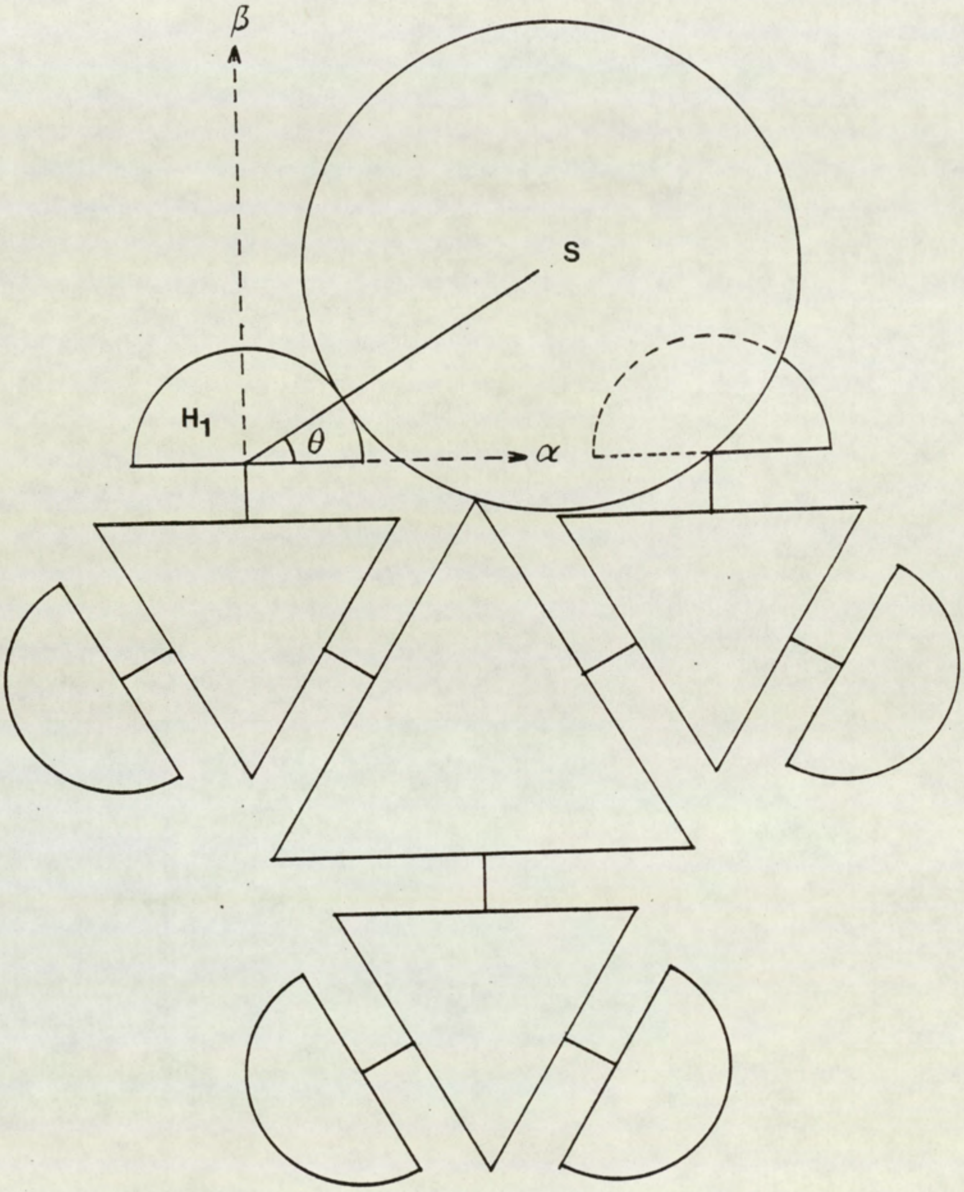

Figure 5.1: Two dimensional representation of a TMS (solute) molecule encountered by an isotropic solvent molecule (solvent molecule in contact with the resonant solute ^1H).

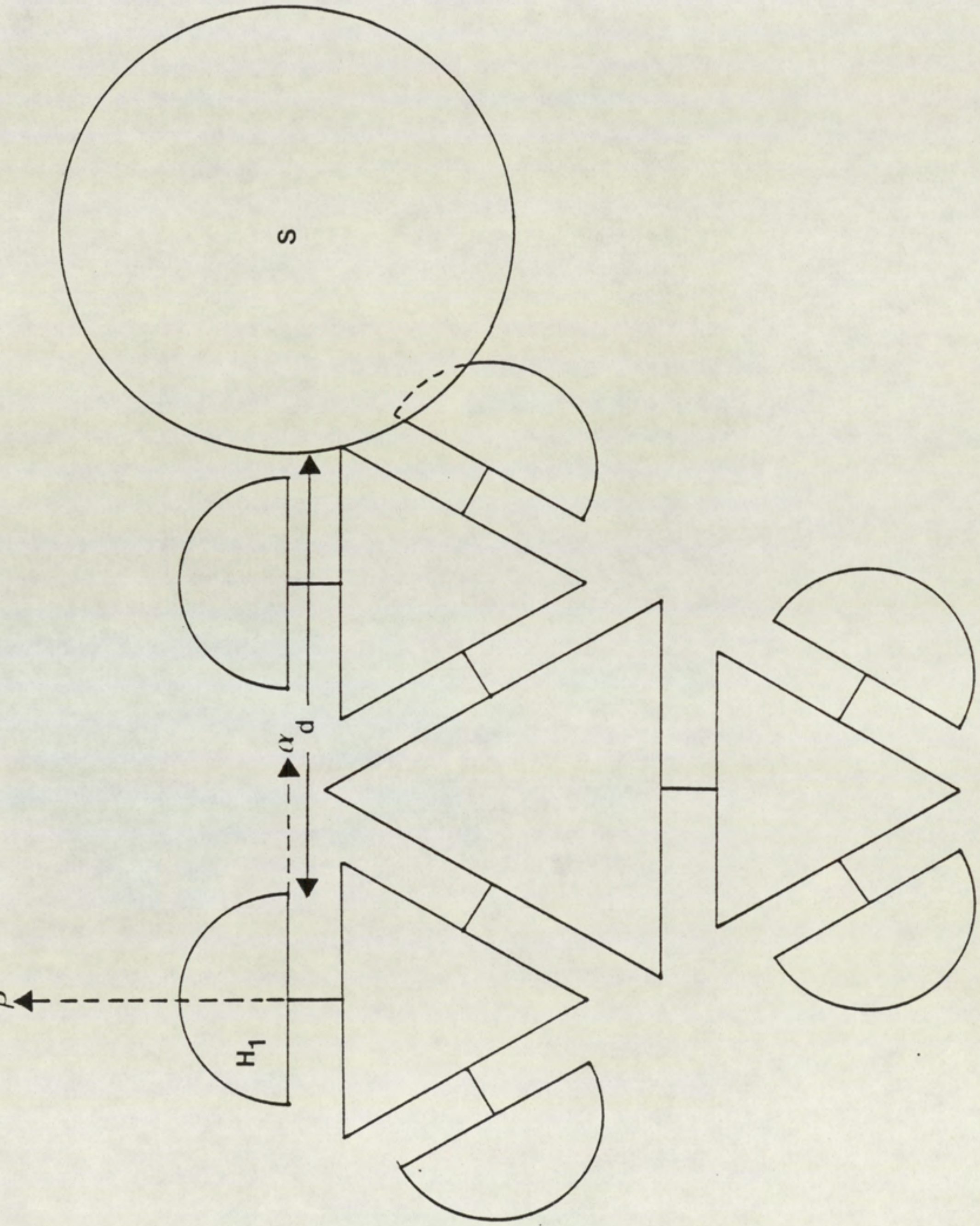

Figure 5.2: Two dimensional representation of a TMS (solute) molecule encountered by an isotropic solute molecule (solvent molecule at a distance d from resonant solute ^{1}H)

contact can be measured. It has been observed that a set of twelve different values of ß and ξ must be considered to provide a realistic estimation of all the geometrical restrictions which a solvent may encounter while approaching a TMS solute molecule. $(2\beta_c - \xi_c)^2$ for each angle of contact must be calculated and then averaged to obtain the precise value of the contact value of the buffeting factor.

To calculate the total value of $(2\beta_T - \xi_T)^2$ the solvent molecule is moved away from the hydrogen atom of interest, while still in contact with the rest of the TMS solute molecule (see Figure 5.2). The distance 'd' (which is the distance between the centre of the hydrogen atom under consideration and the centre of the peripheral atom of the solvent sphere) is then measured. From the value of the angle of contact (Figure 5.2) and the distance d (Figure 5.2), the distance modulated value of the buffeting parameter, $(2\beta_T - \xi_T)^2$ is calculated using equations (4.18, 4.19). The distance modulated value $(2\beta_T - \xi_T)^2$ for each angle of contact and distance d is then averaged to obtain the overall degree of accessibility of a solute nucleus.

5.3.1 Consideration of solvent molecules with peripheral atoms other than hydrogen

If the so called 'buffeting' solvent atom is changed from hydrogen to an atom with more electrons (for example chlorine) it may be expected(109,110) that the effect of 'buffeting' will be greater. However the general theory of buffeting is built up around a theory of hydrogen atom-hydrogen atom encounters and such an extension to other situations on an *ab initio* basis would be a formidible task on account of the increased number of electrons. Yonemoto(111) suggested a Hartee-fock scaling factor, Q, which is equal to unity for a hydrogen atom and is replaced by

$$Q = \frac{\langle \Sigma X_i^2 \rangle}{a_o^2}$$

for atoms such as the halogens. These values of Q can be multiplied into equation 3.26 to obtain the 'buffeting effect' of a non-hydrogen atom. However, the value of Q must be distance modulated by the sums of the van der Waals radii of the interacting atoms in the appropriate way. Homer and Percival[39] modified their equation (3.26) in more general terms to account for this and decided that:

$$\sigma_{BI} = \frac{-B\,K^H}{r^6_{HH}} \left(2\beta_T - \xi_T\right)^2 Q^x \left[\frac{r_{HH}}{r_{HX}}\right]^6 \qquad ..... \; 5.2$$

where X refers to the interacting solvent atom.

In order to test the validity of equation 5.2 some solvents with peripheral cholorine atoms have been selected for investigation.

5.3.2 Choice of the solute and the solvents

Measurement of the parameters ß and ξ is a very tedious process and demands extreme caution. It can be very taxing and extremely difficult to measure these parameters specially if a linear or non-symmetrical molecule is selected as a solute. Even for a symmetrical solute molecule at least twelve different measurements are required to calculate these parameters for each solute atom with one chosen solvent. For non symmetrical molecules, it may be necessary to measure between twenty four and sixty different ß and ξ's. Hence TMS was an ideal choice for the present investigation.

As mentioned in Section 4.3 (Chapter 4) Homer and Percival assume that all the solvent molecules can be represented by spheres proportional to their relevant molecular volumes. Difficulties in selecting the solvents are drastically reduced due to this simple assumption. Hence, a wide range of solvents with varying shapes and molecular volumes were selected.

Measurement and calculations of the buffeting parameters for various solvents in TMS solute are reported in Table 5.5. Three sets of four readings encountered by a solute atom from all four octants, are systematically enlisted reflecting the changes in values of ß and ξ due to three different orientations of the $Si(CH_3)_3$ fragment of the TMS (solute) molecule. For solvent having similar molar volumes the same value of $(2ß_T - \xi_T)^2$ is reported.

In the case of solvents containing peripheral chlorine atoms, $(2ß_T - \xi_T)^2$ is calculated by using the modified equation 5.2 for various values of Hartree Fock scaling factor Q which reflects 'the buffeting effect' of non-hydrogen atoms. Buffeting parameters for different Q values are listed in Table 5.11.

Table 5.5: Measurement and calculation of the buffeting parameter $(2\beta_T - \xi_T)^2$ for TMS (solute) in various solvents

Solvents: 2,2-dimethyl butane
2,3-dimethyl butane
2-Methyl pentane

Angle of contact θ°	α_c	β_c	$(2\beta_c-\xi_c)^2$	distance Å	α_T	β_T	$(2\beta_T-\xi_T)^2$
			ORIENTATION A				
83.08	0	0.1538	0.0946	3.42	0.1387	0.2712	0.0702
20.05	0.5544	1	0.7944	1.38	0.6934	1	0.3761
14.32	0.6817	1	0.4053	0.3	0.9084	1	0.0336
20.05	0.5544	1	0.7944	1.38	0.6934	1	0.3761
			ORIENTATION B				
68.75	0	0.4721	0.8916	3.66	0.1299	0.5407	0.675
20.05	0.5544	1	0.7944	1.38	0.6934	1	0.3761
14.32	0.6817	1	0.4053	0.3	0.9084	1	0.0336
20.05	0.5544	1	0.7944	1.38	0.6934	1	0.3761
			ORIENTATION C				
83.08	0	0.1538	0.0946	3.48	0.1364	0.2692	0.0706
20.05	0.5544	1	0.7944	1.38	0.6934	1	0.3761
14.32	0.6817	1	0.4053	0.3	0.9084	1	0.0336
20.05	0.5544	1	0.7944	1.38	0.6934	1	0.3761

Average $(2\beta_T - \xi_T)^2$: 0.2644

Table 5.5 cont ...

Solvent: TMS

Angle of contact θ°	α_c	β_c	$(2\beta_c-\xi_c)^2$	distance Å	α_T	β_T	$(2\beta_T-\xi_T)^2$
			ORIENTATION A				
83.08	0	0.1538	0.0946	4.02	0.1185	0.2541	0.0735
22.92	0.4907	1	1.0375	1.2	0.6676	1	0.442
15.76	0.6499	1	0.4904	0.3	0.8992	1	0.0406
22.92	0.4907	1	1.0375	1.2	0.6676	1	0.442
			ORIENTATION B				
68.75	0	0.4721	0.8916	4.26	0.112	0.5312	0.703
22.92	0.4907	1	1.0375	1.2	0.6676	1	0.442
15.76	0.6499	1	0.4904	0.3	0.8992	1	0.0406
22.92	0.4907	1	1.0375	1.2	0.6676	1	0.442
			ORIENTATION C				
83.08	0	0.1538	0.0946	4.02	0.1185	0.2541	0.0735
22.92	0.4907	1	1.0375	1.2	0.6676	1	0.442
15.76	0.6499	1	0.4904	0.3	0.8992	1	0.0406
22.92	0.4907	1	1.0375	1.2	0.6676	1	0.442

Average $(2\beta_T - \xi_T)^2$: 0.302

Table 5.5 cont ...

Solvent: Decalin

Angle of contact θ°	α_c	β_c	$(2\beta_c-\xi_c)^2$	distance Å	α_T	β_T	$(2\beta_T-\xi_T)^2$
			ORIENTATION A				
83.08	0	0.1538	0.0946	4.56	0.1048	0.2424	0.0758
24.35	0.4589	1	1.171	1.32	0.6337	1	0.5368
17.19	0.618	1	0.5836	0.48	0.8465	1	0.0943
24.35	0.4589	1	1.171	1.32	0.6337	1	0.5368
			ORIENTATION B				
68.75	0	0.4721	0.8916	4.74	0.1008	0.4681	0.5395
24.35	0.4589	1	1.171	1.32	0.6337	1	0.5368
17.19	0.618	1	0.5836	0.48	0.8465	1	0.0943
24.35	0.4589	1	1.171	1.32	0.6337	1	0.5368
			ORIENTATION C				
83.08	0	0.1538	0.0946	4.62	0.1034	0.2413	0.0761
24.35	0.4589	1	1.171	1.32	0.6337	1	0.5368
17.19	0.618	1	0.5836	0.48	0.8465	1	0.0943
24.35	0.4589	1	1.71	1.32	0.6337	1	0.5368

Average $(2\beta_T - \xi_T)^2$: 3496

Table 5.5 cont ...

Solvent: Bicylohexyl
Solvent: Decane

Angle of contact θ°	α_c	β_c	$(2\beta_c-\xi_c)^2$	distance Å	α_T	β_T	$(2\beta_T-\xi_T)^2$
			ORIENTATION A				
88.81	0	0.0265	0.0028	4.92	0.0972	0.1211	0.0023
25.78	0.427	1	1.313	1.62	0.5839	1	0.6925
22.92	0.4907	1	1.0375	0.66	0.7512	1	0.2477
25.78	0.427	1	1.313	1.62	0.5839	1	0.6925
			ORIENTATION B				
74.48	0	0.3448	0.4755	5.22	0.9167	0.4049	0.3923
25.78	0.427	1	1.313	1.62	0.5839	1	0.6925
22.92	0.4907	1	1.0375	0.66	0.7512	1	0.2477
25.78	0.427	1	1.313	1.62	0.5839	1	0.6925
			ORIENTATION C				
91.67	0	0.0372	0.0055	5.04	0.0949	0.06125	0.0045
25.78	0.427	1	1.313	1.62	0.5839	1	0.6925
22.92	0.4907	1	1.0375	0.66	0.7521	1	0.2477
25.78	0.427	1	1.313	1.62	0.5839	1	0.6925

Average: $(2\beta_T - \xi_T)^2$: 0.4414

Table 5.5 cont ...

Solvent: Hexadecane

Angle of contact θ°	α_c	$ß_c$	$(2ß_c-\xi_c)^2$	distance Å	α_T	$ß_T$	$(2ß_T-\xi_T)^2$
			ORIENTATION A				
91.67	0	0.0372	0.0055	5.22	0.0917	0.0579	0.0046
31.51	0.2997	1	1.961	1.74	0.4803	1	1.0806
27.22	0.395	1	1.463	0.78	0.676	1	0.4192
31.51	0.2997	1	1.961	1.74	0.4803	1	1.0806
			ORIENTATION B				
77.35	0	0.2811	0.3161	5.52	0.0867	0.3435	0.2637
31.51	0.2997	1	1.961	1.74	0.4803	1	1.0806
27.22	0.395	1	1.463	0.78	0.676	1	0.4192
31.51	0.2997	1	1.961	1.74	0.4803	1	1.0806
			ORIENTATION C				
91.67	0	0.0372	0.0055	5.28	0.0906	0.0568	0.0046
31.51	0.2997	1	1.961	1.74	0.4803	1	1.0806
27.22	0.395	1	1.463	0.78	0.676	1	0.4192
31.51	0.2997	1	1.961	1.74	0.4803	1	1.0806

Average: $(2ß_T - \xi_T)^2$: 0.6678

Table 5.5 cont ...

Solvent: Chloroform
Solvent: 1,2,-dichloro ethane

Angle of contact θ°	α_c	$ß_c$	$(2ß_c-\xi_c)^2$	distance Å	α_T	$ß_T$	$(2ß_T-\xi_T)^2$
			ORIENTATION A				
80.21	0	0.2175	0.1892	2.7	0.1737	0.3534	0.1292
14.32	0.6817	1	0.4053	0.84	0.823	1	0.1253
11.46	0.7454	1	0.2594	0.24	0.9384	1	0.0152
14.32	0.6817	1	0.4053	0.84	0.823	1	0.1253
			ORIENTATION B				
68.75	0	0.4721	0.8916	2.82	0.1667	0.5601	0.6191
14.32	0.6817	1	0.4053	0.84	0.823	1	0.1253
11.46	0.7454	1	0.2594	0.24	0.9284	1	0.0152
14.32	0.6817	1	0.4053	0.84	0.823	1	0.1253
			ORIENTATION C				
80.21	0	0.2175	0.1892	2.7	0.1737	0.3534	0.1292
14.32	0.6817	1	0.4053	0.84	0.823	1	0.1253
11.46	0.7454	1	0.2594	0.24	0.9384	1	0.0152
14.32	0.6817	1	0.4053	0.84	0.823	1	0.1253

Average: $(2ß_T - \xi_T)^2$: 0.1396

Table 5.5 cont ...

Solvent: 1,1-dichloro ethane

Angle of contact $\theta°$	α_c	β_c	$(2\beta_c-\xi_c)^2$	distance Å	α_T	β_T	$(2\beta_T-\xi_T)^2$
			ORIENTATION A				
80.21	0	0.2175	0.1892	2.73	0.1719	0.3520	0.1297
14.32	0.6817	1	0.4053	0.9	0.8169	1	0.1341
11.46	0.7454	1	0.2594	0.3	0.9267	1	0.0215
14.32	0.6817	1	0.4053	0.9	0.8169	1	0.1341
			ORIENTATION B				
68.75	0	0.4721	0.8916	2.82	0.1667	0.5601	0.6191
14.32	0.6817	1	0.4053	0.9	0.8169	1	0.1341
11.46	0.7454	1	0.2594	0.3	0.9267	1	0.0215
14.32	0.6817	1	0.4053	0.9	0.8169	1	0.1341
			ORIENTATION C				
80.21	0	0.2175	0.1892	2.73	0.1719	0.3520	0.1297
14.32	0.6817	1	0.4053	0.9	0.8169	1	0.1341
11.46	0.7454	1	0.2594	0.3	0.9267	1	0.0215
14.32	0.6817	1	0.4053	0.9	0.8169	1	0.1341

Average: $(2\beta_T - \xi_T)^2P$: 0.1456

Table 5.5 cont ...

Solvent: Carbon Tetrachloride

Angle of contact θ°	α_c	β_c	$(2\beta_c-\xi_c)^2$	distance Å	α_T	β_T	$(2\beta_T-\xi_T)^2$
			ORIENTATION A				
83.08	0	0.1538	0.0946	2.76	0.1701	0.2978	0.0652
17.19	0.618	1	0.5836	0.96	0.7735	1	0.2052
14.13	0.6817	1	0.4053	0.3	0.9084	1	0.0336
17.19	0.618	1	0.5836	0.96	0.7735	1	0.2052
			ORIENTATION B				
68.75	0	0.4721	0.8916	2.88	0.1634	0.5583	0.6240
17.19	0.618	1	0.5836	0.96	0.7735	1	0.2052
14.13	0.6817	1	0.4053	0.3	0.9084	1	0.0336
17.19	0.618	1	0.5836	0.96	0.7735	1	0.2052
			ORIENTATION C				
83.08	0	0.1538	0.0946	2.76	0.1701	0.2978	0.0652
17.19	0.618	1	0.5836	0.96	0.7735	1	0.2052
14.13	0.6817	1	0.4053	0.3	0.9084	1	0.0336
17.19	0.618	1	0.5836	0.96	0.7735	1	0.2052

Average: $(2\beta_T - \xi_T)^2$: 0.1739

Table 5.5 cont ...

Solvent: Cyclohexane
Solvent: 1,1,2,2-tetra chloro ethane

Angle of contact θ°	α_c	$ß_c$	$(2ß_c-\xi_c)^2$	distance Å	α_T	$ß_T$	$(2ß_T-\xi_T)^2$
			ORIENTATION A				
83.08	0	0.1538	0.0946	3.06	0.1543	0.2844	0.0677
17.19	0.618	1	0.5836	1.08	0.761	1	0.2279
14.33	0.6817	1	0.4053	0.3	0.9084	1	0.0336
17.19	0.618	1	0.5836	1.08	0.761	1	0.2279
			ORIENTATION B				
68.75	0	0.4721	0.8916	3.18	0.1487	0.5506	0.6461
17.19	0.618	1	0.5836	1.08	0.761	1	0.2279
14.33	0.6817	1	0.4053	0.3	0.9084	1	0.0336
17.19	0.618	1	0.5836	1.08	0.761	1	0.2279
			ORIENTATION C				
83.08	0	0.1538	0.0946	3.06	0.1543	0.2844	0.0677
17.19	0.618	1	0.5836	1.08	0.761	1	0.2279
14.33	0.6817	1	0.4053	0.3	0.9084	1	0.0336
17.19	0.618	1	0.5836	1.08	0.761	1	0.2279

Average: $(2ß_T - \xi_T)^2$: 0.1875

5.4 The Evaluation of Reaction Field

The reaction field values used to correct the experimental chemical shifts in the author's laboratory were calculated using equation 3.18 and are tabulated in Table 5.6 (number of decimal places quoted are not intended to imply accuracy, but are left to avoid rounding up errors).

Table 5.6: Primary $\langle R_1^2 \rangle$, Secondary $\langle R_2^2 \rangle$ and Total Reaction Field $\langle R_T^2 \rangle$ for TMS (Solute) in different solvents

Solvent	Primary reaction field $\langle R_1^2 \rangle \times 10^{12}$ esu	Secondary reaction field $\langle R_2^2 \rangle \times 10^{12}$ esu	Total reaction field $\langle R_T^2 \rangle \times 10^{12}$ esu
1,2-dichloro ethane	3.9054	28.1402	32.0456
$CHCl_3$	3.9237	28.2725	32.1963
1,1-dichloroethane	3.5333	21.0621	24.5954
CCl_4	4.0308	23.0634	27.0942
1,1,2,2-tetrachloroethane	4.5649	23.1969	27.7620
Cyclohexane	3.6621	12.5299	16.1921
2,3-dimethyl butane	3.0037	6.8222	9.8258
2-Methyl pentane	2.9531	6.5469	9.4999
2,2,-dimethyl butane	2.9255	6.3002	9.2257
TMS	2.708	5.416	8.124
Decalin	4.3905	9.1239	13.5144
Bicyclohexyl	4.3297	6.1020	10.4317
n-Decane	3.4679	4.5504	8.0183
Hexadecane	3.7586	2.6558	6.4145

5.5 Gas-to-liquid NMR Chemical Shifts

The factors affecting the nuclear screening constant (σ) were discussed in Section 1.10.1 (Chapter One). To study the effect of the reaction field and buffeting interaction equations 4.24 and 3.6 have been utilized in the present chapter, ie.

$$\sigma_{soln} = \sigma_o + \sigma_b + \sigma_w \qquad \text{..... 4.24}$$

and

$$\sigma_w = \sigma_{RF} + \sigma_{BI} \qquad \text{..... 3. 6}$$

Substituting σ_w in equation 4.24:

$$\sigma_{soln} = \sigma_o + \sigma_b + \sigma_{RF} + \sigma_{BI} \qquad \text{..... 5.3}$$

So that

$$\delta_{g\text{-}1} = \sigma_b + \sigma_{RF} + \sigma_{BI}$$

Assuming that σ_b, σ_{RF} and σ_{BI} effects are negligible in the gas phase, to obtain $\delta_{g\text{-}1}$ it is first necessary to determine the shift of the chosen solute (in this case TMS) at zero pressure in the gas phase and then at effectively infinite dilution in the chosen solvents.

5.5.1 Experimental Measurement of the Gas Phase Shifts of ^1H of TMS

To ensure that there was negligible dissolved oxygen which could contribute to the shifts, possibly due to σ_b the TMS samples were prepared in 10mm OD NMR tubes under vacuum, using special glassware as described in Section 4.4.2 (Chapter 4).

The gas phase shifts of ^1H of TMS, measured on JEOL FX 90Q FT NMR spectrometer at various pressures, are given in Table 5.7. The data were extrapolated as shown in Figure 5.3 to zero pressure and values obtained are given in Table 5.8. These values were used in subsequent analysis.

Table 5.7 - Proton gas shifts of TMS at different pressures. Measurements were made using a JEOL FX 90Q FT NMR spectrometer locked onto ^2H of D_2O, at 30°C operating at an irradiation frequency of 89.60405 MHz

TMS sample	^1H shift/Hz
Gas P = 16cm Hg	125.49
Gas P = 24cm Hg	124.51
Gas P = 33cm Hg	124.51
Gas P = 47cm Hg	123.78

Table 5.8 - Gas-to-liquid chemical shifts for ^{1}H in TMS. Measurements were made on JEOL FX 90Q FT NMR spectrometer at 30˚C operating at an irradiation frequency of 89.60405 MHz

Sample	^{1}H shift/Hz
σ_o = Gas (P = O) (Hz)	126.2
Observed δ liquid (Hz)	0.98
$-2\pi/3\chi_v$	100.59
True δ liquid (Hz)	101.57
δ gas to liquid (Hz)	-24.63
δ gas to liquid (ppm)	-0.275

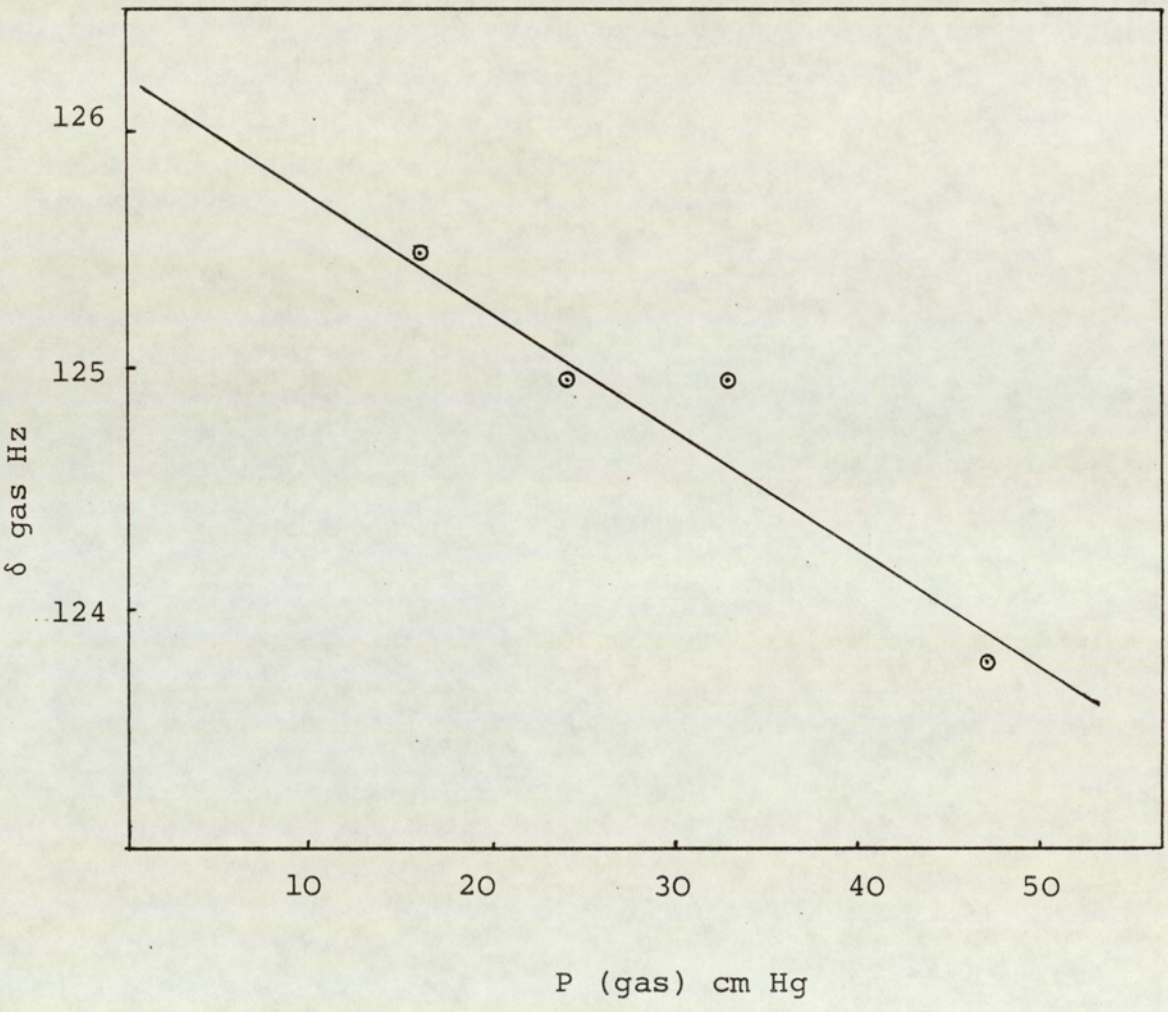

Figure 5.3: Evaluation of Proton gas shift at zero pressure for TMS

5.5.2 Liquid Phase Shifts

All the samples investigated were prepared at effectively infinite dilution to eliminate any effects of concentration. As TMS has been used as a solute, throughout the investigation, a concentration of 0.5M TMS in various solvents has been maintained.

To ensure that there was negligible dissolved oxygen that could contribute to the shifts, the samples were prepared and sealed under vacuum. The transference of the solution to NMR tube under vacuum was effected using special glassware designed for this purpose. The procedure was discussed in detail in Section 4.4.2, (Chapter Four).

The magnetic susceptibilities of the species being investigated are reported in Table 5.9.

The observed gas-to-liquid shifts corrected for bulk susceptibility are cited in Table 5.10 along with total reaction field and the buffeting parameters $(2\beta_T - \xi_T)^2$.

Table 5.9: Magnetic susceptibilities of the species

	$-X_v \times 10^{-6}$(20°C)
1,2-dichloro ethane	0.757
$CHCl_3$	0.740
1,1-dichloro ethane	0.681
CCl_4	0.691
1,1,2,2-tetra chloro ethane	0.856
Cyclohexane	0.627
Si Me_4	0.536
Decalin	0.6814
Bicyclohexyl	0.6889
n-Decane	0.6143
Hexadecane	0.6421
2,3-dimethyl butane	0.5853
2-Methyl pentane	0.5705
2-2 dimethyl butane	0.5744

Collected from reference (85)

Table 5.10: Values of experimental shifts $-\sigma_W$ (corrected for bulk susceptibility) and reaction field $\langle R_T^2 \rangle$ for various solvents in TMS (solute) at 30°C

Solvent	$-\sigma_W$ ppm	$-B^* \langle R_T^2 \rangle$ ppm	$-\sigma_W - B \langle R_T^2 \rangle$
1,2-dichloroethane	0.347	0.2788	0.0682
$CHCl_3$	0.347	0.2801	0.0669
1,1-dichloroethane	0.340	0.214	0.126
CCl_4	0.376	0.2357	0.1403
1,1,2,2-tetrachloro-ethane	0.350	0.2415	0.1085
Cyclohexane	0.283	0.141	0.142
2,3-dimethyl butane	0.254	0.0855	0.169
2,2-dimethyl butane	0.260	0.0803	0.18
2-Methyl pentane	0.260	0.0827	0.177
Si Me_4	0.276	0.071	0.205
Decalin	0.374	0.1176	0.256
Bicyclohexyl	0.364	0.0976	0.266
n-Decane	0.324	0.0698	0.254
Hexadecane	0.339	0.0558	0.283

* $B = 0.87 \times 10^{-18}_{\text{esu}}$ for ref (39)

5.6 Interpretation of Results

A careful scrutiny of Table 5.5 reveals that the ß and ξ values in three octants about the hydrogen atom of one of the methyl groups are fairly constant as compared to the value of ß and ξ calculated for the first octant. This is because only one octant (ie. the first) experiences different degrees of restriction due to the rotation of the rest of the TMS molecule with respect to the methyl group. In the case of TMS (being a symmetrical molecule) all the twelve peripheral hydrogen atoms experience the same degree of exposure. The average of twelve readings thus completely characterizes the buffeting effect on the TMS molecule.

The linear regression of $(2\beta_T - \xi_T)^2$ on σ_w for solvents with peripheral hydrogen atoms (Figure 5.4) show acceptable correlation with a correlation coefficient of 0.882. However, the slope of 0.3088 which represents BK/r^6 is approximately half of the expected value of 0.6205 as reported by Homer and Percival(39). Moreover the unexpected intercept of 0.1058 ppm, indicate that Homer and Percival's "buffeting model" is by no means complete and requires further refinement.

In the case of solvents with peripheral chlorine atoms the regressions for different values of Q are presented in Table 5.11. The best value of BK/r^6 obtainable is 0.6465 ppm (Figure 5.5) which is in good agreement with Homer and Percival's reported value of 0.6205 ppm. The most interesting fact is that the intercept is -0.044ppm which for the first time indicates the success of Homer and Percival's "buffeting model". Although the Q value of 5.5 is comparable with predicted value of 6.5 by Homer and Percival(39), the poor correlation coefficient of 0.623 clearly warrants further investigation into the matter.

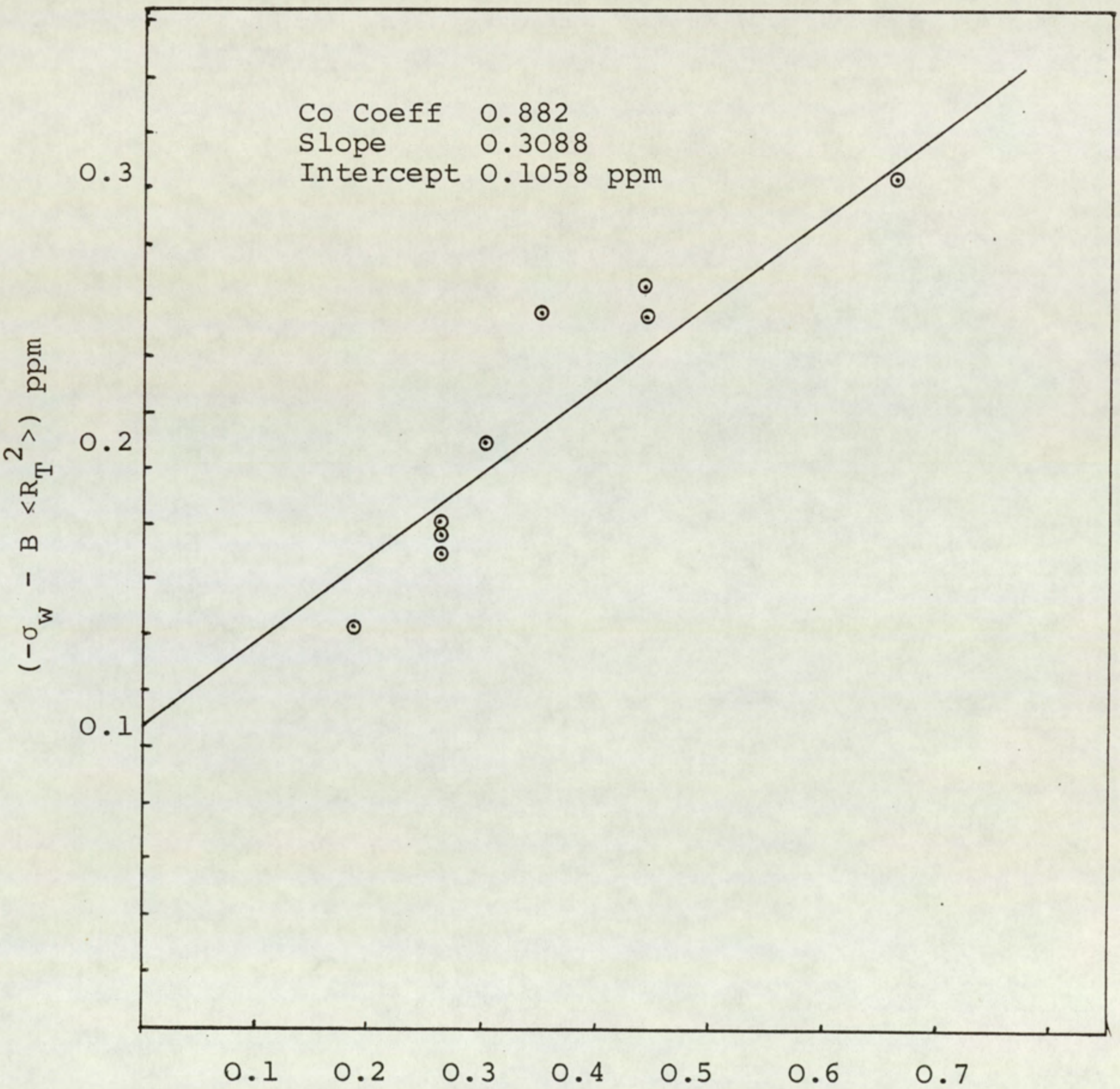

Figure 5.4: Linear regression of $(2\beta_T - \xi_T)^2$ for TMS in solvents with peripheral hydrogen atoms on $(-\sigma_W - B \langle R_T^2 \rangle)$

Table 5.11: Results of linear regression of $(2\beta_T - \xi_T)^2$ for different values of Q for TMS (solute) in solvents containing peripheral chlorine atoms on $(-\sigma_w - B <R_T^2>)$ $-\sigma_w$ is the gas-to-liquid shift corrected for bulk susceptibility)

Solvent		Q $(2\beta_T-\xi_T)^2$ for different values of Q				
	$-\sigma_w-(B<R_T^2>)$ (ppm)	5.0	5.1	5.2	5.3	5.4
1,2-dichlorethane	0.0682	0.182	0.186	0.189	0.193	0.197
$CHCl_3$	0.0669	0.182	0.186	0.189	0.193	0.197
1,1-dichloro ethane	0.126	0.191	0.195	0.199	0.203	0.207
CCl_4	0.1403	0.228	0.233	0.237	0.242	0.246
1,1,2,2-tetrachloro-ethane	0.1085	0.245	0.25	0.255	0.26	0.265
Co coeff		0.615	0.616	0.619	0.619	0.614
Slope		0.707	0.694	0.681	0.669	0.6568
Intercept		-0.043	-0.044	-0.044	-0.044	-0.044
	$-\sigma_w-(B<R_T^2>)$ (ppm)	5.5	5.6	5.7	5.8	5.9
1,2-dichloroethane	0.0682	0.2	0.205	0.209	0.212	0.216
$CHCl_3$	0.0669	0.2	0.205	0.209	0.212	0.216
1,1-dichloroethane	0.126	0.211	0.214	0.218	0.221	0.225
CCl_4	0.1403	0.251	0.255	0.260	0.264	0.269
1,1-dichloroethane	0.1085	0.27	0.275	0.280	0.285	0.29
Co coeff		0.623	0.601	0.602	0.598	0.598
Slope		0.6465	0.623	0.6137	0.594	0.585
Intercept		-0.044	-0.041	-0.042	-0.039	-0.04

Table 5.11 cont ..

Solvent		$Q\,(2\beta_T-\xi_T)^2$ for different values of Q				
	$-\sigma_w-(B\langle R_T^2\rangle)$ (ppm)	6.0	6.1	6.2	6.3	6.4
1,2-dichloro ethane	0.0682	0.22	0.223	0.227	0.231	0.234
$CHCl_3$	0.0669	0.22	0.223	0.227	0.231	0.234
1,1-dichloro ethane	0.126	0.229	0.232	0.237	0.24	0.244
CCl_4	0.1403	0.274	0.278	0.283	0.287	0.292
1,1,2,2-tetrachloro-ethane	0.1085	0.295	0.300	0.305	0.31	0.315
Co coeff		0.599	0.595	0.603	0.591	0.599
Slope		0.576	0.559	0.559	0.5417	0.5355
Intercept		-0.041	-0.038	-0.041	-0.039	-0.039
	$-\sigma_w-(B\langle R_T^2\rangle)$ (ppm)	6.5	6.6	6.7	6.8	6.9
1,2,-dichloroethane	0.0682	0.238	0.242	0.245	0.249	0.253
$CHCl_3$	0.0669	0.238	0.242	0.245	0.249	0.253
1,1-dichloroethane	0.126	0.248	0.252	0.256	0.26	0.263
1,1,2,2-tetrachloro-ethane	0.1085	0.319	0.324	0.329	0.334	0.339
Co coeff		0.599	0.595	0.602	0.603	0.597
Slope		0.536	0.527	0.521	0.514	0.5
Intercept		-0.041	-0.041	-0.041	-0.04	-0.04

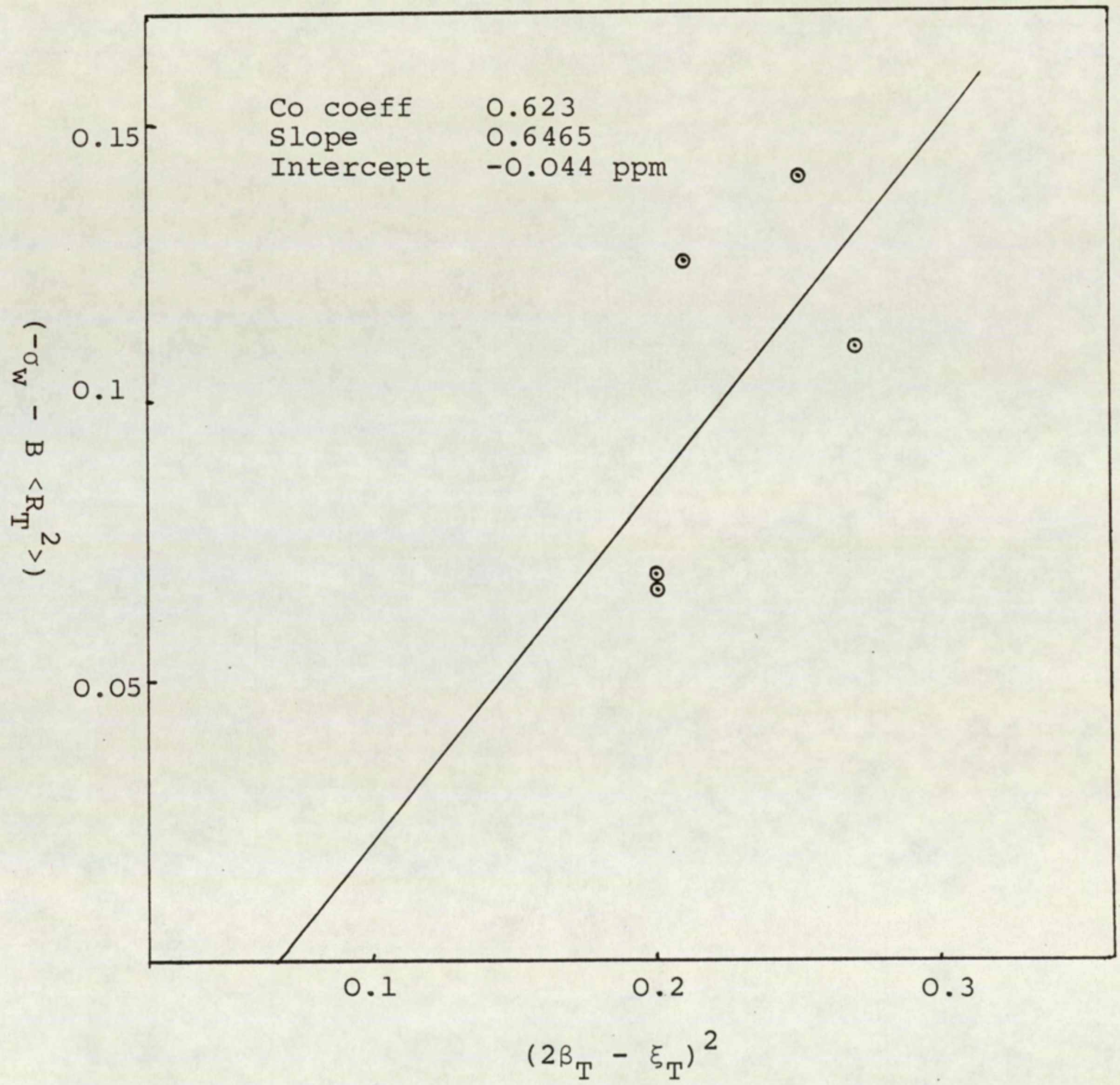

Figure 5.5: Linear regression of $(2\beta_T - \xi_T)^2$ for TMS in solvents with peripheral chlorine atoms on $(-\sigma_W - B \langle R_T^2 \rangle)$

5.7 Conclusions

Correlation analysis of σ_w and the reaction field of Homer and Percival highlights the unexpected intercepts which led to the development of their "Buffeting model".

The significance of the "buffeting model" has been successfully established in the case of solvents with peripheral chlorine atoms. However the unexpected intercept and poor values of BK/r^6, while studying larger solvents with peripheral hydrogen atoms has prompted the author to modify the present "buffeting model" which is explained and tested in Chapter Six.

CHAPTER SIX

A NEW METHOD FOR EVALUATING THE BUFFETING PARAMETERS ß AND ξ

6.1 Introduction

The original 'Buffeting Model' of Homer and Percival[39] was thoroughly investigated in Chapter Five. The unexpected intercepts of regression of $(2ß_T - \xi_T)^2$ on σ_W that were obtained for solvents containing peripheral hydrogen atoms and the poor correlation coefficients in case of solvents with peripheral chlorine atoms indicate that further refinements are necessary to fully understand the buffeting phenomena.

A modified treatment of buffeting is now reported and tested by its application to the analysis of experimental data.

6.2 Theoretical

One basic assumption made by Homer and Percival when presenting their 'buffeting model' has been the use of spheres to represent the solvent molecules; the radii of these spheres may be deduced from their molecular volumes. The solute however is represented by a scaled molecular model that identifies the constituent atoms. Although the success of Homer and Percivals 'buffeting model' is beyond the realm of chance, one may however question the limitations of representing the solvent molecules by spheres.

The sphere is an admirable shape, upon which, in hard, soft and flexible versions, many molecular theories have been based. Nevertheless, the macroscopic properties of liquids are mainly related to properties of the molecules themselves, such as their dynamic behaviour and their arrangement in the liquid state, and more importantly in the present context, to the nature and arrangement of their constituent atoms. Consequently, the use of spheres to represent solvent molecules must be questioned.

Of course, the use of spheres to represent solvent molecules is probably acceptable when investigating the intermolecular effect involving spherically symetric molecules. An excellent example is in the results obtained in Chapter Five for solvents such as CCl_4, and 1,1,2,2-tetrachloro ethane. However the extension of such an assumption to anisotropic linear or cyclic molecules appears to be fraught with difficulties, which may lead to erronious results.

The purpose of the work reported in this chapter is to develop an approach to the evaluation of the parameters ß and ξ that incorporates the steric realities of contacting molecules. In doing so, it is hoped to assess whether the characterisation of the buffeting contribution to nuclear screening can be improved.

The generalisation of Homer and Percival's 'buffeting theory' that is applicable to molecules of different shapes and sizes is by no means an easy task, but it appears that there are no 'short cuts'. To fully investigate the effect of the intermolecular forces, the author feels that a more rigorous approach together with some modifications to the original 'buffeting model' of Homer and Percival is essential. In the following sections a new treatment of the buffeting parameters ß and ξ is proposed that successfully overcomes the shortcomings of the original 'buffeting model'.

6.3 Modified Buffeting Model

The intial hypothesis here is that the buffeting effect depends not only on the shape and size of the solute molecule but also on the shape and size of the solvent molecule. It should be remembered that the work of Homer and Percival indicated that buffeting does depend on the shape and size of the solute but is less sensitive to the shape and size of the solvent.

Essentially at least the following three major factors are involved in the characterisation of the buffeting screening:

1 The shape and the size of the solute and the solvent molecule.

2 The internal rotation within the solute and the solvent molecule.

3 The number and the nature of the peripheral atoms of the solute and the solvent molecule.

Although Homer and Percival's 'buffeting model' is based on hydrogen atom-hydrogen atom interaction (as explained in Chapter Five section 5.3.1) they do incorporate a Hartree-Fock type scaling factor Q, as suggested by Yonometo(111) to generalise their approach to accommodate the effects of peripheral atoms other than hydrogen.

The unexpected intercept from the regression of $(2\beta_T - \xi_T)^2$ on experimentally observed shifts (gas-to-liquid chemical shift corrected for volume magnetic susceptibility and reaction field screenings) that were obtained for solvents with peripheral hydrogen atoms (Chapter Five, Figure 5.4) may be due to taking insufficiently rigorous account of the first two factors (1&2) stated earlier in this section.

6.4 A new approach to the measurement of the buffeting parameters ß and ξ

In order to accurately measure the buffeting parameters, Courteauld molecular models may be used for both the solute and the solvent molecule. In so doing, this will incorporate the effect of both the shape and the size of the solute and the solvent molecules. The details of the approach adapted are given below.

Similar to Homer and Percival's 'buffeting model', one of the peripheral hydrogen atoms (the resonant nucleus) of the solute molecule is divided into four octants. The centre of this hydrogen atom can be assumed to be at the origin of a set of cartesian co-ordinates, with the Z axis along the C-H bond along which ß is effective and a perpendicular X-axis along which α acts. One of the peripheral (hydrogen or non-hydrogen) atoms of the solvent molecule is brought in contact with the solute hydrogen of interest. All approach directions in the four different octants are considered. The degree of accessibility of the solvent proton to the solute atom is obtained by measuring the four different angles of contact relative to X axis (ie. one in each octant) (see Position A, Figure 6.1). Let us denote the solute atom as H_1 and the solvent atom as H_2.

Having measured the angle of contact θ in position A, H_2 is moved away from H_1 while both the solute and the solvent molecule are still in contact with each other, until the centres of H_1 and H_2 coincide with the X-axis (position B). The distance d between the centres of H_1 and H_2 is measured which is utilized to calculate the effect of the distance modulation on the solute molecule by the solvent molecule.

Keeping the position of H_2 fixed, the rest of the solvent molecule is rotated, normally reflecting the internal rotation between the carbon-carbon bond containing H_2, which may or may not alter the shape of the solvent molecule (relative to the solute molecule) depending on its symmetry. If any change in the shape of the solvent molecule is observed, four more measurements (one in each octant) are made between H_1 and H_2 in position A and another four in position B respectively.

The angle of contact is normally unaltered but the distance d may change depending on the new orientation of the solvent molecule. This should essentially account for the effect of internal rotation of the solvent molecule.

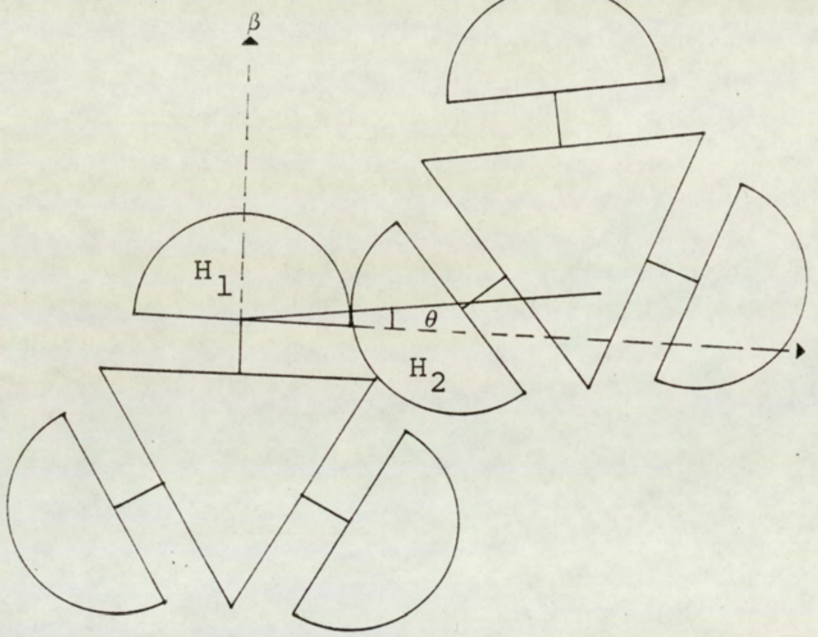

Position A

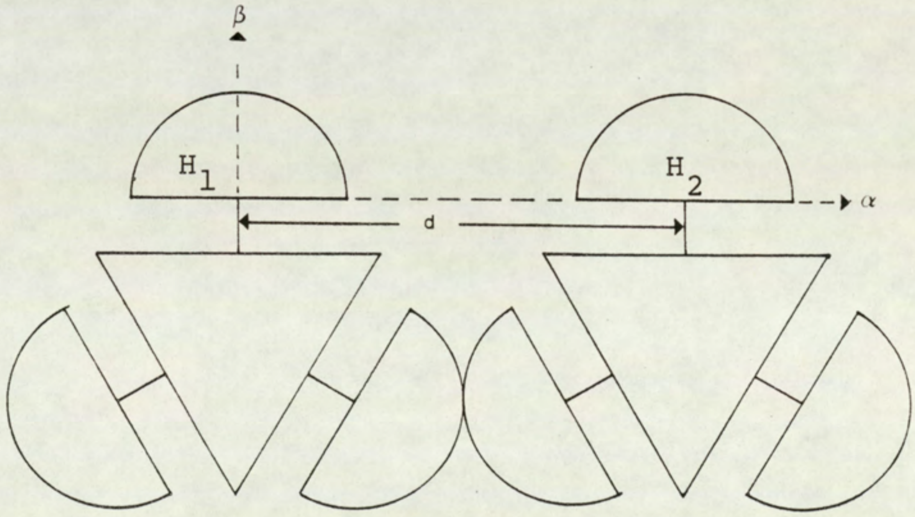

Position B

Figure 6.1: Two positions of methane (solute)-methane solvent encounter.

Position A: shows the limiting contact position, which is utilized to obtain angle of contact Θ

Position B: shows the methane (solvent) at a distance d from H_1 which is used to calculate the distance modulated buffeting parameters

It is equally important to take into consideration the internal rotation of the solute molecule in a similar manner to that described above for the solvent, but this can be avoided if the solute is a spherically symmetrical molecule. For this reason TMS has been selected as the solute molecule. Since the internal rotation between the C-Si bond does not alter the shape of the TMS molecule, the effect of internal rotation is naturally accounted for.

The buffeting parameters must be measured and calculated individually for every solute-solvent-encounter situation and the overall average taken to represent $(2\beta_T - \xi_T)^2$. Hydrogen atoms in the same geometrical environment as H_2 should normally have the same angle of contact and the distance d. However protons in different geometrical situations must be measured separately. The weighted (by number of atoms) average of the parameter $(2\beta_T - \xi_T)^2$ for all the peripheral atoms will eventually reflect the effect of the total number of the peripheral atoms of the solvent molecule on the solute molecule. This can be demonstrated by the following example:

Consider one of the peripheral atoms of a symmetrical solute molecule, represented by A. Let us divide it into four octants 1, 2, 3 and 4. Consider a non symmetrical solvent molecule containing eight peripheral atoms. Five of its peripheral atoms are assumed to be in a similar geometrical environment represented by X_1 and three of its peripheral atoms are assumed to be in different geometrical environment represented by X_2.

As any of the peripheral solvent-atoms can approach A from all four octants, at least four measurements (one in each octant) are required to calculate the buffeting parameter $(2\beta_T - \xi_T)^2$ for type X_1, similarly four more measurements are required to determine the effect of buffeting by X_2.

This can be represented schematically as follows:

No of peripheral solvent atoms of type X_1	Octant	Angle of contact	Distance (d)	$(2\beta_T - \xi_T)^2$
	1	θ_1	d_1	$(2\beta_T - \xi_T)_1{}^2$
5	2	θ_2	d_2	$(2\beta_T - \xi_T)_2{}^2$
	3	θ_3	d_3	$(2\beta_T - \xi_T)_3{}^2$
	4	θ_4	d_4	$(2\beta_T - \xi_T)_4{}^2$

$$\text{Average } (2\beta_T - \xi_T)^2\, X_1 = \frac{(2\beta_T - \xi_T)_1{}^2 + (2\beta_T - \xi_T)_2{}^2 + (2\beta_T - \xi_T)_3{}^2 + (2\beta_T - \xi_T)_4{}^2}{4} \quad \text{..... 6.1}$$

No of peripheral solvent atoms of type X_2	Octant	Angle of contact	Distance (d)	$(2\beta_T - \xi_T)^2$
	1	θ_3	d_5	$(2\beta_T - \xi_T)_5{}^2$
3	2	θ_4	d_6	$(2\beta_T - \xi_T)_6{}^2$
	3	θ_5	d_7	$(2\beta_T - \xi_T)_7{}^2$
	4	θ_6	d_8	$(2\beta_T - \xi_T)_8{}^2$

$$\text{Average } (2\beta_T - \xi_T)^2\, X_2 = \frac{(2\beta_T - \xi_T)_5{}^2 + (2\beta_T - \xi_T)_6{}^2 + (2\beta_T - \xi_T)_7{}^2 + (2\beta_T - \xi_T)_8{}^2}{4} \quad \text{..... 6.2}$$

$$\text{Weighted average } (2\beta_T - \xi_T)^2 = \frac{5\,(2\beta_T - \xi_T)^2\, X_1 + 3\,(2\beta_T - \xi_T)^2\, X_2}{5 + 3} \quad \text{..... 6.3}$$

A generalised equation for the total degree of accessibility can be expressed as follows:

$$\text{Wt ave } (2\beta_T - \xi_T)^2 = \frac{X_1 (2\beta_T - \xi_T)^2 X_1 + X_2 (2\beta_T - \xi_T)^2 X_2 \ldots X_n (2\beta_T - \xi_T)^2 X_n}{X_1 + X_2 \ldots\ldots + X_n} \qquad \ldots\ldots 6.4$$

In the case of a symmetrical solvent molecule the effect on H_1 will be the same for all the peripheral atoms of the solvent and hence the number of the peripheral atoms in the solvent molecule will be automatically accounted for.

For peripheral atoms other than hydrogen, a similar approach to Homer and Percivals 'buffeting model' can be applied by using the Hartree-fock type scaling factor 'Q' which is an electron dependent term that takes into consideration the nature of the peripheral solvent atoms (eg. Cl, F, Br, I etc). To incorporate the effect of peripheral atoms other than hydrogen, equation 6.4 can be modified as follows:

$$\text{wt ave } (2\beta_T - \xi_T)^2 = \frac{X_1 (2\beta_T - \xi_T)^2 X_1 + X_2\, Q \left[\frac{r\,\text{H-H}}{r\,\text{H-X}}\right]^6 (2\beta_T - \xi_T)^2 X_2 \ldots + X_n (2\beta_T - \xi_T)^2 X_n}{X_1 + X_2 \ldots\ldots + X_n} \qquad \ldots\ldots 6.5$$

where X may be Cl, Br, I etc...

Before reporting the values for the buffeting parameters for various solvents with TMS as solute, the following simple example will be used to visualize the factors mentioned in Section 6.3.

6.4.1 Measurement in the buffeting parameters for methane gas (solute) in various hydrocarbons (solvents)

A succession of molecular courtauld models representing solvents from methane to heptadecane were used with the methane (gas) molecular model as a solute, to measure the buffeting parameters as explained in Section 6.4.

The measurement of the buffeting parameters for the methane (solute)-methane (solvent) system is straight forward because the molecules are small, symmetrical and there are no added problems of internal rotation. However when considering the next solvent, ie. ethane, some very interesting features specially due to the effect of internal rotation along the C-C bond in ethane molecule are clearly noticeable.

Two conformations of the ethane molecule are depicted in Figure 6.2.

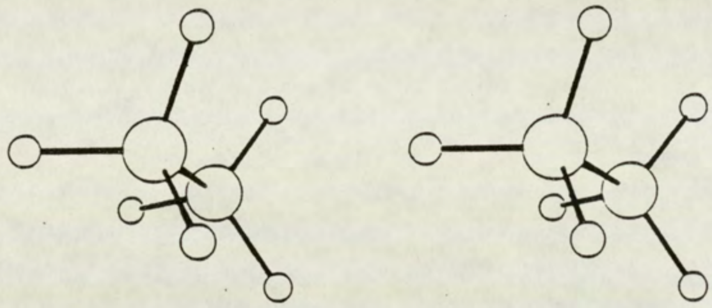

(a) eclipsed structure of ethane

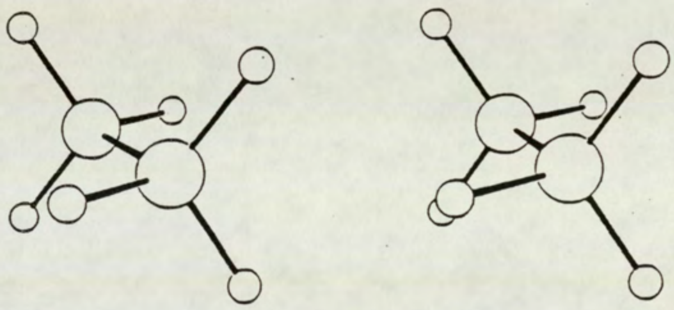

(b) staggered structure of ethane

Figure 6.2: Two conformations of the ethane molecule

A close scrutiny of ethane molecular model reveals that, in the staggered conformation all the six peripheral hydrogen atoms of the ethane solvent molecule are equally exposed to the solute molecule. Hence it is possible for the ethane molecule to approach the solute with minimum degree of geometrical restriction. However in the eclipsed form the six hydrogens experience a greater degree of restriction, while approaching the solute molecule. It is therefore necessary to consider them separately.

It is assumed for the present investigations, that both the conformations of ethane are equally probable; this is not necessarily true, because in practice we find that staggered conformation of ethane molecule is more stable than the strained eclipsed form[112].

Essentially, two different sets of measurements are necessary to obtain the weighted averaged $(2\beta_T - \xi_T)^2$ for the ethane solvent molecule, ie.

(a) One set of readings that apply to all six hydrogen atoms in the staggered conformation.

(b) One set of readings that apply to all six hydrogen atoms in the eclipsed conformation.

Note that each set of readings consists of four measurements (ie. one in each of the four octants about the centre of the resonant nucleus). To obtain the weighted average of the buffeting parameters, at least eight measurements are necessary (ie. $4\ [\ (2\beta_T - \xi_T)^2_A + 4\ (2\beta_T - \xi_T)^2_B]$.

The weighted average $(2\beta_T - \xi_T)^2$ can be calculated as follows:

$$(2\beta_T - \xi_T)^2_{\text{Wt ave}} = \frac{6_{(A)} \times \text{ave}\ (2\beta_T - \xi_T)^2\ (\text{staggered}) + 6_{(B)} \times \ \text{ave}\ (2\beta_T - \xi_T)^2\ (\text{eclipsed})}{12} \qquad \text{..... 6.6}$$

where $6_{(A)}$ is the number of peripheral hydrogen atoms in staggered conformation, A $6_{(B)}$ is the number of peripheral hydrogen atoms in eclipsed conformation B.

Some of the measured values of $(2\beta_T - \xi_T)^2$ are recorded in Table 6.1. The first column in Table 6.1 under the heading "number of peripheral solvent atoms: n*" indicates the location and the number of peripheral solvent atoms which are in a similar geometrical environment (relative to the solute resonant atom). This can be explained by the following example:

In the case of propane solvent molecule $C^1H_3\ C^2H_2\ C^3H_3$, three hydrogen atoms attached to the methyl carbon in position 1 are equally exposed to the solute molecule as the three hydrogen atoms attached to the methyl carbon in position 3, and hence they will experience the same degree of restriction while approaching a solute molecule. This has been reported in column one as $6\,^1H$ from 2 - CH_3 groups.

The two hydrogen atoms attached to the methylene carbon, which experience a different degree of restriction are reported in column one as $2\,^1H$ from 1 - CH_2 group.

It is apparent from Table 6.1 that to fully implement the new approach for determining $(2\beta_T - \xi_T)^2$ some duplication when reporting the measurements is unavoidable. In order to avoid further repetition of the measured values, only three examples (ie. methane, ethane and propane) are cited in their entirety. The values for the buffeting parameters for the rest of the solvents are reported in a condensed form in Table 6.2.

Table 6.1: Measurement and calculation of the buffeting parameter $(2\beta_T - \xi_T)^2$ for methane (gas) solute in various solvents

Solvent: Methane

No of peripheral solvent atoms: n*	Angle of contact θ	α_c	β_c	$(2\beta_T - \xi_T)^2$	distance (d) Å	α_T	β_T	$(2\beta_T - \xi_T)^2$
$4\,^1H$	5.73	0.8727	1	0.0648	1.08	0.9204	1	0.0253
	5.73	0.8727	1	0.0648	1.26	0.9853	1	0.0287
	5.73	0.8727	1	0.0648	1.26	0.9153	1	0.0287
	5.73	0.8727	1	0.0648	1.26	0.9153	1	0.027

Average $(2\beta_T - \xi_T)^2 = 0.0279$

Table 6.1 cont ...

Solvent: Ethane (staggered form)

No of peripheral solvent atoms: n*	Angle of contact θ	α_c	β_c	$(2\beta_T - \xi_T)^2$	distance (d) Å	α_T	β_T	$(2\beta_T - \xi_T)^2$
6^1H	5.73	0.8727	1	0.0648	1.08	0.9204	1	0.0253
	5.73	0.8727	1	0.0648	1.26	0.9153	1	0.0287
	5.73	0.8727	1	0.0648	1.26	0.9153	1	0.0287
	5.73	0.8727	1	0.0648	1.26	0.9153	1	0.0287

Average $(2\beta_T - \xi_T)^2$: 0.0279

Solvent: Ethane (eclipsed form)

No of peripheral solvent atoms: n*	Angle of contact θ	α_c	β_c	$(2\beta_T - \xi_T)^2$	distance (d) Å	α_T	β_T	$(2\beta_T - \xi_T)^2$
6^1H	5.73	0.8727	1	0.0648		0.9152	1	0.0287
	5.73	0.8727	1	0.0648		0.9075	1	0.0341
	5.73	0.8727	1	0.0648		0.9035	1	0.0341
	5.73	0.8727	1	0.0648		0.9075	1	0.0341

Average $(2\beta_T - \xi_T)^2$: 0.0328

Weighted average $(2\beta_T - \xi_T)^2$: 0.0304

n*: gives the number of peripheral solvent atoms which are in a similar geometrical environment (relative to the solute resonant atom) and the location or the group of solvent molecule to which they are bonded.

Solvent: Propane

No of peripheral solvent atoms: n*	Angle of contact θ	α_c	β_c	$(2\beta_T - \xi_T)^2$	distance (d) Å	α_T	β_T	$(2\beta_T - \xi_T)^2$
$6\,^1H$ from	5.73	0.8727	1	0.0648	1.08	0.9204	1	0.0253
2 - CH_3	5.73	0.8727	1	0.0648	1.26	0.9153	1	0.0287
groups	5.73	0.8727	1	0.0648	1.26	0.9153	1	0.0287
	5.73	0.8727	1	0.0648	1.26	0.9153	1	0.0287
$2\,^1H$ from	5.73	0.8727	1	0.0648	1.56	0.9086	1	0.0333
1 - CH_2	5.73	0.8727	1	0.0648	2.28	0.8985	1	0.0412
group	5.73	0.8727	1	0.0648	2.28	0.8985	1	0.0412
	5.73	0.8727	1	0.0648	2.28	0.8985	1	0.0412

Weighted average: $(2\beta_T - \xi_T)^2$: 0.0306

Table 6.2: $(2\beta_T - \xi_T)^2$ for methane (gas) solute in various solvents

Solvent	Molar volume[112] cm^3	$(2\beta_T - \xi_T)^2 \times 10^2$
Methane	37.83	2.79
Ethane	55.05	3.04
Propane	75.74	3.06
Butane	100.41	3.24
Pentane	115.18	3.35
Hexane	130.66	3.44
Heptane	146.57	3.5
Octane	162.54	3.54
Nonane	175.75	3.58
Decane	192.18	3.61
Undecane	211.13	3.64
Dodecane	227.33	3.66
Tridecane	243.62	3.68
Tetradecane	258.06	3.7
Pentadecane	276.30	3.71
Hexadecane	292.23	3.72
Heptadecane	309.62	3.72

A regression of molar volume of the solvents against $(2\beta_T - \xi_T)^2$ obtained by the approach just described is shown in Figure 6.3, and indicates that the increase in buffeting parameter is not directly proportional to the molar volume of the solvent. The progressive change in the values of $(2\beta_T - \xi_T)^2$ appears to diminish with increasing molar volume, and appears to become essentially constant for the largest molecules. It is interesting to note that large molecules, with the greater number of peripheral atoms would have been expected on the basis of linear extrapolation to result in the larger values of the buffeting parameter, but in fact this extrapolation appears to be offset by the fact that $(2\beta_T - \xi_T)^2$ becomes constant due to steric inaccessibility. This confirms the results obtained in Chapter 3, where on the basis of a crude two dimensional model it was concluded that large solvent molecules may not necessarily have large values of $(2\beta_T - \xi_T)^2$.

Having confirmed the general trend of the buffeting parameters, the intention now is to use the new approach to calculate the buffeting parameters for the TMS molecule (solute) in various solvents and compare them with the experimental shifts reported in Chapter Five.

6.5 Measurement of the buffeting parameters for TMS solute molecule in various solvents

It must be emphasised that while measuring the angles of contact using Courteauld molecular models, some degree of human error is unavoidable despite making the measurements with great care. It is suggested that the measurements must be repeated for the same solute and solvent molecules on several different occasions to minimize the human error. The new approach for these measurements is explained in detail in Section 6.4.

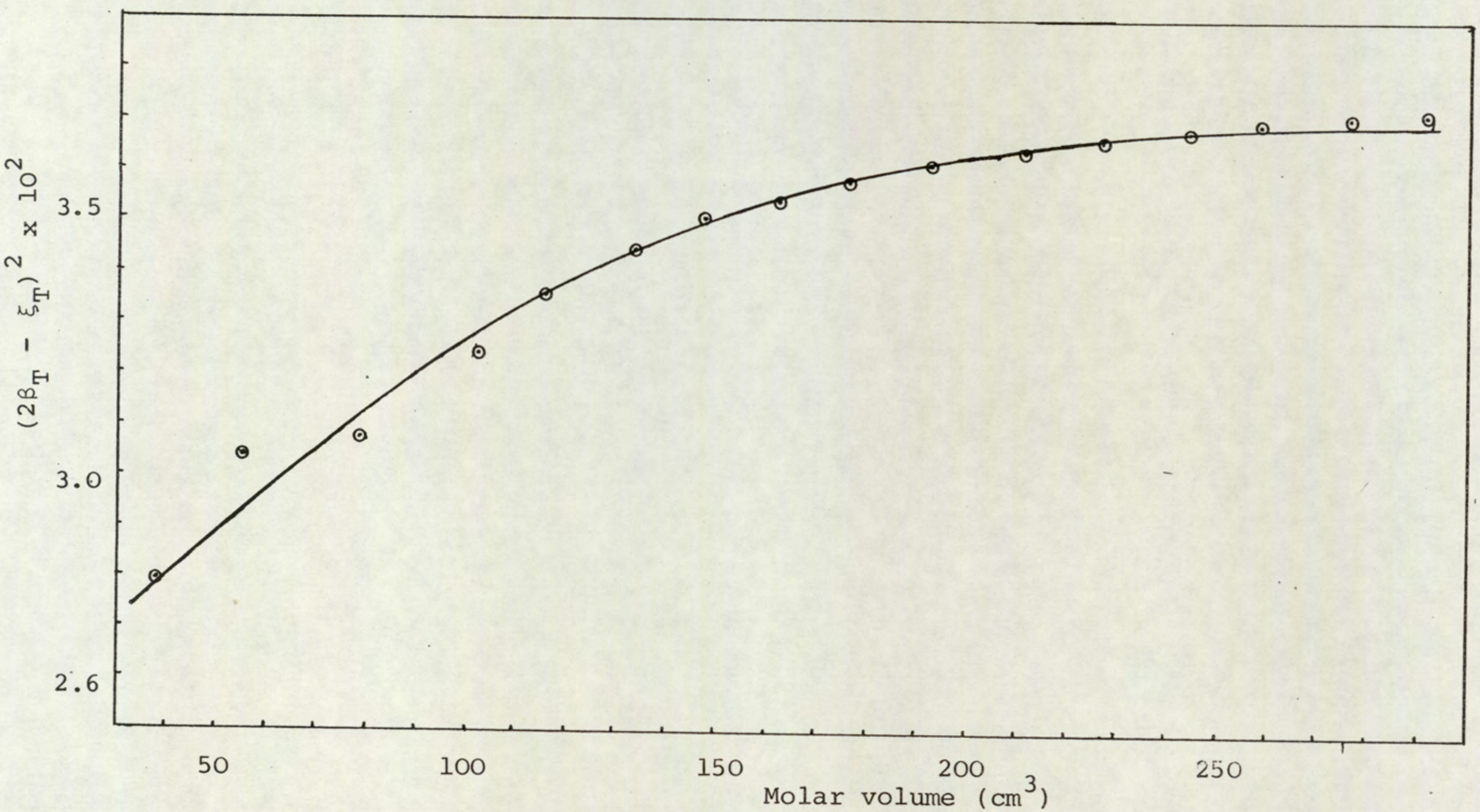

Figure 6.3: Regression of $(2\beta_T - \xi_T)^2$ for methane gas (solute) in various solvents on molar volume

The values of the buffeting parameters for TMS solute in various solvents are reported in detail in Table 6.3. Three sets of four readings encountered by a solute atom from all four octants are systematically enlisted reflecting changes in the values of ß and ξ due to three different orientations of the Si $(CH_3)_3$ fragment of the TMS solute molecule.

One cannot avoid noticing that a fair amount of repetition of the measured values has occurred. However this is a constant reminder that while measuring the buffeting parameters from all four directions of approach in each of the four octants, the degree of accessibility is essentially altered in only one octant.

The effect of the buffeting parameters on the remaining three octants is very small. This is because three of the octants are exposed more or less equally to the solvent molecule. This particularly reflects the symmetrical structure of the TMS (solute) molecule. In order to completely visualize the effect of buffeting, it is felt necessary to report all the measured values in their entirety.

At this stage it would be appropriate to explain the terminology used in Table 6.3, under the first column, ie. number of peripheral solvent atoms: n*. This column shows the number of peripheral solvent atoms which are in a similar geometrical environment (relative to the solute resonant atom) and also the location or the group of the solvent molecule to which they are bonded (ref: Section 6.4.1). In the case of decalin and bicyclohexyl, terminology such as ^{1}H internal and ^{1}H external is used. For example, while reporting the buffeting parameters for bicyclohexyl, the term ^{1}H internal simply indicates the type of hydrogen atoms which are in the proximity of the central C-C bond, which joins the two cyclic ring structures. On the other hand, ^{1}H external indicates the hydrogen atoms in the rest of the bicyclohexyl molecule which have a greater degree of accessibility to the solute molecule compared with the ^{1}H internal hydrogen atoms.

The buffeting parameters reported in Table 6.3 for solvents with peripheral chlorine atoms are the measured values based on molecular models and are not corrected for the Hartree-Fock type scaling factor Q. Note that when the buffeting atom is other than H the value of r^6_{H-H} in the equation (3.26) has to be replaced by r^6_{H-X}. The buffeting parameters for these solvents for different values of Q are tabulated in Table 6.5.

The value of $(2\beta_T - \xi_T)^2$ is obtained by weighted averaging of the peripheral hydrogen atom effects and the non-hydrogen atom effects (corrected for the electron displacement term Q).

Table 6.3: Measurement and calculation of the buffeting parameters for TMS solute in various solvent

Solvent: TMS

No of peripheral solvent atoms: n*	Angle of contact θ	α_c	β_c	$(2\beta_T - \xi_T)^2$	distance (d) Å	α_T	β_T	$(2\beta_T - \xi_T)^2$
12^1H	68.75	0	0.472	0.892	6.7	0.1185	0.5347	0.6927
from	5.73	0.8727	1	0.0648	1.6	0.9245	1	0.0228
4 Methyl	5.73	0.8727	1	0.0648	2.4	0.9111	1	0.0316
groups	5.73	0.8727	1	0.0648	2.4	0.9111	1	0.0316
	34.48	0.2361	1	2.3344	7.6	0.3161	1	1.8709
	5.73	0.8727	1	0.0648	1.6	0.9245	1	0.0228
	5.73	0.8727	1	0.0648	2.4	0.9111	1	0.0316
	5.73	0.8727	1	0.0648	2.4	0.9111	1	0.0316
	22.92	0.4907	1	1.0375	6.5	0.5529	1	0.7997
	5.73	0.8727	1	0.0648	1.6	0.9245	1	0.0228
	5.73	0.8727	1	0.0648	2.4	0.9111	1	0.0316
	5.73	0.8727	1	0.0648	2.4	0.9111	1	0.0316

Weight average $(2\beta_T - \xi_T)^2$: 0.3018

*n: shows the number of peripheral solvent atoms which are in similar geometrical environment (relative to the solute resonant atom) and the location or the group of solvent molecule to which they are bonded.

Table 6.3 cont ...

Solvent: Cyclohexane

No of peripheral solvent atoms: n*	Angle of contact θ	α_c	β_c	$(2\beta_T - \xi_T)^2$	distance (d) Å	α_T	β_T	$(2\beta_T - \xi_T)^2$
6^1H	71.62	0	0.4085	0.6673	3.18	0.1487	0.4964	0.4836
axial	5.73	0.8727	1	0.0648	0.72	0.9347	1	0.0171
	5.73	0.8727	1	0.0648	1.08	0.9204	1	0.0253
	5.73	0.8727	1	0.0648	1.08	0.9204	1	0.0253
	28.65	0.3634	1	1.6211	3.3	0.4548	1	1.1892
	5.73	0.8727	1	0.0648	0.72	0.9347	1	0.0171
	5.73	0.8727	1	0.0648	1.08	0.9204	1	0.0253
	5.73	0.8727	1	0.0648	1.08	0.9204	1	0.0253
	20.05	0.5544	1	0.7944	3.0	0.6244	1	0.5642
	5.73	0.8727	1	0.0648	0.72	0.9347	1	0.0171
	5.73	0.8727	1	0.0648	1.08	0.9204	1	0.0253
	5.73	0.8727	1	0.0648	1.08	0.9204	1	0.0253
				Ave $(2\beta_T - \xi_T)^2$	0.2033			
6^1H	71.62	0	0.4085	0.6673	3.48	0.1364	0.4891	0.4977
equa-	5.73	0.8727	1	0.0648	0.78	0.9318	1	0.0186
torial	5.73	0.8727	1	0.0648	1.26	0.9153	1	0.0287
	5.73	0.8727	1	0.0648	1.26	0.9153	1	0.0287
	28.65	0.3634	1	1.6211	3.6	0.4474	1	1.2215
	5.73	0.8727	1	0.0648	0.78	0.9318	1	0.0186
	5.73	0.8727	1	0.0648	1.26	0.9153	1	0.0287
	5.73	0.8727	1	0.0648	1.26	0.9153	1	0.0287
	20.05	0.5544	1	0.7944	3.54	0.6141	1	0.5955
	5.73	0.8727	1	0.0648	0.78	0.9318	1	0.0186
	5.73	0.8727	1	0.0648	1.26	0.9153	1	0.0287
	5.73	0.8727	1	0.0648	1.26	0.9153	1	0.0287
				Ave $(2\beta_T - \xi_T)^2$:	0.2119			

Wt ave $(2\beta_T - \xi_T)^2$: 0.2076

Table 6.3 cont

Solvent: 2,3-dimethyl butane

No of peripheral solvent atoms: n*	Angle of contact θ	α_c	ß$_c$	$(2ß_T - \xi_T)^2$	distance (d) Å	α_T	ß$_T$	$(2ß_T - \xi_T)^2$
12^1H	71.62	0	0.4085	0.6673	3.66	0.1299	0.4833	0.505
from	5.73	0.8727	1	0.0297	1.32	0.9138	1	0.0297
4-CH_3	5.73	0.8727	1	0.0297	3.42	0.8903	1	0.0481
groups	5.73	0.8727	1	0.0297	3.42	0.8903	1	0.0481
	31.51	0.2997	1	1.9616	3.72	0.3892	1	1.492
	5.73	0.8727	1	0.0297	1.32	0.9138	1	0.0297
	5.73	0.8727	1	0.0297	3.42	0.8903	1	0.0481
	5.73	0.8727	1	0.0297	3.42	0.8903	1	0.0481
	22.92	0.4907	1	1.0375	3.78	0.5548	1	0.7928
	5.73	0.8727	1	0.0297	1.32	0.9138	1	0.0297
	5.73	0.8727	1	0.0297	3.42	0.8903	1	0.0481
	5.73	0.8727	1	0.0292	3.42	0.8903	1	0.0481
				Ave $(2ß_T - \xi_T)^2$:	0.2640			
2^1H	71.62	0	0.4085	0.6673	3.84	0.1239	0.4818	0.512
from	5.73	0.8727	1	0.0297	1.5	0.9138	1	0.0325
2-CH	5.73	0.8727	1	0.0297	1.86	0.8903	1	0.0371
groups	5.73	0.8727	1	0.0297	1.86	0.8903	1	0.0371
	31.51	0.2997	1	1.9616	3.9	0.3852	1	1.5118
	5.73	0.8727	1	0.0297	1.5	0.9138	1	0.0325
	5.73	0.0727	1	0.0297	1.86	0.8903	1	0.0371
	5.73	0.8727	1	0.0297	1.86	0.8903	1	0.0371
	22.92	0.4907	1	1.0375	3.78	0.5548	1	0.792
	5.73	0.8727	1	0.0297	1.5	0.9138	1	0.0325
	5.73	0.8727	1	0.0292	1.86	0.8903	1	0.0371
	5.73	0.8727	1	0.0297	1.86	0.8903	1	0.0371
				Ave $(2ß_T - \xi_T)^2$:	0.2613			

Wt ave $(2ß_T - \xi_T)^2$: 0.2636

Table 6.3 cont ...

Solvent: 2,2 dimethyl butane

No of peripheral solvent atoms: n*	Angle of contact θ	α_c	β_c	$(2\beta_T - \xi_T)^2$	distance (d) Å	α_T	β_T	$(2\beta_T - \xi_T)^2$
9^1H from 3-CH_3 groups		12 readings same as for 2,3-dimethyl butane (*n = 12 ^1H for 4-CH_3 groups) Ave $(2\beta_T - \xi_T)^2$: 0.2640						
2^1H from 1-CH group		12 readings same as for 2,3-dimethyl butane (*n = 2^1H from 2-CH group) Ave $(2\beta_T - \xi_T)^2$ = 0.2613						
3^1H from 1-CH_3 group	71.62	0	0.4085	0.6673	3.72	0.1278	0.4841	0.508
	5.73	0.8727	1	0.0297	1.32	0.9138	1	0.0297
	5.73	0.8727	1	0.0297	3.42	0.8903	1	0.0481
	5.73	0.8727	1	0.0297	3.42	0.8903	1	0.0481
	31.51	0.2997	1	1.9616	3.84	0.3865	1	1.505
	5.73	0.8727	1	0.0297	1.32	0.9138	1	0.0297
	5.73	0.8727	1	0.0297	3.42	0.8903	1	0.0481
	5.73	0.8727	1	0.0297	3.42	0.8903	1	0.0481
	22.92	0.4907	1	1.0375	3.36	0.5625	1	0.7655
	5.73	0.8727	1	0.0297	1.32	0.9138	1	0.0297
	5.73	0.8727	1	0.0297	3.42	0.8903	1	0.0481
	5.73	0.8727	1	0.0297	3.42	0.8903	1	0.0481

Ave $(2\beta_T - \xi_T)^2$: 0.2630

Wt ave $(2\beta_T - \xi_T)^2$: 0.2634

Table 6.3 cont ...

Solvent: 2-methyl pentane

No of peripheral solvent atoms: n*	Angle of contact θ	α_c	β_c	$(2\beta_T - \xi_T)^2$	distance (d) Å	α_T	β_T	$(2\beta_T - \xi_T)^2$

6^1H from 2-CH_3 methyl groups

12 readings same as for 2,3-dimenthyl butane
(*n = 12 ^1H for 4 - CH_3 groups)
Ave $(2\beta_T - \xi_T)^2$: 0.2640

1^1H from 1-CH group and 4^1H from 2-CH_2 groups

12 readings same as for 2,3-dimethyl butane
(*n = 2^1H from 2-CH groups)
Ave $(2\beta_T - \xi_T)^2$: 0.2613

3^1H from 1-CH_3 group

12 readings same as for 2,2-dimethyl butane
(n* = 3^1H from 1 CH_3 group)
Ave $(2\beta_T - \xi_T)^2$: 0.2630

$$\text{Wt ave } (2\beta_T - \xi_T)^2: \frac{6 \times 2640 + 5 \times 0.2613 + 3 \times 0.2630}{14}$$

Wt ave $(2\beta_T - \xi_T)^2$: 0.2628

Table 6.3 cont ...

Solvent: Decalin

No of peripheral solvent atoms: n*	Angle of contact θ	α_c	β_c	$(2\beta_T - \xi_T)^2$	distance (d) Å	α_T	β_T	$(2\beta_T - \xi_T)^2$
6^1H	71.62	0	0.4085	0.6673	4.32	0.1105	0.4738	0.5280
internal	5.73	0.8727	1	0.0648	2.7	0.8948	1	0.0443
	8.59	0.809	1	0.1459	3.96	0.832	1	0.1129
	8.59	0.809	1	0.1459	3.96	0.832	1	0.1129
	40.11	0.1087	1	3.1774	4.74	0.1986	1	2.569
	5.73	0.8727	1	0.0648	2.7	0.8948	1	0.0443
	8.59	0.809	1	0.1459	3.96	0.832	1	0.1129
	8.59	0.809	1	0.1459	3.96	0.832	1	0.1129
	22.92	0.4907	1	1.0375	4.26	0.5477	1	0.8182
	5.73	0.8727	1	0.0648	2.7	0.8948	1	0.0443
	8.59	0.809	1	0.1459	3.96	0.832	1	0.1129
	8.59	0.809	1	0.1459	3.96	0.832	1	0.1129
				Ave $(2\beta_T - \xi_T)^2$:	0.3928			
	71.62	0	0.4085	0.6673	3.66	0.1299	0.4853	0.5053
12^1H	5.73	0.8727	1	0.0648	1.08	0.9204	1	0.0253
external	8.59	0.809	1	0.1459	1.44	0.8666	1	0.071
	8.59	0.809	1	0.1459	1.44	0.8666	1	0.071
	40.11	0.1087	1	3.1774	4.02	0.2144	1	2.4688
	5.73	0.8727	1	0.0648	1.08	0.9204	1	0.0253
	8.59	0.809	1	0.1459	1.44	0.8666	1	0.071
	8.59	0.809	1	0.1459	1.44	0.8666	1	0.071
	22.92	0.4907	1	1.0375	3.72	0.5558	1	0.7892
	5.73	0.8727	1	0.0648	1.08	0.9204	1	0.0253
	8.59	0.809	1	0.1459	1.44	0.8666	1	0.071
	8.59	0.809	1	0.1459	1.44	0.8666	1	0.071
				Wt ave $(2\beta_T - \xi_T)^2 = 0.3554$				

Wt ave $(2\beta_T - \xi_T)^2 = 0.3682$

Table 6.3 cont ...

Solvent: Bicyclohexyl

No of peripheral solvent atoms: n*	Angle of contact θ	α_c	β_c	$(2\beta_T - \xi_T)^2$	distance (d) Å	α_T	β_T	$(2\beta_T - \xi_T)^2$
10^1H internal	71.62	0	0.4085	0.6673	4.8	0.0996	0.4674	0.541
	5.73	0.8727	1	0.0648	2.46	0.8968	1	0.0426
	8.59	0.809	1	0.1459	3.96	0.832	1	0.1129
	8.59	0.809	1	0.1459	3.96	0.832	1	0.1129
	42.97	0.0451	1	3.6476	5.88	0.1229	1	3.077
	5.73	0.8727	1	0.0648	2.46	0.8968	1	0.0426
	8.59	0.809	1	0.1459	3.96	0.832	1	0.1129
	8.59	0.809	1	0.1459	3.96	0.832	1	0.1129
	22.92	0.4907	1	1.0375	5.22	0.5374	1	0.856
	5.73	0.8727	1	0.0648	2.46	0.8968	1	0.0426
	8.59	0.809	1	0.1459	3.96	0.832	1	0.1129
	8.59	0.809	1	0.1459	3.96	0.832	1	0.1129

Ave $(2\beta_T - \xi_T)^2 = 0.4399$

12^1H external	71.62	0	0.4085	0.6673	3.72	0.1278	0.4841	0.5076
	5.73	0.8727	1	0.0648	1.08	0.9204	1	0.0253
	8.59	0.809	1	0.1459	1.44	0.8666	1	0.0712
	8.59	0.809	1	0.1459	1.44	0.8666	1	0.0712
	42.97	0.0451	1	3.6476	4.08	0.1566	1	2.8451
	5.73	0.8727	1	0.0648	1.08	0.9204	1	0.0253
	8.59	0.809	1	0.1459	1.44	0.8666	1	0.0712
	8.59	0.809	1	0.1459	1.44	0.8666	1	0.0712
	22.92	0.4907	1	1.0375	3.78	0.5548	1	0.8872
	5.73	0.8727	1	0.0648	1.08	0.9204	1	0.0253
	8.59	0.809	1	0.1459	1.44	0.8666	1	0.0712
	8.59	0.809	1	0.1459	1.44	0.8666	1	0.0712

Ave $(2\beta_T - \xi_T)^2 = 0.3953$

Wt ave $(2\beta_T - \xi_T)^2 = 0.4155$

Table 6.3 cont ...

Solvent: Decane

No of peripheral solvent atoms: n*	Angle of contact θ	α_c	β_c	$(2\beta_T - \xi_T)^2$	distance (d) Å	α_T	β_T	$(2\beta_T - \xi_T)^2$
$16\,^1H$	71.62	0	0.4085	0.6673	4.26	0.112	0.4747	0.5262
from	5.73	0.8727	1	0.0648	1.56	0.9086	1	0.0334
$8 - CH_2$	8.59	0.809	1	0.1459	1.68	0.8597	1	0.0787
groups	8.59	0.809	1	0.1459	1.68	0.8597	1	0.0787
	42.97	0.0451	1	3.6476	4.5	0.1464	1	2.9145
	5.73	0.8727	1	0.0648	1.56	0.9806	1	0.0334
	8.59	0.809	1	0.1459	1.68	0.8597	1	0.0787
	8.59	0.809	1	0.1459	1.68	0.8597	1	0.0787
	22.92	0.4907	1	1.0375	4.2	0.5485	1	0.8153
	5.73	0.8727	1	0.0648	1.56	0.9086	1	0.0334
	8.59	0.809	1	0.1459	1.68	0.8597	1	0.0787
	8.59	0.809	1	0.1459	1.68	0.8597	1	0.0787

Ave $(2\beta_T - \xi_T)^2 = 0.4024$

$6\,^1H$	71.62	0	0.4085	0.6673	3.66	0.1299	0.4853	0.5053
from	5.73	0.8727	1	0.0638	1.08	0.9204	1	0.0253
$2\text{-}CH_3$	8.59	0.809	1	0.1459	1.44	0.8666	1	0.0712
groups	8.59	0.809	1	0.1459	1.44	0.8666	1	0.0712
	42.97	0.0451	1	3.6476	3.9	0.1617	1	2.8113
	5.73	0.8727	1	0.0648	1.08	0.9204	1	0.0253
	8.59	0.809	1	0.1459	1.44	0.8666	1	0.0712
	8.59	0.809	1	0.1459	1.44	0.8666	1	0.0712
	22.92	0.4907	1	1.0375	3.72	0.5558	1	0.7892
	5.73	0.8727	1	0.0648	1.08	0.9204	1	0.0253
	8.59	0.809	1	0.1459	1.44	0.8666	1	0.0712
	8.59	0.809	1	0.1459	1.44	0.8666	1	0.0712

Ave $(2\beta_T - \xi_T)^2 = 0.384$

Wt ave $(2\beta_T - \xi_T)^2 = 0.3974$

Table 6.3 cont ...

Solvent: Hexadecane

No of peripheral solvent atoms: n*	Angle of contact θ	α_c	β_c	$(2\beta_T - \xi_T)^2$	distance (d) Å	α_T	β_T	$(2\beta_T - \xi_T)^2$
28 ^1H	71.62	0	0.4085	0.6673	5.46	0.0877	0.4603	0.5554
from	5.73	0.8727	1	0.0648	1.56	0.9086	1	0.0334
14-CH_2	8.59	0.809	1	0.1459	1.62	0.8613	1	0.0769
groups	8.59	0.809	1	0.1459	1.62	0.8613	1	0.0769
	45.84	0	0.9814	3.8526	5.7	0.085	0.983	3.2325
	5.73	0.8727	1	0.0648	1.56	0.9086	1	0.0334
	8.59	0.809	1	0.1459	1.62	0.8613	1	0.0769
	8.59	0.809	1	0.1459	1.62	0.8613	1	0.0769
	25.78	0.427	1	1.3131	5.4	0.4778	1	1.0906
	5.73	0.8727	1	0.0648	1.56	0.9086	1	0.0334
	8.59	0.809	1	0.1459	1.62	0.8613	1	0.0769
	8.59	0.809	1	0.1459	1.62	0.8613	1	0.0769

Ave $(2\beta_T - \xi_T)^2 = 0.4533$

6^1H	71.62	0	0.4085	0.6673	3.66	0.1299	0.4853	0.5053
from	5.73	0.8727	1	0.0648	1.08	0.9204	1	0.0253
2-CH_3	8.59	0.809	1	0.1459	1.44	0.8667	1	0.0712
groups	8.59	0.809	1	0.1459	1.62	0.8613	1	0.0769
	42.97	0.0451	1	3.6476	3.9	0.1617	1	2.8113
	5.73	0.8727	1	0.0648	1.08	0.9204	1	0.0253
	8.59	0.809	1	0.1459	1.44	0.8667	1	0.0712
	8.59	0.809	1	0.1459	1.44	0.8667	1	0.0712
	22.92	0.4907	1	1.0375	3.72	0.5558	1	0.7892
	5.73	0.8727	1	0.0648	1.08	0.9204	1	0.0253
	8.59	0.809	1	0.1459	1.44	0.8667	1	0.0712
	8.59	0.809	1	0.1459	1.44	0.8667	1	0.0712

Ave $(2\beta_T - \xi_T)^2 = 0.384$

Wt ave $(2\beta_T - \xi_T)^2 = 0.4411$

Table 6.3 cont ...

Solvent: Carbon tetrachloride

No of peripheral solvent atoms: n*	Angle of contact θ	α_c	β_c	$(2\beta_T - \xi_T)^2$	distance (d) Å	α_T	β_T	$(2\beta_T - \xi_T)^2$
4 Cl atoms attached to central carbon atom	83.08	0	0.1538	0.0946	4.44	0.1075	0.2448	0.0754
	8.59	0.809	1	0.1459	0.9	0.8901	1	0.0483
	11.46	0.7454	1	0.2594	0.84	0.8584	1	0.0802
	11.46	0.7454	1	0.2594	0.84	0.8584	1	0.0802
	74.48	0	0.3448	0.4755	4.56	0.1048	0.4134	0.3811
	8.59	0.809	1	0.1459	0.9	0.8901	1	0.0483
	11.46	0.7454	1	0.2594	0.84	0.8584	1	0.0802
	11.46	0.7454	1	0.2594	0.84	0.8584	1	0.0802
	68.75	0	0.4721	0.8916	4.38	0.1089	0.5296	0.7078
	8.59	0.809	1	0.1459	0.9	0.8901	1	0.0483
	11.46	0.7454	1	0.2594	0.84	0.8584	1	0.0802
	11.46	0.7454	1	0.2594	0.84	0.8584	1	0.0802

Ave $(2\beta_T - \xi_T)^2 = 0.1492$

Table 6.3 cont ...

Solvent: Chloroform

No of peripheral solvent atoms: n*	Angle of contact θ	α_c	β_c	$(2\beta_T - \xi_T)^2$	distance (d) Å	α_T	β_T	$(2\beta_T - \xi_T)^2$
1H attached to the central carbon atom	88.81	0	0.0265	0.0028	4.08	0.1168	0.1402	0.0022
	5.73	0.8727	1	0.0648	1.8	0.9046	1	0.0364
	5.73	0.8727	1	0.0648	1.8	0.9046	1	0.0364
	5.73	0.8727	1	0.0648	1.8	0.9046	1	0.0364
	85.94	0	0.0901	0.0325	4.2	0.1136	0.1935	0.02554
	5.73	0.8727	1	0.0648	1.8	0.9046	1	0.0364
	5.73	0.8727	1	0.0648	1.8	0.9046	1	0.0364
	5.73	0.8727	1	0.0648	1.8	0.9046	1	0.0364
	83.08	0	0.1538	0.0946	4.14	0.1152	0.2513	0.0741
	5.73	0.8727	1	0.0648	1.8	0.9046	1	0.0364
	5.73	0.8727	1	0.0648	1.8	0.9046	1	0.0364
	5.73	0.8727	1	0.0648	1.8	0.9046	1	0.0364

Ave $(2\beta_T - \xi_T)^2 = 0.03578$

No of peripheral solvent atoms: n*	Angle of contact θ	α_c	β_c	$(2\beta_T - \xi_T)^2$	distance (d) Å	α_T	β_T	$(2\beta_T - \xi_T)^2$
3 Cl attached to the central carbon atom	83.08	0	0.1538	0.0946	3.0	0.1572	0.2868	0.0672
	8.59	0.809	1	0.1459	0.3	0.945	1	0.0121
	11.46	0.7454	1	0.2594	0.3	0.945	1	0.0121
	11.46	0.7454	1	0.2594	0.3	0.9267	1	0.0215
	74.48	0	0.3448	0.4755	3.06	0.1543	0.4459	0.3401
	8.59	0.809	1	0.1459	0.3	0.945	1	0.0121
	11.46	0.7454	1	0.2594	0.3	0.9267	1	0.0215
	11.46	0.7454	1	0.2594	0.3	0.9267	1	0.0215
	68.75	0	0.4721	0.8916	2.94	0.1603	0.5567	0.6287
	8.59	0.809	1	0.1459	0.3	0.945	1	0.0121
	11.46	0.7454	1	0.2594	0.3	0.9267	1	0.0215
	11.46	0.7454	1	0.2594	0.3	0.9267	1	0.0215

Ave $(2\beta_T - \xi_T)^2 = 0.1001$

Table 6.3 cont ...

Solvent: 1,1-Dichloro ethane

No of peripheral solvent atoms: n*	Angle of contact θ	α_C	β_C	$(2\beta_T - \xi_T)^2$	distance (d) Å	α_T	β_T	$(2\beta_T - \xi_T)^2$
1H	88.81	0	0.0265	0.0028	4.2	0.1136	1.137	0.0022
attached	5.73	0.8727	1	0.0648	2.1	0.9005	1	0.0396
to CCl_2	5.73	0.8727	1	0.0648	2.1	0.9005	1	0.0396
group	5.73	0.8727	1	0.0648	2.1	0.9005	1	0.0396
	85.94	0	0.0901	0.03251	4.32	0.1105	0.1906	0.0257
	5.73	0.8727	1	0.0648	2.1	0.9005	1	0.0396
	5.73	0.8727	1	0.0648	2.1	0.9005	1	0.0396
	5.73	0.8727	1	0.0648	2.1	0.9005	1	0.0396
	83.08	0	0.1538	0.0946	4.08	0.1168	0.2527	0.0738
	5.73	0.8727	1	0.0648	2.1	0.9005	1	0.0396
	5.73	0.8727	1	0.0648	2.1	0.9005	1	0.0396
	5.73	0.8727	1	0.0648	2.1	0.9005	1	0.0396

Ave $(2\beta_T - \xi_T)^2 = 0.0382$

3H from	68.75	0	0.4721	0.8916	3.18	0.1487	0.5506	0.6461
one	5.73	0.8727	1	0.0648	1.08	0.9204	1	0.0253
methyl	5.73	0.8727	1	0.0648	0.96	0.9245	1	0.0228
group	5.73	0.8727	1	0.0648	0.96	0.9245	1	0.0228
	34.38	0.2361	1	2.3344	2.94	0.3585	1	1.6461
	5.73	0.8727	1	0.0648	1.08	0.9204	1	0.0253
	5.73	0.8727	1	0.0648	0.96	0.9245	1	0.0228
	5.73	0.8727	1	0.0648	0.96	0.9245	1	0.0228
	22.92	0.4907	1	1.0375	3.06	0.5693	1	0.7421
	5.73	0.8727	1	0.0648	1.08	0.9204	1	0.0253
	5.73	0.8727	1	0.0648	0.96	0.9245	1	0.0228
	5.73	0.8727	1	0.0648	0.96	0.9245	1	0.0228

Ave $(2\beta_T - \xi_T)^2 = 0.271$

2 Cl	83.08	0	0.1538	0.0946	4.8	0.0996	0.2381	0.0767
from	8.59	0.809	1	0.1459	1.26	0.8729	1	0.0646
2 C-Cl	11.46	0.7454	1	0.2594	1.2	0.8338	1	0.1105
groups	11.46	0.7454	1	0.2594	1.2	0.8338	1	0.1105

Table 6.3 cont

Solvent: 1,1-Dichloro ethane (cont ...)

74.48	0	0.3448	0.4755	4.92	0.0972	0.4085	0.3876
8.59	0.809	1	0.1459	1.26	0.8729	1	0.0646
11.46	0.7454	1	0.2594	1.2	0.8338	1	0.1105
11.46	0.7454	1	0.2594	1.2	0.8338	1	0.1105
68.75	0	0.4721	0.8916	4.68	0.1021	0.526	0.7188
8.59	0.809	2	0.1459	1.26	0.8729	1	0.0646
11.46	0.7454	1	0.2594	1.2	0.8338	1	0.1105
11.46	0.7454	1	0.2594	1.2	0.8338	1	0.1105

Ave $(2\beta_T - \xi_T)^2 = 0.1699$

Table 6.3 cont ...

Solvent: 1,2-Dichloro ethane

No of peripheral solvent atoms: n*	Angle of contact θ	α_c	β_c	$(2\beta_T - \xi_T)^2$	distance (d) Å	α_T	β_T	$(2\beta_T - \xi_T)^2$
4H (set	88.81	0	0.0265	0.0028	4.86	0.0984	0.1222	0.0023
of two	5.73	0.8727	1	0.0648	2.1	0.9005	1	0.0396
$-CH_2$	5.73	0.8727	1	0.0648	2.1	0.9005	1	0.0396
groups)	5.73	0.8727	1	0.0648	2.1	0.9005	1	0.0396
	85.94	0	0.0901	0.0325	5.16	0.0927	0.1745	0.0268
	5.73	0.8727	1	0.0648	2.1	0.9005	1	0.0396
	5.73	0.8727	1	0.0648	2.1	0.9005	1	0.0396
	5.73	0.8727	1	0.0648	2.1	0.9005	1	0.0396
	83.08	0	0.1538	0.0946	4.38	0.109	0.246	0.0751
	5.73	0.8727	1	0.0648	2.1	0.9005	1	0.0396
	5.73	0.8727	1	0.0648	2.1	0.9005	1	0.0396
	5.73	0.8727	1	0.0648	2.1	0.9005	1	0.0396

Ave $(2\beta_T - \xi_T)^2 = 0.0384$

2 Cl	83.08	0	0.1538	0.0946	4.74	0.1009	0.2391	0.0765
	8.59	0.809	1	0.1459	1.26	0.8729	1	0.0646
	11.46	0.7454	1	0.2594	1.26	0.8306	1	0.1148
	11.46	0.7454	1	0.2594	1.26	0.8306	1	0.1148
	74.48	0	0.3448	0.4755	4.86	0.0984	0.4092	0.3866
	8.59	0.809	1	0.1459	1.26	0.8729	1	0.0646
	11.46	0.7454	1	0.2594	1.26	0.8306	1	0.1148
	11.46	0.7454	1	0.2594	1.26	0.8306	1	0.1148
	68.75	0	0.4721	0.8916	4.68	0.1021	0.526	0.7188
	8.59	0.809	1	0.1459	1.26	0.8729	1	0.0646
	11.46	0.7454	1	0.2594	1.26	0.8306	1	0.1148
	11.46	0.7454	1	0.2594	1.26	0.8306	1	0.1148

Ave $(2\beta_T - \xi_T)^2 = 0.1721$

Table 6.3 cont ...

Solvent: 1,1,2,2-tetra chloroethane

No of peripheral solvent atoms: n*	Angle of contact θ	α_c	β_c	$(2\beta_T - \xi_T)^2$	distance (d) Å	α_T	β_T	$(2\beta_T - \xi_T)^2$
2H from	88.81	0	0.0265	0.0028	5.76	0.0832	0.1074	0.0024
the two	5.73	0.8727	1	0.0648	2.4	0.8973	1	0.0422
-CH	5.73	0.8727	1	0.0648	2.4	0.8973	1	0.0422
groups	5.73	0.8727	1	0.0648	2.4	0.8973	1	0.0422
	85.94	0	0.0901	0.0325	5.46	0.0877	0.1699	0.0271
	5.73	0.8727	1	0.0648	2.4	0.8973	1	0.0422
	5.73	0.8727	1	0.0648	2.4	0.8973	1	0.0422
	5.73	0.8727	1	0.0648	2.4	0.8973	1	0.0422
	83.08	0	0.1538	0.0946	5.22	0.0917	0.2314	0.0781
	5.73	0.8728	1	0.0648	2.4	0.8973	1	0.0422
	5.73	0.8727	1	0.0648	2.4	0.8973	1	0.0422
	5.73	0.8727	1	0.0648	2.4	0.8973	1	0.0422

Ave $(2\beta_T - \xi_T)^2 = 0.041$

4 Cl	83.08	0	0.1538	0.0946	5.1	0.0938	0.2332	0.0777
attached	8.59	0.809	1	0.1459	1.32	0.8707	1	0.0669
to two	11.46	0.7454	1	0.2594	1.26	0.8306	1	0.1148
$C Cl_2$ groups	11.46	0.7454	1	0.2594	1.26	0.8306	1	0.1148
	74.48	0	0.3448	0.4755	5.16	0.0927	0.4055	0.3914
	8.59	0.809	1	0.1459	1.32	0.8707	1	0.0669
	11.46	0.7454	1	0.2594	1.26	0.8306	1	0.1148
	11.46	0.7454	1	0.2594	1.26	0.8306	1	0.1148

Ave $(2\beta_T - \xi_T)^2 = 0.174$

Table 6.4

Comparison of the values of $(2\beta_T - \xi_T)^2$ obtained by the new approach (section 6.5) against the values measured using the Homer and Percival method (Table 5.5, Chapter 5) for TMS solute in various solvents

Solvent	Molar volume of 30° (ref: Table 5.3)	$(2\beta_T - \xi_T)^2$ (Homer & Percival method)	$(2\beta_T - \xi_T)^2$ New approach
1,2-dichloroethane	79.92	0.2	0.1249
Chloroform	81.17	0.2	0.1387
1,1-dichloroethane	85.3	0.126	0.2399
Carbon tetrachloride	97.0	0.1403	0.2581
1,1,2,2-tetra chloro-ethane	106.33	0.1085	0.2581
Cyclohexane	110.13	0.1875	0.2076
2,3-dimethyl butane	132.08	0.2644	0.2628
2-Methyl pentane	133.49	0.2644	0.2628
2,2-dimethyl butane	134.08	0.2644	0.2634
TMS	139.6	0.302	0.3018
Decalin	157.84	0.3496	0.3682
Bicyclohexyl	195.13	0.4414	0.4155
n-Decane	196.78	0.4414	0.3974
Hexadecane	295.37	0.6678	0.4411

6.6 Comparison of the buffeting parameters obtained by Homer and Percivals method and those obtained by the present approach

A careful scrutiny of the buffeting parameters depicted in Table 6.4 reveal some very interesting facts, which are considered below.

1 The value of $(2\beta_T - \xi_T)^2$ for TMS (solute)-TMS (solvent) obtained by the present approach is 0.3018 which is very similar to the value of 0.302 (Table 5.5) obtained using Homer and Percival's original buffeting model.

This confirms the suggestion made by Homer and Percival that to represent the solvent molecule with spheres of an appropriate size derived from the molar volume of the solvents is totally acceptable when the solvents are spherical and symmetrical. However the values for non-spherical solvents obtained by the two approaches to buffeting show marked differences.

2 The same value of 0.2644 for $(2\beta_T - \xi_T)^2$ (Table 5.5) was reported for the three solvent solvents, 2-Methyl pentane, 2,2-dimethyl butane and 2,3-dimethyl butane on the basis of the original buffeting model. This is because the difference in the molar volumes of these solvents is so small that they can be represented by just one sphere and this necessarily leads to the same value of $(2\beta_T - \xi_T)^2$. However, when using the modified approach proposed here (that accounts for the size and the shape of the solvents) it is possible to actually obtain three slightly different values for all three solvents, ie. 0.2628, 0.2634 and 0.2613 respectively. In spite of the marginal differences between them (due to the similarity in size and structure) this appears to be more realistic. Nevertheless, the differences between the three values obtained by the present approach and that obtained by Homer and Percival's model appear to be marginal. This once again confirms that these molecules can be safely assumed to be spherical for the purpose of measuring the buffeting parameters.

3 A totally different situation emerges when comparing the buffeting parameters for bicyclohexyl and decane. Although these molecules have rather similar molar volumes, ie. 195.13 cm^3 and 196.78 cm^3 respectively, the differences in the buffeting parameters obtained by the present approach is clearly noticable (0.4155 and 0.3974 respectively). This is essentially due to the marked differences in their molecular structures. Using Homer and Percival's model a single value of 0.4414 was deduced for both molecules. The failure to incorporate the effect of molecular structure of such solvent molecules may be one of the reasons for the poor correlations obtained in Figure 5.4, Chapter 5.

4 The two values for the buffeting parameters for hexadecane using Homer and Percival's method and the present approach are 0.6678 and 0.4411 respectively. The value of 0.6678 appears to be unrealistically high, because of the invalid assumption of assuming that such a large linear solvent molecule can be represented by a sphere. This assumption necessitates that the measured value of buffeting parameter incorporates the possibility that all peripheral atoms on the solvent molecule have an equal probability of coming into contact with the TMS solute molecule. This would appear to be unrealistic. However with the present approach, a value of 0.4411 was obtained. This reflects the effect of sterically different peripheral atoms.

It is not appropriate to compare the values of the buffeting parameters obtained by the two different methods for solvents containing peripheral chlorine atoms, because the values for both the methods are reported for different values of Q, ie. Q = 5.5 for Homer and Percival's method and Q = 6.6 for the present approach.

Having analysed some of the basic differences between the two approaches for measuring the buffeting parameters, it is now appropriate to utilize the values obtained by the present approach to analyse experimental chemical shifts and so assess its validity.

6.7 Regressional analysis of the buffeting parameters obtained by the modified approach to $(2\beta_T - \xi_T)^2$ on experimentally obtained chemical shifts

The linear regression of $(2\beta_T - \xi_T)^2$ on the observed shifts (gas-to-liquid chemical shifts, corrected for bulk susceptibility and reaction field screenings) for TMS (solute) in various solvents containing peripheral hydrogen atoms is shown in Figure 6.4.

In order to establish the effect of the electron displacement term Q, solvents with peripheral chlorine atoms are treated separately to those with peripheral hydrogen atoms.

The results of the regression of the buffeting parameters for various values of Q (for solvents with peripheral chlorine atoms) on the experimental shifts are incorporated in Table 6.5. Inspection of these results reveals that the best correlation coefficient is obtained for Q = 6.6. The regression is depicted in Figure 6.5.

An additional Figure 6.6 shows the linear regression of $(2\beta_T - \xi_T)^2$ for all the solvents in the present investigation on the experimentally observed gas-to-solution shifts (corrected for χ and $-B \langle R_T^2 \rangle$).

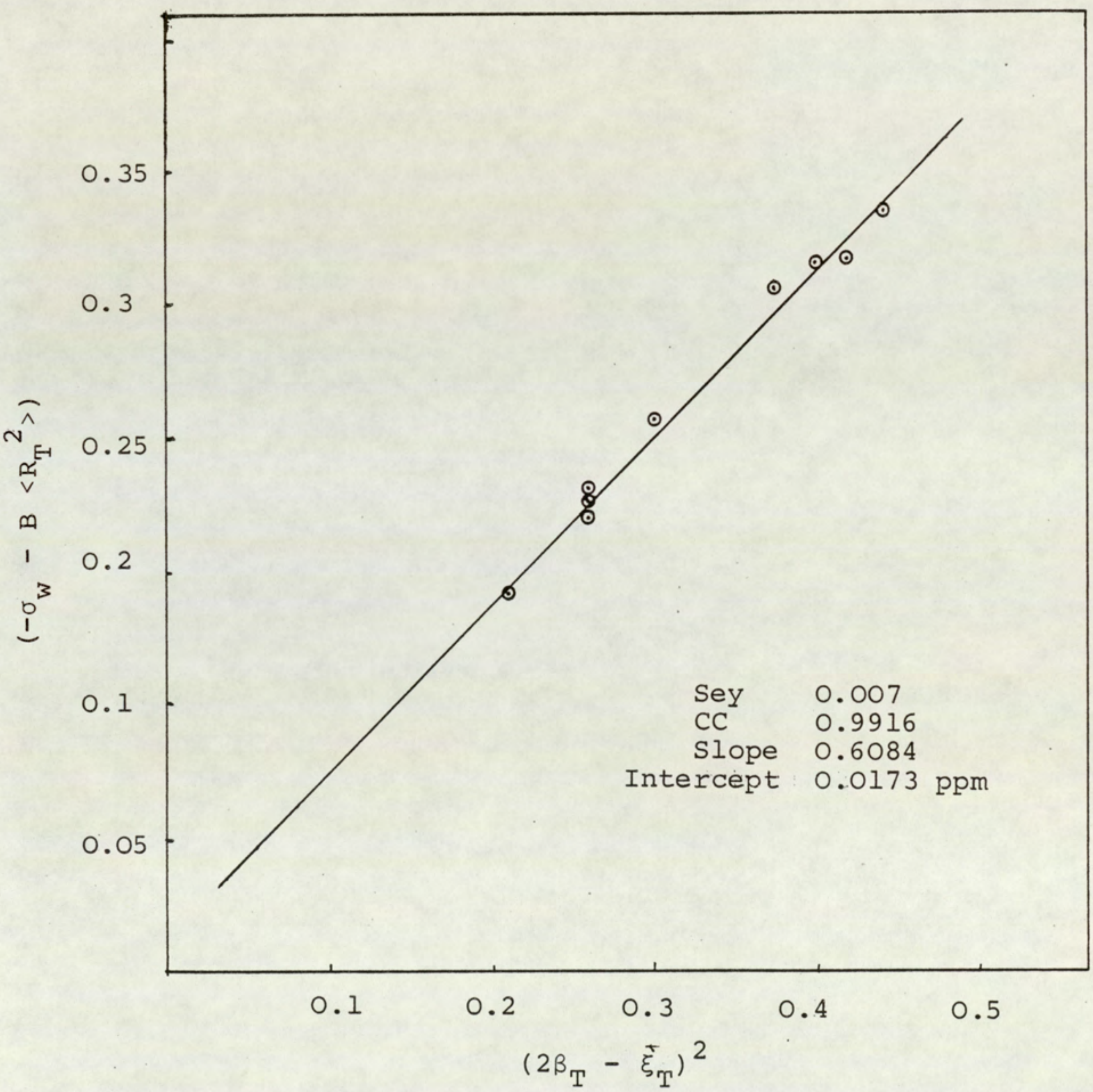

Figure 6.4: Linear regression of $(2\beta_T - \xi_T)^2$ for solvents with peripheral hydrogen atoms on $(-\sigma_w - B \langle R_T^2 \rangle$

Table 6.5 - Results of linear regression of $(2\beta_T - \xi_T)^2$ for different values of Q for TMS (solute) in solvents containing peripheral chlorine atoms on $-\sigma_w - B \langle R_T^2 \rangle$ ($-\sigma_w$ is the gas-to-liquid chemical shift corrected for bulk susceptibility)

	$-\sigma_w - B \langle R_T^2 \rangle$	Q $(2\beta_T - \xi_T)^2$ for different values of Q				
Solvent	ppm	5.0	5.1	5.2	5.3	5.4
1,2-dichloroethane	0.0682	0.1009	0.1023	0.1039	0.1053	0.1069
$CHCl_3$	0.0669	0.1072	0.1094	0.1109	0.1132	0.1154
1,1-dichloroethane	0.126	0.2162	0.2175	0.2192	0.2205	0.2222
CCl_4	0.1403	0.1956	0.1995	0.2034	0.2073	0.2112
1,1,2,2-tetrachloro-ethane	0.1085	0.1656	0.1687	0.1717	0.1747	0.1778
Co coeff		0.9553	0.9606	0.9649	0.9691	0.9723
Slope		0.6172	0.6163	0.6126	0.6113	0.6084
Intercept		0.005	0.004	0.003	0.002	0.001
		5.5	5.6	5.7	5.8	5.9
1,2-dichloroethane	0.0682	0.1083	0.1099	0.1113	0.1129	0.1143
$CHCl_3$	0.0669	0.1169	0.1192	0.1214	0.1229	0.1252
1,1-dichloro ethane	0.126	0.2235	0.2249	0.2265	0.2279	0.2295
CCl_4	0.1403	0.2151	0.2190	0.2229	0.2268	0.2308
1,1,2,2-tetrachloro-ethane	0.1085	0.1808	0.1839	0.1869	0.1899	0.1930
Co coeff		0.9761	0.979	0.9813	0.984	0.9857
Slope		0.6043	0.6021	0.5979	0.5932	0.5885
Intercept		0.00	-0.001	-0.002	-0.003	-0.003

Table 6.5 cont ...

	$-\sigma_W - B \langle R_T^2 \rangle$	$Q\,(2\beta_T - \xi_T)^2$ for different values of Q				
Solvent	ppm	6.0	6.1	6.2	6.3	6.4
1,2-dichloroethane	0.0682	0.1158	0.1173	0.1188	0.1203	0.1218
$CHCl_3$	0.0669	0.1267	0.1289	0.1312	0.1327	0.1349
1,1-dichloroethane	0.126	0.2308	0.2325	0.2339	0.2355	0.2369
CCl_4	0.1492	0.2347	0.2385	0.2425	0.2464	0.2503
1,1,2,2-tetrachloro-ethane	0.1085	0.196	0.199	0.2021	0.2051	0.2082
Co coeff		0.9877	0.9888	0.9898	0.9909	0.9914
Slope		0.5833	0.5785	0.5739	0.5674	0.5625
Intercept		-0.004	-0.004	-0.005	-0.005	-0.005
		6.5	6.6	6.7	6.8	6.9
1,2-dichloroethane	0.0682	0.1233	0.1249	0.1264	0.1279	0.1294
$CHCl_3$	0.0669	0.1372	0.1387	0.1409	0.1424	0.1447
1,1,-dichloroethane	0.126	0.2382	0.2399	0.2412	0.2429	0.2442
CCl_4	0.1492	0.2542	0.2581	0.262	0.266	0.2699
1,1,2,2-tetrachloro ethane	0.1085	0.2112	0.2143	0.2173	0.2203	0.2233
Co coeff		0.9917	0.9921	0.992	0.9920	0.9913
Slope		0.5579	0.5511	0.5460	0.5387	0.5356
Intercept		-0.005	-0.006	-0.006	-0.006	-0.006

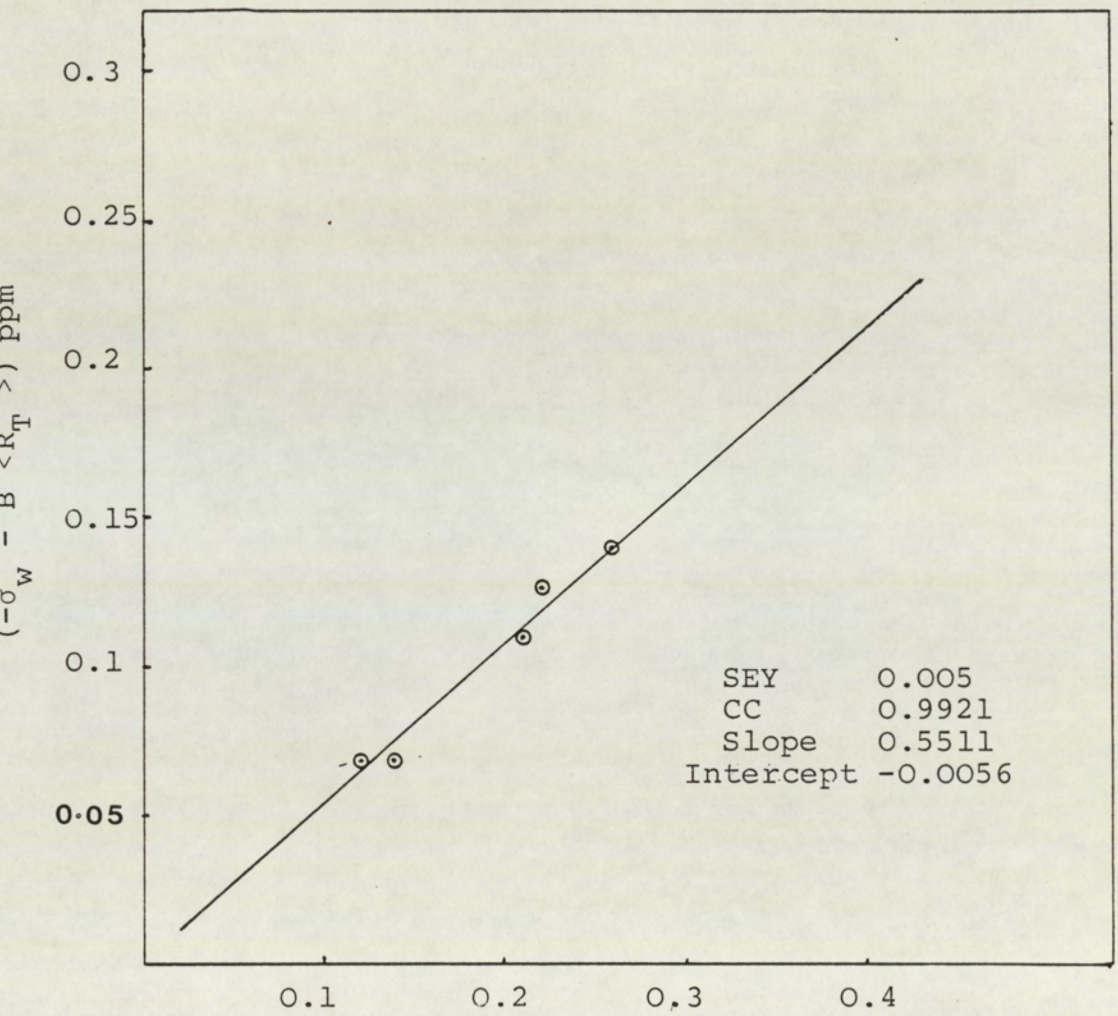

Figure 6.5: Linear regression of $(2\beta_T - \xi_T)^2$ for solvents with peripheral chlorine atoms on $(-\sigma_W - B \langle R_T^2 \rangle)$

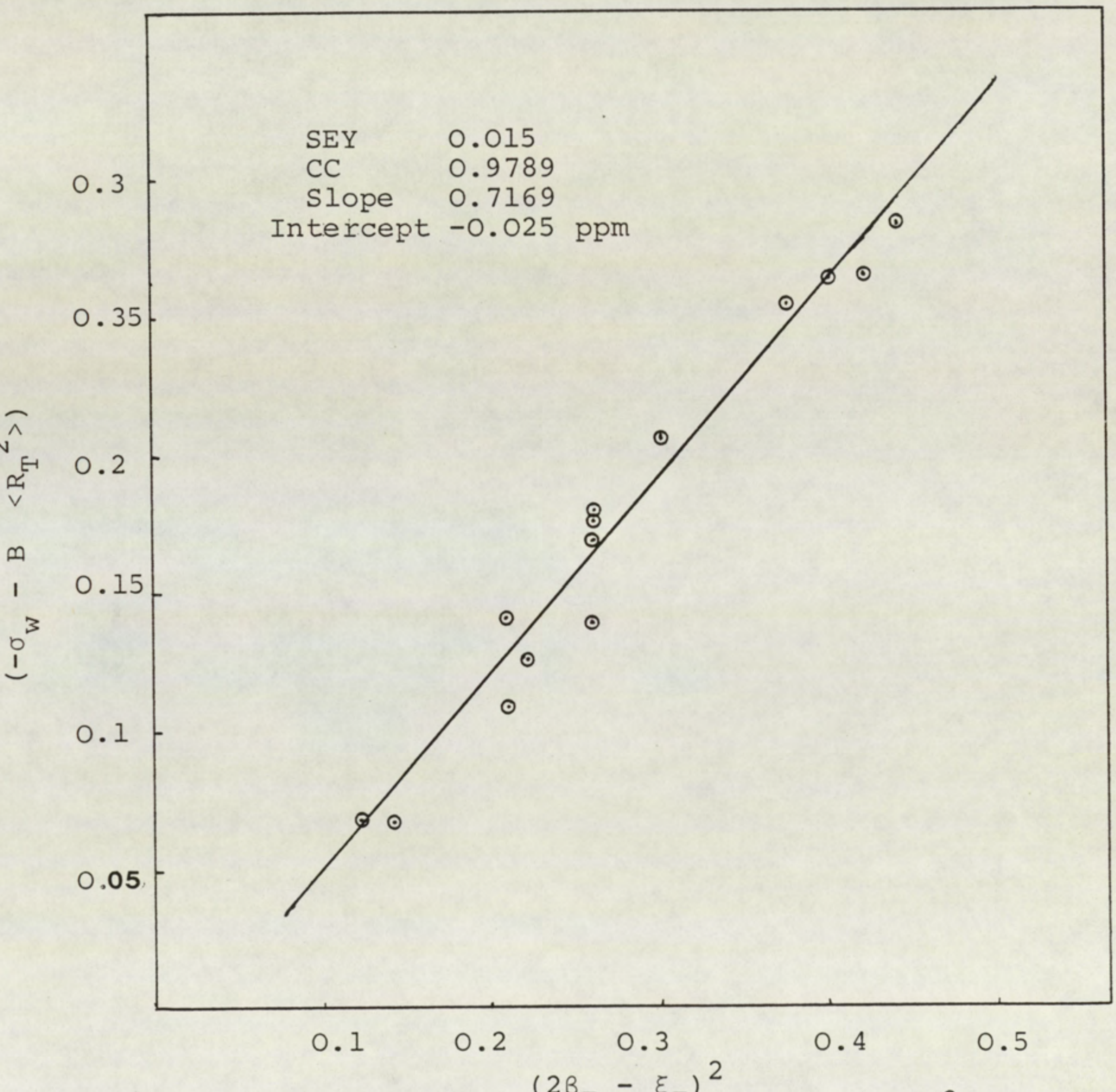

Figure 6.6: Linear regression of $(2\beta_T - \xi_T)^2$ for all the solvents on $(-\sigma_W - B^T<R_T^{2T}>)$

6.7.1 Results and Discussion

It is apparent from equation 3.26 that the slopes of the regressions depicted in Figures 6.4, 6.5 and 6.6 should represent the value for $-BK/r^6$.

The value for $-BK/r^6$ obtained for TMS as solute in various solvents with peripheral hydrogen atoms is 0.6084 ppm (Figure 6.4), which is in good agreement with Homer and Percival's value of 0.6206. The correlation coefficient is 0.9916 with a standard deviation of 0.007 and intercept of 0.0173 ppm.

Figure 6.5 shows a value of 0.5511 ppm for BK/r^6 for TMS solute in various solvents containing peripheral chlorine atoms, which is reasonably comparable with Homer and Percival's value of 0.6206 ppm. The correlation coefficient is 0.9921 with standard deviation of 0.005 and negligible intercept of -0.0056ppm. These values have been obtained for the best-fit Q values of 6.6 which is in good agreement with the value of 6.5 predicted by Yonomoto[112].

The linear regression of $(2\beta_T - \xi_T)^2$ for all the solvents against the experimental shifts (Figure 6.6) shows a value of 0.6084 ppm for BK/r^6 which is once again comparable with Homer and Percival's value of 0.6206. The correlation coefficient is 0.9916, with standard deviation of 0.007 and negligible intercept of 0.0173 ppm.

The negligible intercepts, good correlation coefficients and values for the parameters BK/r^6 and Q that compare with those reported elsewhere clearly indicate the success of the new approach to the buffeting model. This overcomes the shortcoming of the approach of Homer and Percival.

6.8 Conclusions

The refinements to the original buffeting model proposed by Homer and Percival that are reported here, facilitate the more precise evaluation of the buffeting parameters for solvents of any size and shape. Eventually this may, through the use of computer simulation enable a better understanding of the geometrical factors affecting the intermolecular forces.

Probably the most promising aspect of the present investigation is the standardization of the treatment of the buffeting interaction and the characterization of the nuclear screening constant σ_{BI}.

CHAPTER SEVEN

AN INVESTIGATION AND JUSTIFICATION OF THE INDIVIDUAL CONTRIBUTIONS THOUGHT TO CHARACTERIZE VAN DER WAALS NUCLEAR SCREENING

7.1 Introduction

The original work of Homer and Percival[39] suggested that van der Waals dispersion forces can be characterized by three discrete effects. Justification for these three effects emerge from the self-consistency of their composite analysis of a vast range of experimental data. Similarly the work presented earlier in this thesis has revealed that the use of the primary and secondary mean square reaction fields together with the buffeting square field, ie. $<R_1^2> + <R^2{}_2> + <E^2>_{BI}$ can be used in a satisfactorily self-consistent way to analyse the chemical shifts in a range of complex molecules. However, at no time has there been conclusive experimental proof that each of the three contributing terms exist separately. The purpose of this chapter is to demonstrate that $<R_1^2>$, $<R_2^2>$ and $<E^2>_{BI}$ have been adequately characterized and act separately.

7.2 Theoretical

The derivation of $<R_1^2>$ from an Onsager type treatment indicates that all points in the hypothetical cavity will experience the full value of $<R_1^2>$. The original derivation of the extra-solvent cavity mean square field $<R_2^2>$, however, yields an equation slightly different to that presented earlier in this thesis. In essence the correct formulation of $<R_2^2>$ would be given by:

$$<R_2^2> = \left[\frac{8\pi}{9}\right]^2 \cdot 2\left[\frac{r_1}{r_2}\right]^2 \frac{<\mu_2^2>}{V_2^2} \cdot \frac{(n_2^2+2)^2\,(n_2^2-1)^2}{9\,n_2^4} \left[\frac{r}{a}\right]^6 \qquad \text{..... 7.1}$$

from which it can be seen that $(r/a)^6$ is included; where r is the solvent molecule radius and a = r + d where d is the distance between the centre of the resonant nucleus and the periphery of the solute molecule. To all intents and purposes when considering regions at the periphery of the solute, $(r/a)^6$ may be taken as unity as assumed by Homer and Percival. If, however, the screening of nuclei within the solute molecular cavity is considered, the value of $(r/a)^6$ should be evaluated and used in equation 7.1. In a similar way when considering the buffeting square field E^2_{BI}, this was also derived for a position at the periphery of the solute molecule. However, when considering the screening of nuclei within a molecule, it is evident that E^2_{BI} may be reduced or indeed zero.

The above principles that are implicit in the derivation of these three terms contributing to dispersion forces can be tested by investigating the screening of nuclei at different locations within a molecule. To this end the ^1H and ^{13}C of tetraethylmethane $C\,(CH_2\,CH_3)_4$ have been studied as well as ^1H, ^{13}C and ^{29}Si of tetramethylsilane $Si\,(CH_3)_4$.

The procedure adopted was to measure the appropriate shifts in the somewhat limited range of readily available and suitable solvents(113). These are TMS, CCl_4, C_6H_{12}, CEt_4 and C_6H_6 for TMS; and TMS, CCl_4, C_6H_{12} and CEt_4 for CEt_4. The measurements were carried out by Dr HK Al-Daffaee at 30°C using a JEOL FX 90Q NMR spectrometer locked to the ^2H resonance of D_2O contained in a 5mm OD NMR tube co-axial with the main 10mm OD NMR tube so that the system of interest was contained in the annulus. For each particular nuclide the irradiation frequency was kept constant and the shifts measured relative to the irradiating frequency (mentioned in appropriate tables). Because of the difference in the volume magnetic susceptibilities of the solvents used, each shift was corrected(113) for the appropriate susceptibility of the solution; this was deduced by the solution volume fraction weighting of the susceptibilities of the pure materials (given in Table 7.1).

Table 7.1 - The volume magnetic susceptibilities of the solvents used at 30°C

Compound	$-\chi/10^{-6}$ at 30°C
$C\,(CH_2\,CH_3)_4$	0.6657
$Si\,(CH_3)_4$	0.536
$C_6\,H_{12}$	0.627
$C\,Cl_4$	0.681
C_6H_6	0.611
D_2O	0.708

7.3 Studies of Tetraethylmethane $C\,(CH_2CH_3)_4$

The observed[113] ^1H and ^{13}C shifts together with volume magnetic susceptibility corrected shifts for $C\,(CH_2\,CH_3)_4$ in various solvents are recorded in Tables 7.2 and 7.3 respectively.

The present objective is to ascertain whether the definitions of $\langle R_1{}^2\rangle$, $\langle R_2{}^2\rangle$ and $E^2{}_{BI}$ as given in Chapter 3 and also by Homer and Percival for peripheral nuclei are adequate or whether it is necessary to modify the latter two terms consistent with the principles implicit in their derivation. Concurrently, it is hoped to obtain experimental evidence for their separate existance.

Solvent	$^1H_{obs}$ group	$^1H\delta_{obs}$ Hz	$H\delta_{obs}$ Hz	$\frac{-2\pi}{3}\chi_v$ ppm	$^1H\delta_{true}$ ppm	$^1H\delta_{true}$ Hz
$SiMe_4$	CH_2	-7.42	-0.083	1.226	+1.04	93.17
	CH_3	+30.86	+0.3444		+1.467	131.45
CEt_4	CH_2	-31.25	-0.3488	1.3942	+1.045	93.68
	CH_3	+6.25	+0.0698		+1.464	131.18
C_6H_{12}	CH_2	-23.24	-0.2594	1.3132	+1.054	94.43
	CH_3	+14.26	+0.1591		+1.4723	131.92
CCl_4	CH_2	-39.83	-0.4445	1.4263	+0.9818	87.97
	CH_3	-3.7	-0.0413		+1.385	124.10

Table 7.2 - ^1H observed[113] and susceptibility corrected shifts from ^2H, of CEt_4 in various solvents. Measurements were made employing a JEOL FX 90Q NMR spectrometer at 30°C, with irradiation frequency of 89.60415 MHz.

Solvent	^{13}C	δ^{obs} Hz	δ^{obs} ppm	$\frac{-2\pi}{3}\chi_v$ ppm	δ^t ppm
	C	1213.38	53.85		54.97
TMS	CH_2	1440.43	63.93	1.12	65.05
	CH_3	1887.20	83.75		84.87
	C	1208.50	53.63		55.02
CEt_4	CH_2	141.88	63.55	1.39	64.94
	CH_3	1881.10	83.48		84.87
	C	1210.94	53.74		55.05
C_6H_{12}	CH_2	1435.54	63.71	1.31	65.02
	CH_3	1887.20	83.75		85.06
	C	1198.73	53.20		54.63
CCl_4	CH_2	1425.78	63.28	1.43	64.71
	CH_3	1865.23	82.78		84.21

Table 7.3 - ^{13}C observed(113) and susceptibility corrected shifts, from 2H, of C $(CH_2\ CH_3)_4$ in different solvents. The measurements were made using a JEOL FX 90Q NMR spectrometer operating at 30°C with an irradiating frequency of 22.533 MHz.

Using the data provided in Table 7.4, the appropriate values of $<R_1^2>$, $<R_2^2>$ and $<R^2_T>$ are calculated and recorded in Table 7.5. Additionally, the values of the buffeting parameters β_T and ξ_T were deduced for the methyl and methylene protons and carbon atoms by using the new approach which was discussed in Chapter 6. Values of $(2\beta_T - \xi_T)^2$ and E^2_{BI} are given in Table 7.6 in a condensed form (to avoid repetition of the measured values). However, all the relevant measurements necessary to calculate the buffeting parameters are incorporated in Table 7.6. For the calculation of the buffeting effects of CCl_4 the value of 6.5 for Q deduced by Homer and Percival[39] for chlorine atom was used. Given below are the values of K/r^6 which were used to calculate E^2_{BI}.

$E^2_{BI} = K/r^6\ (2\beta_T - \xi_T)^2$

$K^H/r^6_{HH} = 0.7133 \times 10^{12}$ esu

$K^{Cl}/r^6_{HCl} = 1.2715 \times 10^{12}$ esu

$Q = 6.5$

$r_{HH} = 2.4$ Å, $r_{HCl} = 3.0$ Å

Table 7.4 - Data required for reaction field calculations (ref: Chapter 4)

Compound	r Å	$\alpha/10^{-23}$ cm^{-3}	$I/10^{-12}$ erg	Molar volume cm^3	n^2_D
$C(C_2H_5)_4$	4.358	1.64928	16.5	171.91	2.0181
$Si(CH_3)_4$	4.079	1.19	15.7	139.6	1.8266
CCl_4	3.613	1.05	18.3	97.0	2.1144
C_6H_{12}	3.746	1.04196	157.2	110.13	2.034

r - molecular radius

α - polarizability
I - ionization potential
n_D - refractive index

Table 7.5 - The calculated mean square reaction fields $\langle R_1^2 \rangle$, $\langle R_2^2 \rangle$, and $\langle R_T^2 \rangle$ for C Et_4 in different solvents

Solvent	$\langle R_1^2 \rangle/10^{11}$ (esu)	$\langle R_2^2 \rangle/10^{11}$ (esu)	$\langle R_T^2 \rangle/10^{11}$ (esu)
$Si(CH_3)_4$	0.2867	0.6222	0.909
$C(C_2H_5)_4$	0.3933	0.7867	1.180
C_6H_{12}	0.3899	1.439	1.8294
CCl_4	0.4299	2.6496	3.0795

Table 7.6 - Measurement of $(2\beta_T - \xi_T)^2$ for CEt_4 (solute) in various solvents

Solvent: C_6H_{12} (for ^1H (CH_3) shifts of CEt_4

No of solvent atoms: n*	Angle of contact θ	Distance d Å	$(2\beta_T - \xi_T)^2$	No of similar measurements	Ave $(2\beta_T - \xi_T)^2$
6 ^1H	5.73	2.22	0.041	3	
equatorial	5.73	3.0	0.046	6	
	73.35	4.5	0.25	1	0.4514
	42.97	5.7	3.06	1	
	31.51	7.2	1.7089	1	
6 ^1H	5.73	1.92	0.038	3	
axial	5.73	1.8	0.036	6	
	77.35	4.26	0.025	1	0.4058
	42.97	4.5	2.91	1	
	28.65	6.36	1.38	1	

Wt ave $(2\beta_T - \xi_T)^2$: 0.4086

E^2_{BI}: 0.3057

Solvent: C Cl_4 (for ^1H (CH_3) shifts of CEt_4)

4 Cl	11.46	1.26	0.115	3	
	11.46	1.8	0.146	6	
	34.38	4.44	1.859	1	0.394
	68.75	6.0	0.754	1	
	22.92	6.72	0.895	1	
4 Cl	11.46	2.34	0.167	3	
	11.46	3.42	0.192	6	0.423
	34.38	5.82	1.966	1	
	68.75	6.6	0.767	1	
	20.05	7.32	0.693	1	

Wt ave $(2\beta_T - \xi_T)^2$: 0.4085

E^2_{BI}: 0.5194

n*: gives the number of peripheral solvent atoms which are in a similar geometrical environment (relative to the solute resonant atom) and where appropriate, the location or the group of solvent molecule to which they are bonded.

Table 7.6 cont ...

Solvent: TMS (for ^1H (CH_3) shifts of CEt_4)

No of solvent atoms: n*	Angle of contact θ	Distance d Å	$(2\beta_T - \xi_T)^2$	No of similar measurements	Ave $(2\beta_T - \xi_T)^2$
12 ^1H from	5.73	3.42	0.0481	3	
4 methyl	5.73	2.94	0.046	6	
groups	22.92	3.42	0.77	1	0.4309
	40.11	3.54	2.38	1	
	57.3	3.66	1.6	1	
12 ^1H from	5.73	4.86	0.053	3	
4 methyl	5.73	4.62	0.052	6	
groups	22.92	4.2	0.815	1	0.4713
	40.11	5.22	2.16	1	
	57.3	5.52	1.76	1	

Wt ave $(2\beta_T - \xi_T)^2$: 0.4511

E^2_{BI}: 0.3218

Solvent: CEt_4 (for ^1H (CH_3) shift of CEt_4)

12 ^1H from	5.73	1.26	0.029	3	
4 methyl	5.73	1.68	0.035	6	0.5064
groups	22.92	4.8	0.0841	1	
	42.97	7.56	3.199	1	
	57.3	5.22	1.74	1	
8 ^1H from	5.73	1.86	0.037		
4 methylene	5.73	2.16	0.04		
groups	22.92	8.6	0.865	0.5235	
	42.97	8.16	3.231		
	57.3	7.08	1.836		

Wt ave $(2\beta_T - \xi_T)^2$: 0.5132

E^2_{BI}: 0.366

Table 7.6 cont ...

Solvent: CEt_4 (For ^1H (CH_2) shifts of CEt_4)

No of solvent atoms: n*	Angle of contact θ	Distance d Å	$(2\beta_T - \xi_T)^2$	No of similar measurements	Ave $(2\beta_T - \xi_T)^2$
12^1H from	5.73	2.04	0.039	3	
4 methyl	5.73	2.46	0.043	6	
groups	40.11	5.4	2.639	1	0.498
	37.24	7.74	2.41	1	
	71.62	5.34	3.02	1	
8^1H from	5.73	5.34	0.054	3	
4 methylene	5.73	7.92	0.057	6	
groups	40.11	5.22	2.62	1	0.579
	42.97	5.82	3.07	1	
	68.75	5.94	0.754	1	

Wt ave $(2\beta_T - \xi_T)^2$: 0.530

E^2_{BI}: 0.378

Solvent: TMS (for ^1H CH_2) shifts of CEt_4

12^1H from	5.73	2.4	0.042	3	
4 methyl	5.73	2.82	0.045	6	0.5035
groups	68.75	6.06	0.756	1	
	37.24	5.46	2.28	1	
	40.11	5.1	2.61	1	
	5.73	2.4	0.042	3	
	5.73	2.82	0.045	6	
	68.75	6.42	0.7634	1	0.5102
	37.24	5.82	2.3073	1	
	40.11	5.58	1.1627	1	

Wt ave $(2\beta_T - \xi_T)^2$: 0.507

E^2_{BI}: 0.3616

Table 7.6 cont ...

Solvent: C_6H_{12} (for ^1H (CH_2) shifts of CEt_4)

No of solvent atoms: n*	Angle of contact θ	Distance d Å	$(2\beta_T - \xi_T)^2$	No of similar measurements	Ave $(2\beta_T - \xi_T)^2$
$6\,^1H$ axial	5.73	2.46	0.0426	6	
	5.73	1.92	0.0378	3	
	77.48	5.4	0.3949	1	0.3791
	37.24	6.36	2.3423	1	
	31.51	4.8	1.4426	1	
$6\,^1H$ equatorial	5.73	2.22	0.0407	6	
	5.73	1.8	0.0364	3	0.3572
	77.35	5.88	0.2667	1	
	37.24	6.54	2.3528	1	
	28.65	4.8	1.314	1	

Wt ave $(2\beta_T - \xi_T)^2$: 0.3682

E^2_{BI}: 0.2626

Solvent: CCl_4 (for ^1H (CH_2) shifts of CEt_4)

4 Cl	14.32	3.0	0.288	3	
	14.32	3.3	0.297	6	
	34.38	6.0	1.9765	1	0.645
	68.75	6.72	0.7689	1	
	37.24	6.54	2.3528	1	
4 Cl	14.32	3.0	0.288	3	
	14.32	3.3	0.297	6	
	34.38	5.7	1.9586	1	0.6262
	68.75	5.64	0.7466	1	
	37.24	4.32	2.1678	1	

Wt ave $(2\beta_T - \xi_T)^2$: 0.6356

E^2_{BI}: 0.8081

Table 7.6 cont

Solvent: CEt_4 (for ^{13}C (CH_3) shifts of CEt_4)

No of solvent atoms: n*	Angle of contact θ	Distance d Å	$(2\beta_T - \xi_T)^2$	No of similar measurements	Ave $(2\beta_T - \xi_T)^2$
12 ^1H from 4 methyl groups	37.24	3.84	2.102	3	1.721
	30.08	3.54	1.339	3	
8 ^1H from 4 methyl groups	37.24	4.68	2.209	3	1.811
	30.08	4.32	1.414	3	

Wt ave $(2\beta_T - \xi_T)^2$: 1.757

E^2_{BI}: 1.253

Solvent: TMS (for ^{13}C (CH_3) shifts of CEt_4)

12 ^1H from 4 methyl groups	37.24	3.48	2.043	3	1.642
	30.08	2.82	1.241	3	

Solvent: C_6H_{12} (for ^{13}C (CH_3) shifts of CEt_4)

6 ^1H	37.24	2.7	1.8707	3	1.5097
	30.08	2.34	1.1487	3	

E^2_{BI}: 1.0768

Solvent: CCl_4 (for ^{13}C (CH_3) shifts of CEt_4)

4 Cl	37.24	2.64	1.854	3	1.480
	30.08	2.16	1.106	3	

E^2_{BI}: 1.8818

Table 7.6 cont ...

Solvent: CEt_4 (for ^{13}C (CH_2) shifts of CEt_4)

No of solvent atoms: n*	Angle of contact θ	Distance d Å	$(2ß_T - \xi_T)^2$	No of similar measurements	Ave $(2ß_T - \xi_T)^2$
$12\,^1H$ from	83.5	5.46	0.0695	2	
4 methyl	79.5	5.16	0.1793	1	0.0796
groups	89.5	5.28	0.0004	1	
$8\,^1H$ from	83.5	6.12	0.0709	2	
4 methyl	79.5	6.0	0.1844	1	0.0817
groups	89.5	6.48	0.0004	1	

Ave $(2ß_T - \xi_T)^2$: 0.0804

E^2_{BI}: 0.0573

Solvent: TMS (for ^{13}C (CH_2) shifts of CEt_4)

$12\,^1H$ from	83.5	5.4	0.0693	2	
4 methyl	79.5	5.1	0.1788	1	0.0795
groups	89.5	5.22	0.0004	1	

E^2_{BI}: 0.0567

Solvent: C_6H_{12} (for ^{13}C (CH_2) shifts of CEt_4)

$6\,^1H$	83.5	4.98	0.0682	2	
	79.5	4.68	0.1756	1	0.078
	89.5	4.86	0.0004	1	

E^2_{BI}: 0.0556

Solvent: CCl_4 (for ^{13}C (CH_2) shifts of CEt_4)

4 Cl	83.5	4.8	0.0677	2	
	79.5	4.32	0.1723	1	0.0769
	89.5	4.74	0.0004	1	

E^2_{BI}: 0.0978

7.3.1 Analysis of Proton Shifts of C $(CH_2 CH_3)_4$

In the case of the methyl group in tetraethyl methane, Figure 7.1 shows the regression of $(\langle R_T^2 \rangle + E^2_{BI})$ on the susceptibility corrected shifts. This yields a B value of 0.359 x 10^{-18} esu which is evidently too small to correspond with Homer and Percival's average value of 0.87 x 10^{-18} esu. Figure 7.2 shows the regression with the square buffeting field E^2_{BI} eliminated and this again gives a low value for B of 0.381 x 10^{-18} esu. At the other extreme the regression of $\langle R_1^2 \rangle$ on the corrected shifts (Figure 7.3) gives an unacceptably high value for B of 3.94 x 10^{-18} esu.

Evidently the best value of B will be obtained from the appropriate regression that lies somewhere between $\langle R_1^2 \rangle$ and $(\langle R_T^2 \rangle + E^2_{BI})$ on the corrected shifts.

Figure 7.4 presents a two-dimensional representation of the C $(CH_2\ CH_3)_4$ molecule, from which the appropriate value for the $(r/a)^6$ modification implicit in the equation 7.1 can be estimated. For the two extremes for the methyl protons indicated in Figure 7.4 values of d = 1.0Å and d = 2.25Å. The average of these together with the possible positions at the periphery resulting from the rotation of the methyl group gives an average d value of 0.8Å. This was used to calculate the values of $\langle R_2^2 \rangle (r/a)^6$ that are given in Table 7.7 together with other immediately relevant data.

The regression of $\langle R_1^2 \rangle + \langle R_2^2 \rangle\ (r/a)^6 + K/r^6\ (2\beta_T - \xi_T)^2$ is shown in Figure 7.5. From this a value of 0.969 x 10^{-18} esu for B is deduced.

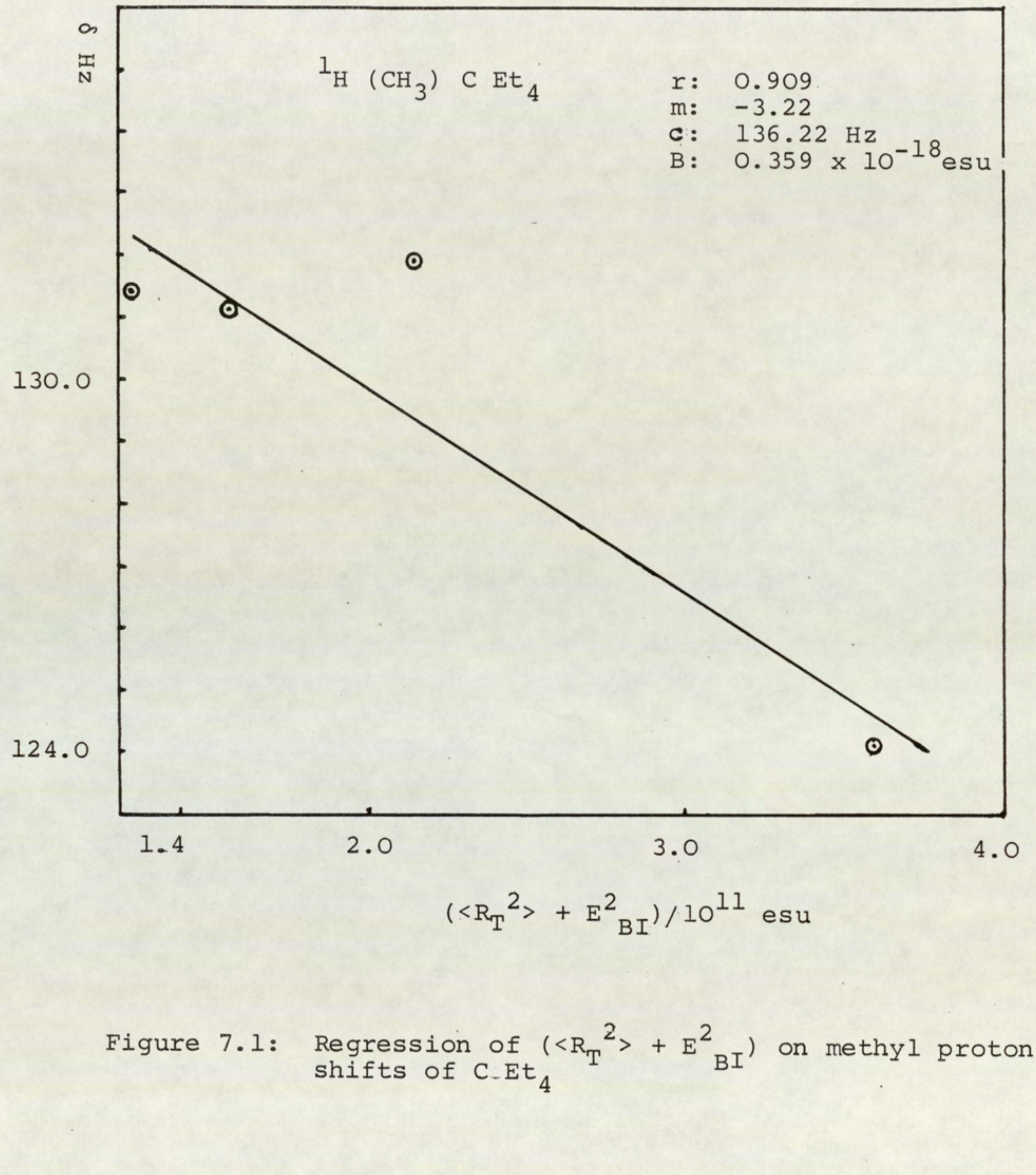

Figure 7.1: Regression of $(\langle R_T^2\rangle + E^2_{BI})$ on methyl proton shifts of $C\text{-}Et_4$

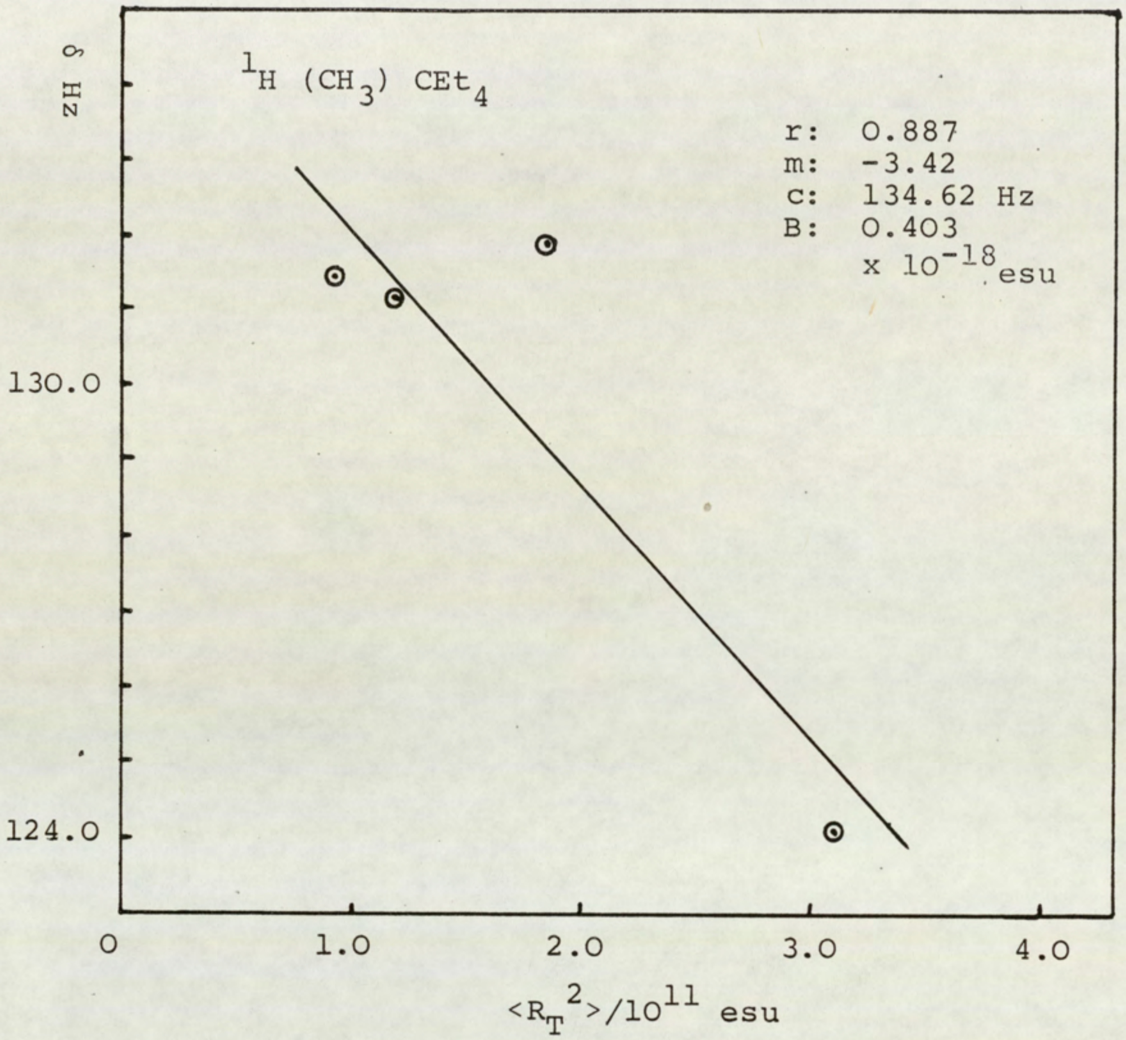

Figure 7.2: Regression of $\langle R_T^{\,2}\rangle$ on methyl proton shifts of C Et_4

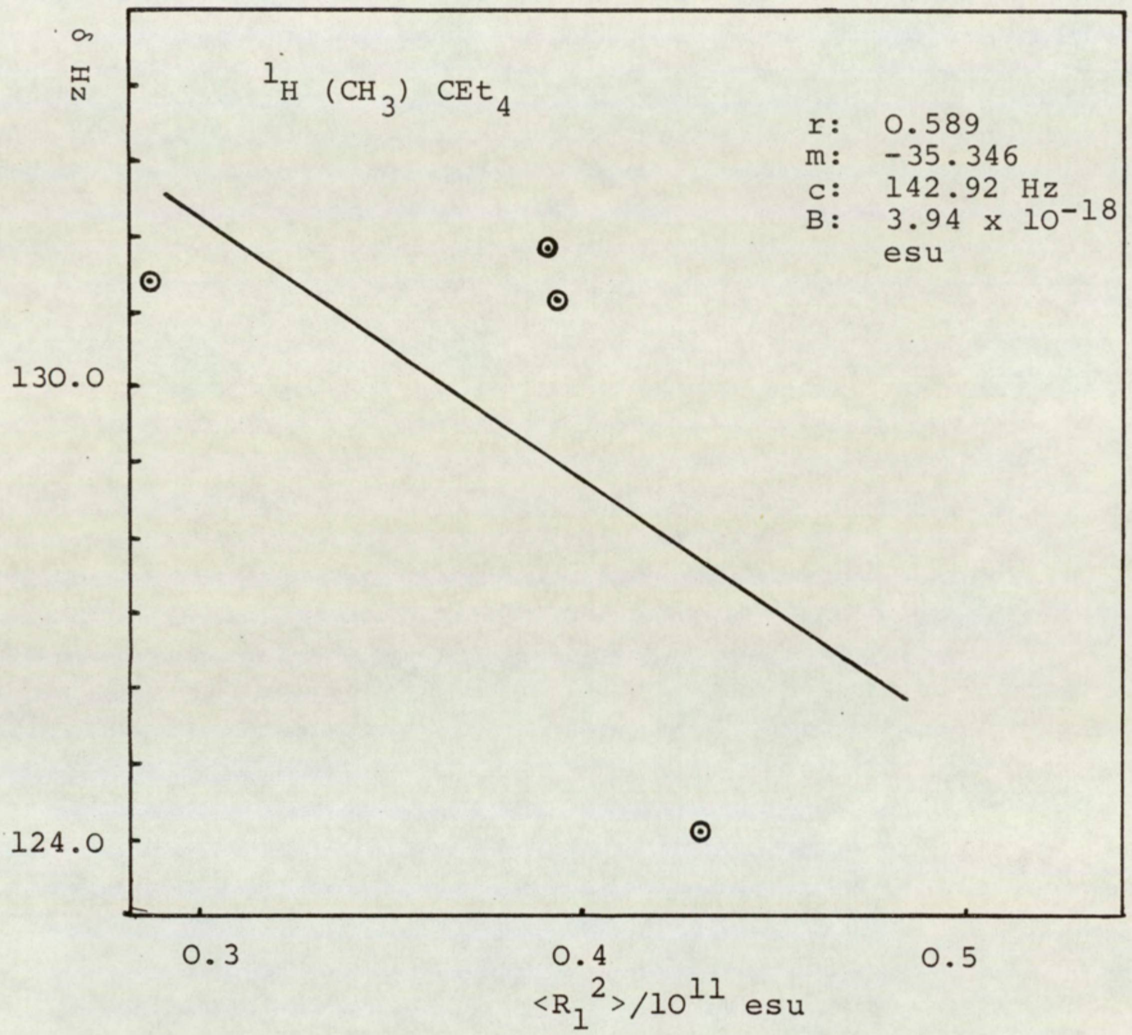

Figure 7.3: Regression of $<R_1{}^2>$ on methyl proton shifts of CEt_4

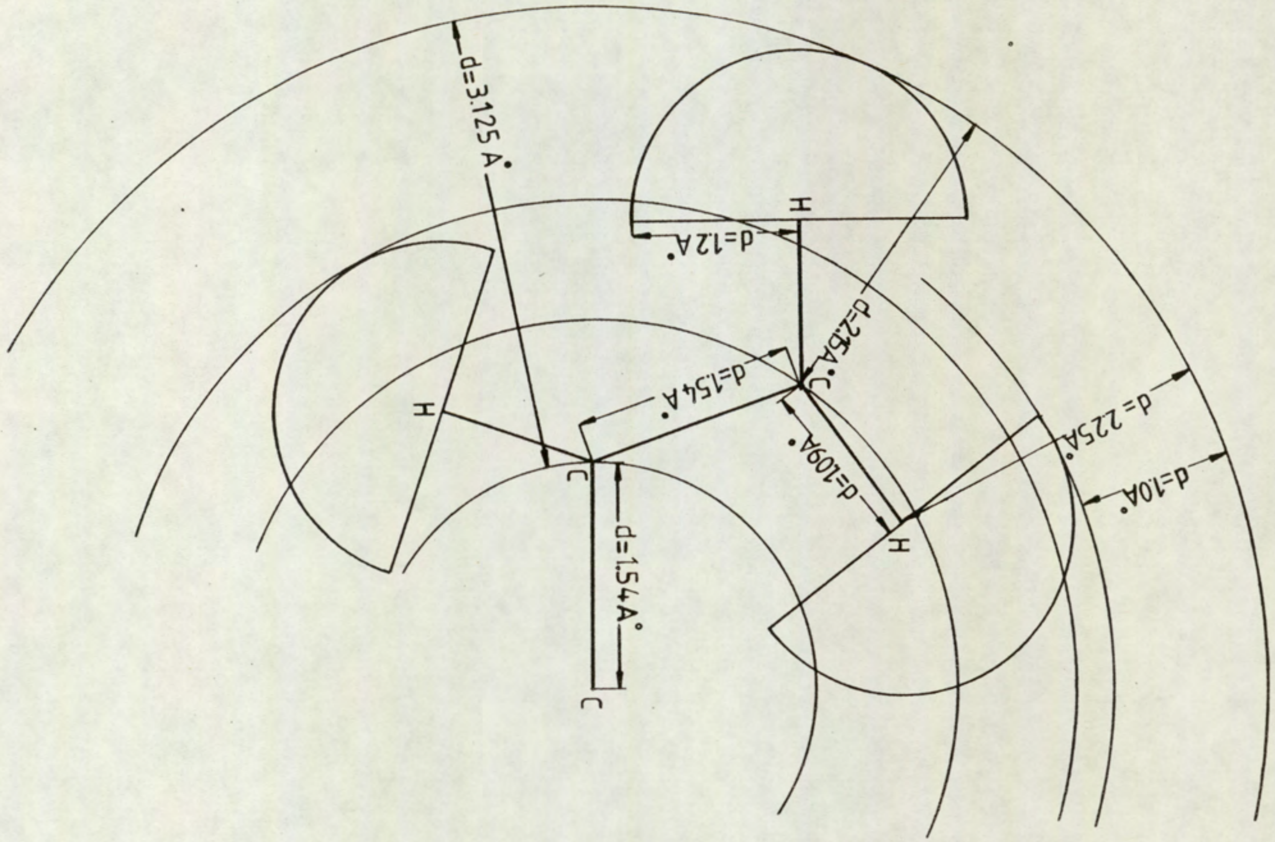

Figure 7.4: Two dimensional representation of CEt_4 molecule

^{1}H (CH_3) CEt_4 d = 0.8 Å; a = r_2+ d

Solvent	$\left(\frac{r}{r+d}\right)^6$	$\langle R_1^2\rangle/10^{11}$	$\langle R_2^2\rangle/10^{11}$	$\langle R_2^2\rangle (r/a)^6/10^{11}$	$\langle R_T^2\rangle/10^{11}$	$E^2_{BI}/10^{11}$	$(\langle R_T^2\rangle + E^2_{BI})/10^{11}$	$\langle R_1^2\rangle + \langle R_2^2\rangle (r/a) + E^2_{BI}/10^{11}$	δ^1H CH_3 Hz
TMS	0.341	0.2867	0.6222	0.212	0.909	0.322	1.231	0.8207	131.45
CEt_4	0.364	0.3933	0.7867	0.286	1.180	0.366	1.546	1.0453	131.18
C_6H_{12}	0.313	0.3899	1.439	0.4504	1.8294	0.306	2.1354	1.1463	131.92
CCl_4	0.301	0.4299	2.6496	0.7975	3.0795	0.519	3.599	1.7464	124.10

Table 7.7 - The mean square reaction fields $\langle R_1^2\rangle$, $\langle R_2^2\rangle$, $\langle R^2_T\rangle$ with the modulated term $\langle R_2^2\rangle (r/a)^6$ together with E^2_{BI}, for the methyl protons of CEt_4 where a = r_2 + 0.8 Å

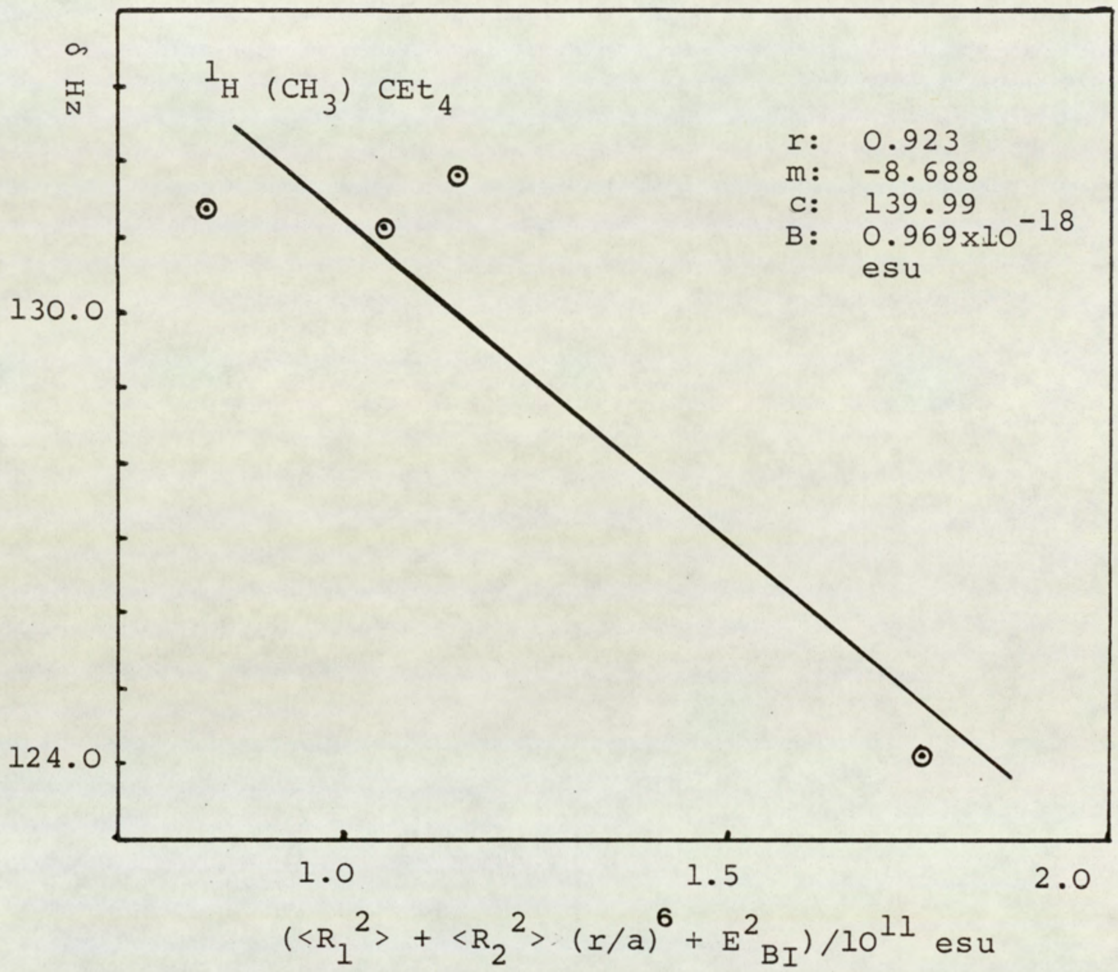

Figure 7.5: Regression of $(\langle R_1{}^2\rangle + \langle R_2{}^2\rangle\,(r/a)^6 + E^2{}_{BI})/10^{11}$ esu on methyl proton shifts of CEt_4

If the regression is only for $<R_1^2> + <R_2^2> (r/a)^6$ on the corrected shifts a value of 1.161×10^{-18} esu for B is obtained. Table 7.8 shows the collective B values obtained.

Table 7.8 - Collected B values from the different regressions for methyl protons in CEt_4

Regression of	B value/10^{-18} esu
$<R_1^2>$	3.91
$<R_T^2>$	0.0381
$<R_T^2> + E^2_{BI}$	0.359
$<R_1^2> + <R_2^2> (r/a)^6 + E^2_{BI}$	0.969
$<R_1^2> + <R_2^2> (r/a)^6$	1.161

It is evident that the value of 0.969×10^{-18} esu is in most satisfactory agreement with that of 0.87×10^{-18} esu established before.

This gives an initial indication that $<R_1^2>$ is induced uniformly through the cavity, and that $<R_2^2>$ decreases with the distance from the centre of the solvent molecule, and that the buffeting is effective at the periphery of the methyl protons.

For the case of the methylene protons, Table 7.6 shows the deduced values of the buffeting parameters with $(2\beta_T - \xi_T)^2$ and E^2_{BI}. The values were calculated for $<R_1^2>$, $<R_2^2> (r/a)^6$ and for the buffeting contribution and are given in Table 7.9 with the d values deduced for the methyl protons from Figure 7.4 for calculations of the distance modulation of $<R_2^2>$. The same approach as before was used in that the various regression applied to the case of the methyl protons were used for the methylene protons. These are shown in Figures 7.6, 7.7, 7.8 and 7.9. The values of B obtained there are summarized in Table 7.10. From the various values obtained for B, it can be seen that there is little to choose between those obtained from the

$^{1}H\ (CH_2)\ C\ Et_4$ d = 2.51 Å; a = r_2+ d

Solvent	$\left(\frac{r}{r+d}\right)^6$	$\langle R_1 2\rangle/10^{11}$	$\langle R_2 2\rangle/10^{11}$	$\langle R_2^2\rangle (r/a)^6/10^{11}$	$\langle R^2 T\rangle/10^{11}$	$E^2BI/10^{11}$	$(\langle R_T^2\rangle + E^2_{BI})/10^{11}$	$\langle R_1^2\rangle + \langle R_2 2\rangle (r/a) + E^2_{BI}/10^{11}$	$\delta^1H\ CH_2$ Hz
TMS	0.0563	0.2867	0.6222	0.035	0.909	0.362	0.6487	0.6837	93.17
$C\ Et_4$	0.0653	0.3933	0.7867	0.0514	1.180	0.378	0.7713	0.8227	93.68
C_6H_{12}	0.0461	0.3899	1.439	0.066	1.8294	0.2626	0.6525	0.7185	94.43
$C\ Cl_4$	0.0422	0.4299	2.6496	0.1118	3.0795	0.808	1.2379	1.3497	87.97

Table 7.9 - The mean square reaction fields $\langle R_2^2\rangle$ (r/a)^6 together with E^2_{BI} for the methylene protons of CEl_4, where a = r_2+ 2.51 Å

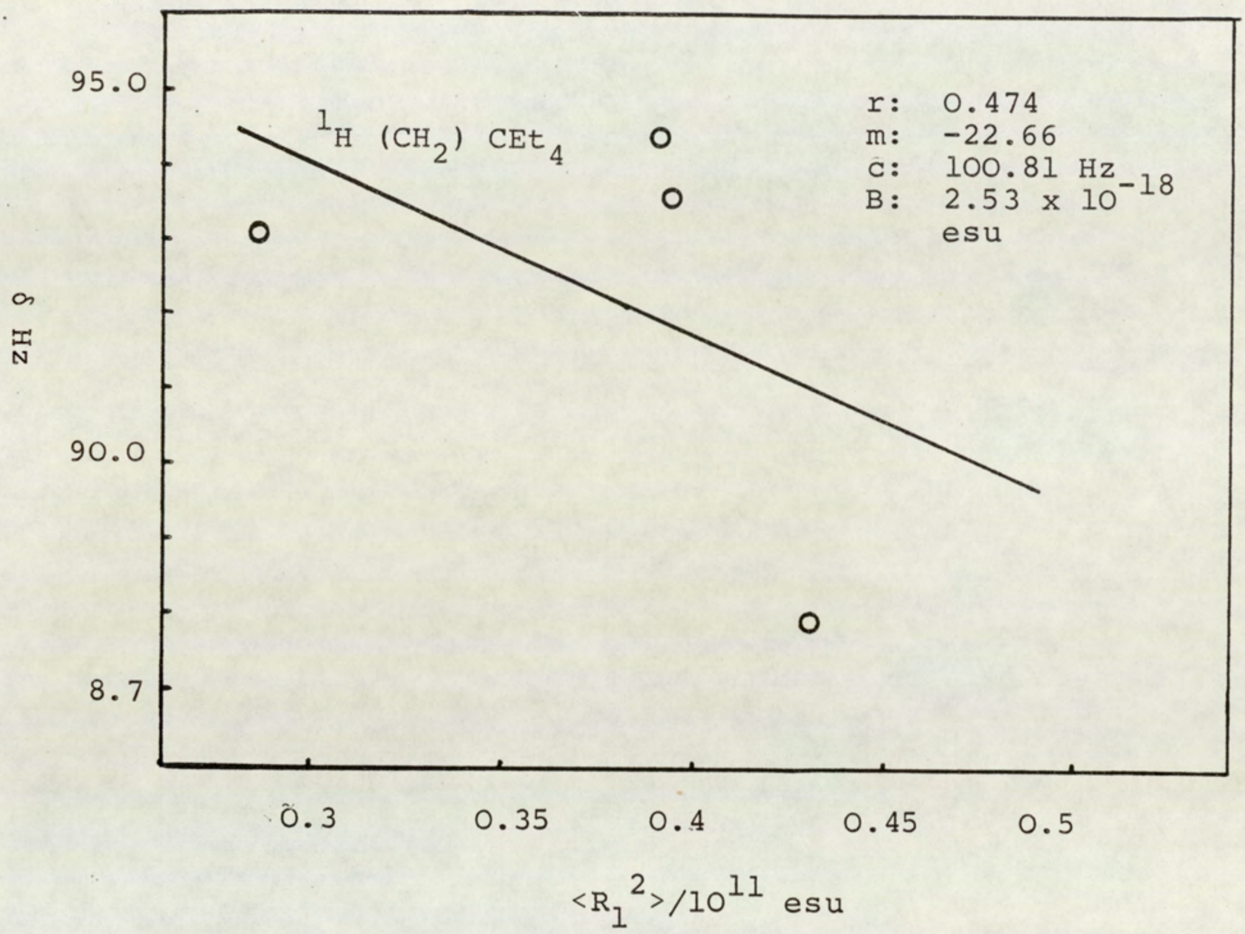

Figure 7.6: Regression of $\langle R_1^2 \rangle$ on methylene proton shifts of CEt_4

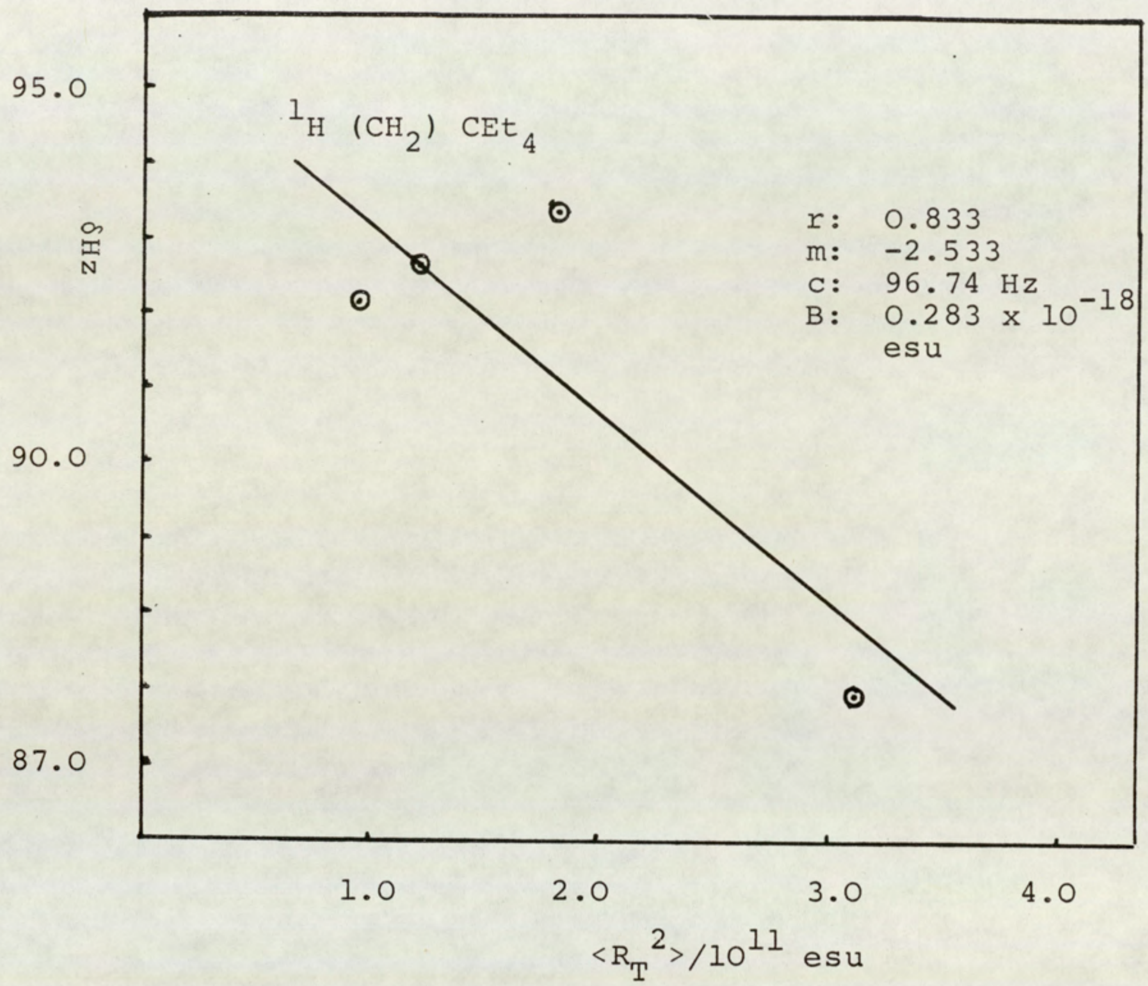

Figure 7.7: Regression of $\langle R_T^2 \rangle$ on the methylene proton shifts of CEt_4

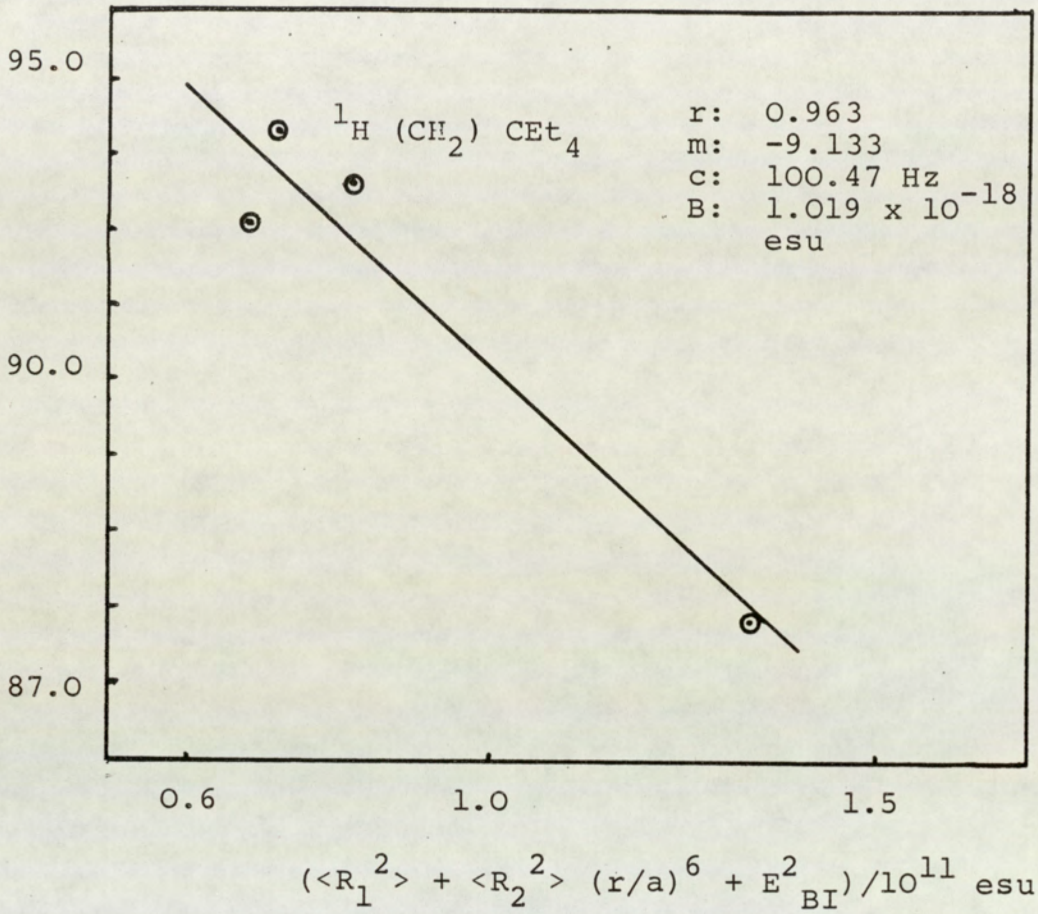

Figure 7.8: Regression of $(\langle R_1^2\rangle + \langle R_2^2\rangle (r/a)^6 + E^2_{BI})$ on methylene proton shifts of CEt_4

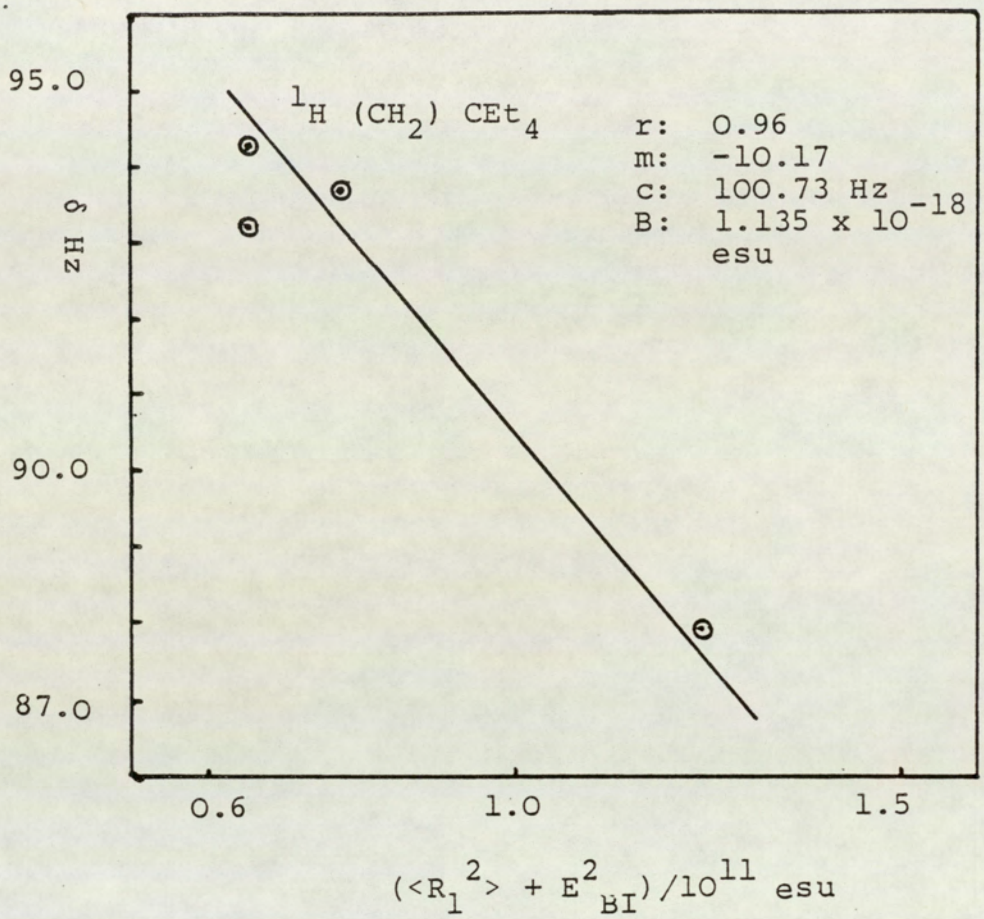

Figure 7.9: Regression of $(\langle R_1^{\,2}\rangle + E^2_{BI})$ on the methylene proton shifts of CEt_4

regressions involving $<R_1^2> + E^2_{BI}$ and $<R_1^2> + <R_2^2> + E^2_{BI}$. This is because the distance modulation for the methylene protons essentially eliminates $<R_2^2>$. This is a particularly important result because it is to be expected that $<R_2^2>$ for nuclei not at periphery of the molecule will be attenuated very rapdily with the distance of the resonant site from the centre of the solvent molecule.

Table 7.10 - Collected B values from the different regressions for methylene protons in CEt_4

Regression of	B value/10^{-18} esu
$<R_1^2>$	2.53
$<R_T^2>$	0.283
$<R_1^2> + <R_2^2> (r/a)^6 + E^2_{BI}$	1.019
$<R_1^2> + E^2_{BI}$	1.135

In reaching the above conclusion the similarity between the values of B deduced with that obtained by Homer and Percival of 0.87×10^{-18} esu[39] has been used as the criterion for assessing the contributions of $<R_1^2>$, $<R_2^2>$ and E^2_{BI} to the intermolecular forces. This would appear reasonable because for a proton Sp^3 bonded to carbon, it is to be expected that they will always have similar B values. This follows from the fact that while in general, the B values for some nucleus X bonded to an atom Y may well be of similar magnitude for different Y, their precise values are expected to depend on the nature of Y[27,114].

7.3.2 <u>Analysis of ^{13}C shifts of $C(CH_2CH_3)_4$</u>

The observed[113] and susceptibility corrected shifts of ^{13}C for $C(CH_2CH_3)_4$ are recorded in Table 7.3.

A careful scrutiny of the C $(CH_2\ CH_3)_4$ molecule reveals that although the methyl and the methylene carbon atoms are protected by the bonded protons, they are still exposed to the peripheral solvent atoms. This indicates that the buffeting field is effective on the methyl and methylene carbon atoms. However the central carbon atom is deeply embedded within the C $(CH_2\ CH_3)_4$ molecule and should not experience any buffeting. The values of the buffeting parameters $(2\beta_T - \xi_T)^2$ and E^2_{BI} for the methyl and methylene carbon atoms are given in Table 7.6

For the estimation of the B values for ^{13}C, the same approach as in section 7.3.1 was used in that the various regressions as were applied in the case of the methyl protons were used for the methyl, methylene and the central carbon atom of C $(CH_2\ CH_3)_4$. The values for $\langle R_2^2 \rangle (r/a)^6$ obtained for ^{13}C methyl and ^{13}C methylene by using the two dimensional representation of C $(CH_2\ CH_3)_4$ molecule (Figure 7.4) are reported in Tables 7.11 and 7.13 together with other relevant data. The regressions are shown in Figures 7.10, 7.11, 7.12, 7.13 and 7.14 for methyl ^{13}C, Figures 7.15, 7.16, 7.17 and 7.18 for methylene ^{13}C and Figures 7.19 and 7.20 for the central ^{13}C. The values of B obtained therefore are summarised in Tables 7.12, 7.13 and 7.14 for the methyl, methylene and central carbon respectively.

Before interpreting the results obtained, it would be appropriate to establish the range of B values expected for ^{13}C in general.

It is known that the value of B for a proton attached to an Sp^3 hybridized carbon is 0.87×10^{-18} esu. Unfortunately, neither theoretical nor practical estimates of the value of ^{13}C or ^{29}Si are available. The B value of ^{29}Si is analysed later for the TMS molecule and the results will be discussed in the appropriate section. Consequently it would be reasonable to establish a trend for the values of B for ^{29}Si on a competitive basis with the B values for ^1H and ^{13}C.

It is possible to make some crude predictions as to the relative magnitude expected for the value of B for the three nuclei. Gas-to-solution shifts for ^{13}C are of the order of 15 times those of analogous proton shifts(115) and it would not be unreasonable to suppose that B for carbon will be about 15 times that of hydrogen. Interestingly, in the ethyl halides the variation of the methyl ^{13}C shifts with halogen electronegitivity is also about 15 times that of the similarly sited methylene protons(116). If in fact these shift variations are dominated by intra-molecular electric fields rather than substituent electronegitivity(117) it may be that the relative magnitudes of the intra-molecular shifts for the two nuclides may be taken to a first approximation as indication of the relative magnitudes of the corresponding inter-molecular shifts. If this is so it is pertinent to note that substituent effects on ^{29}Si shifts sometimes operate in an almost equivalent, if opposite manner, to those of the corresponding ^{13}C shifts(118). It would not be too unreasonable to expect therefore, that the values of B for ^{13}C and ^{29}Si should be similar.

According to Mohammadi(71) the B value of a selected resonant nucleus falls somewhere between the B value of its corresponding inert gas nucleus and that of the inert nucleus of the next row in the periodic table. This indicates that the B value for ^{13}C should be in the proximity of the B value of its inert gas nucleus (ie. Neon which has a B value of 4.1×10^{-18} esu or more).

The B value of proton is already established. On the basis of the above discussions it appears that the B value for ^{13}C should be somewhere between 4.1 and 15×10^{-18} esu. Table 7.12 presents possible values for B for the methyl ^{13}C of the TEM.

Figure 7.13 shows the regression of $(\langle R_T^2 \rangle + E^2_{BI})$ on the susceptibility corrected shifts for methyl ^{13}C. This yields a B value of 2.54×10^{-18} esu which in the light of above discussion is evidently too small. Figure 7.11 shows the regression with the square field buffeting E^2_{BI} eliminated and this again gives a low B value of

^{13}C (CH_3) CEt_4 d = 2.15 Å, a = r_2 + 2.15 Å

Solvent	$\left(\frac{r}{r+d}\right)^6$	$\langle R_1^2\rangle/10^{11}$	$\langle R_2^2\rangle/10^{11}$	$\langle R_2^2\rangle (r/a)^6/10^{11}$	$\langle R_T^2\rangle/10^{11}$	$\langle R_1^2\rangle+\langle R_2^2\rangle (r/a)^6/10^{11}$	E^2_{BI}	$\langle R_T^2\rangle+E^2_{BI}/10^{11}$	$\langle R_1^2\rangle+\langle R_2^2\rangle (r/a)^6 + E^2_{BI}/10^{11}$	$\delta^{13}C$ CH_3 ppm
TMS	0.079	0.2867	0.6222	0.0492	0.909	0.3359	1.171	2.08	1.5069	84.87
$C Et_4$	0.09	0.3933	0.7867	0.0708	1.180	0.4641	1.253	2.433	1.7171	84.87
C_6H_{12}	0.066	0.3899	1.439	0.0949	1.8294	0.4849	1.0769	2.9063	1.5618	85.06
$C Cl_4$	0.0607	0.4299	2.6496	0.1608	3.0795	0.5907	1.8818	4.9613	2.4725	84.21

Table 7.11 - The mean square reaction fields $\langle R_1^2\rangle$, $\langle R_2^2\rangle$, $\langle R_T^2\rangle$ and the modulated term $\langle R_2^2\rangle (r/a)^6$ for the methyl ^{13}C of CEt_4 where a = r_2 + 2.15Å

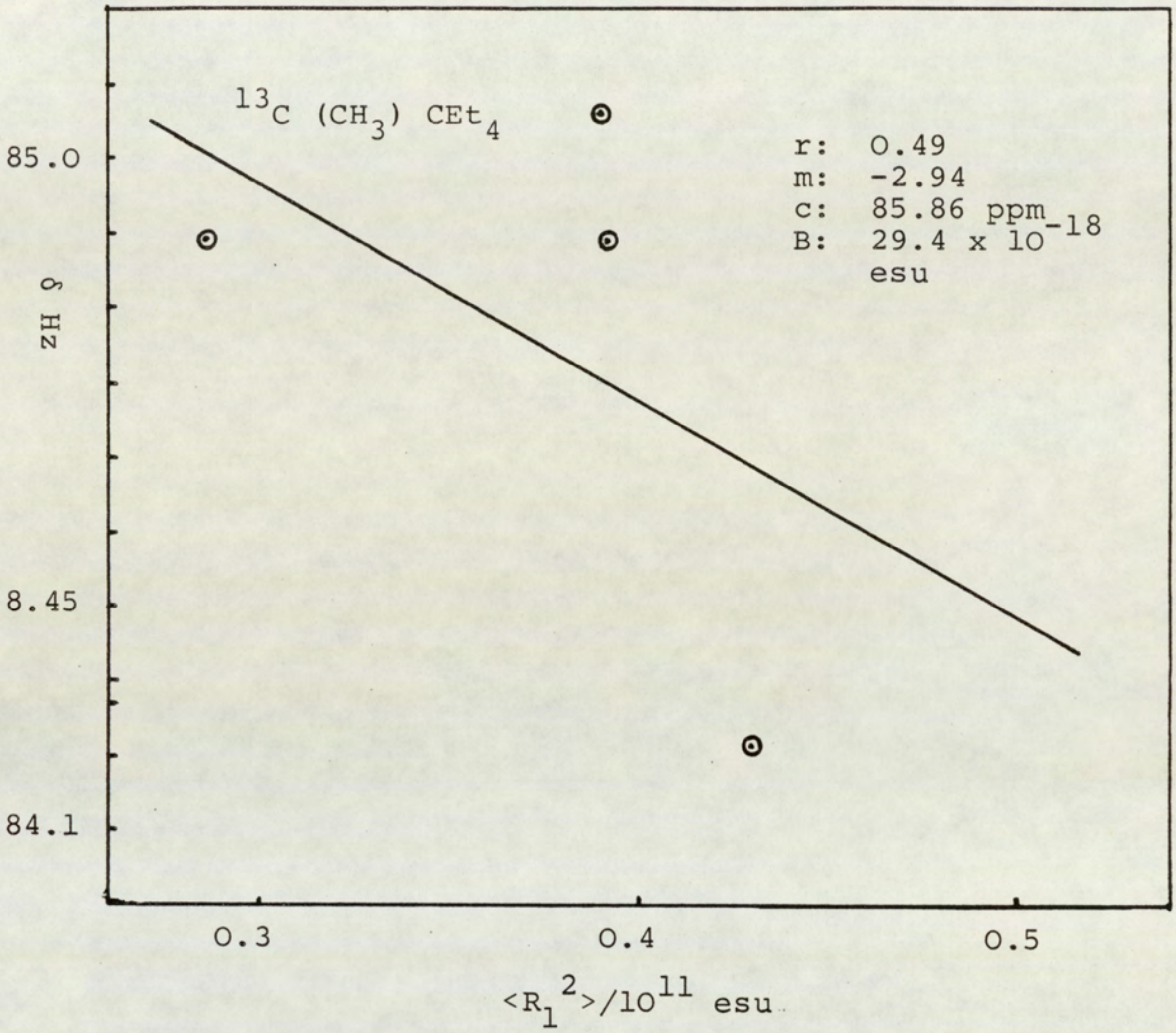

Figure 7.10: Regression of $\langle R_1^{\,2}\rangle$ on ^{13}C Methyl shifts of CEt_4

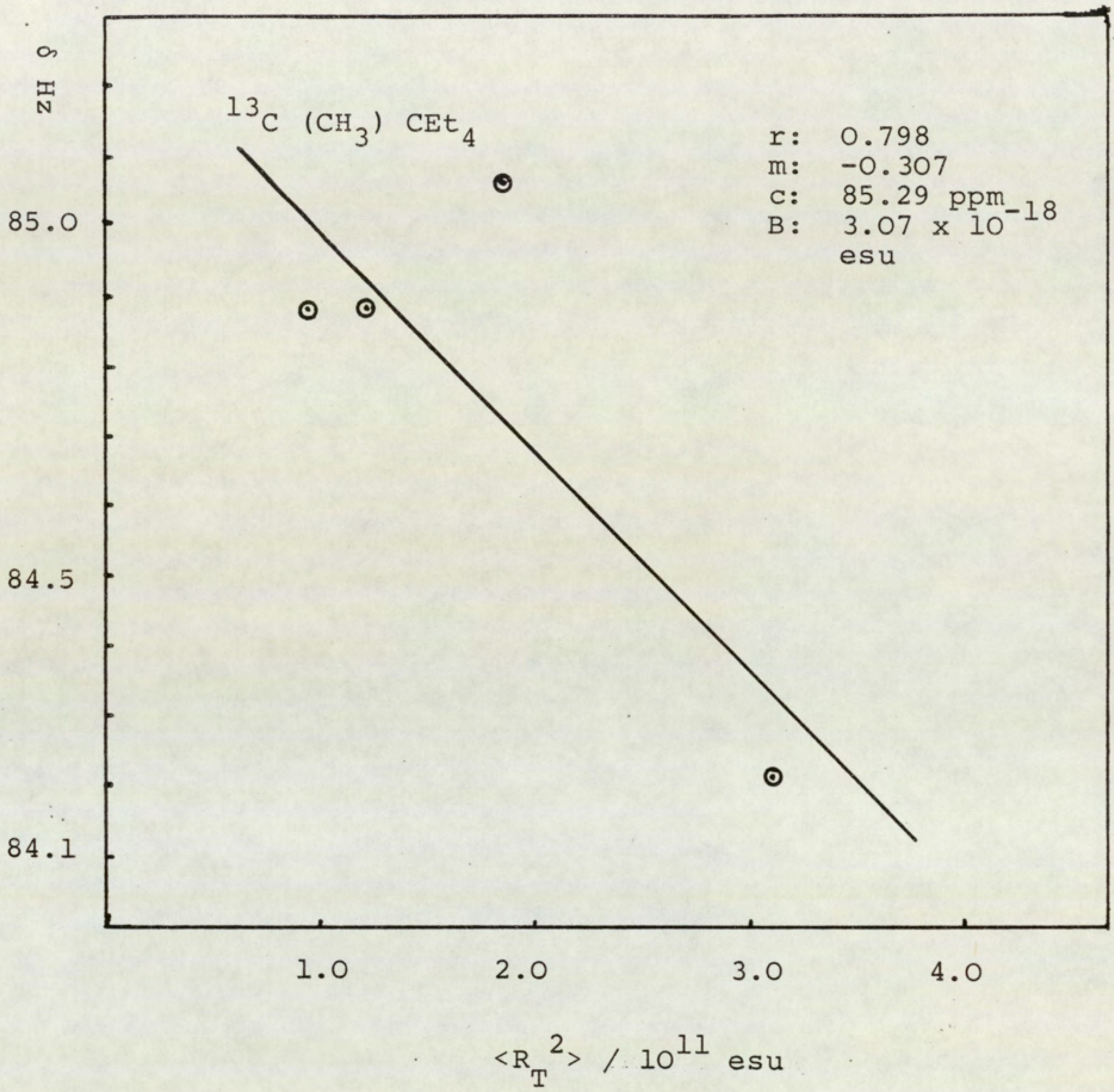

Figure 7.11: Regression of $<R_T^{\ 2}>$ on ^{13}C methyl shifts of CEt_4

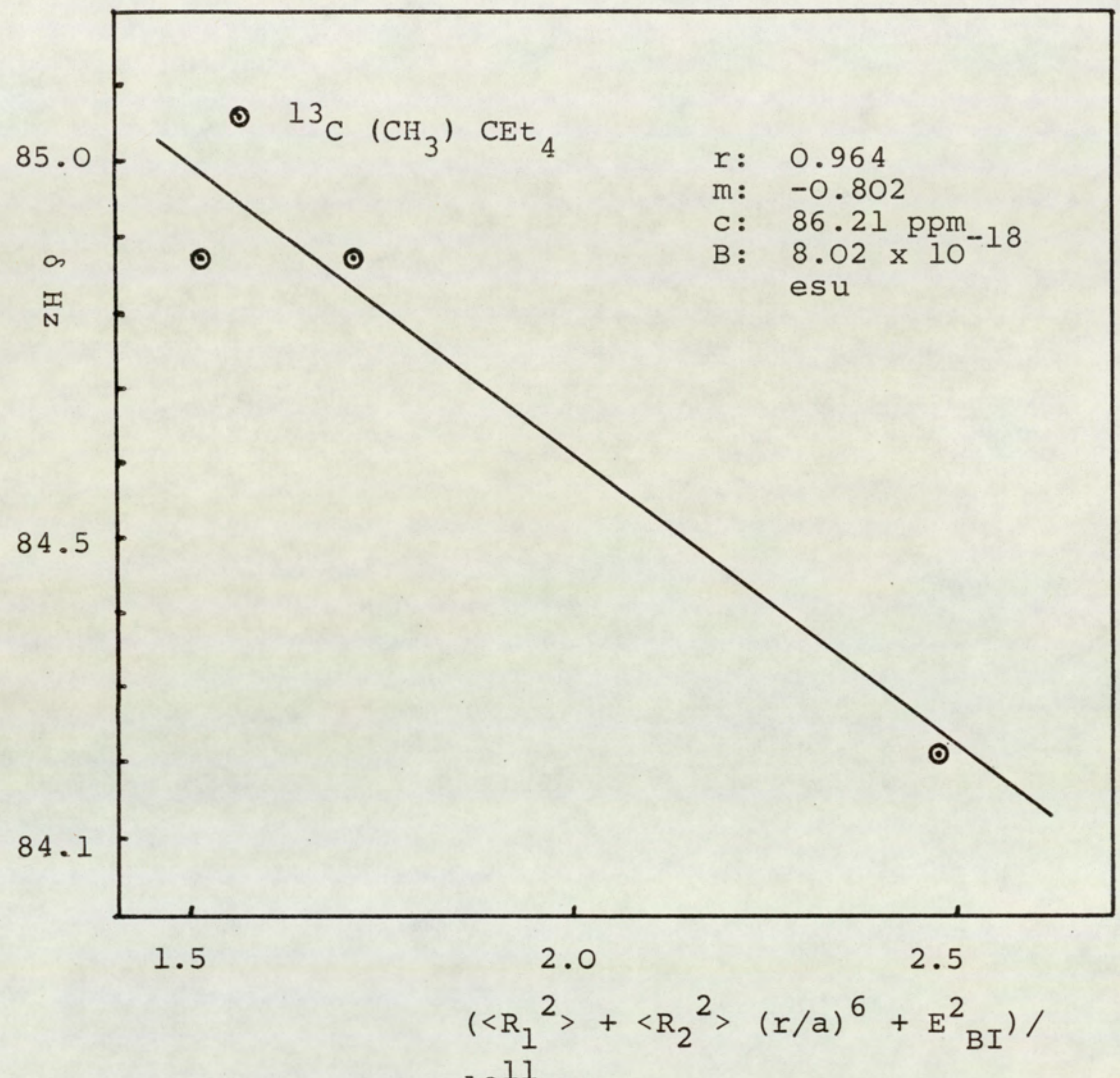

Figure 7.12: Regression of $(\langle R_1^2\rangle + \langle R_2^2\rangle (r/a)^6 + E^2_{BI})$ on ^{13}C methyl shifts of CEt_4

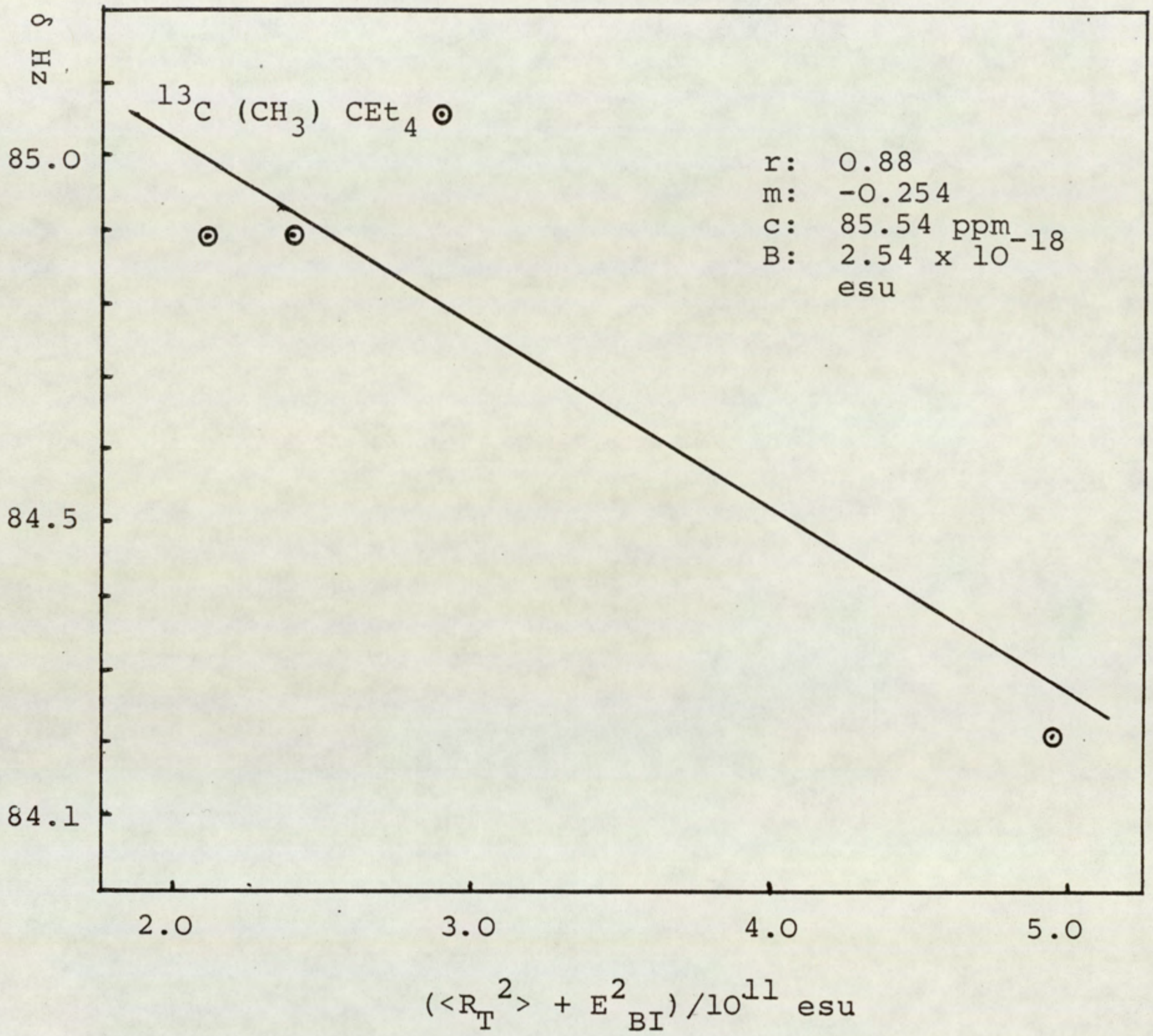

Figure 7.13: Regression of $(\langle R_T{}^2\rangle + E^2{}_{BI})$ on ^{13}C Methyl shifts of CEt_4

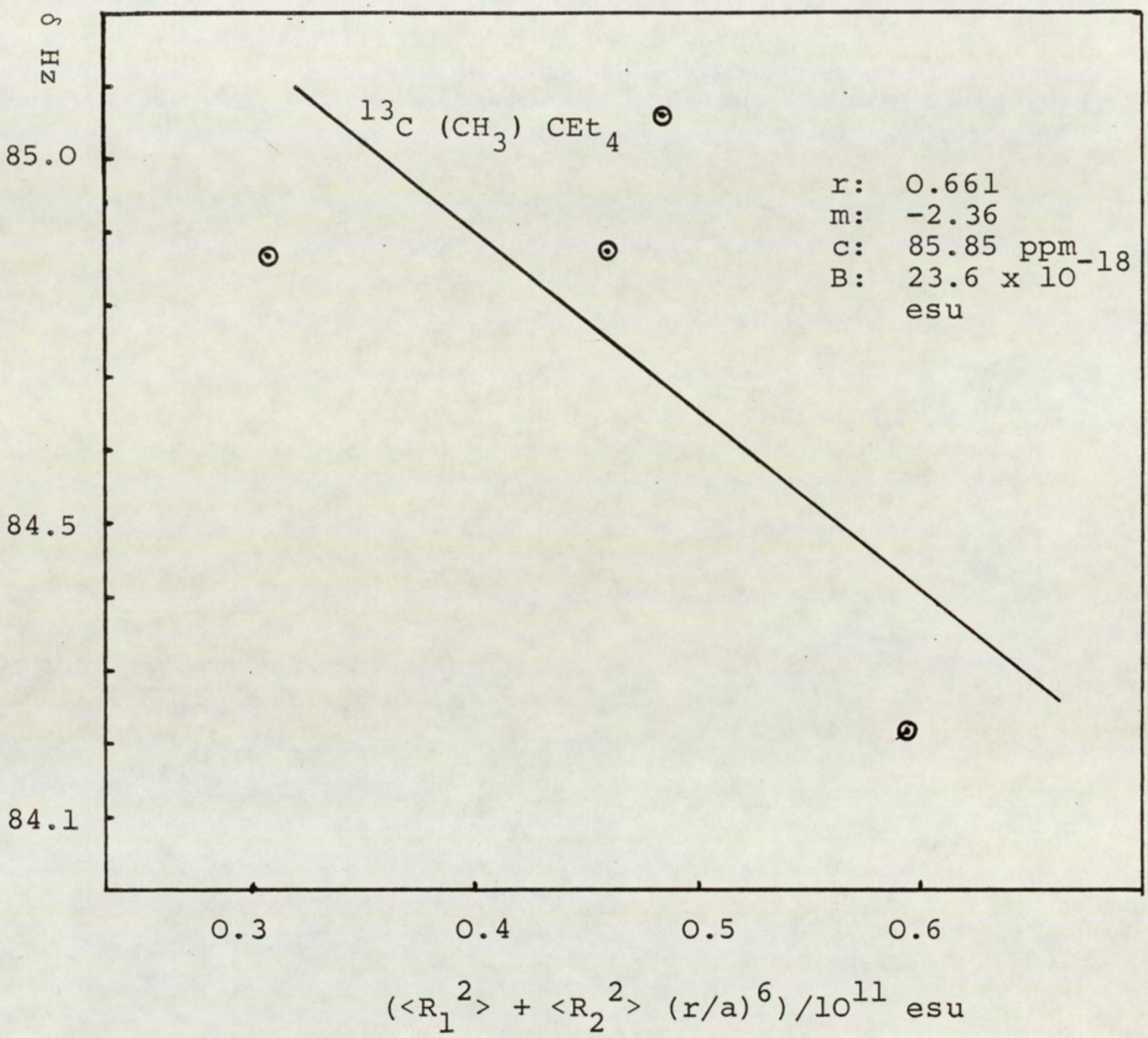

Figure 7.14: Regression of $(<R_1^2> + <R_2^2>\ (r/a)^6)$ on ^{13}C Methyl shifts of CEt_4

3.07×10^{-18} esu. At the other extreme the regression of $<R_1^2>$ (Figure 7.10) on the corrected shifts for methyl ^{13}C gives rather high value for B of 29.4×10^{-18} esu.

Table 7.12 - Collected B values for various regression ^{13}C methyl of CEt_4

^{13}C (CH_3) CEt_4	B value/10^{-18} esu
$<R_1^2>$	29.4
$<R_T^2>$	3.07
$<R_1^2> + <R_2^2> (r/a)^6 + E^2_{BI}$	8.02
$<R_T^2> + E^2_{BI}$	2.54
$<R_1^2> + <R_2^2> (r/a)^6$	23.6

Evidently, the best value of B will be obtained from appropriate regression that lies somewhere between $<R_1^2>$ and $(<R_T^2> + E^2_{BI})$ on the corrected shift.

The regression of $(<R_1^2> + <R_2^2> (r/a)^6 + E^2_{BI})$ (Figure 7.12) yields a value of 8.02×10^{-18} esu for B of methyl ^{13}C, whereas the regression of $(<R_1^2> + <R_2^2> (r/a)^6)$ on the corrected shifts of methyl ^{13}C gives a value of 23.6×10^{-18} esu. It is evident that the value of 8.02×10^{-18} esu is in most satisfactory agreement with the aforementioned prediction.

This once again confirms that $<R_1^2>$ is induced uniformly through the cavity and that $<R_2^2>$ decreases with the distance from the centre of the solvent molecule and that the buffeting extends to the methyl carbon atoms.

The same approach applied in the case of the methylene carbon, once again indicates the emergence of a similar pattern. The results obtained for various regressions (Figures 7.15, 7.16, 7.17 and 7.18) (Table 7.14) show that the values lie on the extreme ends of the range for the predicted values of B [$<R_1^2>$ (B value = 18.6

$^{13}C\ (CH_2)\ CEt_4\ d = 3.125$ Å $a = r_2 + d$

Solvent	$(\frac{r}{r+d})^6$	$\langle R_1^2\rangle / 10^{11}$	$\langle R_2^2\rangle / 10^{11}$	$\langle R_2^2\rangle (r/a)^6 / 10^{11}$	$\langle R_T^2\rangle / 10^{11}$	E^2_{BI}	$\langle R_T^2\rangle + E^2_{BI} / 10^{11}$	$\langle R_1^2\rangle + \langle R_2^2\rangle (r/a)^6 + E^2_{BI} / 10^{11}$	$\delta^{13}C$ CH_3 ppm
TMS	0.033	0.2867	0.6222	0.0205	0.909	0.0567	0.9657	0.3639	65.05
CEt_4	0.039	0.3933	0.7867	0.0307	1.180	0.0573	1.2373	0.4813	64.94
C_6H_{12}	0.0263	0.3899	1.439	0.0378	1.8294	0.0556	1.885	0.4833	65.02
CCl_4	0.0238	0.4299	2.6496	0.063	3.0795	0.0978	3.6072	0.5907	64.71

Table 7.13 - The reaction fields $\langle R_1^2\rangle$, $\langle R_2^2\rangle$, $\langle R_T^2\rangle$ and the modulated term $\langle R_2^2\rangle (r/a)^6$ for the methylene ^{13}C of $C\ El_4$ where $a = r_2 + 3.125$ Å

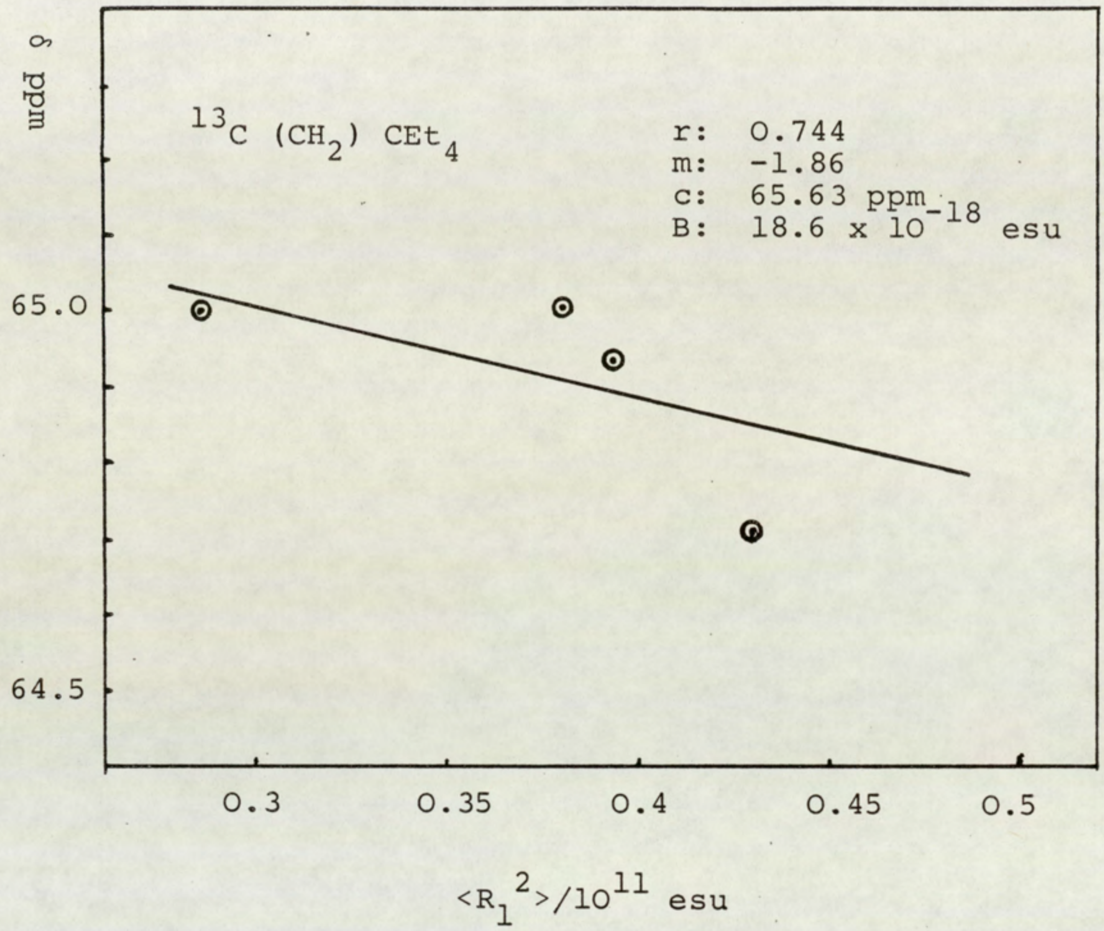

Figure 7.15: Regression of $\langle R_1^2 \rangle$ on ^{13}C Methylene shifts of CEt_4

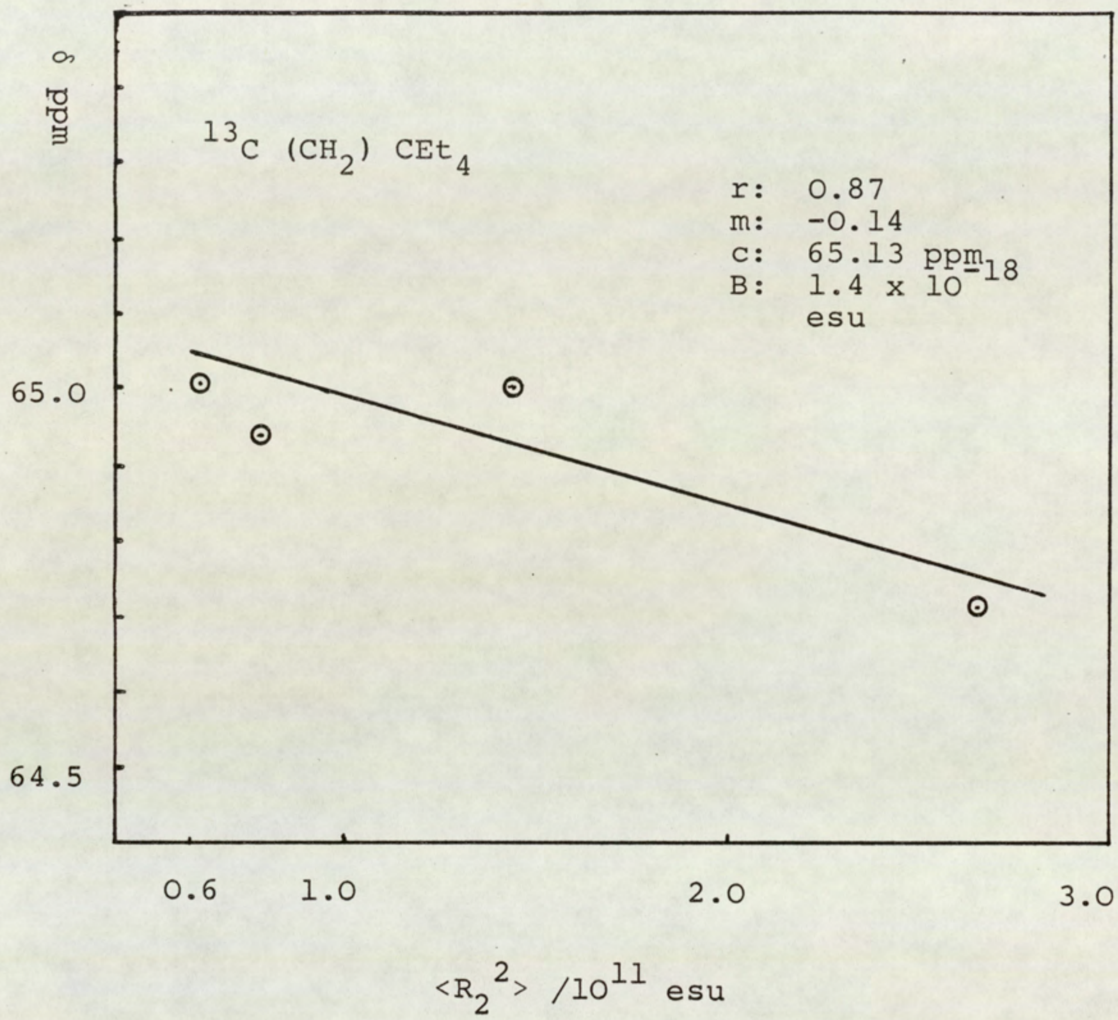

Figure 7.16: Regression of $<R_2{}^2>$ on ^{13}C Methylene of CEt_4

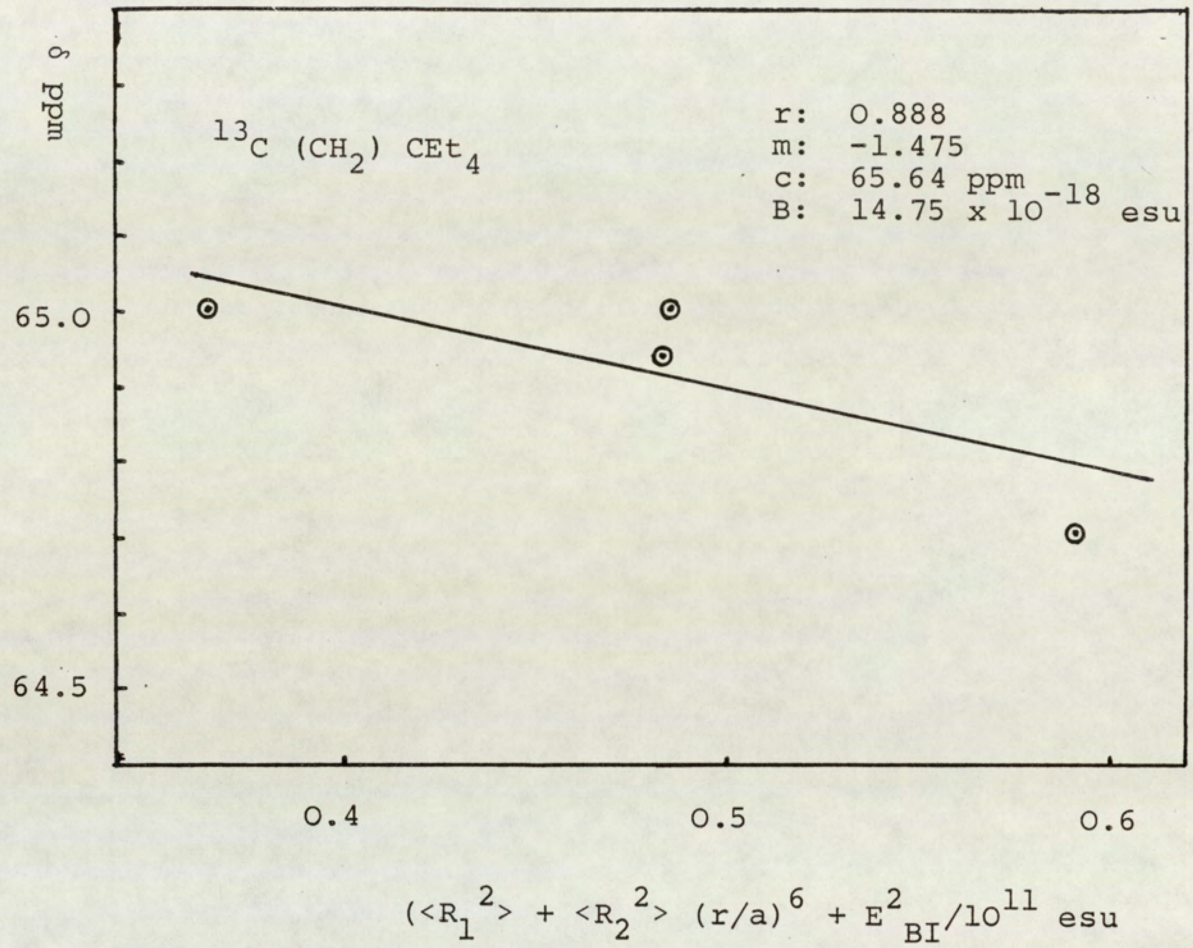

Figure 7.17: Regression of $(\langle R_1{}^2\rangle + \langle R_2{}^2\rangle\ (r/a)^6 + E^2{}_{BI})$ on ^{13}C Methylene shifts of CEt_4

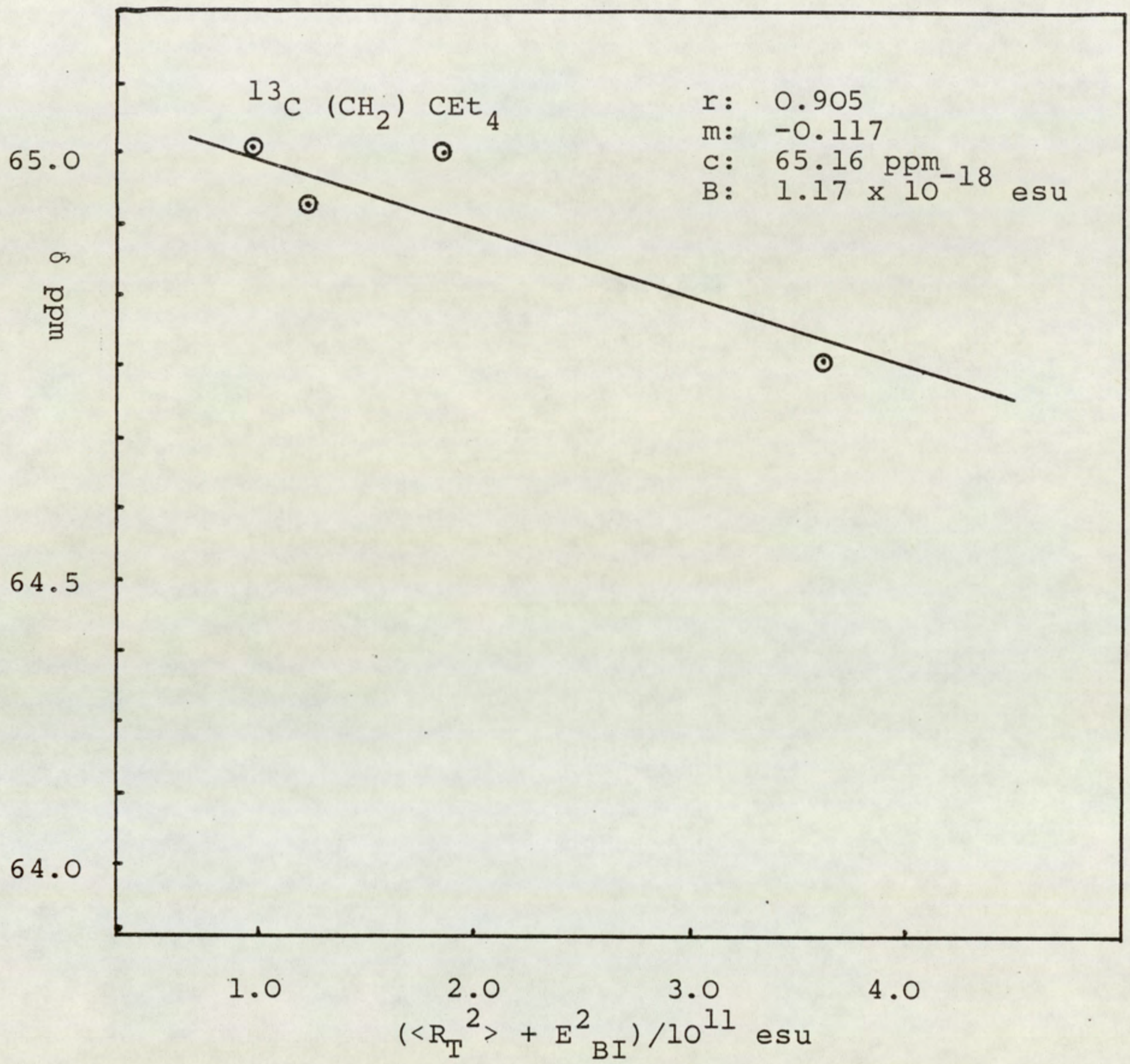

Figure 7.18: Regression of $(\langle R_T^2\rangle + E^2_{BI})$ on ^{13}C Methylene shifts of CEt_4

x 10^{-18} esu) and ($<R_1^2> + <R_2^2> + E^2_{BI}$) (B value = 1.17 x 10^{-18} esu)]. The most appropriate value of B for the methylene carbon results from the regression of ($<R_1^2> + <R_2^2> (r/a)^6) + E^2_{BI}$) (B value = 14.75 x 10^{-18} esu) on the susceptibility corrected shifts.

Table 7. 14 - Collected B values for various regression on ^{13}C methylene of CEt_4

^{13}C (CH_2) CEt_4	B value/10^{-18} esu
$<R_1^2>$	18.6
$<R_2^2>$	1.4
$<R_1^2> + <R_2^2> (r/a)^6 + E^2_{BI}$	14.75
$<R_T^2> + E^2_{BI}$	1.17

This once again confirms that $<R_1^2>$ is induced uniformly through the cavity and that $<R_2^2>$ decreases with the distance from the centre of the solvent molecule and that buffeting is effective at the methylene carbon atom.

Results for the regression of $<R_1^2>$ and $<R_2^2>$ (Figures 7.19 and 7.20) for the central carbon atom gives values for B of 14.57 x 10^{-18} esu and 1.69 x 10^{-18} esu respectively. Evidently E^2_{BI} and $<R_2^2> (r/a)^6$ would not be expected to operate at the central carbon and the value of 14.57 x 10^{-18} esu would seem most appropriate.

It seems from the set of B values obtained in Tables 7.12, 7.14 and Figure 7.19 that the value of 8.02 x 10^{-18} esu, 14.75 x 10^{-18} esu and 14.57 x 10^{-18} esu for methyl, methylene and central carbons respectively are eminently reasonable, and consistant. Moreover the procedure by which they are obtained suggests again that $<R_1^2>$ is uniform through the cavity and that $<R_2^2>$ is modulated by the distance parameter.

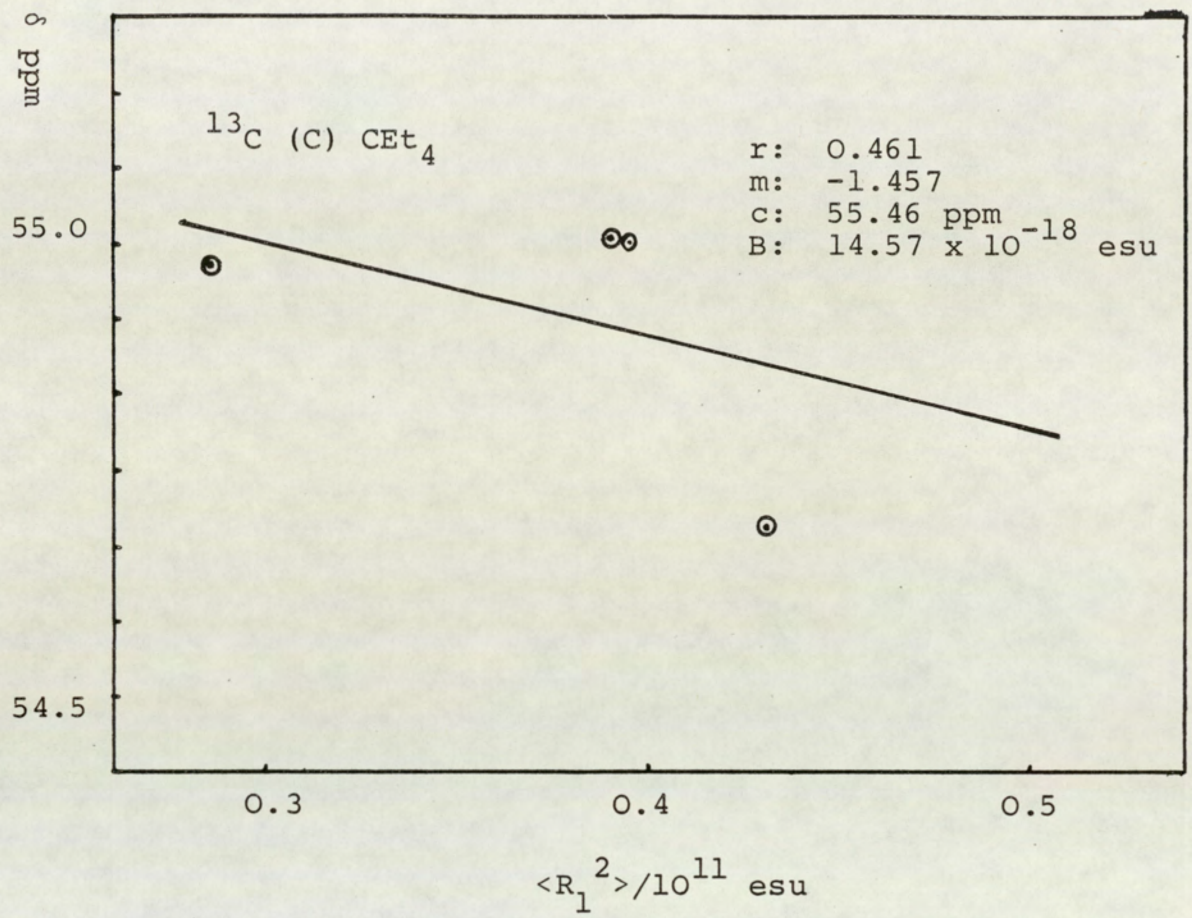

Figure 7.19: Regression of $<R_1^2>$ on the central ^{13}C shifts of CEt$_4$

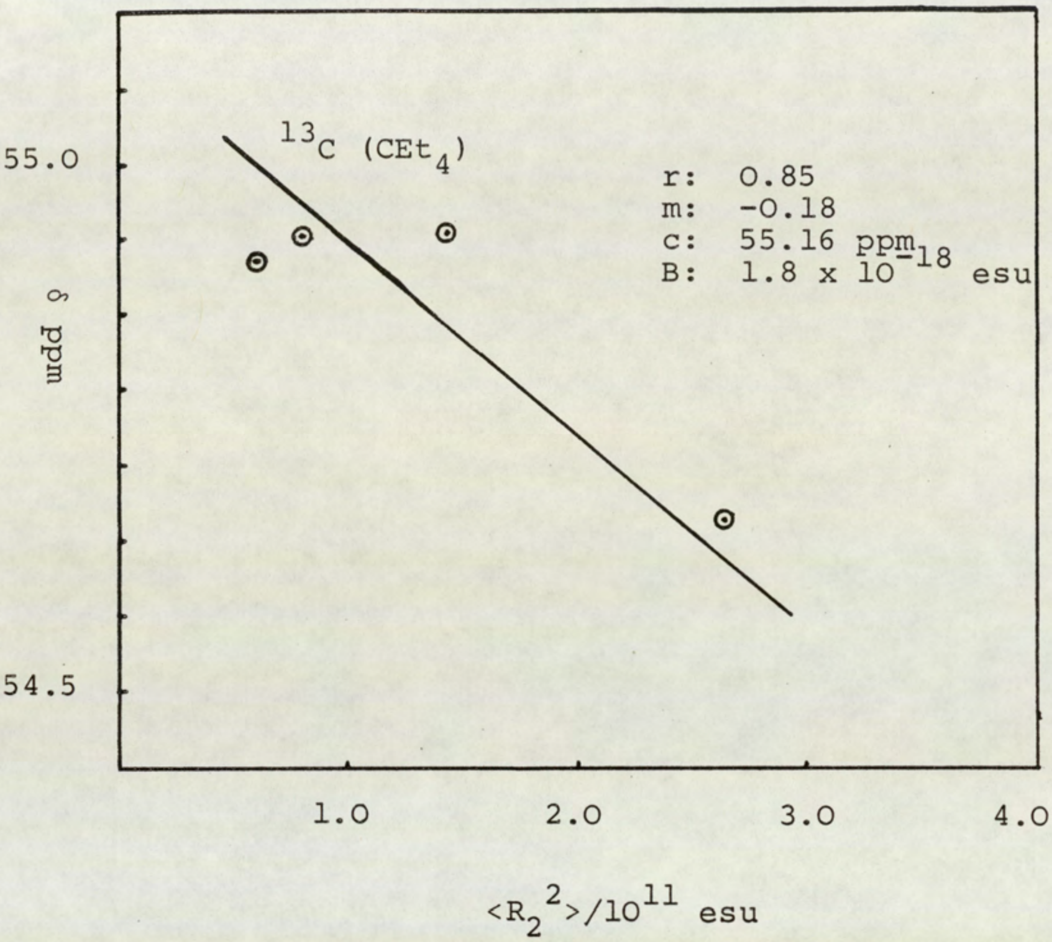

Figure 7.20: Regression of $\langle R_2^{\,2} \rangle$ on the central ^{13}C shifts of CEt_4

7.4 Studies of Tetramethylsilane ($Si(CH_3)_4$)

In view of the encouraging analysis of ^1H and ^{13}C shifts of CEt_4 just discussed, similar analysis for the ^1H, ^{13}C and ^{29}Si of TMS were undertaken.

7.4.1 Analysis of ^1H shifts of $Si(CH_3)_4$

The observed(113) and susceptibility corrected shifts of the methyl protons of TMS in various solvents are given in Table 7.15. Using data collected earlier in Table 7.4 and Chapter Five, the values of the square fields $\langle R_1^2 \rangle$, $\langle R_2^2 \rangle$ and $\langle R_T^2 \rangle$ are calculated and given in Table 7.16. The measured values of $(2\beta_T - \xi_T)^2$ and E^2_{BI} for ^1H, ^{13}C and ^{29}Si are reported in a condensed form in Table 7.17. The values of $(2\beta_T - \xi_T)^2$ for the solvents CCl_4, C_6H_{12} and $Si(CH_3)_4$ in $Si(CH_3)_4$ (solute) for ^1H are already reported in detail in Chapter Six and hence are not included in the present table.

Table 7.15 - The observed(113) and susceptibility corrected proton shifts of $SiMe_4$ in different solvents obtained by using a JEOL FX 90Q NMR spectrometer locked at ^2H of D_2O, operating at 30°C and an irradiation frequency of 89.60425 MHz.

^1H in TMS

Solvent	Obs δ^1H Hz	obs δ^1H ppm	$-2\pi/3\chi_v$	true δ^1H ppm
None gas (P = 0)	326.16	3.540	0	3.640
TMS	200.00	2.232	1.123	3.355
CCl_4	164.31	1.834	1.442	3.276
C_6H_{12}	184.08	2.054	1.327	3.381
CEt_4	175.98	1.964	1.403	3.367
C_6H_6	217.29	2.425	1.296	3.721

Table 7.16 - The calculated mean square reaction fields $<R_1^2>$, $<R_2^2>$ and $<R_T^2>$ for TMS in various solvents

Solvent	$<R_1^2>/10^{11}$ esu	$<R_2^2>/10^{11}$ esu	$<R_T^2>/10^{11}$ esu
TMS	0.271	0.5416	0.8124
CCl_4	0.4031	2.306	2.7091
C_6H_{12}	0.3662	1.253	1.6192
CEt_4	0.3589	0.6205	0.9774
C_6H_6	0.461	2.6078	3.0688

Table 7.17 - Measurement and calculation of $(2\beta_T - \xi_T)^2$ for TMS solute in various solvents

Solvent: Tetraethyl methane (for ^1H shift of TMS)

No of solvent atoms: n*	Angle of contact θ	Distance d Å	$(2\beta_T - \xi_T)^2$	No of similar measurements	Ave $(2\beta_T - \xi_T)^2$
12 ^1H from	5.73	1.08	0.0253	3	
4 methyl	5.73	1.56	0.0323	6	
groups	22.92	4.02	0.806	1	0.4381
	40.11	4.56	2.5466	1	
	57.30	3.9	1.6283	1	
8 ^1H from	5.73	1.26	0.0287	3	
3 methylene	5.73	1.86	0.0371	6	
groups	22.92	5.46	0.8636	1	0.4581
	40.11	5.04	2.6029	1	
	57.30	4.92	1.722	1	

Wt ave $(2\beta_T - \xi_T)^2$: 0.4461
E^2_{BI}: 0.2604

Solvent: Benzene (for ^1H, shift of TMS)

6 ^1H	5.73	2.34	0.0417	3	
Horizontal	5.73	2.76	0.0446	6	
	68.75	5.64	0.7466	1	0.3598
	37.24	5.76	2.303	1	
	22.92	5.88	0.8754	1	
6 ^1H	5.73	2.88	0.0454	3	
Vertical	5.73	4.02	0.504	6	
	68.75	6.96	0.773	1	0.3704
	37.24	6.18	2.331	1	
	22.92	7.08	0.9018	1	

Wt ave $(2\beta_T - \xi_T)^2$: 0.3651
E^2_{BI}: 0.3183

n*: gives the number of peripheral solvent atoms which are in a similar geometrical environment (relative to the soslute resonant atom) and where appropriate, the location or the group of solvent molecule to which they are bonded.

Table 7.17 cont ...

Solvent: Tetraethyl methane (for ^{13}C shift of TMS)

No of solvent atoms: n*	Angle of contact θ	Distance d Å	$(2\beta_T - \xi_T)^2$	No of similar measurements	Ave $(2\beta_T - \xi_T)^2$
$12\,^1H$ from 4 methyl groups	37.24	3.66	2.074	3	1.700
	30.08	3.42	1.325	3	
$8\,^1H$ from 4 methylene groups	37.24	4.5	2.189	3	1.797
	30.08	4.2	1.404	3	

Wt ave $(2\beta_T - \xi_T)^2$: 1.7388

E^2_{BI}: 1.240

Solvent: TMS (for ^{13}C shift of TMS)

$12\,^1H$ from 4 methyl groups	37.24	3.3	2.009	3	1.615
	30.08	2.7	1.091	3	

E^2_{BI}: 1.240

Solvent: CCl_4 (for ^{13}C shift of TMS)

4 Cl	37.24	2.4	1.781	3	1.436
	30.08	2.7	1.091	3	

E^2_{BI}: 1.826

Solvent: C_6H_{12} (for ^{13}C shift of TMS)

$12\,^1H$	37.24	2.46	1.8	3	1.468
	30.08	2.28	1.135	3	

E^2_{BI}: 1.047

Table 7.17 cont ...

Solvent: C_6H_6(for ^{13}C shift of TMS)

6^1H	37.24	3.0	1.946	3	1.566
	30.08	2.52	1.187	3	

E^2_{BI}: 1.1117

Solvent: Tetraethyl methane (for ^{29}Si shift of TMS)

12^1H from	88.5	5.4	0.0037	2	0.04485
4 methyl group	82.5	3.96	0.086	2	
8^1H from	88.5	5.52	0.0037	2	0.0464
4 methylene group	82.5	4.56	0.089	2	

Wt ave ($2\beta_T - \xi_T$): 0.0456
E^2_{BI}: 0.0325

Solvent: TMS (for ^{29}Si shift of TMS)

12^1H from	88.5	4.2	0.0035	2	0.0446
4 methyl groups	82.5	3.9	0.0856	2	

E^2_{BI}: 0.0318

Solvent: C_6H_{12}

12 ^1H	88.5	3.24	0.0032	2	0.0385
	82.5	2.52	0.0738	2	

E^2_{BI}: 0.0274

Solvent: CCl_4

4 Cl	88.5	3.78	0.0034	2	0.0399
	82.5	2.76	0.0765	2	

E^2_{BI}: 0.0509

Solvent: C_6H_6

	88.5	3.9	0.0034	2	0.0438
	82.5	3.66	0.0841	2	

E^2_{BI}: 0.0312

By reference to figure 7.21 which shows a two dimensional representation of the Si $(CH_3)_4$ molecule, the values of the relevant distance modulation $\langle R_2^2 \rangle$ can be calculated, and these are presented in the relevant tables, that include the modulated reaction field. Table 7.18 shows the modulated square reaction field with $\langle R_1^2 \rangle$, $\langle R_2^2 \rangle$ and $\langle R_T^2 \rangle$ together with E^2_{BI} for the protons of TMS. Figures 7.22, 7.23, 7.24 and 7.25 show the regressions of $\langle R_1^2 \rangle + \langle R_2^2 \rangle$, $(\langle R_1^2 \rangle + \langle R_2^2 \rangle (r/a)^6$, $(\langle R_1^2 \rangle + \langle R_2^2 \rangle + E^2_{BI})$ and $(\langle R_1^2 \rangle + \langle R_2^2 \rangle (r/a)^6 + E^2_{BI})$ on the susceptibility corrected proton shifts.

The values of B obtained from the various regressions on the protons of TMS mentioned above, are summarized in Table 7.19 which demonstrates again that the regression of $(\langle R_1^2 \rangle + \langle R_2^2 \rangle (r/a)^6 + E^2_{BI})$ yields the most realistic value for B of 1.087×10^{-18} esu this again indicates that $\langle R_2^2 \rangle$ is distance modulated and the buffeting contribution exists on the periphery.

Additionally, this regression has an intercept of 3.45ppm, that is most consistent with the gas phase shift of 3.64 ppm obtained experimentally in Chapter Five.

The data for benzene as a solvent were not included in the regressions, because of the contribution of σ_a. However from Figure 7.25 it can be deduced that σ_a for benzene with TMS is 0.43ppm. This is in good agreement with the value of 0.488 ppm deduced by Homer and Redhead[53].

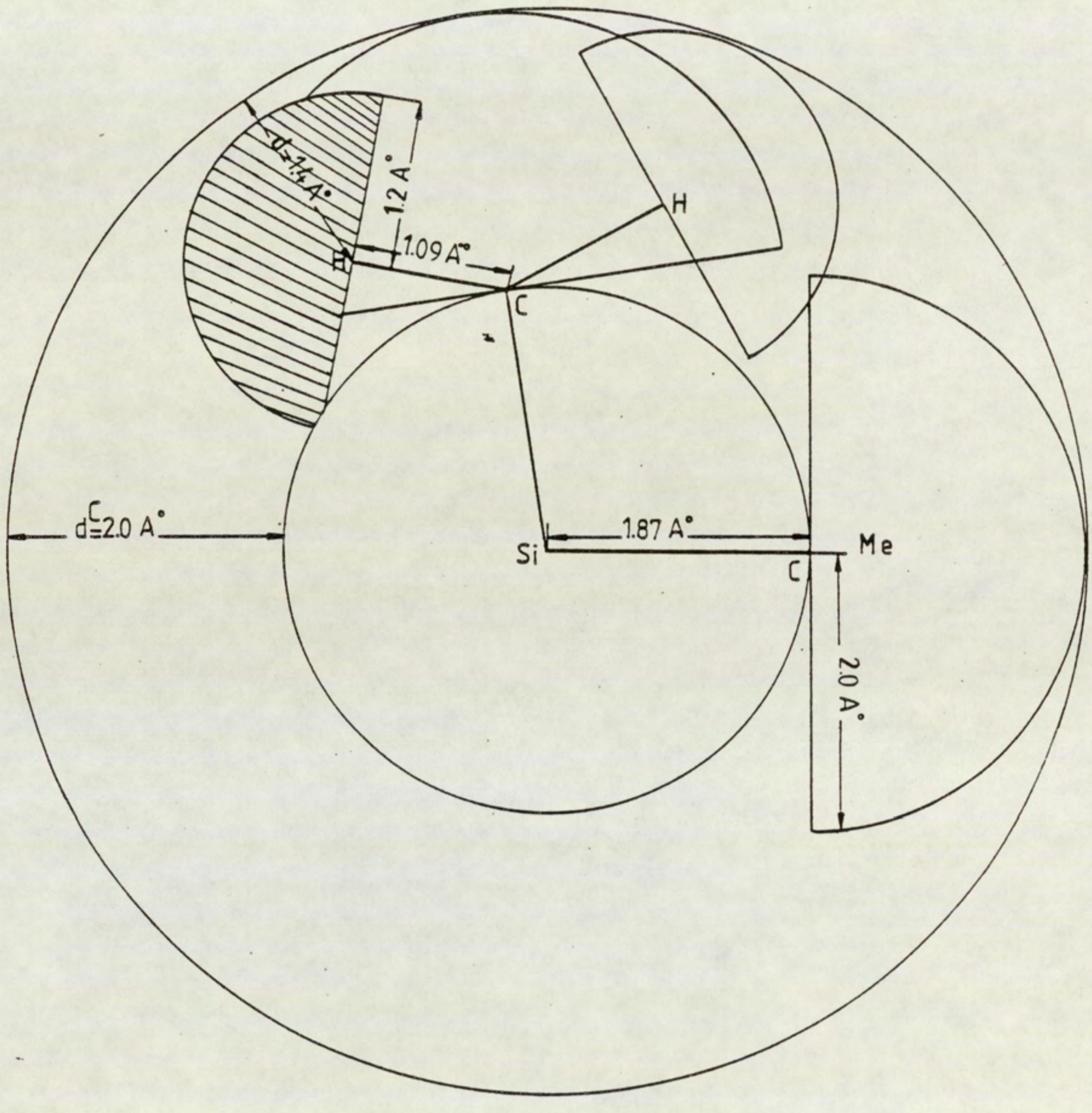

Figure 7.21: Two dimensional representation of Tetramethyl molecule

$^1H\ (CH_3)$ TMS $d = 0.7Å$, $a = r + 0.7$

Solvent	$\left(\frac{r}{r+d}\right)^6$	$\langle R_1^2\rangle/10^{11}$	$\langle R_2^2\rangle/10^{11}$	$\langle R_2^2\rangle (r/a)^6/10^{11}$	$E^2_{BI}/10^{11}$	$\langle R_T^2\rangle/10^{11}$	$\langle R_1^2\rangle+\langle R_2^2\rangle (r/a)^6$	$+ E^2_{BI}$	$\langle R_1^2\rangle+\langle R_2^2\rangle E^2_{BI}$	$\langle R_T^2\rangle + \delta^1H$ ppm
TMS	0.387	0.271	0.5416	0.2096	0.2153	0.8124	0.4806	0.6959	1.0277	3.355
$C\,Cl_4$	0.346	0.4031	2.306	0.7979	0.3232	2.7091	1.201	1.5242	3.0323	3.276
C_6H_{12}	0.358	0.3662	1.253	0.4486	0.148	1.6192	0.8148	0.9628	1.7672	3.381
CEt_4	0.409	0.3589	0.6205	0.2538	0.3183	0.9774	0.6127	0.931	1.2957	3.367
$C_6\,H_6$	0.335	0.461	2.6078	0.8736	0.2604	3.0688	1.3346	1.595	3.3292	3.721

Table 7.18 - The calculated square fields $\langle R_1^2\rangle$, $\langle R_2^2\rangle$ and the modulated term $\langle R_2^2\rangle \left(\frac{r^6}{a}\right)$ together with the square buffeting field for the proton in TMS

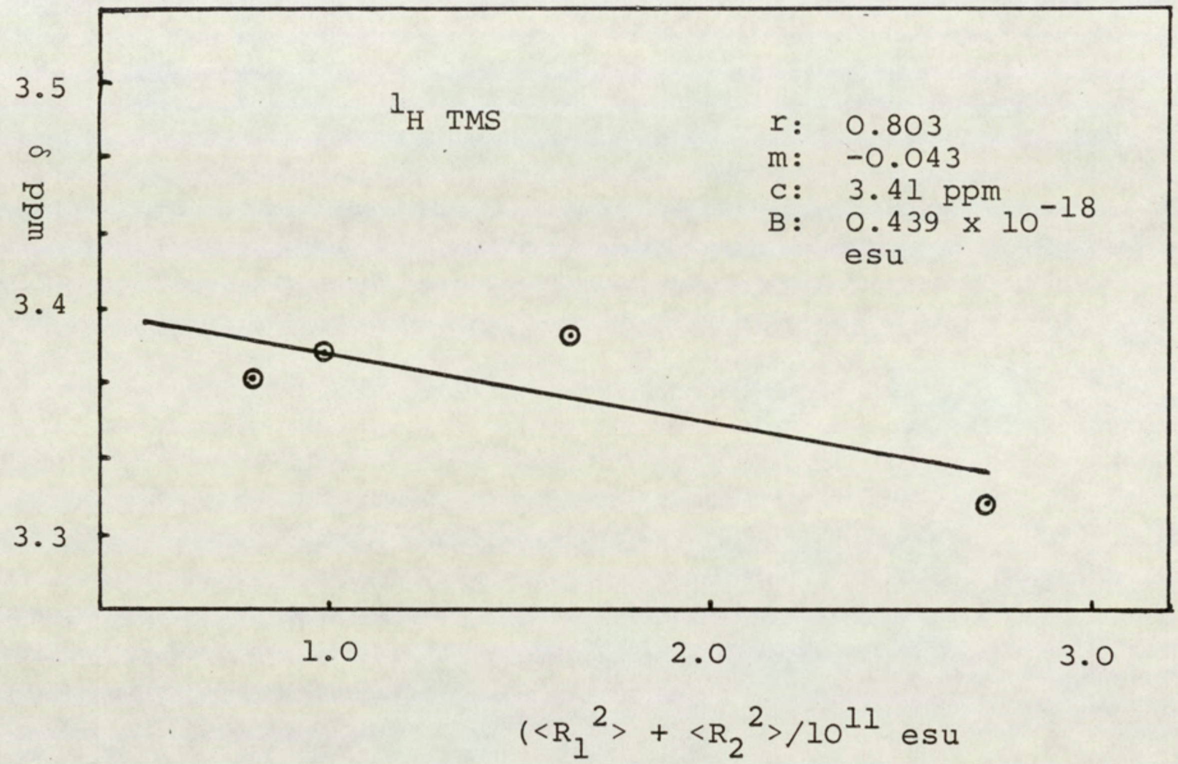

Figure 7.22: Regression of $(\langle R_1^2\rangle + \langle R_2^2\rangle)$ on proton shifts of TMS

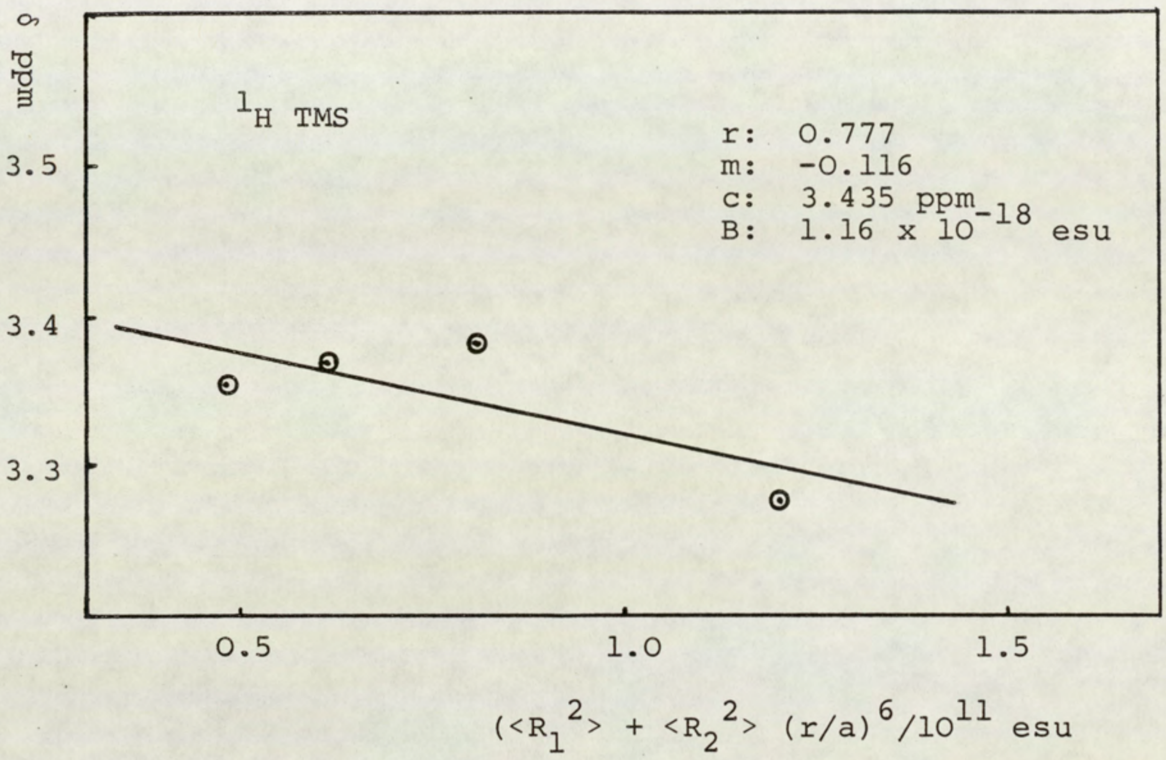

Figure 7.23: Regression of $(\langle R_1^2\rangle + \langle R_2^2\rangle\ (r/a)^6)$ on proton shifts of TMS

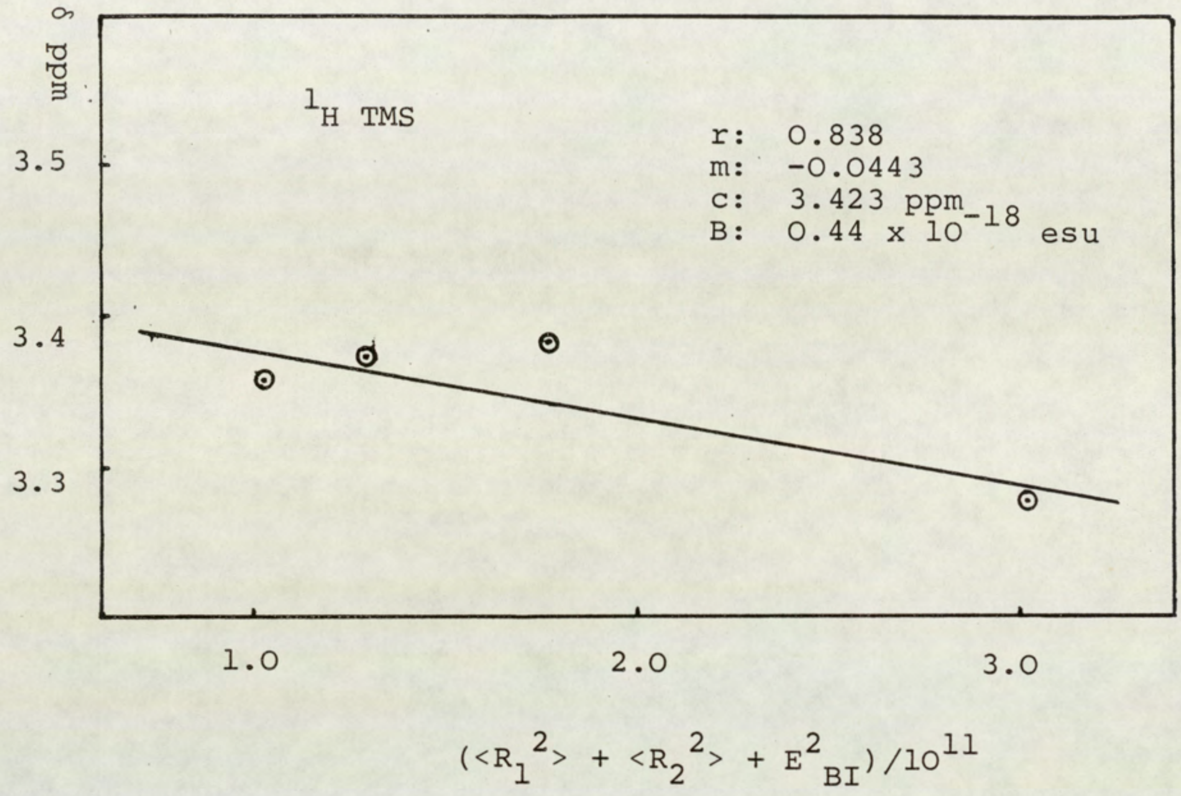

Figure 7.24: Regression of $(\langle R_1^2\rangle + \langle R_2^2\rangle + E^2_{BI})$ on proton shifts of TMS

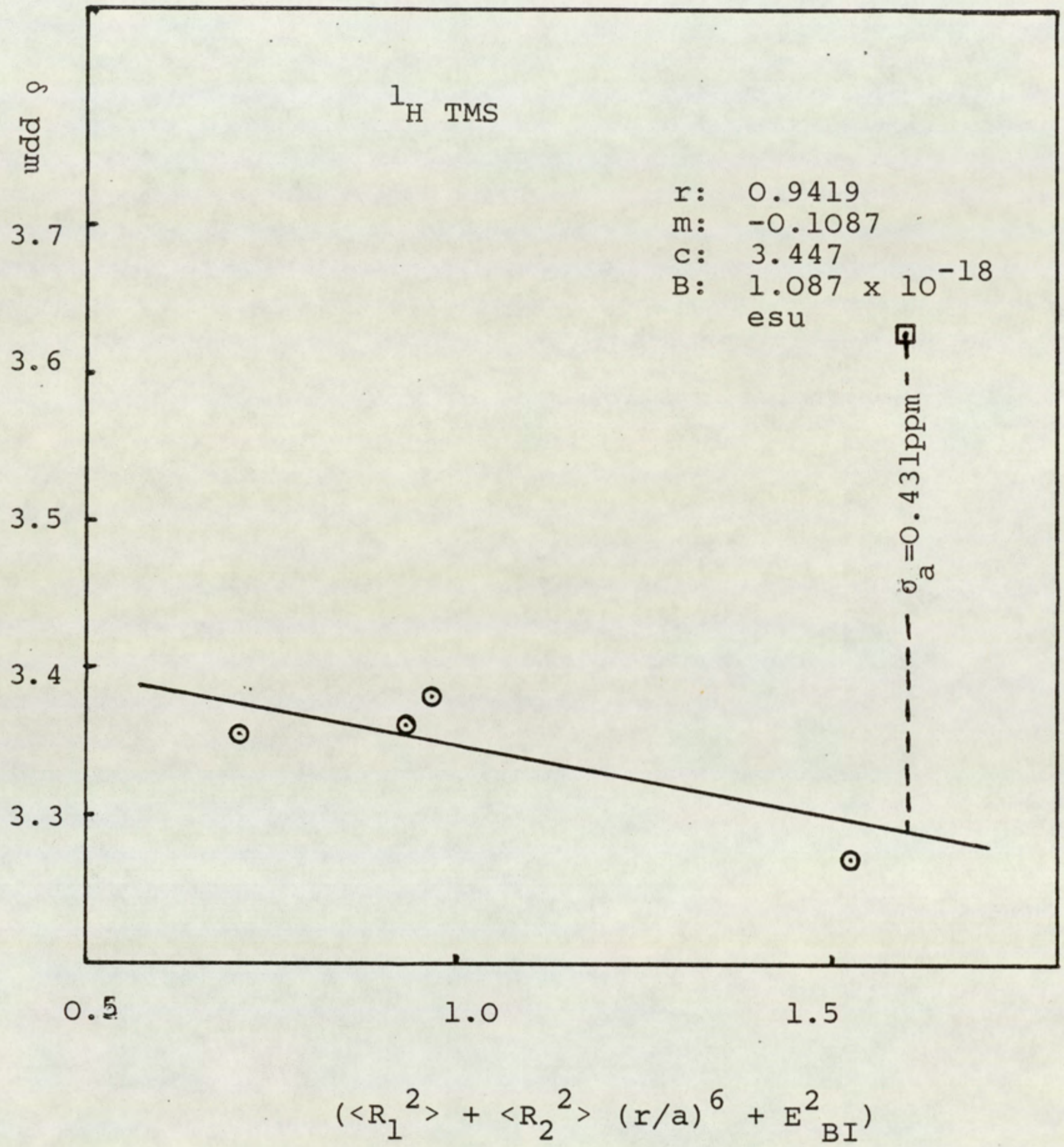

Figure 7.25: Regression of $(\langle R_1{}^2\rangle + \langle R_2{}^2\rangle\ (r/a)^6 + E^2{}_{BI})$ on proton shifts of TMS

Table 7.19 - Collected B values from the different regressions on the ^1H shifts of TMS

Regression of	B value/10^{-18} esu
$\langle R_1{}^2\rangle + \langle R_2{}^2\rangle$	0.439
$\langle R_1{}^2\rangle + \langle R_2{}^2\rangle\ (r/a)^6$	1.16
$\langle R_1{}^2\rangle + \langle R_2{}^2\rangle + E^2{}_{BI}$	0.44
$\langle R_1{}^2\rangle + \langle R_2{}^2\rangle\ (r/a)^6 + E^2{}_{BI}$	1.087

7.4.2 Analysis of ^{13}C shifts of $Si\ (CH_3)_4$

The observed(113) and susceptibility corrected shifts of ^{13}C of TMS are given in Table 7.20. Table 7.21 shows the calculated $\langle R_1{}^2\rangle$, $\langle R_2{}^2\rangle$, $\langle R_T2\rangle$ and the modulated term $\langle R_2{}^2\rangle\ (r/a)^6$ along with other immediately relevant data. The measured values of $(2ß_T - \xi_T)^2$ are reported in Table 7.17. Figures 7.26, 7.27, 7.28, 7.29 and 7.30 show the regression of $(R_T{}^2 + E^2{}_{BI})$, $\langle R_T{}^2\rangle$, $\langle R_1{}^2\rangle$, $(\langle R_1{}^2\rangle + \langle R_2{}^2\rangle\ (r/a)^6) + E^2{}_{BI})$ and $(\langle R_1{}^2\rangle + \langle R_2{}^2\rangle\ (r/a)^6)$ on the susceptibility corrected shifts respectively. It can be seen from Table 7.22, which presents the B values obtained from these regressions that the B value that is most consistent with those found earlier for ^{13}C results from the regression of $(\langle R_1{}^2\rangle + \langle R_2{}^2\rangle\ (r/a)^6 + E^2{}_{BI})$ on the shifts. The value obtained is 10.84×10^{-18} esu, which is in good agreement with the value of $B = 8.02 \times 10^{-18}$ esu obtained for methyl ^{13}C of tetraethylmethane, once again confirming that $\langle R_2{}^2\rangle$ is distance modulated and the buffeting contribution exists on the periphery.

Table 7.20 - Observed(113) and susceptibility corrected ^{13}C shifts of TMS in various solvents. Measurements were made using a JEOL FX 90Q NMR spectrometer locked at ^{2}H of D_2O, operating at 30°C and an irradiation frequency of 22.533 MHz.

Solvent	Obs $\delta^{13}C$ Hz	obs $\delta^{13}C$ ppm	$-2\pi/3\chi_v$	true $\delta^{13}C$ ppm
TMS	2056.88	91.283	1.123	92.406
CCl_4	2030.03	90.091	1.442	91.533
C_6H_{12}	2056.88	91.283	1.327	92.61
CEt_4	2050.77	91.012	1.403	92.415
C_6H_6	2054.33	91.17	1.296	92.466

^{13}C TMS $d = 2.0Å$, $a = r_2 + d$

Solvent	$\left(\frac{r}{r+d}\right)^6$	$\langle R_1^2\rangle/10^{11}$	$\langle R_2^2\rangle/10^{11}$	$\langle R_2^2\rangle (r/a)^6/10^{11}$	$E^2_{BI}/10^{11}$	$\langle R_T^2\rangle/10^{11}$	$\langle R_1^2\rangle+\langle R_2^2\rangle (r/a)^6$	$\langle R_1^2\rangle+\langle R_2^2\rangle$	$\langle R_T^2\rangle+E^2_{BI}{}^1$ $(r/a)^6 + E^2_{BI}$	$\delta^{13}C$ ppm
TMS	0.091	0.271	0.5416	0.0493	1.152	0.8124	0.3203	1.4722	1.9644	92.406
$C Cl_4$	0.071	0.4031	2.306	0.1637	1.826	2.7091	0.5668	2.3928	4.5351	91.533
C_6H_{12}	0.077	0.3662	1.253	0.0965	1.047	1.6192	0.4627	1.5096	3.0324	92.61
CEt_4	0.104	0.3589	0.6205	0.0645	1.24	0.9774	0.4234	1.6634	2.217	92.415
C_6H_6	0.067	0.461	2.6078	0.1747	1.1117	3.0688	0.6357	1.7474	4.1805	91.98*

Table 7.21 - The square fields $\langle R_1^2\rangle$, $\langle R_2^2\rangle$ and the modulated term $\langle R_2^2\rangle (r/a)^6$ together with the square field buffeting field for ^{13}C of TMS. Among the shifts σ_a for benzene with TMS eliminated (as 0.488 ppm) deduced by Homer and Redhead(53).

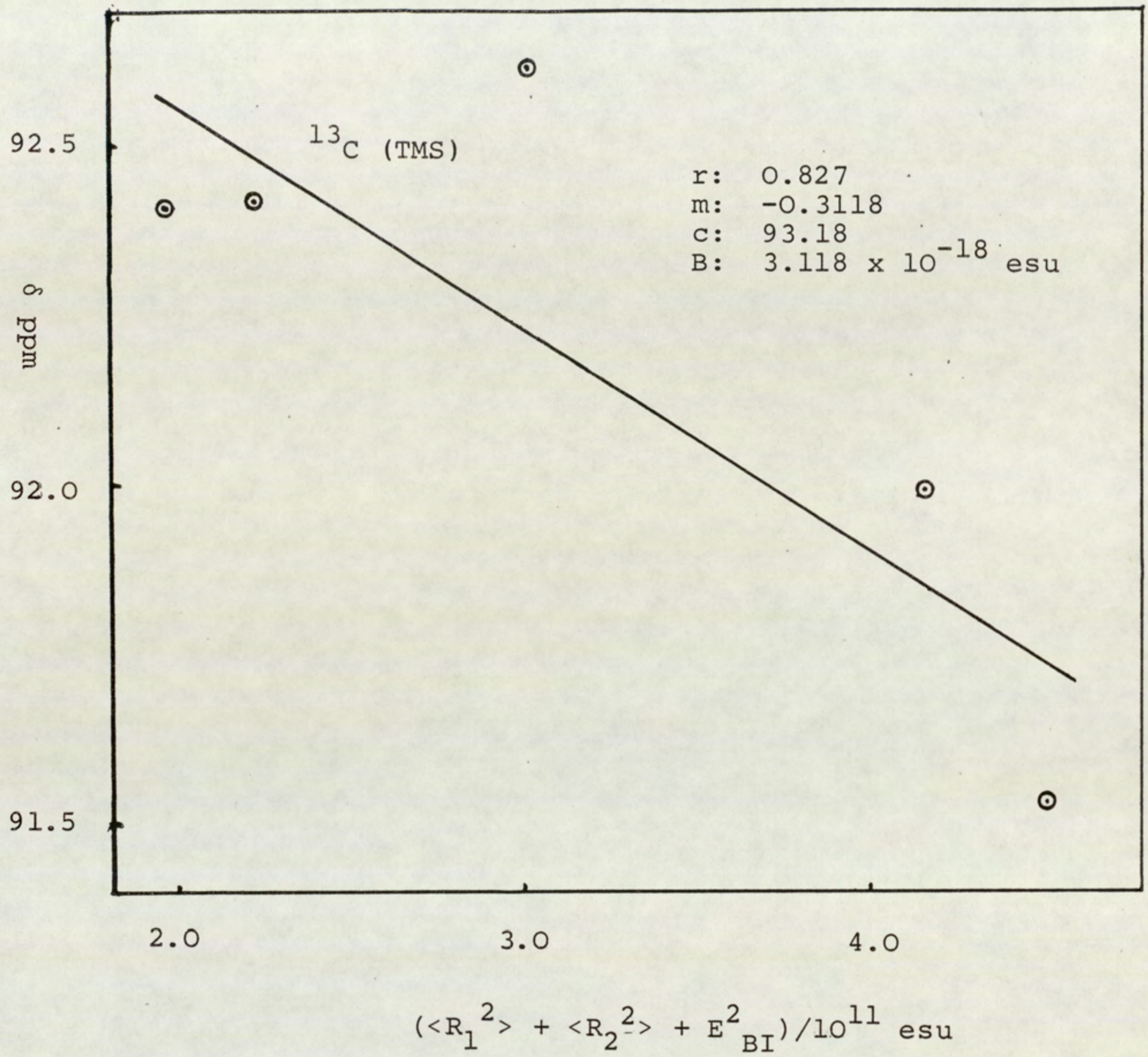

Figure 7.26: Regression of $(\langle R_1{}^2\rangle + \langle R_2{}^2\rangle + E^2{}_{BI})$ on ^{13}C shifts of TMS

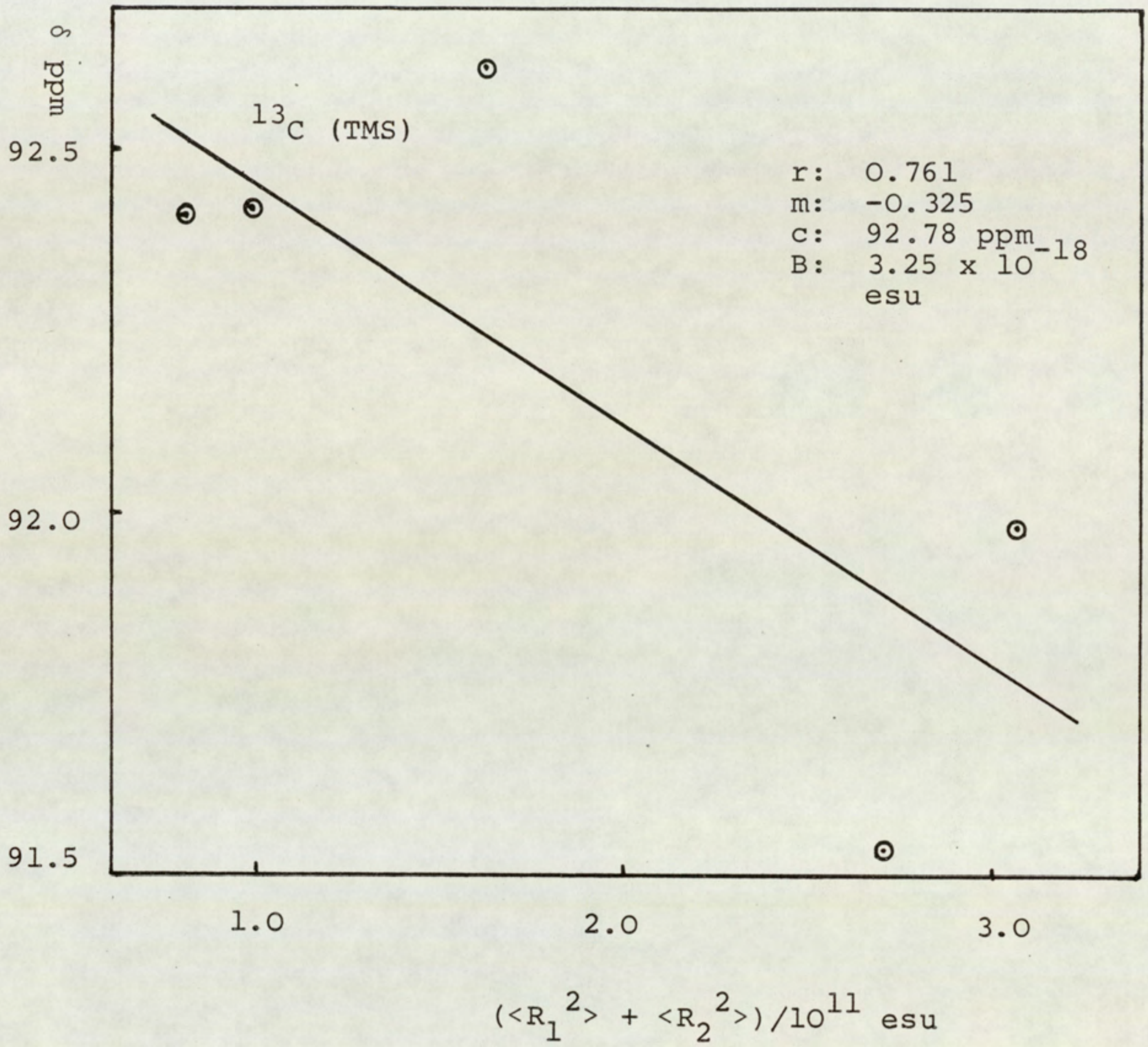

Figure 7.27: Regression of $(\langle R_1^2\rangle + \langle R_2^2\rangle)$ on ^{13}C shifts of TMS

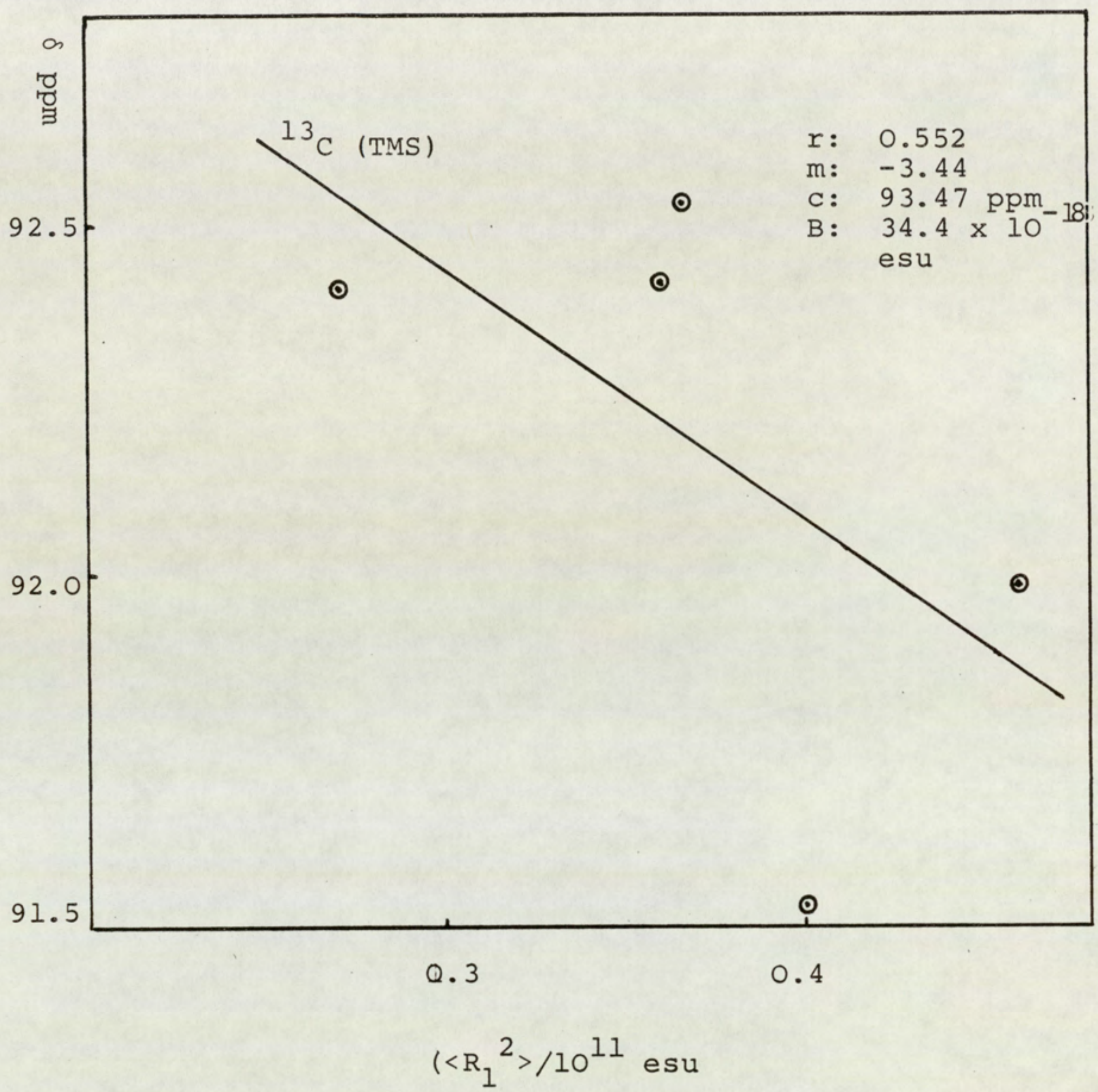

Figure 7.28: Regression of $\langle R_1^2 \rangle$ on ^{13}C shifts of TMS

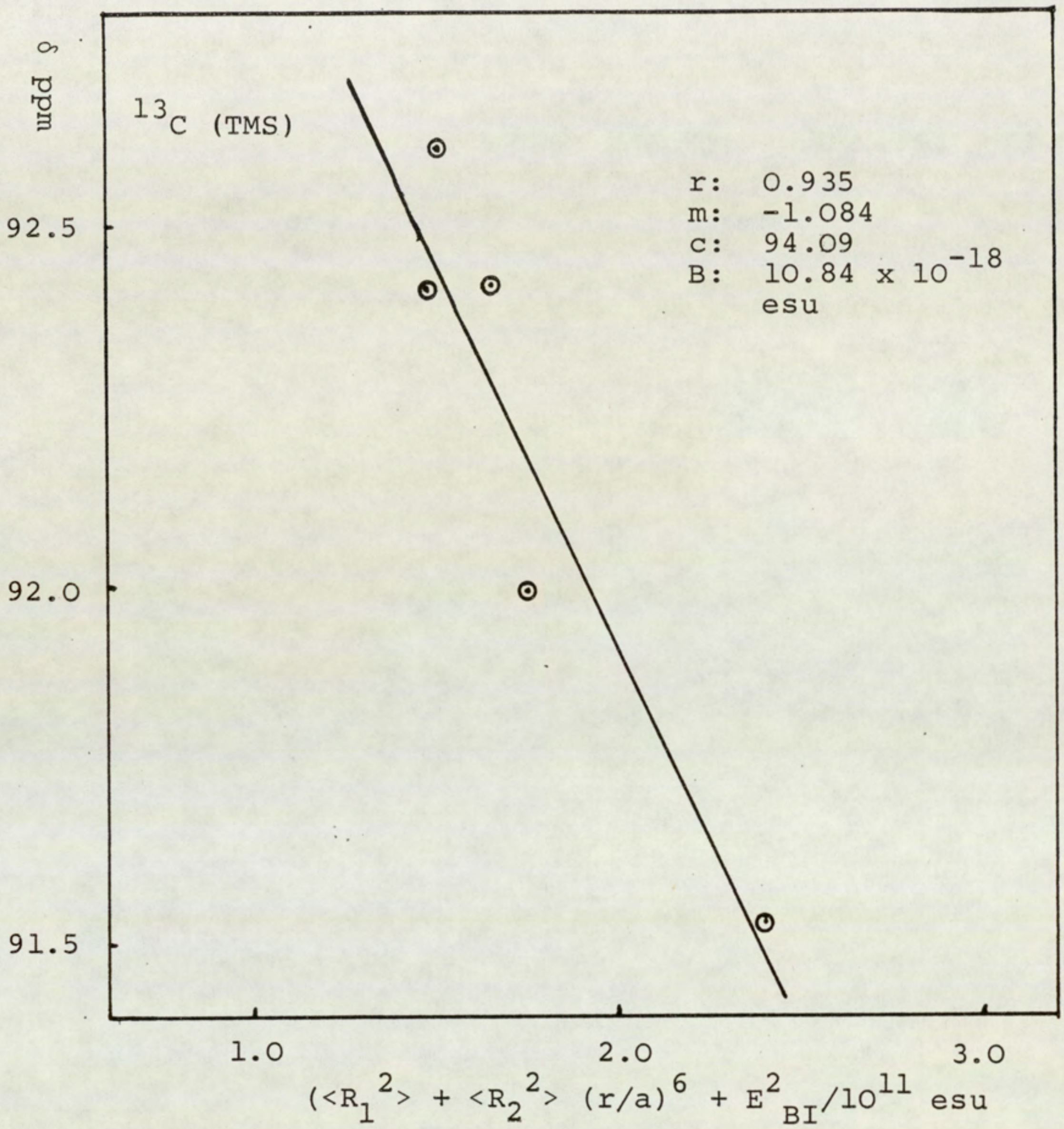

Figure 7.29: Regression of $(\langle R_1{}^2\rangle + \langle R_2{}^2\rangle (r/a)^6 + E^2{}_{BI})$ on ^{13}C shifts of TMS

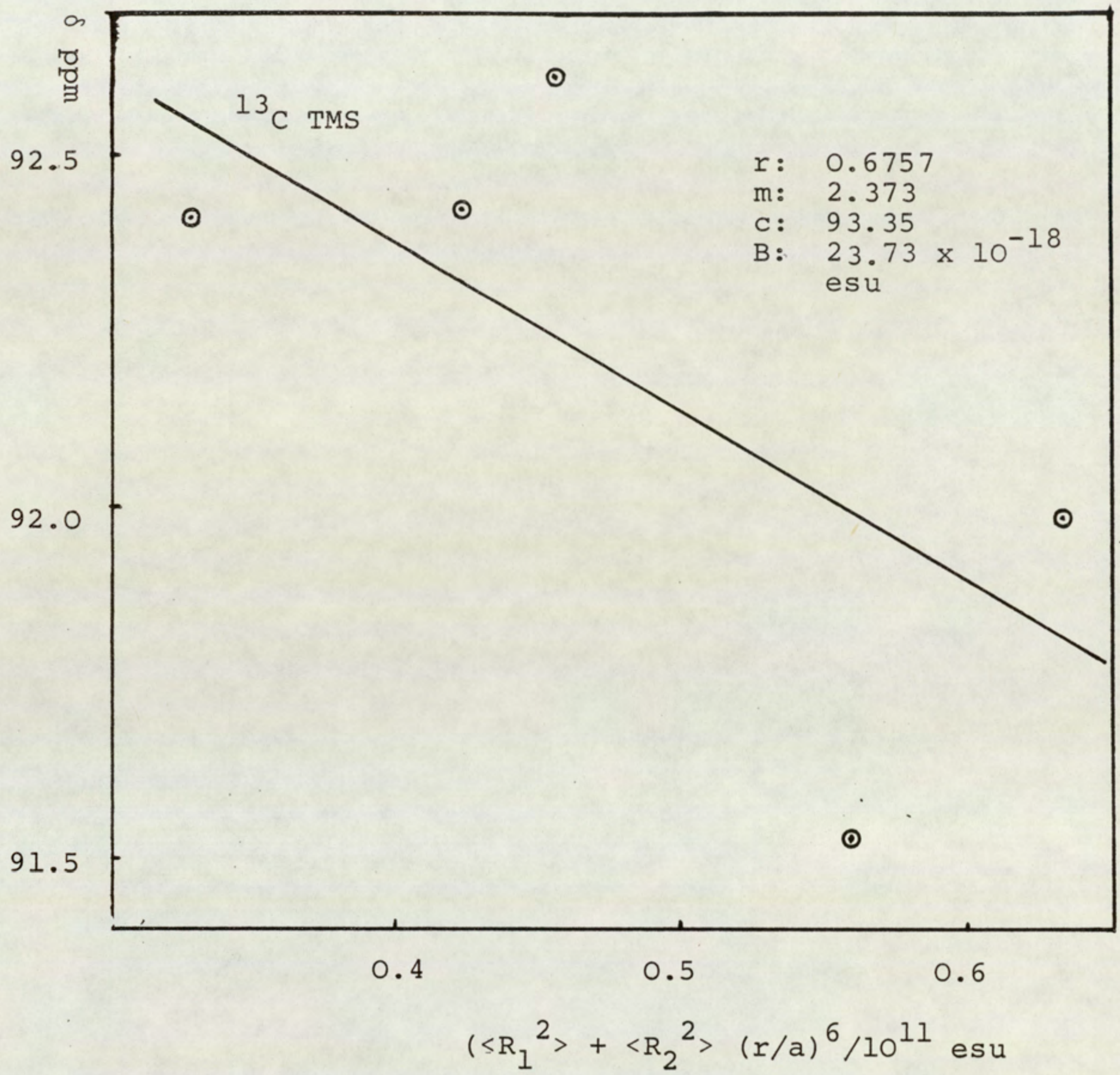

Figure 7.30: Regression of $(\langle R_1^2\rangle + \langle R_2^2\rangle (r/a)^6$ on ^{13}C shifts of TMS

Table 7.22 - Collected B values from the different regression on the ^{13}C shifts of TMS

Regression of	B value/10^{-18} esu
$<R_1^2>$	34.4
$<R_1^2> + <R_2^2>$	3.25
$<R_T^2> + E^2_{BI}$	3.118
$<R_1^2> + <R_2^2> (r/a)^6 + E^2_{BI}$	10.84
$<R_1^2> + <R_2^2> (r/a)^6$	23.73

7.4.3 Analyses of ^{29}Si shifts of $Si(CH_3)_4$

The observed(113) and susceptibility corrected shifts for the ^{29}Si of TMS in various solvents are presented in Table 7.23. As ^{29}Si is at the centre of the molecule, one would expect that the buffeting field should not be effective. However, due to the size of silicon atom the four methyl groups attached to it are far enough from each other to allow a solvent molecule to come in contact with the silicon atom. Hence one could expect a rather diminished buffeting effect due to the hinderance from the adjacent methyl groups. The values of buffeting parameters $(2\beta_T - \xi_T)^2$ are tabulated in Table 7.17. The values of $<R_1^2>$, $<R_2^2>$, $<R_T^2>$, $<R_2^2> (r/a)^6$ along with other immediately relevant data are recorded in Table 7.24.

Table 7.23 - The observed(113) and susceptibility corrected ^{29}Si shifts of $SiMe_4$ in various solvents. Measurements were made using a JEOL FX 90Q NMR spectrometer locked at ^2H of external D_2O, operating at 30°C and irradiation frequency of 17.80188 MHz.

Solvent	Obs $\delta^{29}Si$ Hz	obs $\delta^{29}Si$ ppm	$-2\pi/3\chi_v$	true $\delta^{29}Si$ ppm
TMS	81.05	4.526	1.123	5.649
CCl_4	69.58	3.909	1.442	5.351
C_6H_{12}	76.90	4.320	1.327	5.647
CEt_4	76.9	4.320	1.403	5.723
C_6H_6	86.67	4.869	1.296	6.165

Figures 7.31, 7.32, 7.33, 7.34 and 7.35 show the regression of ($\langle R_T^2\rangle + E^2_{BI}$), $\langle R_T^2\rangle$, $\langle R_1^2\rangle$, ($\langle R_1^2\rangle + \langle R^2\rangle (r/a)^6$) and ($\langle R_1^2\rangle + \langle R_2^2\rangle (r/a)^6 + E^2_{BI}$) respectively, on the corrected shifts of ^{29}Si.

The values of B obtained from these regressions are tabulated in Table 7.25.

It is interesting to note that the B-value obtained from the regression of ($\langle R_1^2\rangle + \langle R_2^2\rangle (r/a)^6 + E^2_{BI}$) is 15.03 x 10^{-18} esu which is marginally higher than 14.16 x 10^{-18} esu obtained from the regression of ($\langle R_1^2\rangle + \langle R_2^2\rangle (r/a)^6$ and $\langle R_1^2\rangle$ respectively. This clearly indicates that the effect of buffeting square field is significantly small. The B value of 15.03 x 10^{-18} esu is comparable with the B values obtained for ^{13}C in tetraethylmethane and is in agreement with the prediction mentioned in Section 7.3.2. It is interesting to note that the B value for ^{29}Si is

^{29}Si TMS d = 3.87 Å, a = r + 3.87

Solvent	$\left(\frac{r}{r+d}\right)^6$	$\langle R_1^2\rangle / 10^{11}$	$\langle R_2^2\rangle / 10^{11}$	$\langle R_2^2\rangle (r/a)^6 / 10^{11}$	$E^2_{BI}/10^{11}$	$\langle R_T^2\rangle / 10^{11}$	$\langle R_1^2\rangle + \langle R_2^2\rangle (r/a)^6$	$\langle R_1^2\rangle + \langle R_2^2\rangle (r/a)^6 + E^2_{BI}$	$\langle R_T^2\rangle + E^2_{BI}$	$\delta^{29}Si$ ppm
TMS	0.0183	0.271	0.5416	0.0099	0.0318	0.8124	0.2809	0.3127	0.8442	5.649
$C\,Cl_4$	0.0127	0.4031	2.306	0.0293	0.0509	2.7091	0.4324	0.4833	2.76	5.351
C_6H_{12}	0.0142	0.3662	1.253	0.0178	0.0274	1.6192	0.384	0.4114	1.6466	5.647
CEt_4	0.0221	0.3694	0.6847	0.0151	0.0325	1.054	0.3845	0.417	1.0865	5.723
C_6H_6	0.012	0.461	2.6078	0.0313	0.0312	3.0688	0.4923	0.5235	3.3808	6.165

Table 7.24 - The calculated square fields $\langle R_1^2\rangle$, $\langle R_2^2\rangle$ and the modulated term $\langle R_2^2\rangle (r/a)^6$ together with the square field buffeting field for ^{29}Si in TMS

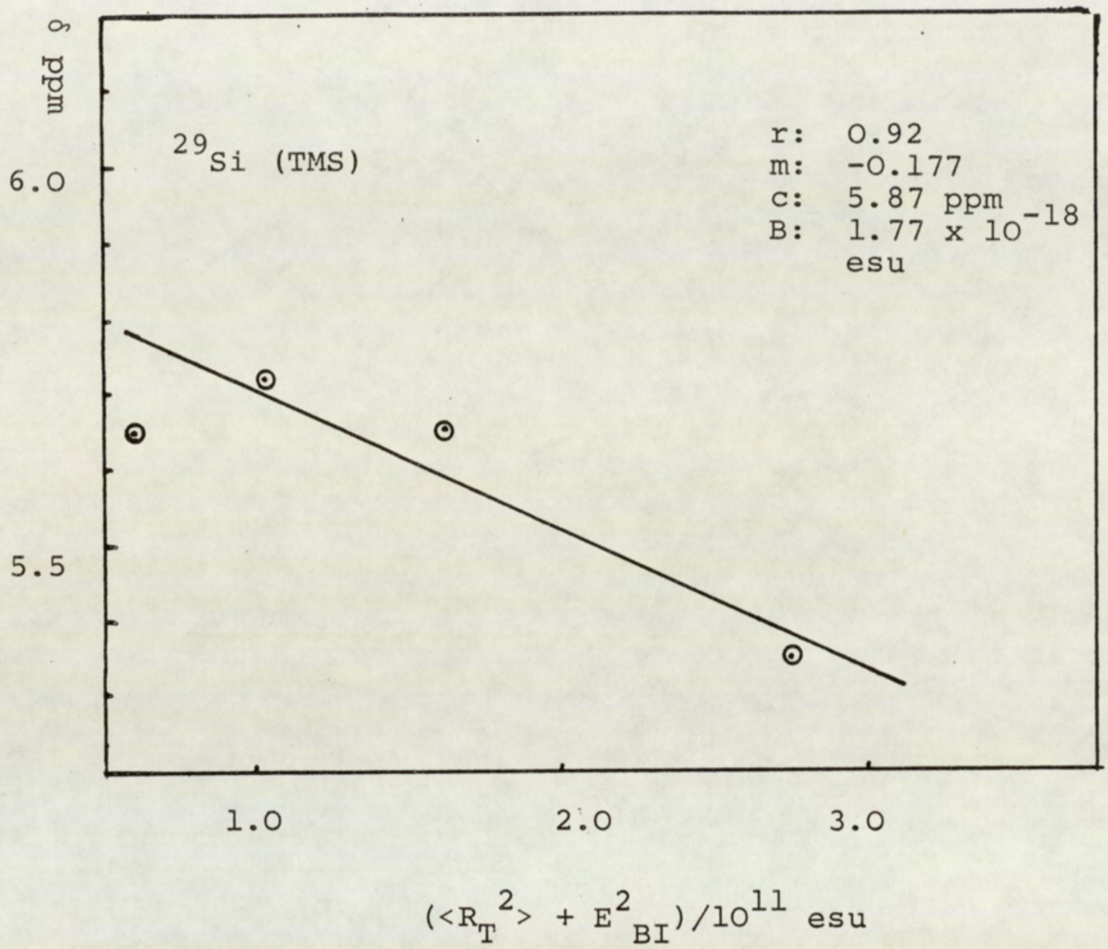

Figure 7.31: Regression of $(\langle R_T^{\ 2}\rangle + E^2_{BI})$ on ^{29}Si shifts of TMS

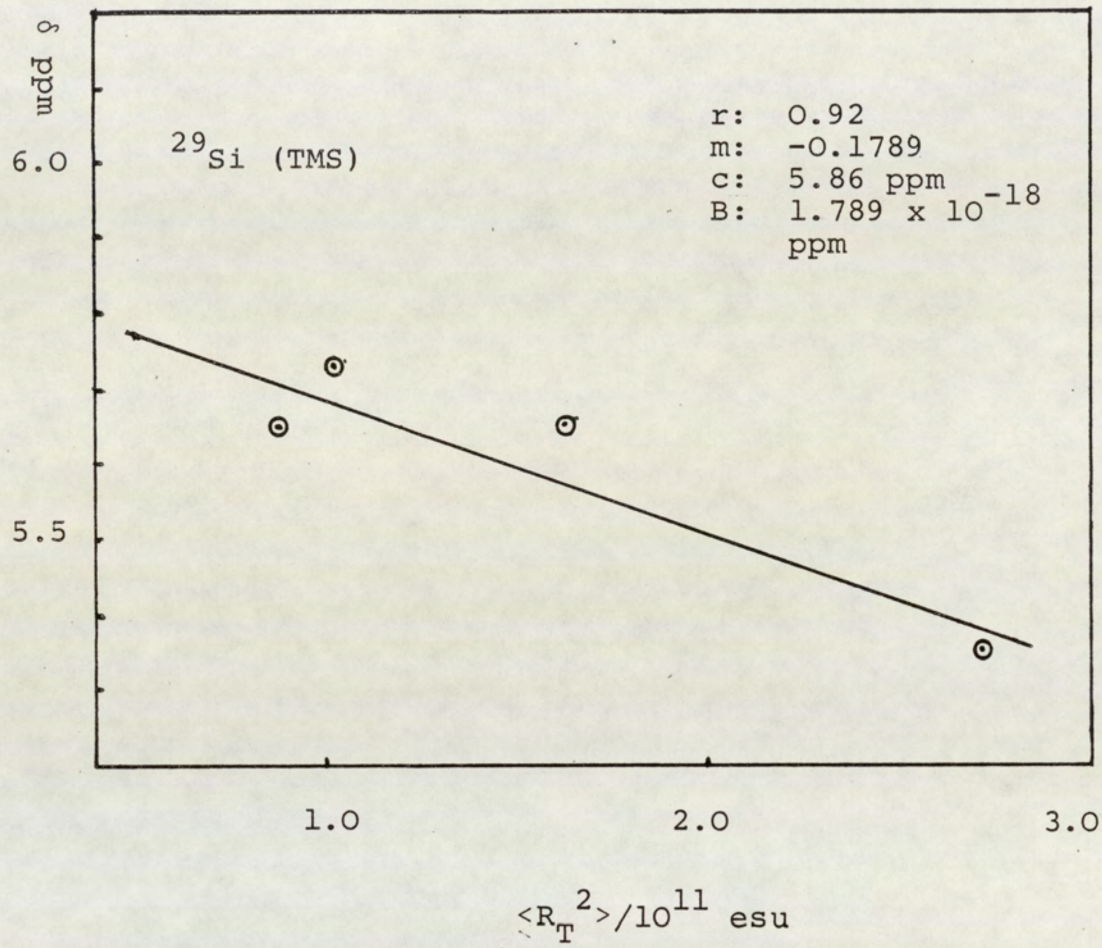

Figure 7.32: Regression of $<R_T^2>$ on ^{29}Si shifts of TMS

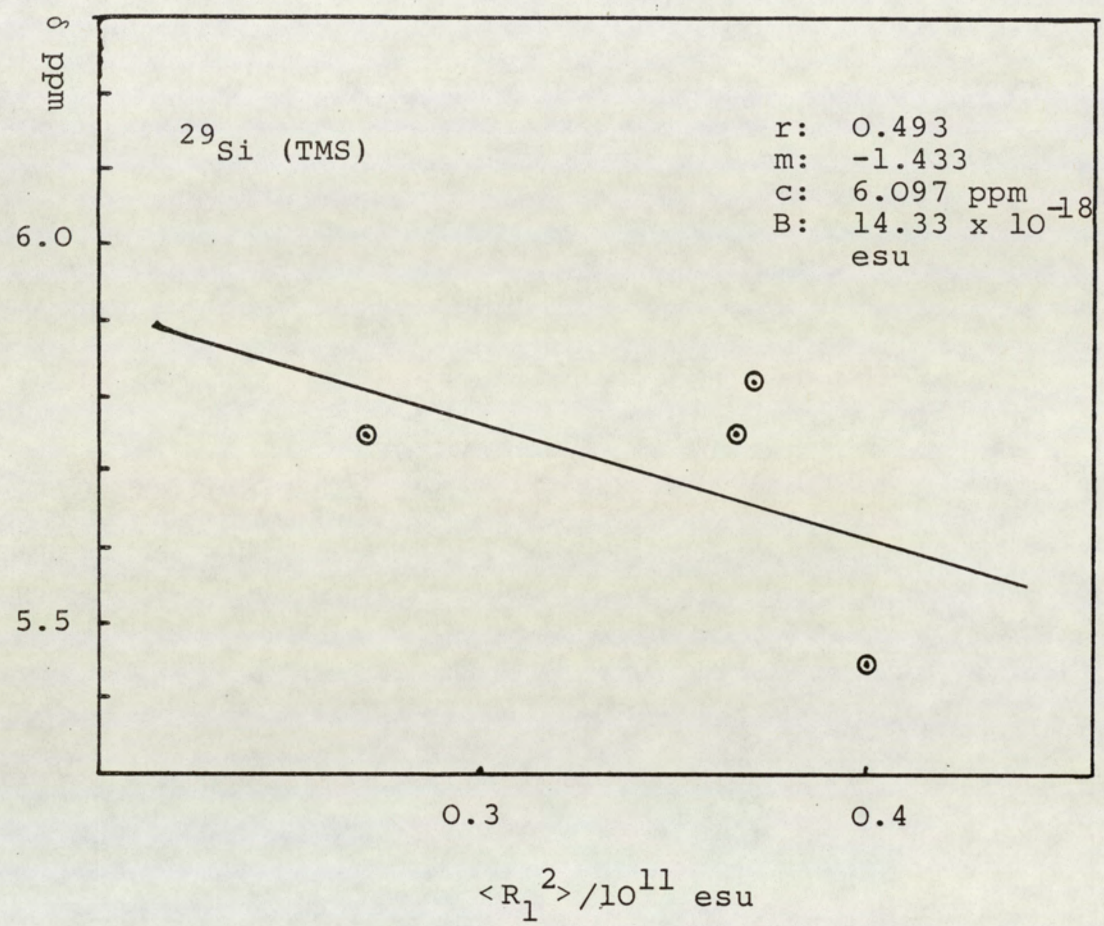

Figure 7.33: Regression of $\langle R_1{}^2 \rangle$ on ^{29}Si shifts of TMS

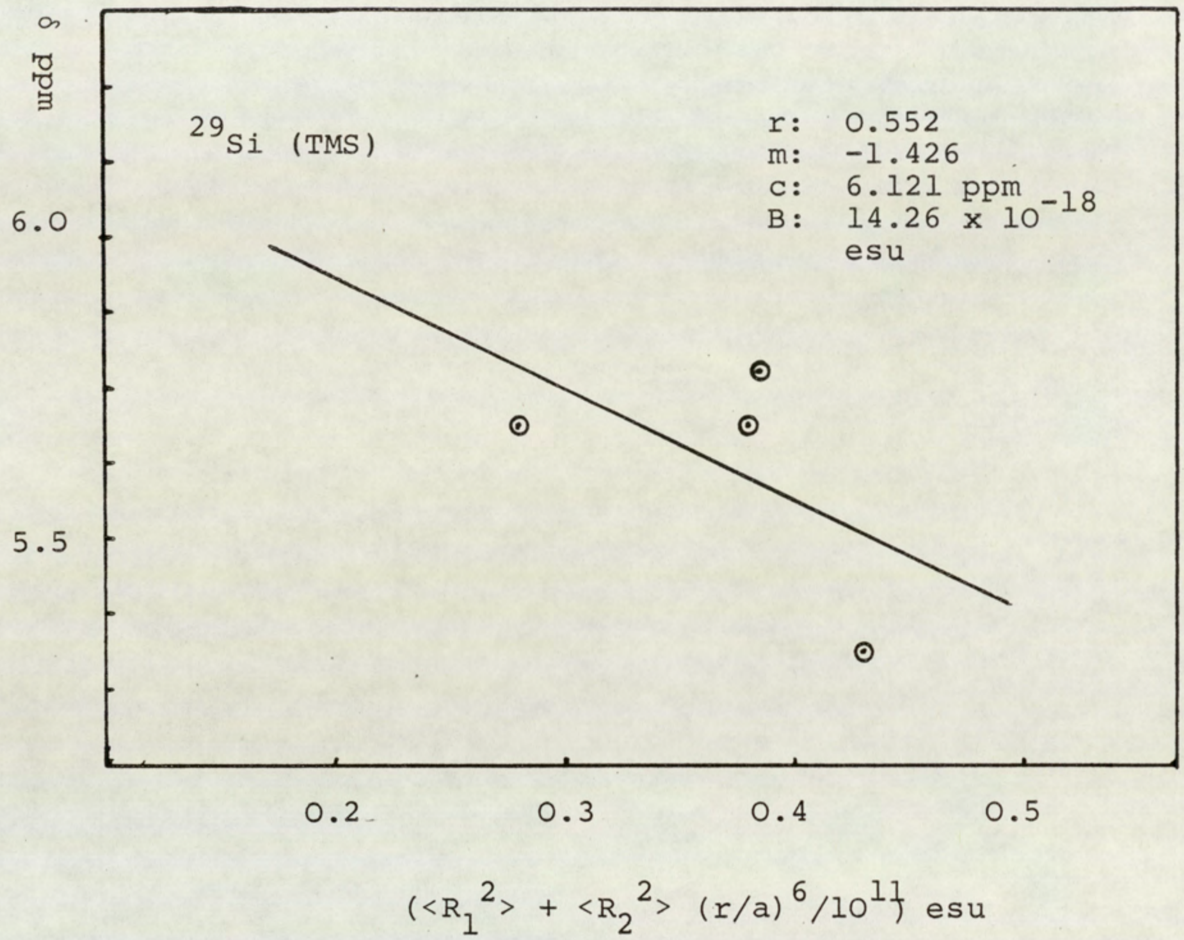

Figure 7.34: Regression of $(\langle R_1^2\rangle + \langle R_2^2\rangle\ (r/a)^6)$ on ^{29}Si shifts of TMS

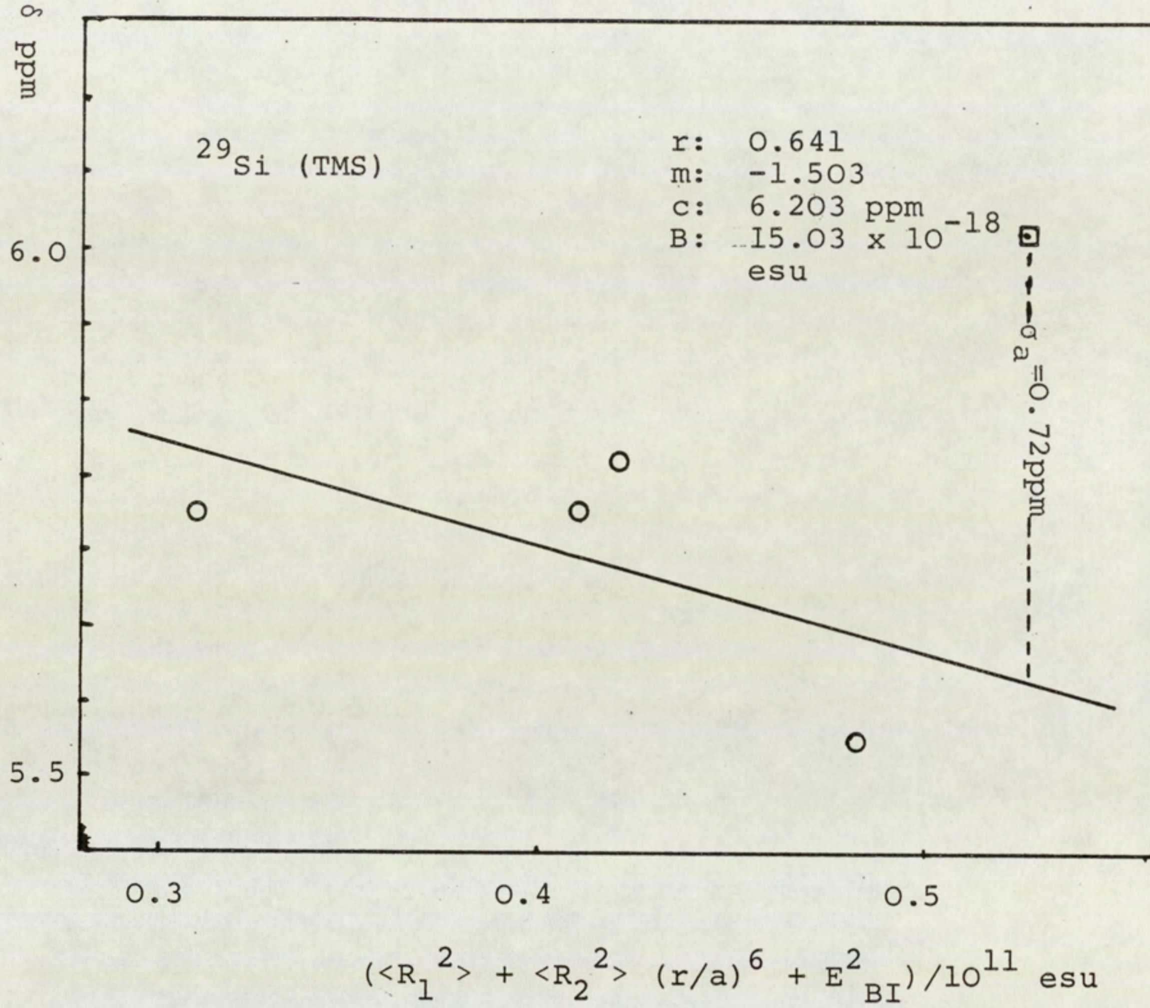

Figure 7.35: Regression of $(\langle R_1{}^2\rangle + \langle R_2{}^2\rangle\ (r/a)^6 + E^2{}_{BI})$ on ^{29}Si shifts of TMS

marginally larger than that of ^{13}C, which confirms Mohammadi(71) hypothesis mentioned in Section 7.3.2. It can be seen that the value of B obtained from the $<R_T^2>$ regression is exceedingly small, as compared to those obtained from the $<R_1^2>$ regression for the similarly sited ^{13}C in the CEt_4. This serves to demonstrate that $<R^2>$ should be distance modulated.

Additionally from Figure 7.35 a sensible value of 0.72 ppm is obtained for σ_a of benzene. This adds further credibility to the foregoing analysis.

Table 7.25 - Collected B values from the different regression on the ^{29}Si shifts of TMS

Regression of	B value/10^{-18} esu
$<R_1^2>$	14.33
$<R_1^2> + <R_2^2>$	1.789
$<R_1^2> + <R_2^2> (r/a)^6$	14.26
$<R_1^2> + <R_2^2> (r/a)^6 + E^2_{BI}$	15.03
$<R_T^2> + E^2_{BI}$	1.77

7.5 Conclusion

The analysis presented in this chapter provides the first substantial evidence that while $<R_1^2>$ is operative in all circumstances throughout the Onsager cavity $<R_2^2>$ has to be distance modulated to account for the distance between the periphery of the solute molecule and the resonant nucleus. It is evident also that the buffeting effect is significant for atoms at the periphery of the solute molecules and its effect diminishes for atoms situated towards the centre of the molecule.

OVERALL CONCLUSIONS

The mean square electric fields associated with intermolecular dispersion (here called van der Waals) forces perturb extra-nuclear electrons. Therefore, particularly in the liquid phase, there is a significant contribution to the nuclear screening (σ_W) and hence the chemical shift of the resonant nuclei due to van der Waals forces. The satisfactory characterization of this nuclear screening may provide the key to a more detailed understanding of other intermolecular screening effects that nuclei may experience.

In 1984, Homer and Percival proposed that σ_W can be characterized by an extended two part Onsager-type reaction field ($\langle R_1^2 \rangle$ and $\langle R_2^2 \rangle$) treatment together with a new buffeting effect that arises from the interaction between the peripheral atoms of the adjacent molecules and the atom containing the resonant nucleus. In their preliminary work, they demonstrated that the buffeting screening term (σ_{BI}) is most significantly influenced by the nature of the solute molecule and that variations in buffeting due to changing solvents, having the same peripheral atoms, could not be detected with any certainty. Moreover, they provided no direct experimental evidence for the discrete contributions of the reaction field terms and the buffeting term (defined by the parameter $(2\beta_T\text{-}\xi_T)^2$ where ß and ξ are geometrical parameters). The work presented in this thesis is principally directed to elucidating various features of the buffeting screening.

Homer and Percival's model requires that buffeting should be enhanced for solvents containing peripheral atoms that contain a large number of electrons. In order to investigate this possibility, the selective use of Lanthanide Shift Reagents (LSR) that do not bond to suitable solutes is investigated. The expected enhancement of buffeting is not found. This arises because, despite the anticipated electronic effects, the high molecular volumes of these LSR compounds reduce the steric parameter $(2ß_T-\xi_T)^2$ and thus the anticipated enhancement. Similar conclusions are reached from the evaluation of $(2ß-\xi)^2$ for a series of hydrocarbons, of increasing molecular volumes, acting on methane as solute. This preliminary work indicates that like the solute, the nature of the solvent molecule should also influence the values of the buffeting parameter $(2ß_T-\xi_T)^2$ and hence σ_{BI}. This suggests the need for a method of estimating ß and ε with improved accuracy.

An improved procedure for deducing ß and ξ is presented which accommodates the effects of the molecular structure of both the solute and the solvent molecules. Values of the buffeting parameter $(2ß_T - \xi_T)^2$ are deduced for a range of solute-solvent systems, with the solvent containing either H or Cl separately, or together, as perepheral atoms. Using these values Homer and Percival's theory is applied to analyse a series of ^1H gas-to-solution shifts. The analyses have enabled the determination of a theoretically acceptable value for the classical screening coefficient B for protons, which is in agreement with literature values.

The general theory of buffeting is built up on the basis of hydrogen atom-hydrogen atom encounters. To incorporate the effect of peripheral Cl (or other) atoms, an electron displacement term Q is utilized which accounts for enhanced buffeting due to the electronic structure of Cl atoms. By detailed analysis of data for appropriate solvents a value of Q = 6.6 is obtained which is in good agreement with those obtained by Yonemoto(111) and Homer and Percival.

The conclusions mentioned above provide confirmation for the fundamental validity of Homer and Percival's approach. Consequently, an attempt is made to demonstrate the existence of the screening effects of the individual contributions of the two reaction field terms ($<R_1^2>$ and $<R_2^2>$) and the buffeting term (E^2_{BI}). For this purpose `^1H, ^{13}C and ^{29}Si shifts for the solutes TEM and TMS in a limited range of solvents are investigated. Although based on limited data, an analysis of the various shifts in terms of the three isolated contributions and various combinations of these is presented to yield values of B for ^1H, ^{13}C and ^{29}Si. Comparison of these values with those expected for the screening coefficient B for ^1H, ^{13}C, ^{29}Si provides some evidence for the discrete contributions of the three screening terms.

All of the above findings indicate that future work in this area could prove profitable. For example: it would be particularly constructive to attempt an analysis of the shifts of a variety of nuclear resonances in an extensive range of solvents in order to establish with greater certainty whether the three screening effects do in fact contribute to σ_w; this would also yield values of B for the nuclei studied. It might also prove profitable to design experiments to explore the possibility that σ_{BI} may be used as a reliable tool for the elucidation of molecular structure. Nevertheless, these possibilities need to be tempered by the knowledge that more recent work (Homer and Mohammadi[71]) has resulted in a generalized London type theorem for molecular dispersion interactions that may be considered to superceded the earlier Homer-Percival theory. However the generalized London approach is only valid for relatively small molecules, eg. up to C_5 hydrocarbons, that rotate sufficiently rapidly in the liquid phase that the average of the inverse sixth power of the intermolecular distance is averaged on the NMR time scale.

As suggested by Homer and Mohammadi, for those molecules for which the London dispersion theorem is expected to fail, it may be profitable to characterize the molecular interactions on an atom-atom, atom-group or even group-group additivity basis. If this is the case, it is possible that the principles underlying the present work may be extended to characterize the intermolecular forces for which the generalized London theorem is no longer suitable. Certainly, the investigation of the buffeting effect of hydrocarbon molecules up to C_{14} that are reported herein show that the presently modified approach to buffeting is capable of adequately characterizing intermolecular forces involving these large solvent molecules that lie outside the scope of the generalized London theorem. Consequently it is proposed that any future work in this field should commence with a detailed comparison of the reaction field plus buffeting theory and the recent London dispersion theory of polyatomic molecules.

REFERENCES

1 Pauli W "Naturwiss"; 12, 741, (1924)

2 Dennison DM "Proc Roy Soc (London)"; A15, 483, (1927)

3 Stern O "Z Physik"; 7, 249, (1921)

4 Estermann I, Stern O "Z Physik"; 85, 17, (1933)

5 Ramsey NF "Molecular beams" Oxford University Press, (1959)

6 Purcell EM, Torrey HC & Pound RV "Phys Review"; 69, 37, (1946)

7 Bloch F, Hansen WW & Packard M "Phys Review"; 69, 127, (1946)

8 Emsley JW, Freeny J & Sutcliffe LH "High resolution nuclear magnetic resonance spectroscopy"; Pergamon Press, Oxford (1965)

9 Pople JA, Schneider WG & Berstein HJ "High resolution nuclear magnetic resonance spectroscopy"; McGraw Hill, New York (1959)

10 Jackmann LM "Application of NMR spectroscopy in organic chemistry"; Pergamon Press, London, (1959)

11 Gutowsky HS & McCall DW "Phys Review"; 82, 748, (1951)

12 Blombergen N, Purcell EM & Pound RV "Phys Review"; 73, 679, (1948)

13 Einstein A "Z Phys"; 18, 121, (1917)

14 Purcell EM "Phys Review"; 69, 681, (1946)

15 Emsley JW, Freeny J & Sutcliffe LH "High resolution nuclear magnetic resonance spectroscopy"; Volume 1, Pergamon Press, Oxford (1965)

16 Bloch F "Phys Review"; 70, 460, (1946)

17 Bloch F "Phys Review"; 102, 104, (1956)

18 Wagsness RK & Bloch F "Phys Review"; 89, 728, (1953)

19 Tires GW "J Phys Chem"; 65, 1916, (1961)

20 Endrew ER "Nuclear magnetic resonance"; Cambridge University Press, (1955)

21 Knight WD "Phys Review"; 76, 1259, (1949)

22 Proctor WG & Yu FC "Phys Review"; 77, 717, (1950)

23 Dickinson WC "Phys Review", 77, 736, (1950)

24 Tires GVD "J Phys Chem"; 63, 1379, (1959)

25 Homer J "Tetrahedron"; 23, 4065, (1967)

26 Lazlo P, Speert A, Ottinger R & Reisse J "J Chem Phys"; 48, 1732, (1968)

27 Homer J "Applied Spectroscopy Review"; 9, 1, (1975)

28 Raynes WT, Buckingham AD & Bernstein HJ "J Chem Phys"; 36, 3481, (1962)

29 Petrakis L & Bernstein HJ "J Chem Phys"; 38, 1562, (1963)

30 Saika A & Slichter CD "J Chem Phys"; 22, 26, (1954)

31 Ramsey NF "Phys Review"; 77, 567, (1950)
78, 699, (1950)
83, 540, (1951)
86, 243, (1952)

32 Buckingham AD, Schaefer T & Schneider WG "J Chem Phys"; 32, 1227, (1960)

33 Dickinson WC "Phys Review"; 81, 717, (1951)

34 Lussan C "J Chem Phys"; 61, 462, (1964)

35 Zimmerman JR & Foster MR; "J Chem Phys"; 61, 282, (1957)

36 Laszlo P "Progress in NMR spectroscopy"; 3, 241, (1967)

37 Frost DJ & Hall GE "Mol Phys"; 10, 191 (1966)

38 Homer J, Everdell MH, Hartland EJ & Jackson CJ "JCS"; A, 1111, (1970)

39 Homer J & Percival CC "J Chem Soc Faraday Trans II"; 80, 1-29, (1984)

40 Proctor WG & Yu FC "Phys Review"; 81, 20, (1951)

41 Gutowsky HS & McCall DW "Phys Review"; 82, 748, (1951)

42 Dixon WT "Theory and interpretation of magnetic resonance spectra"; Plenum (1972)

43 Becconsall JK & McIvor MC "Chem in Britain"; 5, 147, (1969)

44 Anderson WJ "NMR and EPR spectroscopy"; staff of Varian Associates, Pergamon, 176, (1960)

45 Radio Society of Great Britain "The radio communication handbook"; (1968)

46 Perkin-Elmer R12B Model NMR spectroscopy handbook, (1968)

47 Clark WG "Review Sci Inst"; 35, 316, (1964)

48 Lowe IJ & Tarr CE "J Sci Inst"; 1, 320, (1968)

49 McKay RA & Woessner DE "J Sci Inst"; 43, 838, (1966)

50 JEOL FT NMR Spectrometer FX 90Q manual

51 Rummens FA, Raynes WT & Bernstein JH "J Phys Chem"; 72, 211, (1968)

52 Onsager L "J Amer Chem Soc"; 58, 1068, (1936)

53 Homer J & Redhead DL "J of Chem Soc"; Faraday transaction II, 68, (1972)

54 Rummens FHA "Can J Chem"; 54, 254, (1976)

55 Howard BB, Linder B & Emerson MT "J Chem Phys"; 36, 485, (1962)

56 Linder B "J Chem Phys"; 33, 668, (1960)

57 Linder B "J Chem Phys"; 35, 371, (1961)

58 Lumbroso N, Wu TK & Dailey BP "J Phys Chem"; 67, 2469, (1963)

59 Fontaine B, Chenon MT & Lumrosa-Bader N "J Chem Phys"; 62, 1075, (1965)

60 De Montgolfier Ph "CR Acad Sci Paris"; 2G3C, 505, (1966)

61 De Montgolfier Ph "J Chem Phys"; 64, 139, (1967)

62 De Montgolfier Ph "J Chem Phys"; 65, 1618, (1968)

63 De Montgolfier Ph "J Chem Phys"; 66, 685, (1969)

64 Rummens FHA "Chem Phys Letters"; 31, 596, (1975)

65 Rummens FHA "J Chem Phys"; 72, 448, (1975)

66 Rummens FHA "NMR Principles of Progress"; 10, (1975)

67 Rummens FHA "Can J Chem"; 54, 254, (1976)

68 Rummens FHA & Berstein HJ "J Chem Phys"; 43, 2971, (1965)

69 Rummens FHA "Mol Phys"; 19, 423, (1970)

70 Percival CC PhD thesis, (1981), Supervisor: J Homer, Department of Chemistry, University of Aston in Birmingham, "The Effect of Molecular Encounters on NMR Chemical Shifts"

71 Mohammadi MS PhD thesis (1986), Supervisor: J Homer, Department of Chemistry, University of Aston in Birmingham, "Polyatomic London Dispersion Forces"

72 Eisenshitz & London F "Z Phys"; 60, 491, (1930)

73 London F "Trans Faraday Soc"; 33, 8, (1937)

74 Bottcher CJF "Theory of electric polarization", Vol 1, "Dielectrics in static fields"; 2nd ed, Elseview Scientific Publishing Co (1973)

75 Kainosho M "J Phys Chem"; 73, 3516, (1969)

76 Hinckley CC "J Amer Chem Soc"; 91, 5160, (1969)

77 Briggs J, Hart FA, Moss GP & Randall EW "Chem Commun"; 364, (1971)

78 Witanowski M, Stefanaik L, Januszewski H & Wolkowski ZW "Chem Commun"; 1573, (1971)

79 Bleaney B, Dobson RB, Williams RJP & Xaviers AV "Chem Commun"; 791, (1972)

80 Dew Horrocks W Jr "Inorg Chem"; 9, 690, (1970)

81 Jessen JB "J Chem Phys"; 47, 579, (1967)

82 McConnell HM & Robertson RE "J Chem Phys"; 29, 1361, (1958)

83 Cramer RE, Dubois R & Sheff K "J Amer Chem Soc"; 96, 4125, (1974)

84 Coupland A PhD thesis, Supervisor: J Homer; Department of Chemitry, University of Aston in Birmingham (1978)

85 Handbook of Chemistry and Physics, 59th Ed, 1978-79, R Weast, Chemical Rubber Co Ltd

86 Homer J "J Mag Res"; 54, 1, (1983)

87 Sanders JKM & Williams DH "Chem Commun"; 422, (1970)

88 Briggs J, Frost GH, Hart FA, Moss GP & Staniforth ML "Chem Commun"; 749, (1970)

89 Rondeau RE & Sievers RE "J Amer Chem Soc"; 93, 1522, (1971)

90 Ernst L & Mannschreck A "Tetrahedran lett", 3023, (1971)

91 Crump DR, Sanders JKM & Williams DH "Tetrahedron lett"; 4419, (1970)

92 Marshall TW & Pople JA "Mol Phys"; 3, 399, (1960)

93 Raynes WT & Raza MA "Mol Phys"; 20, 555, (1971)

94 Raynes WT & Raza MA "Mol Phys"; 17, 157, (1969)

95 Mohanty S & Berstein HJ "J Chem Phys"; 54, 2254, (1971)

96 Moelwyn Hughes EA "Physical Chemistry"; Pergamon Press, Oxford, 2nd Ed, (1961)

97 Raynes WT "J Chem Phys"; 51, 3138, (1969)

98 Stuart HA & Schiezl SV "Ann Phys"; 2, 321, (1948)

99 LeFevre CG & LeFevre RJW "Rev of Pure and Applied Chem"; 5, 261, (1955)

100 Gordow AJ & Ford RA "The Chemist's Companion"; Wiley-Interscience, New York, (1972)

101 Abraham RJ, Wileman DF & Bedford CR "J Chem Soc", Perkin II, 1027, (1973)

102 Bridge NJ & Buckingham AD "Proc Roy Soc"; A295, 334 (1966)

103 "J Phys and Chem Ref data"; 6, (1977) "Energies of Gaseous Ions, Supplement No 1"

104 Lorentz HA "Theory of electrons"; Dover, New York, (1952)

105 Bretsznajder S "Prediction of transport and other physical properties of fluids"; Pergamon Press, Oxford, (1971)

106 Raza MA & Raynes WT "Mol Phys", 19, 199, (1970)

107 Kromhout RA & Linder B "J Mag Res"; 1, 450, (1969)

108 Handbook of Chemistry and Physics; 53rd Ed, (edited by R Weast); Chemical Rubber Co (1973)

109 Marshall TW & Pople JA "Mol Phys", 1, 199 (1958)

110 Musher JI "J Chem Phys", 41, 2671, (1964)

111 Yonomoto T "Can J Chem"; 44, 223, (1966)

112 Douglas CN & Doyle MP "Organic Chemistry"; John Wisley & Sons, New York, (1977)

113 Al-Daffaee HK PhD thesis (1983) Supervisor: J Homer, Department of Chemistry, University of Aston in Birmingham, "Studies of Sterically Controlled Solvent induced NMR Chemical Shifts"

114 Rummens FHA "NMR Periodicals"; 10, (1960)

115 Private communication

116 Spiesecke H & Schneider WG "J Chem Phys"; 35, 772, (1961)

117 Homer J & Callaghan D "J Chem Soc"; B, 1573 (1970)

118 Lauterbur PC "Determination of organic structures by physical methods"; Vol 2, Chap 7, Ed Nacho FC & Phillips WD; Academic Press, New York, (1962)